Panacea, Inc.
14700 Firestone Blvd., Suite 118
La Mirada, CA 90638
Phone (714) 228-1286
Fax (714) 228-1248

Preliminary Fate and Transport Modeling

• Final •

Brown & Bryant Superfund Site
Arvin, California

Prepared for:
U.S. Army Corps of Engineers
Los Angeles District
Los Angeles, California

Perry Montazer, Ph.D.
Hydrogeologist

Mitra Fiuzat, Ph.D.
Project Manager

Mohammad Estiri, Ph.D.
Project Director

Project No. C00-266 June 2004

Table of Contents

EXECUTIVE SUMMARY ..... **viii**

1.0 INTRODUCTION **1**

1.1 BACKGROUND 1
1.2 SITE GEOLOGY AND HYDROGEOLOGY 2
1.3 PREVIOUS AGENCY INSPECTIONS AND FINDINGS 3
1.4 PREVIOUS INVESTIGATIONS BY OTHERS 3
1.5 PURPOSE AND SCOPE 4
1.6 ORGANIZATION OF REPORT 4

2.0 DEVELOPMENT OF INITIAL HYDROGEOLOGIC CONCEPTUAL MODEL **5**

2.1 INTRODUCTION TO ALTERNATIVE CONCEPTUAL MODELS 5
2.2 ALTERNATIVE CONCEPTUAL MODEL 1 5
2.3 ALTERNATIVE CONCEPTUAL MODEL 2 5
2.4 ALTERNATIVE INFILTRATION RATES 6
2.5 CONCEPTUAL MODELS OF B-ZONE AQUIFER 6
2.6 DATA USED FOR MODELING 6
2.6.1 DATABASE MANAGEMENT 7
2.6.2 PRECIPITATION 7
2.6.3 INFILTRATION 7
2.6.4 SOIL PHYSICAL PROPERTIES 7
2.6.5 PROPERTIES OF CHEMICALS OF CONCERN 9

3.0 NUMERICAL MODELING APPROACH **10**

3.1 OVERVIEW OF THE APPROACH 10
3.2 IDENTIFICATION OF CODE FOR SIMULATIONS 10
3.3 DEVELOPMENT OF MESHES 11
3.3.1 CROSS-SECTIONAL UNSATURATED ZONE MESH 12
3.3.2 SATURATED ZONE PLAN-VIEW MESH 12

4.0 NUMERICAL MODELING RESULTS (BASE CASE) **12**

4.1 HYDROGEOLOGIC SYSTEM 12
4.1.1 UNSATURATED A- AND B-ZONES HYDROGEOLOGIC SYSTEM 12

4.1.2 SATURATED ZONE FLOW IN THE B-ZONE 14
4.2 CONSERVATIVE SIMULATION OF THE TRANSPORT OF COCs.....14
4.2.1 CROSS-SECTIONAL UNSATURATED ZONE NUMERICAL MODEL 16
4.2.2 SATURATED ZONE FLOW IN THE B-ZONE HYDROGEOLOGIC SYSTEM 17

5.0 SENSITIVITY ANALYSES.....18
5.1 HYDRAULIC PARAMETERS 18
5.1.1 PARAMETERS AFFECTING FLOW IN THE UNSATURATED ZONE 18
5.1.2 PARAMETERS AFFECTING FLOW IN THE SATURATED ZONE 19
5.1.3 TRANSPORT PARAMETERS 19

6.0 SUMMARY AND TENTATIVE CONCLUSIONS.....20

7.0 RECOMMENDATION.....21

8.0 REFERENCES.....21

TABLES

1 SUMMARY OF THE PROPERTIES OF THE MATERIAL USED FOR HYDROGEOLOGIC CONCEPTUAL MODELS
2 HYDRAULIC CONDUCTIVITY OF SILT AND CLAY MATERIAL MEASURED IN SAMPLES OBTAINED FROM RECENTLY DRILLED BOREHOLES AT THE SITE
3 RESULTS OF SOIL PROPERTIES TEST FROM PREVIOUS STUDIES
4 TOTAL AND EFFECTIVE POROSITY FROM PREVIOUS STUDIES AT THE SITE
5 MOISTURE CONTENT AND CORRESPONDING SATURATION VALUES FOR VARIOUS SAMPLES AT THE SITE
6 MOISTURE CONTENT VALUES FOR VARIOUS SAMPLES AT THE SITE FROM PREVIOUS STUDIES
7 CALCULATED CAPILLARY PRESSURE AS A FUNCTION OF LIQUID SATURATION FOR VARIOUS SOILS
8 CALCULATED CAPILLARY PRESSURE AS A FUNCTION OF LIQUID SATURATION FOR SELECTED SOILS

FIGURES

1-1 TOPOGRAPHIC MAP OF ARVIN AND VICINITY
1-2 THREE-DIMENSIONAL VIEW OF THE TOPOGRAPHIC MAP OF ARVIN AND VICINITY
1-3 AERIAL PHOTOGRAPH OF ARVIN AND VICINITY WITH THE LOCATION OF VARIOUS WELLS
1-4 BORING LOGS

2-1 TRANSECT OF THE BROWN AND BRYANT SITE

2-2 CROSS SECTION OF THE ALTERNATIVE CONCEPTUAL HYDROGEOLOGIC MODEL 1

2-3 THREE-DIMENSIONAL RENDERING OF THE ALTERNATIVE CONCEPTUAL HYDROGEOLOGIC MODEL 1

2-4 CROSS SECTION OF THE CONCEPTUAL HYDROGEOLOGIC MODEL 2

2-5 THREE-DIMENSIONAL RENDERING OF THE ALTERNATIVE-II CONCEPTUAL HYDROGEOLOGIC MODEL OF THE AREA

2-6 MONTHLY PRECIPITATION DATA FOR BAKERSFIELD PRESENTED IN THREE DIMENSIONAL VIEW (A) AND LINE PLOT (B)

2-7 DISTRIBUTION AVAILABLE HYDRAULIC CONDUCTIVITY DATA

2-8 DISTRIBUTION AVAILABLE EFFECTIVE POROSITY DATA

2-9 DISTRIBUTION AVAILABLE SOIL DRY DENSITY DATA

2-10 DISTRIBUTION AVAILABLE TOTAL ORGANIC CARBON (TOC) DATA

2-11 DATA DISTRIBUTION (MOISTURE CONTENT)

2-12 GRAIN-SIZE DISTRIBUTION FOR VARIOUS SAMPLES FROM BOREHOLES AT THE SITE

2-13 CAPILLARY PRESSURE CURVE FOR CLAYS AT THE SITE

2-14 GRAIN-SIZE DISTRIBUTION CURVE FOR SELECTED SAMPLES AT THE SITE

2-15 MEASURED CAPILLARY-MOISTURE RELATIONS FOR SELECTED SOIL SAMPLES

2-16 MEASURED MOISTURE RETENTION CURVE FOR SELECTED SOIL SAMPLES

2-17 CAPILLARY PRESSURE CURVE FOR SILT GROUP AT THE SITE CALCULATED AS DESCRIBED IN TEXT

2-18 CAPILLARY PRESSURE CURVE FOR SAND GROUP AT THE SITE CALCULATED AS DESCRIBED IN TEXT

2-19 CAPILLARY PRESSURE CURVE FOR FINE SAND AND SILTY SAND GROUP AT THE SITE CALCULATED AS DESCRIBED IN TEXT

2-20 CAPILLARY PRESSURE CURVE FOR CLAY GROUP AT THE SITE CALCULATED AS DESCRIBED IN TEXT COMPARED WITH TYPICAL DISTRIBUTION IN LITERATURE

2-21 CAPILLARY PRESSURE CURVE FOR ALL SOILS AT THE SITE CALCULATED AS DESCRIBED IN TEXT COMPARED WITH TYPICAL DISTRIBUTION IN LITERATURE

3-1 CROSS-SECTIONAL MESH USED FOR SIMULATIONS OF UNSATURATED ZONE

3-2 PLAN VIEW MESH USED FOR SIMULATIONS OF SATURATED B-ZONE

4-1 DISTRIBUTION OF WATER SATURATION OVERLAIN ON CONCEPTUAL HYDROGEOLOGIC MODEL 1

4-2 DISTRIBUTION OF WATER SATURATION OVERLAIN ON CONCEPTUAL HYDROGEOLOGIC MODEL 1

4-3 PRESSURE HEAD (m) OVERLAIN ON CONCEPTUAL HYDROGEOLOGIC MODEL 1

4-4 WATER SATURATION OVERLAIN ON CONCEPTUAL HYDROGEOLOGIC MODEL 1

4-5 WATER SATURATION OVERLAIN ON CONCEPTUAL HYDROGEOLOGIC MODEL 2

4-6 PRESSURE HEAD (m) OVERLAIN ON CONCEPTUAL HYDROGEOLOGIC MODEL 2

4-7 PRESSURE HEAD (m) IN THE B-ZONE

4-8 MAXIMUM CHEMICAL CONCENTRATION DISTRIBUTION IN A-ZONE GROUNDWATER IN 1991

4-9 MAXIMUM CHEMICAL CONCENTRATION DISTRIBUTION IN A-ZONE GROUNDWATER IN 1991

4-10 MAXIMUM CHEMICAL CONCENTRATION DISTRIBUTION IN A-ZONE GROUNDWATER IN 1991

4-11 MAXIMUM CHEMICAL CONCENTRATION DISTRIBUTION IN A-ZONE GROUNDWATER IN 1991

4-12 DISTRIBUTION OF MAXIMUM CONCENTRATION OF 1,2-DCP (µg/l) IN B-ZONE GROUNDWATER IN 1992

4-13 DISTRIBUTION OF MAXIMUM CONCENTRATION OF 1,3-DCP (µg/l) IN B-ZONE GROUNDWATER IN 1992

4-14 DISTRIBUTION OF MAXIMUM CONCENTRATION OF 1,2,3-TCP (µg/l) IN B-ZONE GROUNDWATER IN 1992

4-15 DISTRIBUTION OF MAXIMUM CONCENTRATION OF CHLOROFORM (µg/l) IN B-ZONE GROUNDWATER IN 1992

4-16 DISTRIBUTION OF MAXIMUM CONCENTRATION OF DBCP (µg/l) IN B-ZONE GROUNDWATER IN 1992

4-17 DISTRIBUTION OF MAXIMUM CONCENTRATION OF DINOSEB (µg/l) IN B-ZONE GROUNDWATER

4-18 DISTRIBUTION OF MAXIMUM CONCENTRATION OF EDB (µg/l) IN B-ZONE GROUNDWATER

4-19 CONCENTRATION OF 1,2-DCP (µg/l) IN THE B-ZONE

4-20 CONCENTRATION OF 1,2-DCP (µg/l) IN THE B-ZONE

4-21 CONCENTRATION OF 1,2-DCP (µg/l) IN THE B-ZONE

4-22 CONCENTRATION OF 1,2-DCP (µg/l) IN THE B-ZONE

4-23 CONCENTRATION OF 1,2-DCP (µg/l) IN THE B-ZONE

4-24 CONCENTRATION OF 1,2-DCP (µg/l) AFTER 100 YEARS OVERLAIN ON CONCEPTUAL HYDROGEOLOGIC MODEL 1 USING 10 mm/yr INFILTRATION RATE

4-25 CONCENTRATION OF 1,2-DCP (µg/l) AFTER 100 YEARS OVERLAIN ON CONCEPTUAL HYDROGEOLOGIC MODEL 1 USING 100 mm/yr INFILTRATION RATE ON SITE WITH FLAT WATER TABLE

4-26 SIMULATED CONCENTRATION OF 1,2-DCP (µg/l) AFTER 100 YEARS WITH 10 mm/yr INFILTRATION RATE COMPARED WITH DISTRIBUTION OF 1,2-DCP IN UNSATURATED ZONE

4-27 SIMULATED CONCENTRATION OF 1,2-DCP (µg/l) IN THE UNSATURATED ZONE (CONSERVATIVE)

4-28 SIMULATED CONCENTRATION OF 1,3-DCP (µg/l) IN THE UNSATURATED ZONE (CONSERVATIVE)

4-29 SIMULATED CONCENTRATION OF 1,2,3-TCP (µg/l) IN THE UNSATURATED ZONE (CONSERVATIVE)

4-30 SIMULATED CONCENTRATION OF CHLOROFORM (µg/l) IN THE UNSATURATED ZONE (CONSERVATIVE)

4-31 SIMULATED CONCENTRATION OF DBCP (µg/l) IN THE UNSATURATED ZONE (CONSERVATIVE)

4-32 SIMULATED CONCENTRATION OF DINOSEB (µg/l) IN THE UNSATURATED ZONE (CONSERVATIVE)

4-33 SIMULATED CONCENTRATION OF EDB (µg/l) IN THE UNSATURATED ZONE (CONSERVATIVE)

4-34a SIMULATED CONCENTRATION OF 1,2-DCP (µg/l) IN THE SATURATED ZONE (CONSERVATIVE)

4-34b SIMULATED CONCENTRATION OF 1,2-DCP (µg/l) IN THE SATURATED ZONE (CONSERVATIVE)

4-34c SIMULATED CONCENTRATION OF 1,2-DCP (µg/l) IN THE SATURATED ZONE (CONSERVATIVE)

4-35a SIMULATED CONCENTRATION OF 1,3-DCP (µg/l) IN THE B-ZONE GROUNDWATER (CONSERVATIVE)

4-35b SIMULATED CONCENTRATION OF 1,3-DCP (µg/l) IN THE B-ZONE GROUNDWATER (CONSERVATIVE)

4-35c SIMULATED CONCENTRATION OF 1,3-DCP (µg/l) IN THE B-ZONE GROUNDWATER (CONSERVATIVE)

4-36a SIMULATED CONCENTRATION OF TCP (µg/l) IN THE SATURATED ZONE (CONSERVATIVE)

4-36b SIMULATED CONCENTRATION OF TCP (µg/l) IN THE SATURATED ZONE (CONSERVATIVE)

4-36c SIMULATED CONCENTRATION OF TCP (µg/l) IN THE SATURATED ZONE (CONSERVATIVE)

4-37a SIMULATED CONCENTRATION OF CHLOROFORM (µg/l) IN THE B-ZONE GROUNDWATER (CONSERVATIVE)

4-37b SIMULATED CONCENTRATION OF CHLOROFORM (µg/l) IN THE B-ZONE GROUNDWATER (CONSERVATIVE)

4-37c SIMULATED CONCENTRATION OF CHLOROFORM (µg/l) IN THE B-ZONE GROUNDWATER (CONSERVATIVE)

4-38a SIMULATED CONCENTRATION OF DBCP (µg/l) IN THE B-ZONE GROUNDWATER (CONSERVATIVE)

4-38b SIMULATED CONCENTRATION OF DBCP (µg/l) IN THE B-ZONE GROUNDWATER (CONSERVATIVE)

4-38c SIMULATED CONCENTRATION OF DBCP (µg/l) IN THE B-ZONE GROUNDWATER (CONSERVATIVE)

4-39a SIMULATED CONCENTRATION OF DINOSEB (µg/l) IN THE SATURATED ZONE (CONSERVATIVE)

4-39b SIMULATED CONCENTRATION OF DINOSEB (µg/l) IN THE SATURATED ZONE (CONSERVATIVE)

4-39c SIMULATED CONCENTRATION OF DINOSEB (µg/l) IN THE SATURATED ZONE (CONSERVATIVE)

4-40a SIMULATED CONCENTRATION OF EDB (µg/l) IN THE SATURATED ZONE (CONSERVATIVE)

4-40b SIMULATED CONCENTRATION OF EDB (µg/l) IN THE SATURATED ZONE (CONSERVATIVE)

4-40c SIMULATED CONCENTRATION OF EDB (µg/l) IN THE SATURATED ZONE (CONSERVATIVE)

APPENDICES

A PHOTOGRAPHS OF THE SITE

B SAMPLE OF THE DATABASE USED FOR SIMULATIONS

C EXCERPTS FROM VAN GENUCHTEN

D SUMMARY OF THE RUNS FOR UNSATURATED ZONE FLOW SENSITIVITY ANALYSES

E CALCULATION OF CONCENTRATION OF COCs IN SOIL WATER (AQUEOUS PHASE)

F CALCULATION OF Kd FROM LABORATORY BATCH ADSORPTION TEST

EXECUTIVE SUMMARY

The purpose of this study is to assess and understand the fate and transport process of some of the chemicals of concern (COCs) in the vadose and saturated zones at the Brown & Bryant Superfund site (site). Based on analyses of existing borehole data, two conceptual hydrogeologic models were developed to simulate subsurface flow. This report describes the preliminary fate and transport modeling of seven COCs in the groundwater beneath the site that may be used to assess the potential risk of COCs reaching the City of Arvin water well supply.

Geology beneath the site is comprised of an alluvial deposit of alternating layers and mixtures of unconsolidated sands, silts, and clay. Soil underlying the site to a depth of 80 feet (24.4 m) generally consists of silty fine sand to fine sandy silt. Clean, well-graded sand lenses and thin seams of silty clay occur locally within these soils. The soils are thinly interbedded, with textural changes occurring every few vertical inches. These textural changes are also believed to occur laterally.

Due to varying conditions such as precipitation and soil properties that could affect the fate and transport of fluids and movement of chemicals into the groundwater, different assumptions and variables were used to develop the Alternative Conceptual Hydrogeologic Models 1 and 2. Based on these conceptual models, two numerical models were created using data from existing borehole logs, sampling data, and literature research. The main difference between the hydrogeological conceptual models is the northern extent of the existing clay layer in the saturated B-zone aquifer. In Conceptual Model 1, the saturated B-zone is assumed to consist entirely of sand. In Conceptual Model 2, the B-zone is assumed to consist of a continuous clay layer overlying the sand zone. Subsurface groundwater flow and the potential paths of the spread of the COCs were evaluated using the numerical models.

The preliminary fate and transport modeling results suggest that the COCs in the unsaturated zone persist longer than in the saturated zone. The conservative scenario modeling results show that transport of the COCs occurs primarily in the vertical direction in the unsaturated zone. This is despite the heterogeneous layering of the hydrogeologic units. Very little lateral flow and transport occurs in the unsaturated zone. In the saturated zone, flow and transport are mainly southwesterly toward the city well. This direction of flow and transport is partly due to assumptions made based on available information. These modeling results also show that the COCs in the saturated zone may persist for a maximum of 10 years in the absence of vertical leakage from the unsaturated zone. However, leakage from the unsaturated zone is predicted by these results to persist for more than 100 years. The concentrations of chemicals reaching the city well are estimated to be below their respective maximum contaminant levels (MCLs) with or without contribution from the unsaturated zone. This conclusion is reached based on several assumptions that should be validated by future investigations.

Preliminary Fate and Transport Modeling

Brown & Bryant Superfund Site
Arvin, California

1.0 INTRODUCTION

1.1 BACKGROUND

The Brown and Bryant Superfund site (site) is located at 600 South Derby Street in Arvin, California, approximately 18 miles (29 km) southeast of the city of Bakersfield (Figures 1-1, 1-2, and 1-3 and Appendix A, photo A-1). The site (Appendix A, Photo A-2) is bordered on the east by irrigated agricultural fields (Appendix A, photo A-3), on the north and south by food packing and shipping facilities, and on the west by a residential area. Two schools (Gospel Tabernacle of Arvin and Stepping Stones Child Care Center) and a park (Bear Mountain Recreation and Park Center) are within 0.5 mile (0.8 km) of the site. The Morning Star Preschool, at 416 North Hill Street, is within 1 mile (1.61 km) of the site.

The Brown & Bryant facility operated as a pesticide reformulator and custom applicator facility from 1960 to 1989. This facility formulated agricultural chemicals, including pesticides, herbicides, fumigants, and fertilizers. In 1981, the Brown & Bryant facility was licensed under the Resource Conservation and Recovery Act (RCRA) as a hazardous waste transporter. Contamination of soil and groundwater resulted from inadequate procedural controls, poor housekeeping, chemical spills during operations, and leaks from a surface wastewater pond and sumps. The largest releases onsite were from a waste pond, a sump area, and a dinoseb spill area (Figure 1-3).

The waste pond, in the southwest portion of the site, was originally excavated as an unlined earthen pond in 1960. The pond was used to collect runoff water from the yard and from two sumps (since excavated). The pond was also used to collect rinse water from rinsing tanks used for fumigants. Excess pond water and rainwater runoff also collected in a topographically low area to the east and south of the pond. In addition, ponded water from precipitation and irrigation from the east has occasionally breached the berm in the southeast corner of the pond, and drained into the pond. The pond was double lined with a synthetic liner in November 1979. The liner and additional soil were excavated in August 1987. Approximately 640 cubic yards (489 m^3) of soil that showed visible signs of contamination were removed from the pond at that time. The depths of this excavation ranged from approximately 1.5 feet (0.457 m) on the sides to 5 feet (1.52 m) near the center.

In 1960, an unlined earthen sump was constructed in the center of the site (near wells AMW-2P and AMW-4R). The sump was used to collect washwater from a pad where equipment and tanks used for liquid fertilizers and fumigants were washed. Water from the sump was drained to the pond through an underground pipeline. In 1980, the unlined sump was replaced with two double-lined sumps.

Dinoseb was stored in a smaller tank storage area along the eastern fence, just north of the pond. In 1983, there was a significant dinoseb spill in this area. As a result, the soil and groundwater underlying this

portion of the site has been reported to contain the highest concentrations of dinoseb. The USEPA excavated highly contaminated soil from this area in the mid 1990s.

In 1989, the site was listed on the National Priorities List (NPL). Subsequently, various emergency and removal actions were initiated to minimize or eliminate immediate threats to human health and the environment.

The site is currently vacant. A warehouse, an open metal shed, and an aboveground storage tank are on the property. The property is secured by a chain-link fence (Appendix A, photo A-2). A RCRA cap covers the southern portion of the site and a non-RCRA cap covers the northern portion of the site (Figure 1-3).

1.2 SITE GEOLOGY AND HYDROGEOLOGY

Geology beneath the site is comprised of an alluvial deposit of alternating layers and mixtures of unconsolidated sands, silts, and clay (Figure 1-4). Soil underlying the site to a depth of 80 feet (24.4 m) bgs generally consists of silty fine sand to fine sandy silt. Clean, well-graded sand lenses and thin seams of silty clay occur locally within these soils. The soils are thinly interbedded, with textural changes occurring every few vertical inches. These textural changes are also believed to occur laterally.

The site geology has been divided into two zones: the A-zone and the B-zone. The A-zone includes unsaturated soil to 65 to 75 feet (19.8 to 22.9 meters) below ground surface (bgs) and includes the first water-bearing unit, the A-zone groundwater. The depth to the saturated zone has varied between 65 and 85 feet (19.8 and 25.9 meters) bgs in recent groundwater depth measurements. The base of the A-zone is a thin sandy clay layer from 75 to 85 feet (22.9 to 25.9 meters) bgs. The clay layer and the A-zone groundwater occur beneath the entire site but disappear within 900 feet (274 m) south of the site.

The B-zone includes unsaturated soil beneath the A-zone and the second-lowest water-bearing unit (B-zone groundwater) at 150 to 165 feet (45.7 to 50.3 meters) bgs. The B-zone extends to at least 250 feet (76.2 m) bgs and ends at a clay layer known as the Corcoran Clay that confines the drinking water aquifer (the C-zone aquifer) beneath it. The thickness of this clay layer beneath the site is unknown. Specific data regarding the alluvial soil types within the B-zone were not encountered in previous reports prepared for the site or the adjoining properties. These materials probably comprise mixtures and layers of clay, silt, sand, and gravel.

Groundwater in the A-zone flows in a generally southerly direction, with some mounding of the water table observed extending south from the southwest corner of the site. The saturated thickness of the A-zone groundwater ranges from 0 to 10 feet (0 to 3.05 meters). The groundwater velocity in the A-zone has been estimated at 53 feet (16.2 m) per year. Slug test results suggest that a yield of less than 100 gallons (455 liters [l]) per day can be expected for wells in the A-zone. Aquifer testing of three of the onsite extraction wells showed a groundwater yield of approximately ¼ gallon per minute (gpm) (1.14 l/min) (Morrison Knudson [MK], 1999b). It is the opinion of Panacea, Inc. (Panacea), however, that the wells tested were in a portion of the site that typically yields low water quantities. Wells south of the site, within the A-zone, have significantly greater yield.

The B-zone groundwater comprises a series of water-bearing units. All of the wells in the B-zone were installed in the water-bearing unit located at approximately 170 feet (51.8 m) bgs. The direction of flow in this unit is to the south, and the gradient is flat (0.0004). Permeabilities are much higher than for the A-zone groundwater. Past pump tests indicated that wells screened in the B-zone could be pumped at 7 gpm (MK, 1999b) for an extended period.

1.3 PREVIOUS AGENCY INSPECTIONS AND FINDINGS

Inspections by the California Regional Water Quality Control Board (CRWQCB) have documented numerous instances of poor housekeeping practices during Brown & Bryant's occupancy of the site. As noted above, an onsite tank holding dinoseb and two unlined ponds for pesticide rinse water were noted as being potential contaminant release areas. One 250,000-gallon (11.4×10^6 l) pond was noted as overflowing twice. The onsite UN-32 tank, 560,000 gallons (2.55×10^6 l) in capacity, is also reported to have leaked. In 1984, the California Department of Health Services identified various pesticides and herbicides in onsite wells, including 1,2-dibromo-3-chloropropane, ethylene dibromide, dinoseb, 1,2-dichloropropane, and chlorobenzene.

Subsurface investigations conducted onsite to date (Panacea, 2002) have confirmed the presence of a number of potentially hazardous substances in the groundwater. Fifty-six organic compounds were found within the A-zone groundwater samples and 11 were found in the B-zone groundwater samples. The primary chemicals of concern (COCs) include:

- Chloroform;
- 1,2-dibromo-3-chloropropane (DBCP);
- 1,2-dichloropropane (1,2-DCP);
- 1,3-dichloropropane (1,3-DCP);
- 1,2,3-trichloropropane (1,2,3-TCP);
- Ethylene dibromide (EDB); and
- Dinoseb.

These chemicals were detected during the Operable Unit No. 1 (OU1) investigation. The contamination in the perched aquifer poses a potential threat to the underlying unconfined regional aquifer (B-zone) and the confined C-zone aquifer that is used for municipal drinking water. Public and private wells within 3 miles (4.8 km) of the site provide drinking water to 7,200 people and irrigate 19,600 acres (79.3 km^2) of cropland. City of Arvin Well #1 (Appendix A, A-5) is 1,500 feet (457 m) downgradient from the site (labeled as CW-1 in Figure 1-3). None of these supply wells are known to produce water from A- or B-zones.

1.4 PREVIOUS INVESTIGATIONS BY OTHERS

Background information reviewed by Panacea is presented in *Monitoring Well Installation Report* (Panacea, 2002) and the key investigations by Morrison Knudson (MK) summarized here. In 1999, MK prepared a monitoring well completion report for Wells MW-1, MW-2, and MW-3 (MK, 1999a). These three wells were installed to serve as observation wells during aquifer testing of the three adjacent extraction wells (EW-1, EW-2, and EW-3). The new monitoring wells were placed 8 to 15 feet (2.44 to 4.57 meters) from the extraction wells. The report generally presented well construction procedures and physical characteristics of the collected soil. The physical soil characteristics described by MK are used in the present report. MK also presented the results of a series of aquifer tests that were performed on the newly installed extraction wells (EW-1, EW-2, and EW-3) and injection wells (IW-1 and IW-2) (MK, 1999b). Test results indicated a relatively low yield for extraction and injection wells.

1.5 PURPOSE AND SCOPE

This report present a summary of the technical approach and methodology used for developing alternative conceptual and numerical models for subsurface flow of fluids and transport of COCs at the site. Existing data from boreholes and wells were evaluated and analyzed to develop two alternative conceptual hydrogeologic models of the site. Several laboratory test results were analyzed to verify some of the calculated and assumed parameters for the simulations. This report presents the base-case conservative scenario and does not address sensitivity and uncertainty related to transport of the COCs.

The purpose of this preliminary phase of the fate and transport project was to evaluate possible mechanisms of transport of the COCs in the vadose and saturated zones at the site (. Although one of the major concerns is to evaluate whether there is a potential for these COCs to enter the City of Arvin water supply well at concentrations above maximum contamination levels (MCLs), this preliminary analysis does not address this issue fully. The results of fate and transport analyses will ultimately be used in risk assessment to address the issue of potential risks to the city well. Risk assessment requires uncertainty and sensitivity analyses to evaluate ranges of potential attenuation of the COCs along their exposure pathways. This phase of the fate and transport analysis does not provide the uncertainty and sensitivity analyses to the extent that is needed for the risk assessment.

Uncertainty in various assumptions used to arrive at the conclusions about the fate of the COCs affects the confidence level in assessment of risk to human and the environment. The impact of the uncertainty on the results is greater for parameters to which the calculations are most sensitive to (i.e., parameters that could most significantly influence the results of calculations of fate of the COCs and their risks). Sensitivity of parameters and the resultant uncertainty in calculations need to be performed systematically. Although some sensitivity and uncertainty analyses for the hydraulic parameters are presented in this report, a thorough analysis, which requires evaluation of the effects of retardation, degradation, and other attenuation potentials have not been completed. Analyses of sensitivity and uncertainty are underway but with a limited scope in preparation for risk assessment.

1.6 ORGANIZATION OF REPORT

The following list details the organization of the remainder of this report:

- Section 2: Development of Initial Hydrogeologic Conceptual Model. Describes Alternative Conceptual Models and includes the data used for modeling.
- Section 3: Numerical Modeling Approach. Describes the simulation codes and the development of meshes used for saturated and unsaturated zones.
- Section 4: Numerical Modeling Results (Base Case): Describes the hydrogeologic system and conservative simulation of the transport of COCs.
- Section 5: Sensitivity Analyses: Describes hydraulic parameters and parameters affecting flow in the unsaturated and saturated zones.
- Section 6: Summary and Tentative Conclusion.
- Section 7: Recommendation.
- Section 8: References.

2.0 DEVELOPMENT OF INITIAL HYDROGEOLOGIC CONCEPTUAL MODEL

2.1 INTRODUCTION TO ALTERNATIVE CONCEPTUAL MODELS

Geologic logs from all the pertinent boreholes that were available at the time of this study were evaluated and a set of boreholes was selected to develop a geologic cross section from northeast to southwest (Figure 2-1). This cross section intersects the largest number of boreholes and wells, including the city well and the northernmost borehole, EPA-4 (Appendix A, photo A-4). Based on the physical properties available, the geologic components were divided into four hydrogeologic units: sand, silt, clay, and mixed. The mixed unit consists of relatively thin layers of interbedded sand, silt, and clay. Criteria for distinction between the layers were based on the thickness of the layers encountered in the boreholes. If either the sand layers or silt layers were thicker than 5 feet (1.52 m), they were considered as distinct units of sand or silt, respectively. If these layers were thinner than 5 feet (1.52 m), they were lumped together as a mixed unit. For clay layers, a lower bound for distinction was used. A lower bound for thickness was used for clay layers because of their relative importance as barriers to flow of groundwater and transport of COCs. If a clay layer was thicker than 2 feet (0.61 m), it was assigned as a distinct hydrogeologic unit. Otherwise, it was included in the mixed unit.

Two alternative cross sections were developed based on these criteria. The information from the boring logs was entered into Groundwater Modeling System (GMS; Boss International, Inc., 2002) software to develop three-dimensional alternative conceptual hydrogeologic models for the site. Based on the information entered into GMS, two interpretations of the conceptual hydrogeologic model were developed. These are referred to as Conceptual Model 1 and Conceptual Model 2. Following is a brief description of each model.

2.2 ALTERNATIVE CONCEPTUAL MODEL 1

Figure 2-2 shows the northeast-southwest hydrogeologic cross-section of Conceptual Model 1. This conceptual model is based entirely on the information available from existing boring logs. Adequate information is not available to extend the lowermost clay layer penetrated in boreholes CB-01 and WB2-4 to the north. For this reason, in Conceptual Model 1 this clay layer is considered to be of limited extent. Figure 2-3 shows a three-dimensional view of Conceptual Model 1. This clay layer occurs about 200 feet (61 m) below the ground surface (approximately 100 feet [30.5 m] above the Corcoran confining layer). Its continuity is important as measure of added protection of the regional C-zone aquifer. Therefore, the presence or absence of this layer beneath the site was considered a significant factor in distinguishing between the two conceptual models presented in this report.

2.3 ALTERNATIVE CONCEPTUAL MODEL 2

Figure 2-4 shows the northeast-southwest cross-section corresponding to Conceptual Model 2. Figure 2-5 shows a three-dimensional view of this conceptual model. In this conceptual model, the lowermost clay layer in the B-zone is extended to the north based on information from adjacent sites. However, additional boreholes at the site would be needed to confidently extend this clay layer to the north. In this preliminary evaluation of fate and transport, the impact of this layer on flow and transport has not been analyzed completely and simulations await completion of additional boreholes and wells at the site. Efforts have been undertaken to compile additional information to more accurately define the extent of this layer. At this point, there is uncertainty about the extent of this layer and the results presented should not be considered verified.

2.4 ALTERNATIVE INFILTRATION RATES

As described in the following section (Section 2.5), two infiltration scenarios were considered. One of these corresponds to the natural background infiltration typical of the area and the other considers ponding and excess infiltration due to diversion of water into the previous ponds at the site. Although these are not considered as separate physical conceptual hydrogeologic models, the two infiltration scenarios, combined with the above-mentioned two conceptual hydrogeologic models, provide additional conceptualizations that may significantly affect the fate and transport through both saturated and unsaturated zones. Therefore, variations of the infiltration are considered as sub-alternative conceptual models.

2.5 CONCEPTUAL MODELS OF B-ZONE AQUIFER

The conceptual model of the B-zone was based on the assumption that the clay layer mentioned above is absent. The clay layer of concern would fall partially within the B-zone if it were assumed that it extends to the north. Therefore, this assumption has significant impact on the results of the flow and transport calculations in this aquifer. For the purposes of this report, only Alternative Conceptual Model 1 is used for the B-zone. That is, the entire B-zone aquifer is assumed to consist of a uniform, homogeneous sand layer. Recent evaluation of the data from wells off-site has shown that the clay layer encountered in the CB01 and WB2-4 may be present in other areas. However, whether this clay layer is extensive under the modeled area and what section of its thickness falls within the saturated zone is unknown.

One factor that prevents one from arriving at a firm conclusion about the presence or absence of this clay layer beneath the modeled area is that all B-zone wells north of well WB2-4 have encountered water levels and are relatively productive. There are two possible explanations for this occurrence. Either the clay layer is absent to the north or there is a shallow aquifer in the sandy material above this layer. All wells are producing from sandy material in the B-zone north of well WB2-4. If the latter is the case (i.e., there is a continuous clay layer to the north), then there must be another confined aquifer that exists between this clay layer and the Corcoran Aquitard. It is possible that the wells to the north have not been drilled deep enough to encounter this clay layer or any underlying aquifer that might exist. Regardless of the presence or absence of a continuous clay layer, there is a pathway with relatively high transmissivity in the B-zone between the site and the city well. The questions are:

- What is the thickness of this transmissive layer?
- If another aquifer exists beneath this hypothetical clay layer, has it been contaminated?

The differences between the results of these alternative conceptualizations can be evaluated by assuming approximate extent and properties of this clay layer in the B-zone aquifer. However, there is a plan to drill additional boreholes and install wells to expand the characterization of the B-zone aquifer. Therefore, Panacea believes that it is prudent to await availability of additional data before evaluating the alternative conceptual models of the B-zone aquifer. Also, analyses of multiple hypothetical alternatives were beyond the scope of this preliminary fate and transport analysis.

2.6 DATA USED FOR MODELING

A large amount of data was available for the fate and transport analyses, which were incorporated into a database as will be described in the following section (2.6.1). In addition, several physical parameters that were not available from previous site investigations were measured on samples collected during installation of a new series of monitoring wells by Panacea (2002). These samples were analyzed for

several physical parameters including grain-size distribution, moisture retention curves, saturated and unsaturated hydraulic conductivity, and batch adsorption test.

2.6.1 DATABASE MANAGEMENT

All available soil and groundwater chemical analytical results for the seven COCs mentioned above were entered into the SATURN database. SATURN is a database management software tool that is designed to facilitate access to site investigation data. The data stored in the database can be of a completely heterogeneous nature. That is, the database can store soil and rock physical properties, physical and chemical properties of the COCs (e.g., concentration, density, viscosity of non-aqueous phase liquids (NAPL), and thermodynamic properties needed for simulations), and geologic information. The database is spatially oriented, which means that all data points are referenced to a three-dimensional coordinate system (two geographical coordinates with elevation from boreholes). Input data for simulations and results from post-processing of the simulations also are facilitated by SATURN.

Appendix B presents a summary of some of the pertinent tables. Detailed description of the database structure is beyond the scope of this report. In addition to the site-specific information, chemical properties of the COCs were obtained from various sources including TOXNET (Toxicology Network; U.S. National Library of Medicine, 2002). Various chemical properties that were needed for simulations were incorporated into the database and are listed in Appendix B (Table “Chemical properties”).

2.6.2 PRECIPITATION

Monthly precipitation data for Bakersfield are plotted on Figure 2-6. Figure 2-6a is a three-dimensional column view and Figure 2-6b is a line plot for these data. In Figure 2-6a, it is evident that the precipitation occurs between October and April but is most frequent and intense in February and March. The frequency of recurrence appears to be between once every 17 to 20 years for monthly precipitation intensity of 4 inches (0.1 m) or more. For monthly precipitation intensity between 2 and 4 inches (0.05 and 0.1 meters), the frequency appears to be once every 2 to 7 years. These precipitation patterns may have affected the advective transport of the COCs prior to installation of the RCRA cap at the site and may continue to influence transport in the B-zone.

2.6.3 INFILTRATION

Information about the natural infiltration rate at the site is not readily available. Infiltration rates were assumed to be constant and equivalent to other sites with similar climatic conditions in Nevada. Infiltration rates vary in the area of Arvin because of the irrigation practices. Also, at the Brown & Bryant site, the infiltration rate was influenced significantly by the amount of runoff and wastewater that was redirected to the ponds prior to emplacement of the RCRA cap. Two infiltration rates were assumed for the fate and transport simulations. A lower bound of 0.4 inch per year (in/yr) (10 millimeters per year [mm/yr] was assumed to be a natural overall infiltration rate. An infiltration rate of 4 in/year (100 mm/yr) was assumed as a focused infiltration into the bottom of the pond at the site.

2.6.4 SOIL PHYSICAL PROPERTIES

Distributions of the available soil physical properties data at the time when the preliminary fate and transport task was initiated (May 2002) are shown in Figures 2-7 through 2-11. Additional data have become available since then but are not shown in these figures. A summary of the ranges of values is also shown with colored symbols for each property. Available data are most abundant beneath the site.

Table 1 summarizes some of the parameters and naming conventions used for numerical modeling purposes. Although material types are assigned specific names corresponding to zones A or B, all clay layers were given the same properties except for the layer beneath the A-zone, which was assigned various values for sensitivity analysis. Similarly, all silts, sands, and mixed layers were assigned the same properties appropriate for each group of soil (Hillel, 1980; Parker et al., 1987). In Table 1, "RP" refers to relative permeability function parameters and "CP" refers to capillary pressure function parameters. In the following paragraphs, a brief description of derivation of these parameters is presented.

Saturated hydraulic conductivity values for samples obtained from boreholes recently drilled by Panacea are presented in Table 2. These samples are mostly from silt and clay layers. A maximum value of 3.53×10^{-5} centimeter per second [cm/sec]) and a minimum value of 8.19×10^{-9} cm/sec are reported for hydraulic conductivity of these soil types at the site.

Table 3 reports results of directional hydraulic conductivity testing to range from 1×10^{-8} to 8.5×10^{-5} cm/sec. This range is reported for both horizontal and vertical hydraulic conductivity values.

Statistical parameters are calculated for the values in Table 3. The harmonic mean is more representative of the vertical hydraulic conductivity when vertical flow through a series of horizontal layers is considered. The vertical harmonic mean is calculated to be 9.84×10^{-8} cm/sec and the horizontal mean is 2.42×10^{-8} cm/sec (8.03×10^{-8} cm/sec for Panacea boreholes; Table 2). A hydraulic conductivity of 1.0×10^{-9} cm/sec is approximately equivalent to a permeability of (1×10^{-16} square meter [m^2]). It appears that the harmonic mean is almost the same in both horizontal and vertical directions for finer-grained soils (clays and silts).

For flow parallel to the layers, such as in the saturated sections of both A- and B-zones, geometric mean is a more appropriate statistical parameter. This is because of the heterogeneous nature of the material. Geometric means of hydraulic conductivity values range between 5.37×10^{-7} and 1.6×10^{-7} cm/sec (or permeability values between ~5.0×10^{-16} and 1×10^{-16} m^2) for vertical and horizontal directions, respectively (1.29×10^{-6} cm/sec for Panacea samples).

In simulations of the unsaturated zone, the harmonic mean (for the horizontal direction) has been assigned for the base cases to the clay material. Values of the harmonic mean have also been assigned to the clay material for sensitivity analysis. An upper bound value of 1.0×10^{-4} cm/sec (or permeability values between ~1.0×10^{-13} m^2) was assigned to the silt and mixed layers. A value of 1.0×10^{-5} cm/sec (or permeability values between ~1.0×10^{-14} m^2) was also assigned to these layers to evaluate the sensitivity of calculated flow rates in the unsaturated zone.

Calculation of *in-situ* saturation of the soils requires values of total porosity. Values of total and effective porosities are presented in Table 4 for a few samples. *In-situ* saturation values could only be calculated for the Panacea samples (Table 5) because they were the only samples for which dry bulk density was reported. These saturation values seem to suggest that the soils at the site are at near-residual saturation values. If this is the case, vertical flux of water is expected to be small.

Table 6 presents variation of moisture content with depth for samples taken from MW-23 and MW-4 borehole.

Unsaturated characteristic properties (moisture retention and relative permeability curves) for the hydrogeologic units were calculated in part by using the grain-size distribution from laboratory analyses of the soil samples (Figure 2-12). The empirical calculations were compared with a few moisture characteristic curves that were available from previous reports (Figure 2-13). In Figure 2-13, the dashed

capillary-pressure curves are calculated from grain-size distribution data. From the moisture characteristic curves, van Genuchten parameters (α and m; see Appendix C for definitions and examples), which define the capillary pressure function, were calculated. In Figure 2-13, the calculated saturation and capillary pressure data fall within the range of the actually tested samples from the site. Table 7 summarizes the soil characteristic parameters calculated and used for various layers in the model.

Recently, Panacea conducted a series of more rigorous tests on soil samples collected during installation of the additional monitoring wells. The results of these tests are presented graphically in Figures 2-14, 2-15, and 2-16. The purpose of these latter tests was to compare the results of the calculated moisture retention curve from grain-size distribution with the results of direct laboratory measurements. These data only recently became available and the analyses of the calculation of moisture retention curves have not been completed yet. Table 8 presents the results for some of the recent samples that have been analyzed.

Figures 2-17 through 2-21 present grouping of the moisture retention curves according to the shape of the curves. Some of the soils identified in the geologic boring logs seem to have properties that are more appropriate for a coarser or finer group. Figure 2-17 shows the moisture retention curves for the silt group. There are some silty sands and clays included in this figure because of their similarity to typical silty soil. Figure 2-18 is for fine sand, and the grouping seems to be more consistent with relatively small variation in the shape of the curves. However, clay, silt, and other fine material identified in the field geologic boring logs appear in this group as well. Figure 2-19 shows a few fine sand to silty sand soils that have been used for the mixed layers of the model. Figure 2-20 shows a comparison of the group of soils from the site with some typical curves published in the literature. The mean value of this group has been used for the clays of the site model. In Figure 2-21 all of the available curves are compared with some of the published curves. From this figure, it is evident that all soils at the site have significant fine particle sizes, which is the reason for relatively high residual water content (approximately 40% for most of the soils). Also, the majority of the soils are relatively well graded, meaning the grain-size distribution varies gradually from one size to another as opposed to, for example, a clean sand, which has low residual water content and a relatively flat curve (compare with G.E. No. 2 sand of Table C-1 in Appendix C).

It is recognized that the sensitivity of the flow and transport in the unsaturated zone to the characteristic moisture retention properties and relative permeability is large. However, because of the abundance of the fine-grained material and their intercalation, it is believed that the properties of the fine-grained soils have much stronger influence on the migration of moisture and solutes in the unsaturated zone at the site.

2.6.5 PROPERTIES OF CHEMICALS OF CONCERN

Simulations presented here require a comprehensive definition of the parameters for each COC. These parameters relate thermo-physical properties of the COCs to the equation of state. For example, parameters are used to calculate vapor pressure, liquid viscosity, solubility, and density as a function of temperature and pressure. Experimental data on a full range of temperatures and pressures for these parameters are very scarce. Therefore, empirical equations are used to calculate the functions defining variability of these parameters with temperature and pressure. However, adequate data were available in literature for these parameters for a limited range of temperatures and pressures (most commonly, only one value was found). The database listing (Appendix B) provides the source of these data. In several instances, assumptions had to be made for some properties of the chemicals. References for the source of data are provided in the reference list and are not individually cited here in the text. It is believed that because of the state of the flow and transport at the site, these assumptions have minimal impact on the results.

3.0 NUMERICAL MODELING APPROACH

3.1 OVERVIEW OF THE APPROACH

Development of a numerical model requires adoption of a conceptual physical model. In the previous sections, the conceptual physical models were described briefly. In this section, the corresponding numerical models are described. A brief overview of the procedure and justifications is also provided here.

During development of the hydrogeologic conceptual model of the site, it was realized that the system is best represented by a three-dimensional, saturated-unsaturated (variably-saturated) numerical model. However, for expediency and to avoid complications expected in three-dimensional simulations, Panacea decided to set up a two-stage simulation procedure. In this setup, the unsaturated zone was simulated in a cross-sectional, two-dimensional mode to estimate the COC input into the B-zone. The results of these two-dimensional, cross-sectional simulations were then input as sources into another two-dimensional model in plan view, simulating saturated zone flow and transport in the B-zone. In this manner, multiple alternative simulations could be made within relatively short periods of computer run time.

The following subsections describe the justification of selecting the code and the description of the meshes used to subdivide the zones of interest for computer simulations.

3.2 IDENTIFICATION OF CODE FOR SIMULATIONS

Development of the conceptual numerical model of the site was based entirely on T2VOC numerical code (Falta et al., 1995). GMS also provides several tools for fate and transport analysis, which were evaluated and considered. These are UTCHEM and FEMWATER. Both codes in GMS were evaluated and were considered potentially appropriate for use with the site with some limitations. UTCHEM is relatively new to GMS and was expected to potentially cause unforeseen delays in the project. UTCHEM is developed and has been used for petroleum engineering applications. Therefore, although it appears that UTCHEM has all the capabilities offered by T2VOC, Panacea did not consider UTCHEM as well tested, and its application to solving environmental-related problems seemed limited compared to those of T2VOC code.

FEMWATER has been used more widely in the environmental industry but is limited to a single phase (either unsaturated or saturated). The air phase is considered stagnant in FEMWATER. Although this may not be a serious limitation, many of the COCs at the site are volatile and their partitioning into the air phase was considered potentially important for risk assessment purposes.

T2VOC is efficient computationally for both saturated and unsaturated zone simulations. T2VOC was developed with funding from the USEPA and the United States Department of Energy by Lawrence Berkeley National Laboratory. Quality control and assurance for development and testing of the code has been the most stringent in the industry. Multimedia Environmental Technology, Inc. (MET) received a letter of approval from the CRWQCB in 1994-1995 for use of the code for fate and transport analysis at the San Gabriel Valley Superfund site. The USEPA (Region IX) was consulted by the CRWQCB during this process (although USEPA does not necessarily approve or disapprove of the use of the code for any applications). For these reasons, T2VOC was selected as the preferred numerical code for the simulations presented in this report. MET has developed a preprocessor and a postprocessor for this code (SATURN GEIS©). SATURN uses a Microsoft® Access®-based database management system. The database management system was used for retaining and accessing the pertinent data available from the site as well as physical and chemical properties obtained from literature.

T2VOC has the following capabilities:

- Flow of water and air in subsurface geologic formations,
- Transport of COCs (including VOC and NAPL) in vadose and saturated zones,
- Atmospheric boundary conditions,
- Compressible fluids,
- Chemical gradients,
- Thermal gradients,
- Pressure gradients,
- Density gradients,
- Degradation and COC adsorption,
- Variable porosity and permeability, and
- Variable moisture content.

UTCHEM is a multi-phase flow and transport model. UTCHEM is ideally suited for the simulation of surfactant-enhanced aquifer remediation (SEAR), and DNAPL transport. UTCHEM is a mature model that has been widely used. The UTCHEM solver is efficient and robust. Future versions of the GMS/UTCHEM interface are expected to include the simulation of biodegradation (Boss, 2002). Lack of biodegradation simulation capability limits sensitivity analyses related to this potentially important parameter. It is not certain whether adequate capability for adsorption in various phases is offered by this code. T2VOC provides the capability to simulate first-order decay biodegradation. It also has the capability to simulate oxygen transport, which can be used to simulate the aerobic biodegradation process. This capability is complicated and adequate site-specific information is not available to justify using this feature of the T2VOC code. However, if remedial options include aerobic acceleration, this feature may be useful for predictions.

3.3 DEVELOPMENT OF MESHES

Computer numerical simulations require meshes to subdivide regions of interest into individual blocks for which material properties (such as hydraulic conductivity and porosity) can be assigned. Meshes can be one-, two-, or three-dimensional depending on the need for representation of the regions of special interest.

Two separate two-dimensional meshes were developed for the preliminary fate and transport simulations. Both meshes are rectangular with equal grid sizes as described in the following subsections (3.3.1). Figure 3-1 shows the mesh for the unsaturated zone and Figure 3-2 is the mesh for the saturated B-zone aquifer simulations. In this figure the line of cross section for Figure 3-1 is also shown. It should be noted that the northing coordinate of the unsaturated zone mesh (Figure 3-1) is projected because of the oblique orientation of the cross section. Following is a brief description of the two meshes.

3.3.1 CROSS-SECTIONAL UNSATURATED ZONE MESH

The northeast-southwest cross sections corresponding to Conceptual Models 1 and 2 were used to develop two conceptual unsaturated zone numerical models of the site. These models will be referred to as Conceptual Numerical Models 1 and 2. Discretization, initial conditions, and boundary conditions were set up identically for both models. The only difference between these conceptual numerical models was the material properties of the elements corresponding to the B-zone clay layer. The cross section was divided into a rectangular mesh consisting of seventy 31.724-foot (9.67 m) wide columns and thirty 10-foot (3.05 m) deep rows. The lateral (vertical) boundaries of the mesh were set to no-flow conditions. The bottom of the cross section coincides with the top of the regional confining clay layer (*Corcoran Aquitard*). This boundary was assigned constant head conditions to generate the water table profiles observed and assumed in the B-zone. It is assumed that there is no flow into the lower aquifer (C-zone); therefore, the height of the water table, observed in the boreholes and wells penetrating the B-zone, can be interpreted as the approximate piezometric potential along the boundary between the B-zone and the *Corcoran Aquitard*.

3.3.2 SATURATED ZONE PLAN-VIEW MESH

An area was selected that would be large enough to encompass all the pertinent monitoring wells at the site and include potential receptor points of concern. The main points of concern are the city well and the area immediately around the site. A mesh in the plan view was developed that is 1,200 feet (366 m) in the east-west direction and 2,100 feet (640 m) in the north-south direction (Figure 3-2). The mesh consists of 40 east-west and 70 north-south elements. All elements are 30-foot (9.14 m) squares. The size and spacing of the mesh was designed to correspond with those of the cross-sectional mesh used for the unsaturated zone. At this preliminary stage, the saturated zone is not directly connected to the unsaturated zone mesh. All elements are assigned the properties of sand for the preliminary simulations.

4.0 NUMERICAL MODELING RESULTS (BASE CASE)

In this section, results of the simulations are discussed. Also, comparisons of the results of various scenarios simulated are presented. First, the hydrogeologic simulation results will be discussed followed by the results of the COC transport. In each description, the unsaturated zone results will be described followed by the saturated (B-zone) results.

4.1 HYDROGEOLOGIC SYSTEM

4.1.1 UNSATURATED A- AND B-ZONES HYDROGEOLOGIC SYSTEM

The two-dimensional numerical model described in the previous section was used to simulate the northeast-southwest cross section. Numerous trial and error simulations were performed to develop a static hydraulic equilibrium for both cases of infiltration rates of 0.4 and 4 in/yr (10 and 100 mm/year). Calibration in this case was limited to visual comparison of the simulation results with the field data (mainly saturation distribution).

Although the piezometric surface in the B-zone may be constructed from the water-level elevations in the monitoring wells, the water level in two of the wells (CB01 and WB2-4, Figure 2-2) are not consistent with the general conception of the regional groundwater flow. Water-level elevation in WB2-4 is approximately 20 feet (6.1 m) below the extension of the piezometric surface constructed from other wells north of this well. Water level in CB01, which is a borehole, was measured only once during drilling, on July 15, 1991. This borehole was never completed. Therefore, water level in this borehole at

the time when the simulation is desired to start (1992) is questionable. It is possible that the water level in WB2-4 is lower in response to the pumping of the City of Arvin water supply well, which is approximately 300 feet (91.4 m) southwest of WB2-4. The city well is not screened in the B-zone aquifer and any significant hydraulic connection between the C-zone and B-zone aquifers is not expected. However, examination of the driller's log of the city well shows that the city well is completed by a sand pack from the bottom of the well to near ground surface. Therefore, it is possible that there is a short-circuit path between the two aquifers through the city well completion.

Because of this uncertainty, three cases of water table configuration in the B-zone were evaluated. First was a flat (horizontal water table). This flat water would correspond to interpolation of water levels in the wells, ignoring that of WB2-4. The second case was set up to correspond to the water-level elevations observed in both CB01 and WB2-4. The third case was set up by ignoring the water-level elevation of CB01 and assuming that water-level elevation in WB2-4 represents drawdown in response to pumping of the city well. This latter conceptualization was used for all COC transport simulations presented in this report because it appears to be the most conservative relative to COCs reaching the city well.

Based on precipitation history for Bakersfield, which is approximately 20 miles (32 km) northwest of the site (Figure 2-6), an infiltration rate of 0.4 in/yr (10 mm/yr) was assumed to enter the upper boundary at the top of the model. Although this amount of infiltration is large for the arid climate characteristic of this site, it may be a reasonable assumption considering the irrigation practices in this area (prior to installation of the RCRA cap). Also, because ponding of water has been practiced at the site, larger infiltration rates may have resulted. For this reason, a sub-alternative conceptual model was evaluated in which a 4-in/yr (100-mm/yr) infiltration rate was assumed to occur only at the site. Further studies may be required to fully justify these assumptions of infiltration rates.

Results of simulation of the flat water table are shown in Figure 4-1 with a uniform 0.4-in/yr (10-mm/yr) infiltration rate. Figure 4-1 also shows the distribution of water saturation in the Conceptual Model 1 cross section. As expected, the model predicts high water saturation values for finer-grained material. The results of saturation for the case corresponding to actual water-level measurement in the wells and boreholes are presented in Figure 4-2 with the same infiltration rate as in Figure 4-1. The results are substantially different because of the higher water table and a higher extension of the capillary fringe in the finer-grained material. Figure 4-3 presents the pressure heads for this case. The model predicts the perched groundwater that has been observed in the A-zone beneath the site (at depths between 50 and 70 feet [15.2 and 21.3 meters]). Figure 4-3 also provides some explanation for the observations that water levels in the A-zone vary abruptly in the area. It appears that this perching occurs only in the lower, discontinuous clay layer beneath the site. The interpreted water level of Figure 2-2 is reproduced in Figure 4-3 for comparison.

Figure 4-4 presents the saturation distribution and placement of the water table in the case where the B-zone water table is assumed to be influenced by the city well pumping.

In these cases, only the position of the water table in the B-zone was adjusted. Steady-state equilibrium conditions were established by running simulations for as long as 20 million years. These equilibrium conditions were used as initial hydraulic states to start COC transport simulations.

Figures 4-5 and 4-6 present similar results for Conceptual Model 2. Figure 4-5 shows the saturation distribution for the case with the observed water level. Figure 4-6 shows the pressure heads for the case where the water table is assumed to be affected by the city well. In this case, the bottom boundary condition was adjusted to match the observed water levels in the northern parts of the site. Because of this adjustment, the shallow perched water zone beneath the site does not appear (compare with

Figure 4-3). Therefore, there appears to be some inconsistency in assumption of an extensive clay layer in the B-zone, the piezometric level measured in B-zone, and the presence of perched water in A-zone. The reason for this inconsistency was not evaluated any further and is beyond the scope of this preliminary fate and transport model.

4.1.2 SATURATED ZONE FLOW IN THE B-ZONE

Figure 4-7 shows the result of a steady-state simulation that corresponds to the case where the city well is assumed to be influencing the B-zone aquifer piezometric level. The city well in this case (CW-1) is assumed to be a sink with a constant head assigned equivalent to the interpretation presented previously. The northeastern corner of this model was also kept at constant head. All of the boundaries are assumed no-flow boundary conditions. All saturated-zone COC transport simulations used this configuration.

4.2 CONSERVATIVE SIMULATION OF THE TRANSPORT OF COCs

Available data from the site samples and literature indicate that both sorption and biodegradation processes may be influencing the mechanism of transport in both the saturated and the unsaturated zones at the site. However, for these preliminary simulations, these parameters were ignored to evaluate the conservative (no adsorption and no biodegradation) transport of the COCs. Non-conservative simulations are underway to evaluate the significance of these processes on the fate and transport of the COCs. Realistic (non-conservative) simulations are expected to increase the confidence in assessment of the risk.

To establish the initial conditions for the A-zone perched groundwater, concentration distributions for all seven COCs from April 1991 were interpolated. Similarly, concentrations of the COCs in April 1992 for the B-Zone groundwater were interpolated. Inverse distance method was used for interpolation of these data. Comparison of the A-zone results (Figures 4-8 through 4-11) with the B-zone results (Figures 4-12 through 4-18) shows the substantial difference between the concentrations in the two aquifers. Concentrations in the A-zone perched aquifer are several orders of magnitude larger than those in the B-Zone aquifer.

1,2-DCP was selected for initial evaluation of the transport simulationsbecause this COC is more widespread than any other COC at this site. The presence of this COC at detectable levels in most of the monitoring zones both in the A- and B-zone aquifers provides larger number of control points when the results of simulations are compared with the observed data.

Variation of measured concentrations of 1,2-DCP over time is presented in Figures 4-19 through 4-23. From these figures it appears that the concentration of this COC has substantially declined after emplacement of the RCRA cap in 1992. Reappearance of the plume in May 1997 (Figure 4-21) may be attributed to the unusually wet year (see Figure 2-6). Examination of Figure 2-6 also reveals that a wetter climate existed in 1992 and 1995. In 1995, the plume appears in March but at a reduced level of concentration. Therefore, although the cap has been effective in reducing infiltration, there seems to be some correlation between the climate change and the appearance of the plume in the B-zone aquifer.

It is also of interest to note that the plume that appeared in May 1997 seemed to have moved south to the area of WB2-1 in July 1998, which was during a dry year and dry season (as shown in Figure 2-6, July has consistently been a dry month). Although these variations could possibly be due to changes in sampling procedure and analytical methods, the coincidental recurrence and migration of the plume is of particular interest when compared with the results of simulations.

One of the problems encountered in the interpretation of A-zone concentrations was the inconsistency between the results of the soil sample and groundwater analyses. The source of this inconsistency is currently under investigation by Panacea and will be reported in future reports. The source of this inconsistency is suspected to be the units of measurement reported for the soil samples analyzed in 1991 by MK. Future simulations will use a combination of soil and water concentrations to establish initial conditions for the A-zone if this issue is resolved.

The initial COC conditions used for the unsaturated zone simulation were generated by extracting the concentration values along a line drawn on the interpolated maps of the A-zone COC distribution (Figures 4-8 through 4-11 and Figure 3-2). The interpolation grid was selected to be the same as the plan view mesh of Figure 3-2 for both the A-zone and B-zone aquifers.

The following subsections describe the results of the simulation of the COCs for the conservative base case. The unsaturated zone results are presented first. In the unsaturated zone simulations, Conceptual Model 1 was used with the alternative infiltration scenario. In the alternative infiltration scenario, 4 in/yr (100 mm/yr) was applied over the site and 0.4 in/yr (10 mm/yr) over all other elements at the ground surface.

An experimental verification was used to compare the results of using the two infiltration scenarios. The COC 1,2-DCP was selected for this exercise because of its more pervasive distribution in both aquifers. Figure 4-24 shows the result of a simulation with the uniform 0.4-in/yr (10-mm/yr) infiltration rate after 100 years for Conceptual Model 1. In this case, concentration in the B-zone (approximately 180 feet [54.9 m] depth) remains below 100 µg/l. Figure 4-25 shows the result of the alternative infiltration scenario for Conceptual Model 1. In this simulation, the flat water table was used (see Figure 4-1). This case results in concentrations exceeding 20,000 µg/l in the B-zone. Figure 4-24 underestimates the observed concentrations considering that the results of the simulation are after 100 years. Figure 4-25 results overestimate COC concentrations. Figure 4-26 compares the results of Figure 4-24 with the soil data obtained in 1991. The concentration values are not strictly comparable. The soil concentrations are reported as mass of COC per bulk mass of soil and should be converted to aqueous-phase concentration in the pore water. Distribution coefficient and Henry's law constant are needed for this conversion. Although these values have been estimated for all COCs, their use in converting the soil concentrations to pore-water concentrations have not yet been verified. However, the comparison points to the location of the sources of the COC in the soil relative to the simulated groundwater concentration in the A-zone aquifer. It appears that there is very little lateral diversion of the migration path of the COC except along the mixed layer near the top of the B-zone aquifer (depth of approximately 150 to 200 feet [45.7 to 61 meters] bgs).

The results of simulation for all COCs using the most conservative assumptions are presented in the following. The conservative assumptions used are as follows:

- No degradation
- No adsorption
- Largest value of vertical hydraulic conductivity for clay layers in the A-zone
- Large infiltration rate (4 in/yr [100 mm/yr]) at the site throughout the 100-year simulations
- Largest gradient in the B-zone aquifer (this may not be entirely conservative because of the contribution to the dilution factor)

- Largest hydraulic conductivity in the B-zone (this may not be entirely conservative because of the contribution to the dilution factor)

The conservativeness of the assumptions in the B-zone aquifer is subject to debate. The last two assumptions listed above result in faster migration of the COCs from the source to the city well in the B-zone. However, because of the dilution factor, the concentrations are reduced substantially. On the other hand, if lower hydraulic conductivity and smaller gradients were assumed for the B-zone aquifer simulations, larger concentrations would appear beneath the source but much more time would be required for the plume to reach the city well. The significance of the difference will need to be addressed during risk assessment.

The unsaturated zone results are presented here first followed by the saturated zone results.

4.2.1 CROSS-SECTIONAL UNSATURATED ZONE NUMERICAL MODEL

April 1992 is the start time for all simulations, which continue for 100 years. Explanation for Figures 4-27 through 4-40 shows the corresponding dates for the simulations.

4.2.1.1 Results of Simulation of 1,2-DCP

The results of simulation of 1,2-DCP transport are presented in Figure 4-27. The initial concentration of this COC was extracted from the interpolation results shown in Figure 4-8. The interpolation extends the COC presence farther to the north and south than have been observed. However, the concentrations outside the site boundary are relatively small. Figure 4-27 shows that simulated migration of the COC plume beneath the site reaches the B-zone aquifer after approximately 20 years at concentrations exceeding 100 µg/l. From this time forward, the migration of the plume in the unsaturated zone is not relevant for the purposes of this report because lateral flow in the B-zone aquifer is ignored in the unsaturated zone cross-sectional simulations.

4.2.1.2 Results of Simulation of 1,3-DCP

The results of simulation of 1,3-DCP transport are presented in Figure 4-28. The initial concentration of this COC was extracted from the interpolation results shown in Figure 4-8. The pattern of migration is similar to that of 1,2-DCP, but the concentrations are orders of magnitude smaller.

4.2.1.3 Results of Simulation of 1,2,3-TCP

The results of simulation of 1,2,3-TCP transport are presented in Figure 4-29. The initial concentration of this COC was extracted from the interpolation results shown in Figure 4-9. The distribution of 1,2,3-TCP is more isolated than that for 1,2-DCP, but the concentrations are within the same order of magnitude. Vertical migration of this COC is more predominant.

4.2.1.4 Results of Simulation of Chloroform

The results of simulation of chloroform transport are presented in Figure 4-30. The initial concentration of this COC was extracted from the interpolation results shown in Figure 4-9. The pattern of migration is similar to that of 1,2,3-TCP, but the concentrations are an order of magnitude smaller.

4.2.1.5 Results of Simulation of DBCP

The results of simulation of DBCP transport are presented in Figure 4-31. The initial concentration of this COC was extracted from the interpolation results shown in Figure 4-10. The pattern of migration is similar to that of 1,2-DCP, and the concentrations are similar.

4.2.1.6 Results of Simulation of Dinoseb

The results of simulation of dinoseb transport are presented in Figure 4-32. The initial concentration of this COC was extracted from the interpolation results shown in Figure 4-10. The pattern of migration is similar to that of 1,2-DCP, and the concentrations are similar. However, because the center of the plume falls beneath the site where a higher infiltration rate is applied, vertical migration of the plume to the B-zone is more pronounced.

4.2.1.7 Results of Simulation of EDB

The results of simulation of EDB transport are presented in Figure 4-33. The initial concentration of this COC was extracted from the interpolation results shown in Figure 4-11. The pattern of migration is different from all other COCs. It appears that very little reaches the B-zone.

4.2.2 SATURATED ZONE FLOW IN THE B-ZONE HYDROGEOLOGIC SYSTEM

As noted in Section 4.2.1, lateral migration of the plume in the B-zone aquifer is ignored in the unsaturated zone (cross-sectional) simulations. The mass of the COCs that vertically entered the B-zone in the cross-sectional simulations was used as a source in the saturated zone transport simulations. In addition, the April 1992 concentrations were used as the initial conditions in the B-zone plan view simulations. The simulated concentrations in the plan view are much smaller than those shown for the unsaturated zone at the same elevation. This is because of the dilution factor that occurs as the COCs enter the saturated zone. In other words, the flux of water that carries the COCs in the unsaturated zone is several orders of magnitude smaller than the flux of water that flows horizontally in the plan view simulations.

4.2.2.1 Results of Simulation of 1,2-DCP

The results of simulation of 1,2-DCP transport in the B-zone are presented in Figure 4-34. The initial concentration of this COC was extracted from the interpolation results shown in Figure 4-12. Figure 4-34a shows that the plume migrates into the city well area very rapidly but at substantially reduced concentrations. The plume from the unsaturated zone does not break through the B-zone until 20 years after the start of the simulations. This is not consistent with the observations of relatively high concentrations in the B-zone in 1992. The reason for this inconsistency is the fact that migration in the unsaturated zone had started long before April 1991 (which was used as the initial condition for the unsaturated zone simulations). However, this observation is consistent with the site history, which states that the site was in operation since 1960. Data from 1960 are not available to set up initial conditions. Therefore, for all the saturated zone transport simulations, it is more prudent to use the simulations after 20 years as equivalent to the 1992 time frame. Calibration will be required to estimate the initial concentration of the COCs in the unsaturated zone in 1960. However, such calibration exercises are very time consuming and were not within the scope of these preliminary fate and transport simulations.

4.2.2.2 Results of Simulation of 1,3-DCP

The results of simulation of 1,3-DCP transport are presented in Figure 4-35. The initial concentration of this COC was extracted from the interpolation results shown in Figure 4-13. This COC was not detectable in the B-zone in April 1992 (Figure 4-13). The unsaturated zone contribution appears at small concentrations approximately 60 years after the start of the simulation (Figure 4-35b).

4.2.2.3 Results of Simulation of 1,2,3-TCP

The results of simulation of 1,2,3-TCP transport are presented in Figure 4-36. The initial concentration of this COC was extracted from the interpolation results shown in Figure 4-14. The distribution of

1,2,3-TCP in the B-zone simulations is very similar to that for 1,2-DCP, but the unsaturated zone contribution reaches the B-zone after approximately 9.6 years and continues throughout the entire 100 years.

4.2.2.4 Results of Simulation of Chloroform

The results of simulation of chloroform transport are presented in Figure 4-37. The initial concentration of this COC was extracted from the interpolation results shown in Figure 4-15. The pre-existing chloroform plume persists for 20 years at very small concentrations in the B-zone. In figure 4-37a, migration of the chloroform plume at a very low concentration toward the area of the city well is shown. At approximately 20 years into the simulations, the unsaturated zone contribution appears (Figure 4-37b).

4.2.2.5 Results of Simulation of DBCP

The results of simulation of DBCP transport are presented in Figure 4-38. The initial concentration of this COC was extracted from the interpolation results shown in Figure 4-16. There was no DBCP detected in the B-zone aquifer in April 1992. The unsaturated zone contribution is simulated to start after approximately 40 years at very low concentrations. A slight increase in concentration occurs but the plume continues to persist throughout the 100 years of simulation time.

4.2.2.6 Results of Simulation of Dinoseb

The results of simulation of dinoseb transport are presented in Figure 4-39. The initial concentration of this COC was extracted from the interpolation results shown in Figure 4-17. Dinoseb initial concentrations in the B-zone aquifer were not detectable in 1992. Therefore, Figure 4-39 only shows the contribution from the unsaturated zone, which starts at low concentrations after 9.6 years. The concentration gradually increases and persists throughout the entire 100 years of simulation times.

4.2.2.7 Results of Simulation of EDB

The results of simulation of EDB transport are presented in Figure 4-40. The initial concentration of this COC was extracted from the interpolation results shown in Figure 4-18. Initial concentration of EDB in the B-zone aquifer was below detection limits in April 1992. The unsaturated zone contribution shows after approximately 40 years at very small concentrations in the B-zone. The plume also persists and gradually increases in concentration for 100 years.

5.0 SENSITIVITY ANALYSES

Although a full range of parameters affecting both flow and transport processes should be considered for sensitivity analyses, the following only presents some of the more pertinent parameters that have been evaluated for flow in both the saturated and unsaturated zones. Transport parameters such as biodegradation, retardation, and effective porosity will be addressed in the future.

5.1 HYDRAULIC PARAMETERS

5.1.1 PARAMETERS AFFECTING FLOW IN THE UNSATURATED ZONE

The parameters that were evaluated include infiltration rate, hydraulic conductivity of the unsaturated zone material, and moisture characteristic curves.

5.1.1.1 Infiltration Rate

Two infiltration rates were attempted during the simulations. First, a uniform infiltration rate of 0.4 in/yr (10 mm/yr) was applied at the upper boundary of the model. Alternatively, the boundary elements over the site were subjected to a 4-in/yr (100-mm/yr) infiltration rate. The results show that there is a substantial difference in the arrival time of the COCs in the B-zone saturated zone. The difference is on the order of several tens of years. Only 1,2-DCP was used for this sensitivity analysis. However, the results of simulation of all other COCs corroborate this observation. Comparison of the off-site areas of the model with the area beneath the site in Figures 4-27 through 4-33 shows the significant difference in the migration of the COCs. In areas with 0.4-in/yr (10-mm/yr) infiltration (off-site), COCs migrate less than 25 feet (7.6 m) in 100 years, whereas beneath the site (with 4 in/yr [0.1 meters] infiltration), the COCs migrate a few hundred feet (tens of meters).

5.1.1.2 Saturated Hydraulic Conductivity of Selected Layers

T2VOC, as any other variably saturated zone simulator, is very sensitive to the unsaturated hydraulic properties (moisture retention and relative permeability curves) of the soils. Also, the saturated hydraulic conductivity of the soils is very important. One of the difficulties with simulating a heterogeneous system as conceptualized for the site is the convergence of the numerical solution. When large changes in hydraulic conductivity are assigned across adjacent simulated layers, the simulation converges very slowly, which results in long computer run times. For this reason, performing sensitivity to this parameter was limited to changing the saturated hydraulic conductivity of the clay layers in the A-zone by two orders of magnitude (from $1x10^{-15}$ to $1x10^{-17}$ cm/sec). The results of the sensitivity to the changes in hydraulic conductivity were similar to those for changing infiltration rates. This is expected, as both control the vertical flow rates. Reducing the saturated hydraulic conductivity by an order of magnitude resulted in the same results as reducing the infiltration rate by an order of magnitude (from 4 in/yr to 0.4 in/yr [100 mm/yr to 10 mm/yr]). Appendix D presents a table of simulations for various cases of hydraulic parameters.

5.1.2 PARAMETERS AFFECTING FLOW IN THE SATURATED ZONE

Although it is recognized that the results of the flow and transport simulations are strongly dependent on the properties and extent of the clay layer and the steepness of the hydraulic gradient, sensitivity analyses with respect to these parameters were not completed for this preliminary fate and transport report. Future modeling in support of the risk assessment is planned to address these issues.

5.1.3 TRANSPORT PARAMETERS

The following are the transport parameters that are expected to have the most significant influence on the results of the simulation of the transport processes of the COCs (quantitative evaluation of these effects is underway in support of the risk assessment and is not presented in this report):

- Vapor diffusion
- Initial conditions

  - Unsaturated zone

  - Saturated zone
- Boundary conditions

- Unsaturated zone

- Saturated zone

- Distribution coefficient (K_d)
- Biodegradation
- Effective porosity

Values of these parameters are provided in the database tables. Methods for calculation of the initial condition in the unsaturated zone are briefly described in Appendix E. Calculations of the distribution coefficient from laboratory batch tests are shown in Appendix F. However, for the simulations presented in this report, values from the literature presented in the database tables were used.

6.0 SUMMARY AND TENTATIVE CONCLUSIONS

In preparation of this preliminary fate and transport report, two basic conceptual hydrogeologic models were developed based on the available data and the extrapolation and interpretation of the geologic information. Using these hydrogeologic models, conceptual numerical models of the unsaturated and saturated zones were developed. Flow processes were evaluated for the two conceptual models using various simulation scenarios, which included varying infiltration rates and hydraulic properties of selected hydrogeologic units. The unsaturated-zone model was set up separately from the saturated-zone model. Both models were two-dimensional.

Concentration distributions for seven COCs were interpolated using various interpolation schemes. The results of the interpolations for saturated zones of both A- and B-zone aquifers were used as initial conditions to perform conservative simulations of the transport of the COCs in both zones. Using equilibrium hydraulic conditions for both unsaturated and saturated zones, 100-year simulations were performed.

Results of the preliminary conservative analyses indicate that the COC plumes in the unsaturated zone require between 20 and 40 years to arrive in the B-zone aquifer. Transport in the B-zone aquifer is relatively fast and, without a source, any existing plume would disappear in less than 10 years. However, the slowly moving unsaturated zone COCs' contribution to the B-zone aquifer will continue to persist beyond 100 years, but at very low concentrations. For these preliminary analyses, none of the COCs appears to approach the MCL concentrations near the city well.

Based on evaluation of the data and results of the simulations, it is believed that the process and mechanism of flow and transport are fairly well understood. Synchronization of the flow and transport between the unsaturated zone and the saturated zone would reduce the uncertainty of these conclusions. In general, the flow throughout the unsaturated zone appears to be mostly vertically downward. The layering of the hydrogeologic units does not seem to induce significant lateral migration of the COCs.

The preliminary fate and transport modeling results suggest that the COCs in the unsaturated zone persist longer than in the saturated zone. The conservative scenario modeling results show that transport of the COCs occurs primarily in the vertical direction in the unsaturated zone. This is despite the heterogeneous layering of the hydrogeologic units. Very little lateral flow and transport occurs in the unsaturated zone. In the saturated zone, flow and transport are mainly southwesterly toward the city well. This direction of flow and transport is partly due to the assumptions made based on the available information. These

results also show that the COCs in the saturated zone will persist for a maximum of 10 years in the absence of vertical leakage from unsaturated zone. However, leakage from the unsaturated zone persists for more than 100 years. Concentrations of the chemicals reaching the city well are estimated to be below their MCL with or without contribution from the unsaturated zone. This conclusion is reached by several assumptions that should be validated by future investigations. The limited scope of this fate and transport modeling did not allow considering the impact of the presence of the by-product of degradation of the COCs in these simulations and need to be addressed in future analyses.

7.0 RECOMMENDATION

The sensitivity of the results to the hydraulic gradient in the B-zone emphasizes the need for a better understanding of hydraulic conditions near the city well. Water level in the B-zone and in the city well should be verified accurately. The water level in the B-zone near the city well should be measured in newly installed monitoring wells. In fact, concentrations of COCs near the city well in the B-zone should be monitored at three or more points.

Monitoring water levels near the city well may be used to evaluate the connectivity between the city well and the B-zone aquifer. This would require monitoring flow rates and water-level fluctuations in the city well simultaneously. It is recommended that the water levels in these wells be monitored for a period of a few months. It is desirable to monitor the water levels in these wells during a non-pumping period of about a month before the seasonal active pumping of the city well starts. About a month of monitoring during active pumping of the city well would provide a good basis to assess the impact of pumping of the city well on the water levels in the B-zone aquifer. The water levels should be monitored on an hourly interval for these periods using automated water-level monitoring systems in the observation wells. The flow rates in the city well should be recorded at least several times per day during the monitoring periods.

Once these data become available, the saturated zone model presented in this report may be calibrated to obtain hydraulic parameters in the vicinity of the city well.

8.0 REFERENCES

Boss International, Inc. 2002, *Groundwater Modeling System (GMS),* Version 3.1, 6300 University Avenue, Madison, WI, http://www.bossintl.com/html/gms_details.html.

Desert Research Institute, Western Regional Climate Center, *Western U.S. Climate Historical Summaries,* NOAA Coop. Stations & USDA-NRCS SNOTEL Stations, www.wrcc.dri.edu/summary.

Falta, Ronald W., Karsten Pruess, Stefan Finstrele, and Alfredo Battistelli, 1995, *T2VOC User's Guide*, Lawrence Berkeley Laboratory, Berkeley, California, LBL-36400, 76 p.

Hillel, Daniel, 1980, *Fundamentals of Soil Physics*, Academic Press, New York, NY, 413 p.

Howard, Philip H., Robert S. Bothling, William F. Jarvis, William M. Meylan, and Edward M. Michalenko, 1991, *Environmental Degradation Rates* Lewis Publishers, Chelsea, Michigan, 725 p.

Lide, David R., Ed., 1993, *CRC Handbook of Chemistry and Physics*, 73rd Ed., CRC Press, Ann Arbor, Michigan.

Lyman, Warren J., William F. Reehl, and David H. Rosenblatt, 1982, *Handbook of Chemical Property Estimation Method,* American Chemical Society, Washington, DC.

MK (see Morrison Knudson).

Montgomery, John, H., and Linda M. Welcom, 1989, *Groundwater Chemicals Desk Reference*, Lewis Publisher, Chelsea, Michigan, 640 p.

Morrison Knudson (MK), 1999a, *Groundwater Monitoring Well Completion Report, Brown and Bryant Superfund Site, U.S. Army Corps of Engineers*, dated June 1999.

_____, 1999b, *Aquifer Test Report, Brown and Bryant Superfund Site, U.S. Army Corps of Engineers*, dated August 1999.

National Oceanic & Atmospheric Administration (NOAA), National Climatic Data Center, *National Climatic Data Center Internet Site,* www.ncdc.noaa.gov/pub/data/coop-precip/Nevada.txt.

Panacea, Inc., 2002, *Monitoring Well Installation Report,· Draft, Operable Unit No. 2, Brown & Bryant Superfund Site, Arvin, California*, prepared for U.S. Army Corps of Engineers, Los Angeles District, Los Angeles, California, dated October 2002.

Parker, J.C., J. Lenhard, and T. Kuppusamy, 1987, *A parametric model for constitutive properties governing multiphase flow in porous media,* Water Resources Res., 23, 618-624.

Reid, Robert C., John M. Prausnitz, and Bruce E. Poling, 1987, *The Properties of Gases And Liquids*, Fourth Ed., McGraw-Hill, Inc., San Francisco, California, 741 p.

The Pesticide Management Education Program at Cornell University, 2002, *Dinoseb, Extension Toxicology Network,* http://pmep.cce.cornell.edu/profiles/extoxnet/dienochlor-glyphosate/dinoseb-ext.html.

United States Geological Survey, NWISWeb Data for the Nation, *Daily Mean Discharge data from the National Water Information System Files (ADAPS),* Internet download http:\\waterdata.usgs.gov.

United States Geological Survey, NWISWeb Data for the Nation, *Peak Flow Data from National Water Data Storage and Retrieval System (WATSTORE)*, Internet download http:\\waterdata.usgs.gov.

U.S. National Library of Medicine, 2002, *TOXNET*, 8600 Rockville Pike, Bethesda, MD, http://toxnet.nlm.nih.gov.

Vaerschueren, Karel , 1983, *Handbook of Environmental Data on Organic Chemicals*, Second Ed., Van Nostrand Reinhold, New York, New York, 1310 p.

Van Genuchten, M. Th., 1980, *A closed-form equation for predicting the hydraulic conductivity of unsaturated soils*. Soil Sci. Soc. Am. J. 44:892898.

Van Genuchten, M. Th., and D. R. Nielsen. 1985, *On describing and predicting the hydraulic properties of unsaturated soils*. Ann. Geophys. 3:615628.

Tables

Project No. C02-266 June 2004

TABLE 1

SUMMARY OF THE PROPERTIES OF THE MATERIAL USED FOR HYDROGEOLOGIC CONCEPTUAL MODELS

	IRP	RP(1)	RP(2)	RP(3)	RP(4)	RP(5)	RP(6)	RP(7)	Curve Type	ICP	CP(1)	CP(2)	CP(3)	CP(4)	CP(5)
Atmos	1.00E+01	0.00E+00	0.00E+00	0.00E+00	0.00E+00	0.00E+00	0.00E+00	Power Function	1	0.00E+00	9.00E-01	9.50E-01	1.00E+00	1.00E+00	0.00E+00
ClyA1	2.20E-01	6.00E-01	1.00E+00	0.00E+00	0.00E+00	0.00E+00	0.00E+00	van Genuchten Function	7	2.20E-01	1.00E-01	7.58E-04	1.00E+06	1.00E+00	0.00E+00
MxdA2	1.22E-01	4.50E-01	1.00E+00	0.00E+00	0.00E+00	0.00E+00	0.00E+00	van Genuchten Function	7	1.22E-01	1.00E-01	2.07E-04	1.00E+06	1.00E+00	0.00E+00
SltA2	1.22E-01	4.50E-01	1.00E+00	0.00E+00	0.00E+00	0.00E+00	0.00E+00	van Genuchten Function	7	1.22E-01	1.00E-01	2.07E-04	1.00E+06	1.00E+00	0.00E+00
ClyA2	2.20E-01	6.00E-01	1.00E+00	0.00E+00	0.00E+00	0.00E+00	0.00E+00	van Genuchten Function	7	2.20E-01	1.00E-01	7.58E-04	1.00E+06	1.00E+00	0.00E+00
SndA1	4.85E-01	3.00E-01	1.00E+00	0.00E+00	0.00E+00	0.00E+00	0.00E+00	van Genuchten Function	7	4.85E-01	1.00E-01	2.07E-04	1.00E+06	1.00E+00	0.00E+00
MxdA1	1.22E-01	4.50E-01	1.00E+00	0.00E+00	0.00E+00	0.00E+00	0.00E+00	van Genuchten Function	7	1.22E-01	1.00E-01	2.07E-04	1.00E+06	1.00E+00	0.00E+00
SndA2	4.85E-01	3.00E-01	1.00E+00	0.00E+00	0.00E+00	0.00E+00	0.00E+00	van Genuchten Function	7	4.85E-01	1.00E-01	2.07E-04	1.00E+06	1.00E+00	0.00E+00
SndB1	4.85E-01	3.00E-01	1.00E+00	0.00E+00	0.00E+00	0.00E+00	0.00E+00	van Genuchten Function	7	4.85E-01	1.00E-01	2.07E-04	1.00E+06	1.00E+00	0.00E+00
SndB2	4.85E-01	3.00E-01	1.00E+00	0.00E+00	0.00E+00	0.00E+00	0.00E+00	van Genuchten Function	7	4.85E-01	1.00E-01	2.07E-04	1.00E+06	1.00E+00	0.00E+00
SndB3	4.85E-01	3.00E-01	1.00E+00	0.00E+00	0.00E+00	0.00E+00	0.00E+00	van Genuchten Function	7	4.85E-01	1.00E-01	2.07E-04	1.00E+06	1.00E+00	0.00E+00
MxdB1	1.22E-01	4.50E-01	1.00E+00	0.00E+00	0.00E+00	0.00E+00	0.00E+00	van Genuchten Function	7	1.22E-01	1.00E-01	2.07E-04	1.00E+06	1.00E+00	0.00E+00
ClyB1	2.20E-01	6.00E-01	1.00E+00	0.00E+00	0.00E+00	0.00E+00	0.00E+00	van Genuchten Function	7	2.20E-01	1.00E-01	7.58E-04	1.00E+06	1.00E+00	0.00E+00
SndB2	4.85E-01	3.00E-01	1.00E+00	0.00E+00	0.00E+00	0.00E+00	0.00E+00	van Genuchten Function	7	4.85E-01	1.00E-01	2.07E-04	1.00E+06	1.00E+00	0.00E+00
SltB2	1.22E-01	4.50E-01	1.00E+00	0.00E+00	0.00E+00	0.00E+00	0.00E+00	van Genuchten Function	7	1.22E-01	1.00E-01	2.07E-04	1.00E+06	1.00E+00	0.00E+00
MxdB2	1.22E-01	4.50E-01	1.00E+00	0.00E+00	0.00E+00	0.00E+00	0.00E+00	van Genuchten Function	7	1.22E-01	1.00E-01	2.07E-04	1.00E+06	1.00E+00	0.00E+00
SndB3	4.85E-01	3.00E-01	1.00E+00	0.00E+00	0.00E+00	0.00E+00	0.00E+00	van Genuchten Function	7	4.85E-01	1.00E-01	2.07E-04	1.00E+06	1.00E+00	0.00E+00
MxdB3	1.22E-01	4.50E-01	1.00E+00	0.00E+00	0.00E+00	0.00E+00	0.00E+00	van Genuchten Function	7	1.22E-01	1.00E-01	2.07E-04	1.00E+06	1.00E+00	0.00E+00
AqfC1	4.85E-01	3.00E-01	1.00E+00	0.00E+00	0.00E+00	0.00E+00	0.00E+00	van Genuchten Function	7	4.85E-01	1.00E-01	2.07E-04	1.00E+06	1.00E+00	0.00E+00
ClyC1	2.20E-01	6.00E-01	1.00E+00	0.00E+00	0.00E+00	0.00E+00	0.00E+00	van Genuchten Function	7	2.20E-01	1.00E-01	7.58E-04	1.00E+06	1.00E+00	0.00E+00

TABLE 1 (continued)

SUMMARY OF THE PROPERTIES OF THE MATERIAL USED FOR HYDROGEOLOGIC CONCEPTUAL MODELS

Material	Density	Porosity	Perm. 1	Perm. 2	Perm. 3	Sat. Heat K	Sp. Heat	Compress.	Expans.	Dry Heat K	Tortuosity	Klinken. b	FOC
Atmos	1.00E+00	9.90E-01	5.00E-05	5.00E-05	5.00E-05	2.10E-02	1.01E+03	1.00E-05	0.00E+00	2.10E-02	0.00E+00	0.00E+00	0.00E+00
ClyA1	2.55E+03	4.00E-01	2.42E-15	2.42E-15	2.42E-15	2.00E+00	8.23E+02	0.00E+00	0.00E+00	1.60E+00	0.00E+00	0.00E+00	0.00E+00
MxdA2	2.55E+03	3.50E-01	1.10E-13	1.10E-13	1.10E-13	2.00E+00	8.23E+02	0.00E+00	0.00E+00	1.60E+00	0.00E+00	0.00E+00	0.00E+00
SltA2	2.51E+03	3.50E-01	1.10E-13	1.10E-13	1.10E-13	1.81E+00	8.51E+02	0.00E+00	0.00E+00	1.24E+00	0.00E+00	0.00E+00	0.00E+00
ClyA2	2.55E+03	4.00E-01	2.42E-15	2.42E-15	2.42E-15	2.00E+00	8.23E+02	0.00E+00	0.00E+00	1.60E+00	0.00E+00	0.00E+00	0.00E+00
SndA1	2.38E+03	3.00E-01	1.10E-11	1.10E-11	1.10E-11	1.07E+00	1.04E+03	0.00E+00	0.00E+00	5.00E-01	0.00E+00	0.00E+00	0.00E+00
MxdA1	2.38E+03	3.50E-01	1.10E-13	1.10E-13	1.10E-13	1.07E+00	1.04E+03	0.00E+00	0.00E+00	5.00E-01	0.00E+00	0.00E+00	0.00E+00
SndA2	2.34E+03	3.00E-01	1.10E-11	1.10E-11	1.10E-11	5.00E-01	1.08E+03	0.00E+00	0.00E+00	3.50E-01	0.00E+00	0.00E+00	0.00E+00
SndB1	2.34E+03	3.00E-01	1.10E-11	1.10E-11	1.10E-11	5.00E-01	1.08E+03	0.00E+00	0.00E+00	3.50E-01	0.00E+00	0.00E+00	0.00E+00
SndB2	2.40E+03	3.00E-01	1.10E-11	1.10E-11	1.10E-11	9.70E-01	8.49E+02	0.00E+00	0.00E+00	4.40E-01	0.00E+00	0.00E+00	0.00E+00
SndB3	2.40E+03	3.00E-01	1.10E-11	1.10E-11	1.10E-11	9.70E-01	8.49E+02	0.00E+00	0.00E+00	4.40E-01	0.00E+00	0.00E+00	0.00E+00
MxdB1	2.37E+03	3.50E-01	1.10E-13	1.10E-13	1.10E-13	1.02E+00	1.02E+03	0.00E+00	0.00E+00	4.60E-01	0.00E+00	0.00E+00	0.00E+00
ClyB1	2.55E+03	4.00E-01	2.42E-15	2.42E-15	2.42E-15	2.00E+00	8.23E+02	0.00E+00	0.00E+00	1.60E+00	0.00E+00	0.00E+00	0.00E+00
SndB2	2.37E+03	3.00E-01	1.10E-11	1.10E-11	1.10E-11	1.02E+00	1.02E+03	0.00E+00	0.00E+00	4.60E-01	0.00E+00	0.00E+00	0.00E+00
SltB2	2.26E+03	3.50E-01	1.10E-11	1.10E-11	1.10E-11	8.20E-01	1.33E+03	0.00E+00	0.00E+00	3.50E-01	0.00E+00	0.00E+00	0.00E+00
MxdB2	2.26E+03	3.50E-01	1.10E-13	1.10E-13	1.10E-13	8.20E-01	1.33E+03	0.00E+00	0.00E+00	3.50E-01	0.00E+00	0.00E+00	0.00E+00
SndB3	2.37E+03	3.00E-01	1.10E-11	1.10E-11	1.10E-11	6.70E-01	1.22E+03	0.00E+00	0.00E+00	2.30E-01	0.00E+00	0.00E+00	0.00E+00
MxdB3	2.37E+03	3.50E-01	1.10E-13	1.10E-13	1.10E-13	6.70E-01	1.22E+03	0.00E+00	0.00E+00	2.30E-01	0.00E+00	0.00E+00	0.00E+00
AqfC1	2.51E+03	3.00E-01	1.10E-11	1.10E-11	1.10E-11	1.00E+00	8.34E+02	0.00E+00	0.00E+00	3.70E-01	0.00E+00	0.00E+00	0.00E+00
ClyC1	2.55E+03	4.00E-01	2.42E-15	2.42E-15	2.42E-15	2.00E+00	8.23E+02	0.00E+00	0.00E+00	1.60E+00	0.00E+00	0.00E+00	0.00E+00

TABLE 2

HYDRAULIC CONDUCTIVITY OF SILT AND CLAY MATERIAL MEASURED IN SAMPLES OBTAINED FROM RECENTLY DRILLED BOREHOLES AT THE SITE

Well	Depth	Hydraulic Conductivity
	ft	cm/sec
PWA-2	45	2.39E-08
PWA-2	65	5.47E-06
PWA-4	65	1.68E-05
PWA-4	80	5.05E-07
PWB-1	70	3.53E-05
PWB-3	70	1.03E-06
PWB-3	85	1.05E-06
PWB-3	150	6.15E-07
PWB-4	45	7.86E-06
PWB-4	65	1.67E-06
PWB-4	150	6.76E-06
PWB-5	40	8.19E-09
PWB-5	95	6.93E-06
PWB-5	135	2.76E-07

Harmonic Mean	Arithmatic Mean	Geometric Mean
Vertical	Vertical	Vertical
8.03E-08	6.02E-06	1.29E-06

TABLE 3

RESULTS OF SOIL PROPERTIES TEST FROM PREVIOUS STUDIES (MK, 1999a)

SAMPLE NO.	DEPTH (ft)	MOISTURE CONTENT (%) ASTM D2218	DRY DENSITY (pcf) ASTM D2937	SPECIFIC GRAVITY ASTM D854	EFFECTIVE POROSITY SWRCB	PERMEABILITY (cm/sec) USEPA 9100	REMARKS
Q72/AP-6	72.0	17.7	101.8	-	-	8.50E-05	Ver.Perm
Q82/AP-6	82.0	23.73	101.6	2.74	-	1.70E-08	Ver.Perm
R82/AP-15	82.0	14.51	110.7	2.73	-	5.50E-07	Ver.Perm
S82/AP-7	82.0	23.08	106.4	-	-	4.50E-08	Ver.Perm
T85/AR-2	85.0	14.78	114.7	2.77	N/A	7.30E-08	Ver.Perm
T85/AR-2	85.0	-	-	-	-	1.00E-08	Hor.Perm
T88/AR-2	88.0	15.95	110.2	-	-	1.50E-06	Ver.Perm
U84/AP-17	84.0	16.49	127	-	-	2.20E-07	Ver.Perm
U87/AP-17	87.0	11.18	113	2.71	-	7.50E-05	Ver.Perm
SB26/NN084	84.0	15.09	115.3	-	-	3.90E-08	Ver.Perm
SB26/NN084	84.0	-	-	-	-	1.00E-08	Hor.Perm
SB26/NN087	87.0	13.98	106.6	2.83	0.087	4.70E-05	Ver.Perm
SB26/NN0125	125.0	22.53	101.7	-	-	4.00E-08	Ver.Perm
SB27/MM084	84.0	16.43	110.7	-	-	1.90E-07	Ver.Perm
SB27/MM084	84.0	-	-	-	-	N/A	Hor.Perm
SB27/MM087	87.0	14.07	110.9	2.77	0.072	1.30E-07	Ver.Perm
SB27/MM087	87.0	-	-	-	-	2.20E-07	Hor.Perm
SB27/MM125	125.0	16.2	111.2	-	-	2.20E-06	Ver.Perm
AP-12-A	75.0	22.2	99.9	-	-	1.00E-05	Hor.Perm
AP-12-B	80.0	14.07	108.7	2.65	0.11	5.50E-07	Ver.Perm
AP-14-B	80.0	21.78	104.3	-	-	6.00E-07	Ver.Perm
AP-16-B	80.0	15.11	102.5	2.71	-	5.00E-07	Hor.Perm
AP-16-C	85.0	16.28	113.6	2.71	0.059	3.00E-07	Ver.Perm
N-55-B	N/A	5.15	116	2.69	-	-	
P-55-B	N/A	14		-	-	-	
N-40-D	N/A	16	95.4	-	-	-	
O-55-D	N/A	21.81	105	2.78	-	-	
O-40-D	N/A	16.88	92.1	-	-	-	
P-40-A	N/A	25.06	90.7	-	-	-	

Harmonic Mean		Arithmatic Mean		Geometric Mean	
Vertical	Horizontal	Vertical	Horizontal	Vertical	Horizontal
9.84E-08	2.42E-08	1.26E-05	2.15E-06	5.37E-07	1.62E-07

TABLE 4

TOTAL AND EFFECTIVE POROSITY FROM PREVIOUS STUDIES AT THE SITE (MK, 1999a)

Well	Depth	Total Porosity	Effective Porosity
	ft	%	%
IW-1	70.0-72.0	0.446	0.395
IW-2	65.0-67.0	0.396	0.396
MW-1	65.0-67.0	0.478	0.411
MW-2	70.0-72.0	0.449	0.411
MW-3	60.0-62.0	0.441	0.349
MW-4	75.0-77.0	0.482	0.429

TABLE 5

MOISTURE CONTENT AND CORRESPONDING SATURATION VALUES FOR VARIOUS SAMPLES AT THE SITE

Well	Depth	Moisture Content	Dry Density	Grain Density (pcf)	Porosity	Saturation Water Content	Satration (fraction)
	ft	%	pcf	Assumed			
PWB-1	70	16.84	97.95	165.36	0.41	0.41	0.41
PWA-2	45	17.27	112.33	165.36	0.32	0.32	0.54
PWA-2	65	21.90	101.87	165.36	0.38	0.38	0.57
PWA-4	65	10.21	109.34	165.36	0.34	0.34	0.30
PWA-4	80	17.08	113.47	165.36	0.31	0.31	0.54
PWB-1	70	16.84	97.95	165.36	0.41	0.41	0.41
PWB-3	70	28.32	97.32	165.36	0.41	0.41	0.69
PWB-3	85	14.12	119.02	165.36	0.28	0.28	0.50
PWB-3	150	22.55	103.94	165.36	0.37	0.37	0.61
PWB-4	45	18.28	97.75	165.36	0.41	0.41	0.45
PWB-4	65	32.64	90.32	165.36	0.45	0.45	0.72
PWB-4	150	15.22	113.04	165.36	0.32	0.32	0.48
PWB-5	40	21.47	106.80	165.36	0.35	0.35	0.61
PWB-5	95	16.22	95.69	165.36	0.42	0.42	0.38
PWB-5	135	21.57	108.20	165.36	0.35	0.35	0.62
IW-1	55.0-56.5	7.30	ND				
IW-1	60.0-61.5	6.70	ND				
IW-1	65.0-66.5	26.20	ND				
IW-1	70.0-72.0	27.80	ND				
IW-1	73.5-74.0	26.60	ND				
IW-1	75.0-77.0	32.40	ND				
IW-1	77.0-78.5	31.40	ND				
IW-2	55.0-56.5	14.10	ND				
IW-2	60.0-61.5	18.10	ND				
IW-2	65.0-67.0	17.20	ND				
IW-2	70.0-72.0	28.60	ND				
IW-2	72.0-72.5	30.20	ND				
IW-2	76.0-76.5	33.20	ND				
IW-2	77.0-77.3	32.70	ND				
IW-2	77.3-78.3	21.20	ND				
IW-2	79.5-80.0	13.20	ND				
MW-1	53.0-55.0	21.10	ND				
MW-1	62.0-63.5	25.20	ND				
MW-1	65.0-67.0	28.20	ND				
MW-1	70.0-72.0	30.20	ND				
MW-1	72.0-73.5	29.50	ND				
MW-1	73.5-75.0	24.30	ND				
MW-1	78.0-80.0	29.70	ND				
MW-2	53.0-55.0	12.30	ND				
MW-2	62.0-63.5	18.90	ND				
MW-2	65.0-67.0	27.60	ND				
MW-2	70.0-72.0	29.70	ND				
MW-2	72.0-73.5	29.60	ND				
MW-2	78.0-80.0	29.90	ND				

TABLE 6

MOISTURE CONTENT VALUES FOR VARIOUS SAMPLES AT THE SITE FROM PREVIOUS STUDIES

Well	Depth	Moisture Content
	ft	%
MW-3	55.0-56.0	14.30
MW-3	60.0-62.0	20.90
MW-3	65.0-67.0	27.50
MW-3	70.0-72.0	28.90
MW-3	73.5-75.0	26.40
MW-3	75.0-76.5	25.60
MW-3	76.5-78.0	25.80
MW-3	78.0-80.0	26.40
MW-4	55.0-56.5	8.40
MW-4	60.0-61.5	2.70
MW-4	65.0-66.5	16.60
MW-4	72.0-73.5	25.00
MW-4	75.0-77.0	28.00
MW-4	78.5-80.0	24.90

TABLE 7

CALCULATED CAPILLARY PRESSURE AS A FUNCTION OF LIQUID SATURATION FOR VARIOUS SOILS

		Liquid Saturation	0.1	0.2	0.3	0.4	0.5	0.6	0.7	0.8	0.9	1
		Liquid Saturation	0.1	0.2	0.3	0.4	0.5	0.6	0.7	0.8	0.9	1
Sample No.	**Description**	**Model Assignment**	**Capillary Pressure (Pa)**									
PWA-480	Silty Clay to Clayey Silt	Clay	1.00E+20	1.00E+20	1.11E+06	4.99E+03	2.44E+03	1.54E+03	1.05E+03	7.18E+02	4.42E+02	1.00E-20
PWB-370	Silt very stiff	Clay	1.00E+20	1.00E+20	5.54E+04	3.14E+04	2.39E+04	1.95E+04	1.62E+04	1.32E+04	1.01E+04	1.00E-20
PWB-385	Clay	Clay	1.00E+20	1.00E+20	2.36E+04	3.39E+03	1.62E+03	9.81E+02	6.43E+02	4.22E+02	2.46E+02	4.90E-06
PWB-4150	Sand	Clay	1.00E+20	1.00E+20	1.02E+04	2.78E+03	1.43E+03	8.81E+02	5.79E+02	3.77E+02	2.17E+02	1.09E-06
PWB-445	Modofied	Clay	1.00E+20	1.00E+20	1.00E+20	2.10E+07	2.46E+06	7.51E+05	3.16E+05	1.48E+05	6.29E+04	2.60E-06
PWB-465	Silt	Clay	1.00E+20	1.00E+20	1.63E+07	6.93E+05	1.68E+05	6.50E+04	3.05E+04	1.51E+04	6.66E+03	2.57E-07
PWB-595	Clay	Clay	1.00E+20	1.00E+20	3.07E+05	1.28E+05	7.72E+04	5.23E+04	3.69E+04	2.56E+04	1.57E+04	5.13E-04
MW-165-67	Fine Sandy Silt	Mixed	1.00E+20	1.00E+20	1.00E+20	1.00E+20	2.23E+05	3.12E+04	9.88E+03	4.03E+03	1.59E+03	1.00E-20
MW-170-72	Fine Sand	Mixed	1.00E+20	1.00E+20	1.00E+20	1.00E+20	2.70E+07	2.98E+05	2.33E+04	3.78E+03	7.67E+02	1.00E-20
MW-172-73	Fine Sand	Mixed	1.00E+20	1.00E+20	1.00E+20	1.00E+20	6.54E+04	4.21E+04	3.13E+04	2.38E+04	1.70E+04	1.00E-20
MW-475-77	Silty Sand	Mixed	1.00E+20	1.00E+20	1.00E+20	1.00E+20	6.42E+04	3.95E+04	2.92E+04	2.23E+04	1.59E+04	1.00E-20
IW-272-72	**Fine Sand**	**Sand**	1.00E+20	1.00E+20	1.00E+20	3.83E+17	2.62E+07	2.07E+05	1.17E+04	1.48E+03	2.49E+02	1.92E-11
PWB-445	Clay?	Sand	1.00E+20	1.00E+20	1.00E+20	1.00E+20	1.45E+04	2.72E+03	9.80E+02	4.31E+02	1.80E+02	9.84E-09
PWB-5135	Sand	Sand	1.00E+20	1.00E+20	1.00E+20	1.00E+20	2.88E+03	1.43E+03	8.96E+02	5.89E+02	3.56E+02	3.79E-05
IW-170-72	**Silt?**	Silt	1.00E+20	1.00E+20	1.00E+20	3.19E+05	5.06E+03	1.96E+03	1.06E+03	6.15E+02	3.29E+02	1.36E-06
IW-173-74	**Silt?**	Silt	1.00E+20	1.00E+20	1.00E+20	8.17E+04	1.71E+04	1.16E+04	8.79E+03	6.77E+03	4.87E+03	9.92E-02
IW-177-78	**Silt?**	Silt	1.00E+20	1.00E+20	1.00E+20	1.36E+05	1.88E+04	1.16E+04	8.29E+03	6.06E+03	4.10E+03	1.22E-02
IW-265-67	**Silt?**	Silt	1.00E+20	1.00E+20	1.00E+20	4.63E+05	4.95E+03	1.87E+03	9.92E+02	5.72E+02	3.03E+02	1.02E-06
IW-277-77	**Silt?**	Silt	1.00E+20	1.00E+20	1.00E+20	9.40E+04	2.70E+04	2.01E+04	1.62E+04	1.32E+04	1.01E+04	1.85E+00
MW-265-67	Fine Sand	Silt	1.00E+20	1.00E+20	1.00E+20	7.25E+04	2.23E+04	1.23E+04	7.88E+03	5.16E+03	3.06E+03	1.18E-04
MW-270-72	Silty Sand	Silt	1.00E+20	1.00E+20	1.00E+20	2.47E+06	8.37E+04	1.69E+04	5.69E+03	2.30E+03	8.75E+02	7.13E-09
MW-272-73	Silty Sand	Silt	1.00E+20	1.00E+20	1.00E+20	1.18E+06	8.59E+04	2.47E+04	1.03E+04	4.86E+03	2.11E+03	1.17E-07
MW-370-72	Silt	Silt	1.00E+20	1.00E+20	1.00E+20	2.04E+07	1.54E+05	1.56E+04	3.37E+03	9.98E+02	3.00E+02	2.90E-10
MW-373-75	Silt	Silt	1.00E+20	1.00E+20	1.00E+20	1.25E+05	2.81E+04	1.35E+04	7.83E+03	4.74E+03	2.59E+03	1.14E-05
MW-376-78	Silt	Silt	1.00E+20	1.00E+20	1.00E+20	5.67E+06	1.02E+06	4.40E+05	2.39E+05	1.37E+05	7.11E+04	8.69E-05
PWA-245	Silty Clay with Traces of Sand W Calcm Carb	Silt	1.00E+20	1.00E+20	1.00E+20	8.94E+05	2.04E+04	7.70E+03	4.05E+03	2.32E+03	1.22E+03	3.20E-06
PWA-265	Fine Sandy Silt Stiff	Silt	1.00E+20	1.00E+20	1.00E+20	5.68E+03	2.14E+03	1.25E+03	8.14E+02	5.40E+02	3.24E+02	1.04E-05
PWA-465	Clayey Silt to Silt	Silt	1.00E+20	1.00E+20	1.00E+20	5.91E+05	5.56E+03	1.86E+03	9.17E+02	5.01E+02	2.52E+02	3.88E-07
PWB-170	Fine Sandy Silt or Clay Layer??	Silt	1.00E+20	1.00E+20	1.00E+20	1.21E+04	3.56E+03	1.97E+03	1.26E+03	8.31E+02	4.97E+02	1.00E-20
PWB-3150	Fine Sandy Silt	Silt	1.00E+20	1.00E+20	1.00E+20	5.44E+04	2.86E+04	1.94E+04	1.42E+04	1.03E+04	6.89E+03	5.34E-03
PWB-540	Silt very stiff	Silt	1.00E+20	1.00E+20	1.00E+20	1.21E+09	5.31E+05	5.56E+04	1.38E+04	4.64E+03	1.57E+03	1.00E-20

TABLE 8

CALCULATED CAPILLARY PRESSURE AS A FUNCTION OF LIQUID SATURATION FOR SELECTED SOILS

	Theta (cm^{-1})				N (Dimensionless)					
	Calculated	95% Confidence Limits			Calculated	95% Confidence Limits			Theta R	Theta Q
Sample Number	Value	Lower	Upper		Value	Lower	Upper			
PWB-1 (50')	0.0043	0.0000	0.0088		1.2279	1.1626	1.2933		0	0.3631
PWB-3 (135')	0.0058	0.0000	0.0146		1.3508	1.1079	1.5937		0	0.3589
PWB-5 (75')	0.0019	0.0011	0.0026		1.2354	1.2095	1.2613		0	0.5212
PWB-5 (85')	0.0440	0.0000	0.0883		1.1868	1.1400	1.2337		0	0.4217

Figures

Project No. C02-266 June 2004

Figure 1 - Topographic Map of Arvin and Vicinity

PANACEA, INC.
Environmental Services

Project No. C00-266	Figure 1- 1

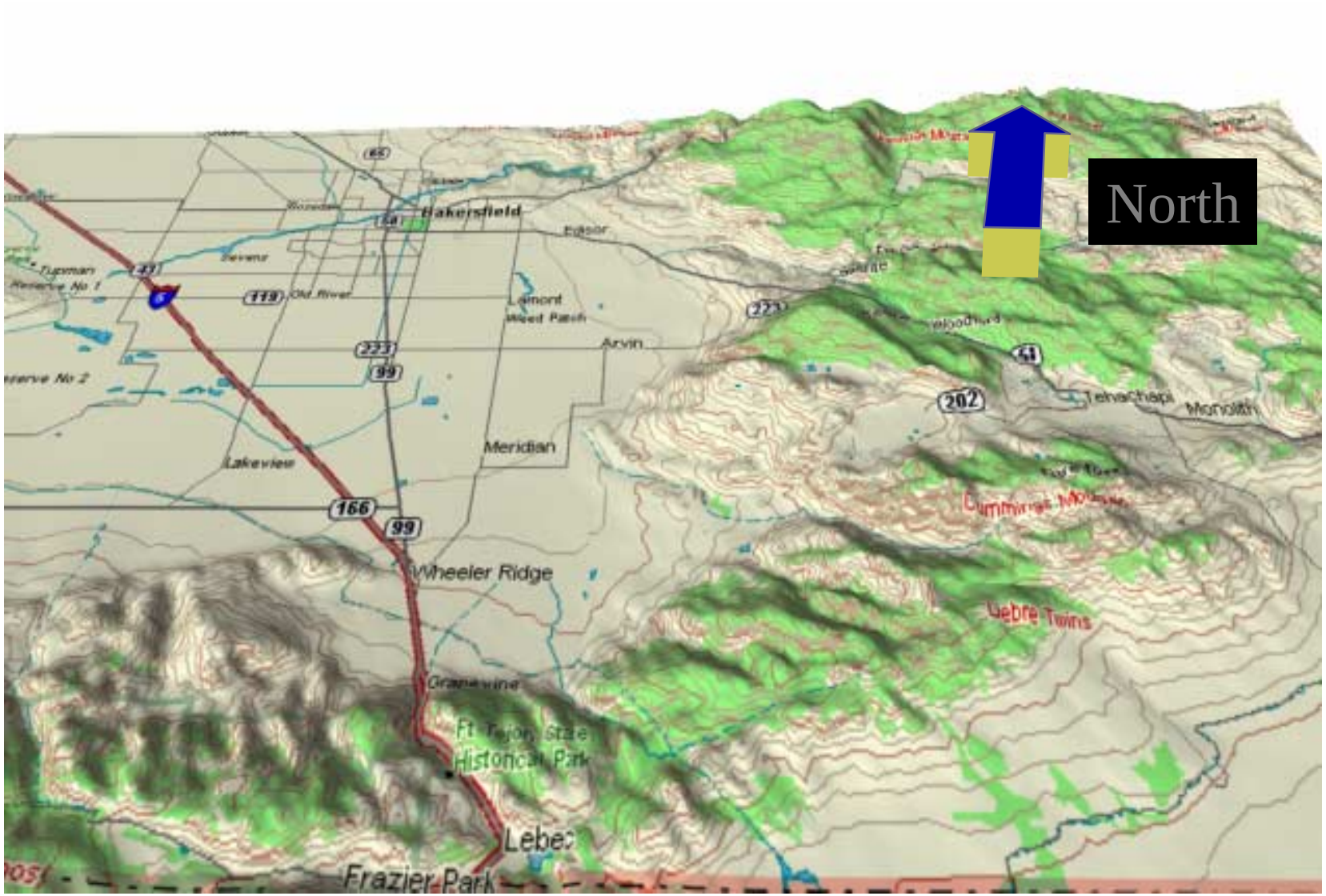

Three-Dimensional View of the Topographic Map of Arvin and Vicinity

PANACEA, INC.
Environmental Services

Project No. C00-266	Figure 1- 2

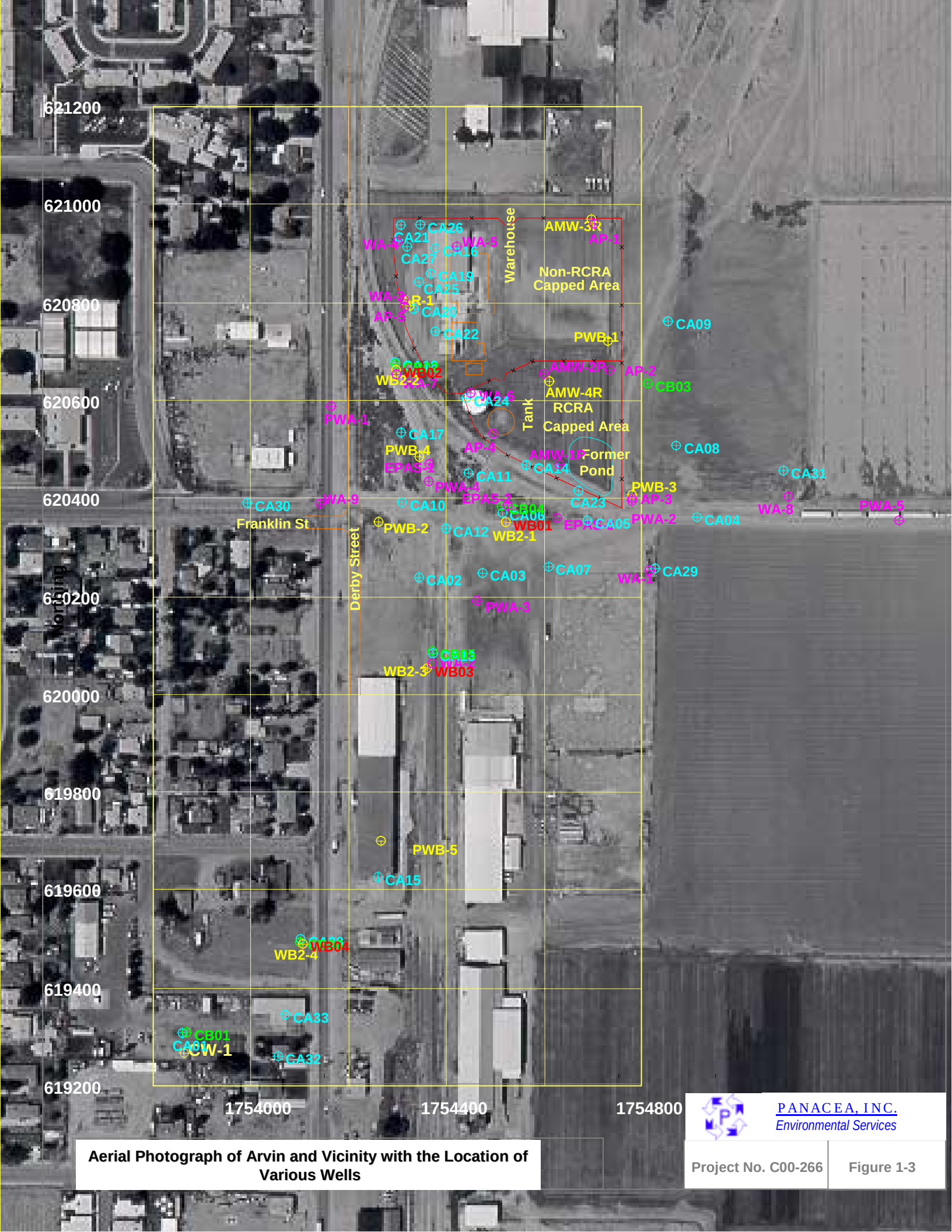

Aerial Photograph of Arvin and Vicinity with the Location of Various Wells

Project No. C00-266	Figure 1-3

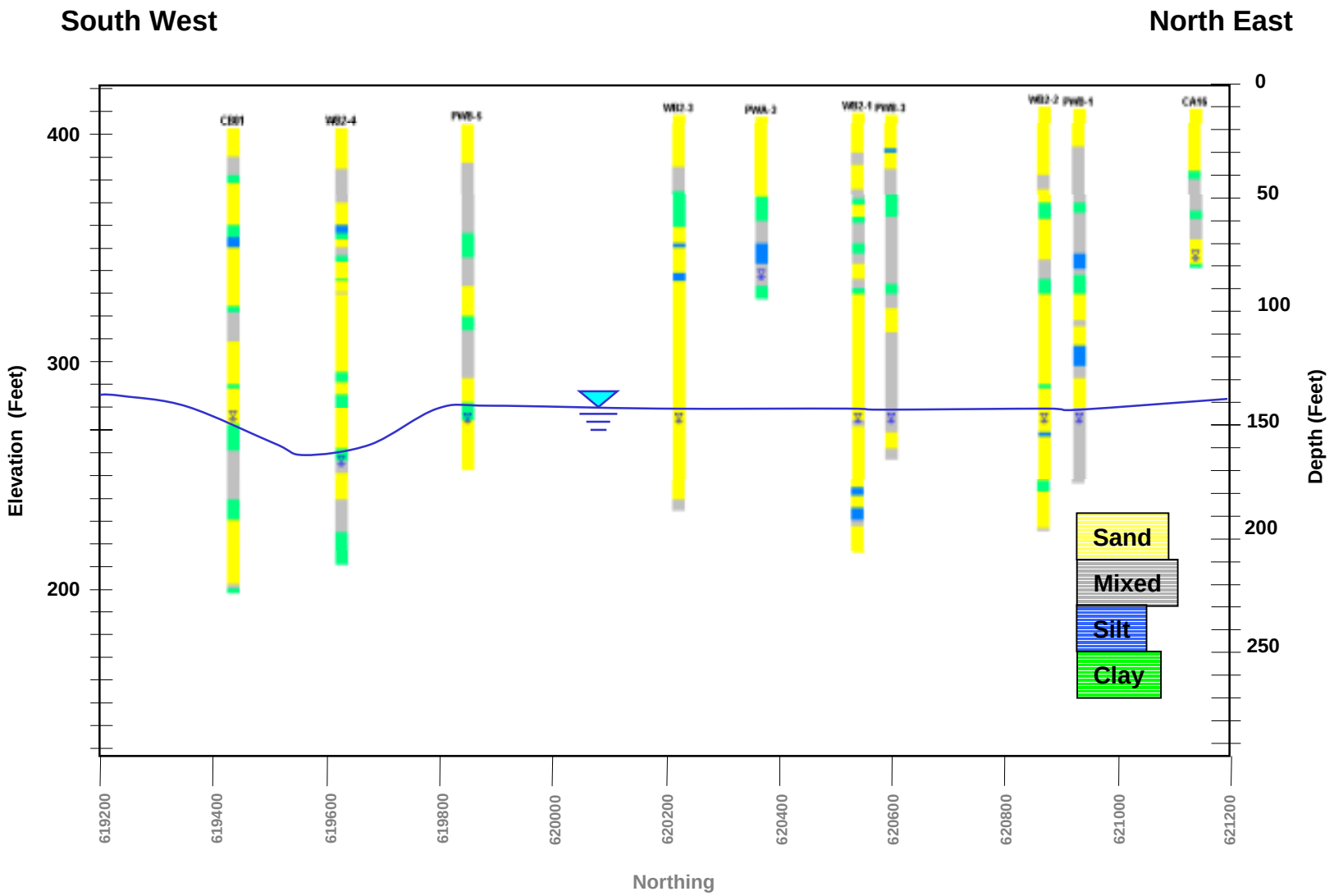

Boring Logs

PANACEA, INC.
Environmental Services

Project No.
C00-266

Figure 1-4

Transect of the Brown and Bryant Site

PANACEA, INC.
Environmental Services

Project No. C00-266	Figure 2- 1

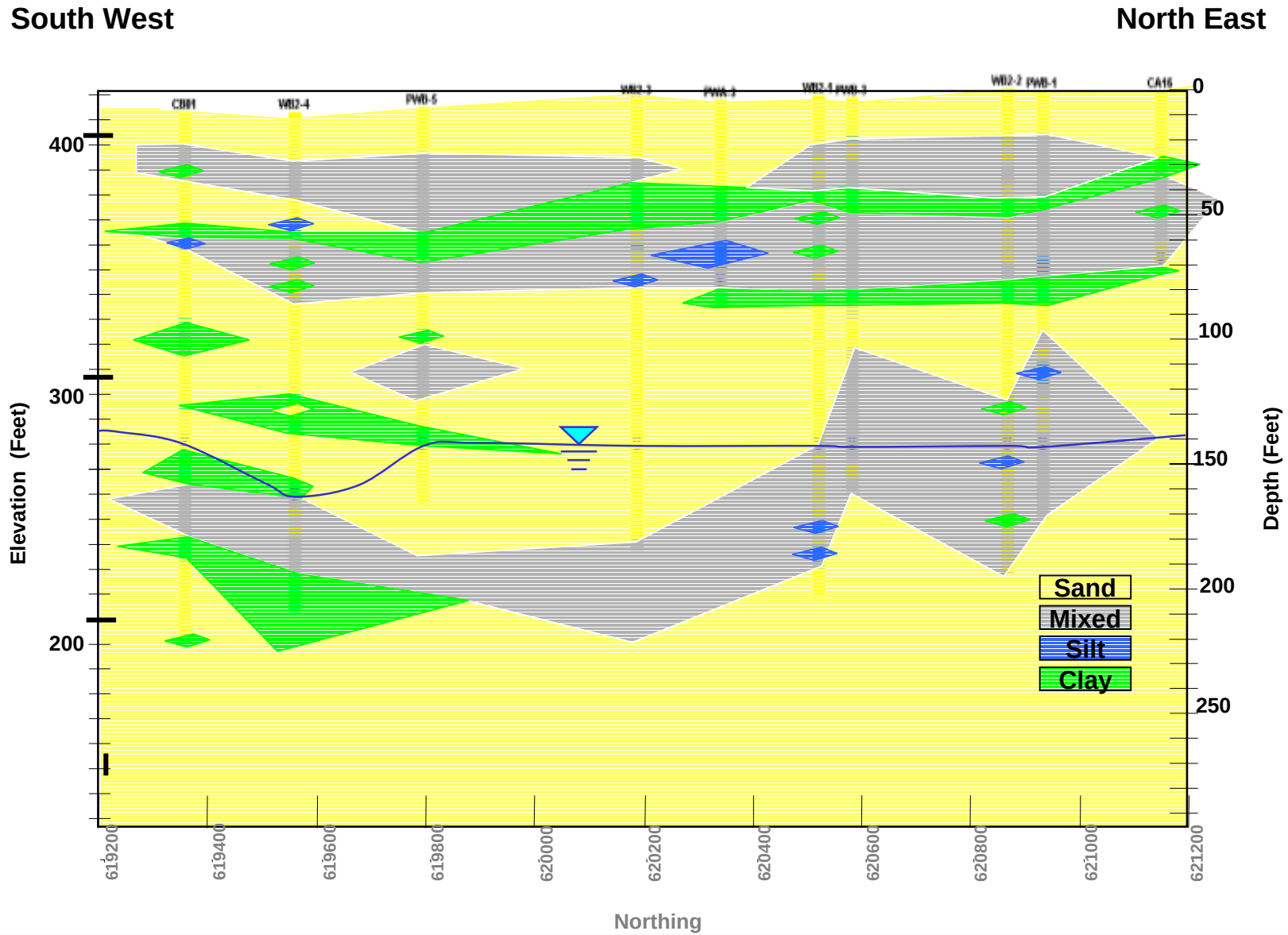

Cross Section of the Alternative Conceptual Hydrogeologic Model 1

PANACEA, INC.
Environmental Services

Project No. C00-266	Figure 2- 2

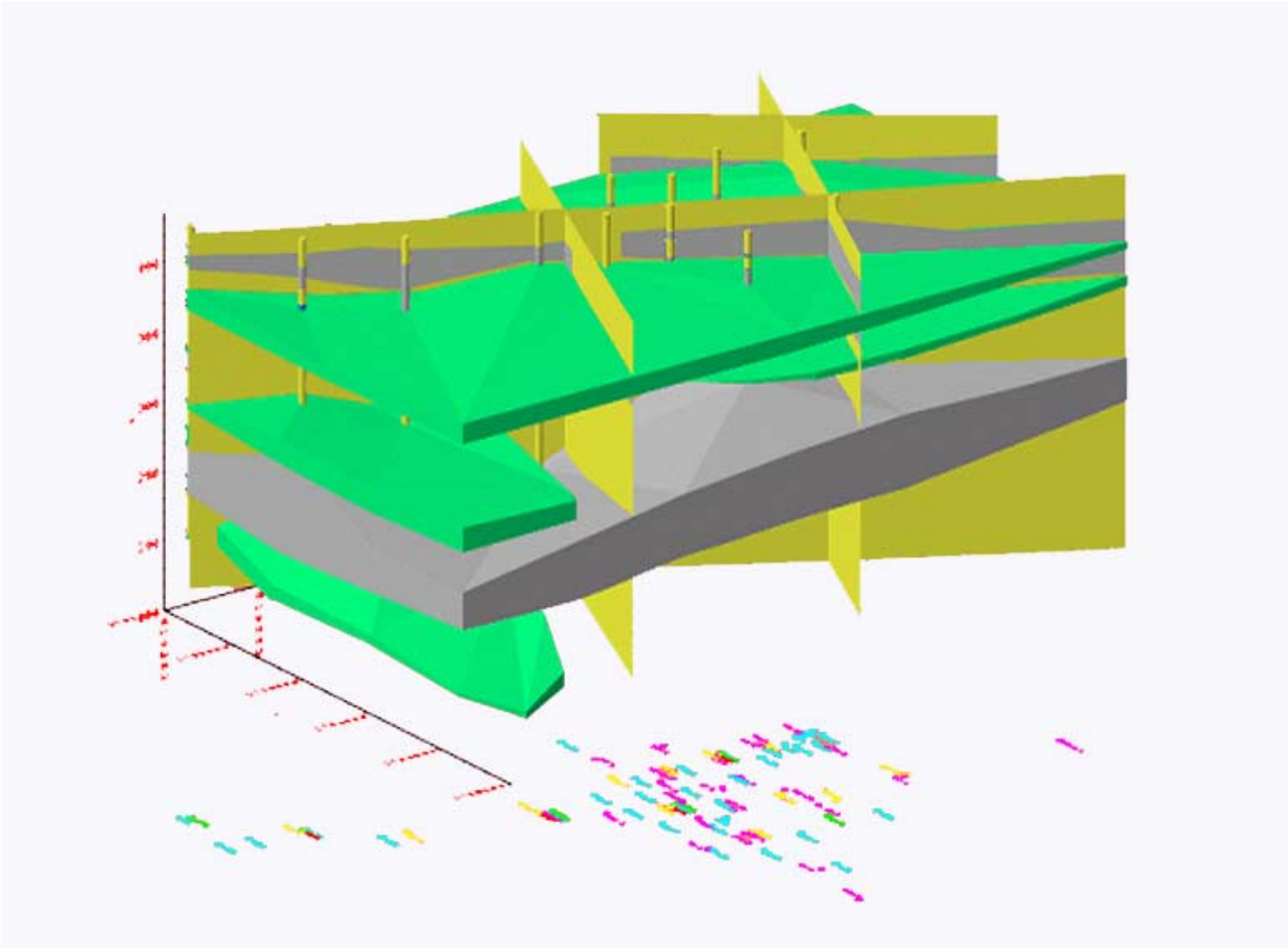

Three-Dimensional Rendering of the Alternative Conceptual Hydrogeologic Model 1

PANACEA, INC.
Environmental Services

Project No. C00-266	Figure 2- 3

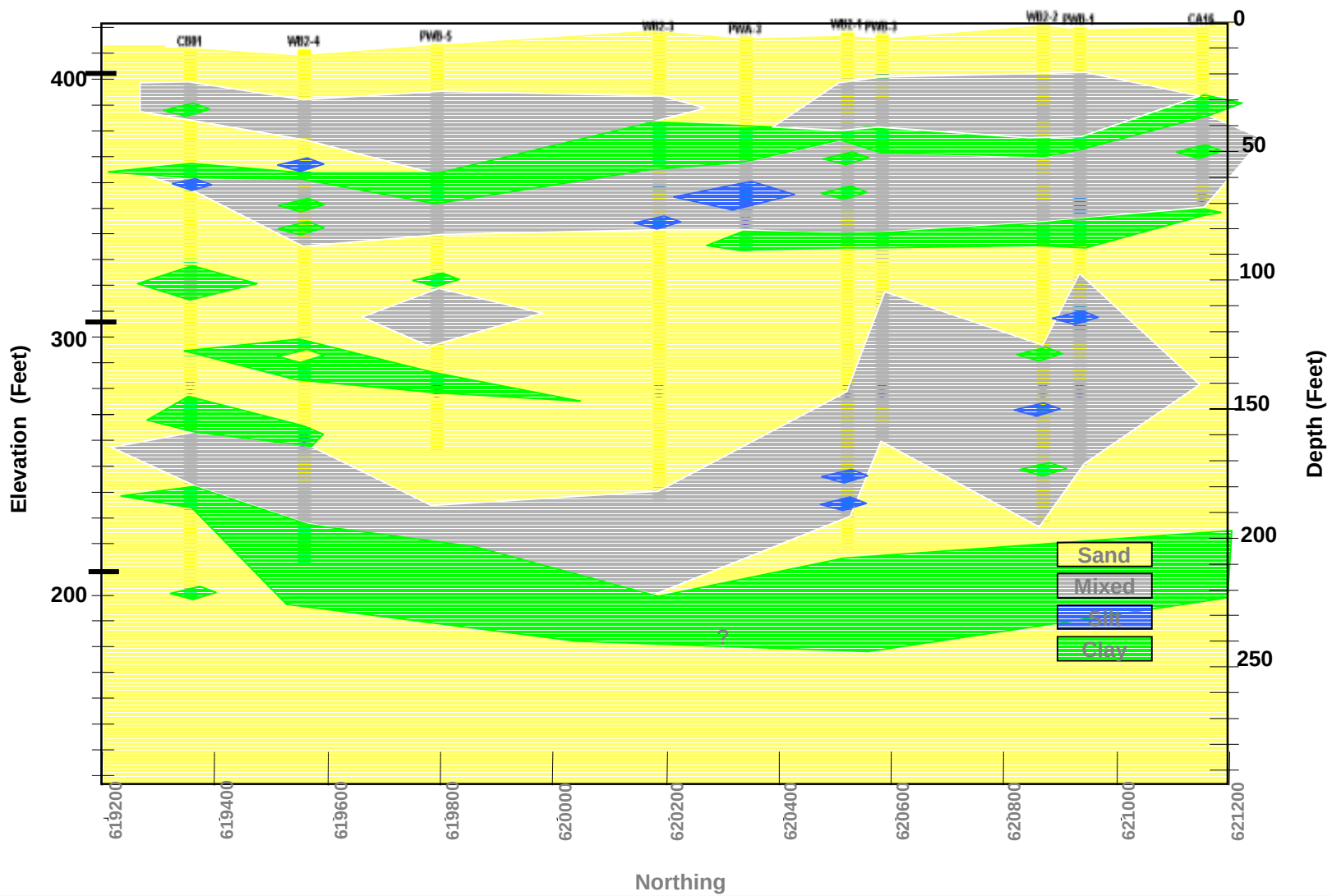

Cross Section of the Conceptual Hydrogeologic Model 2

PANACEA, INC.
Environmental Services

Project No.
C00-266

Figure 2- 4

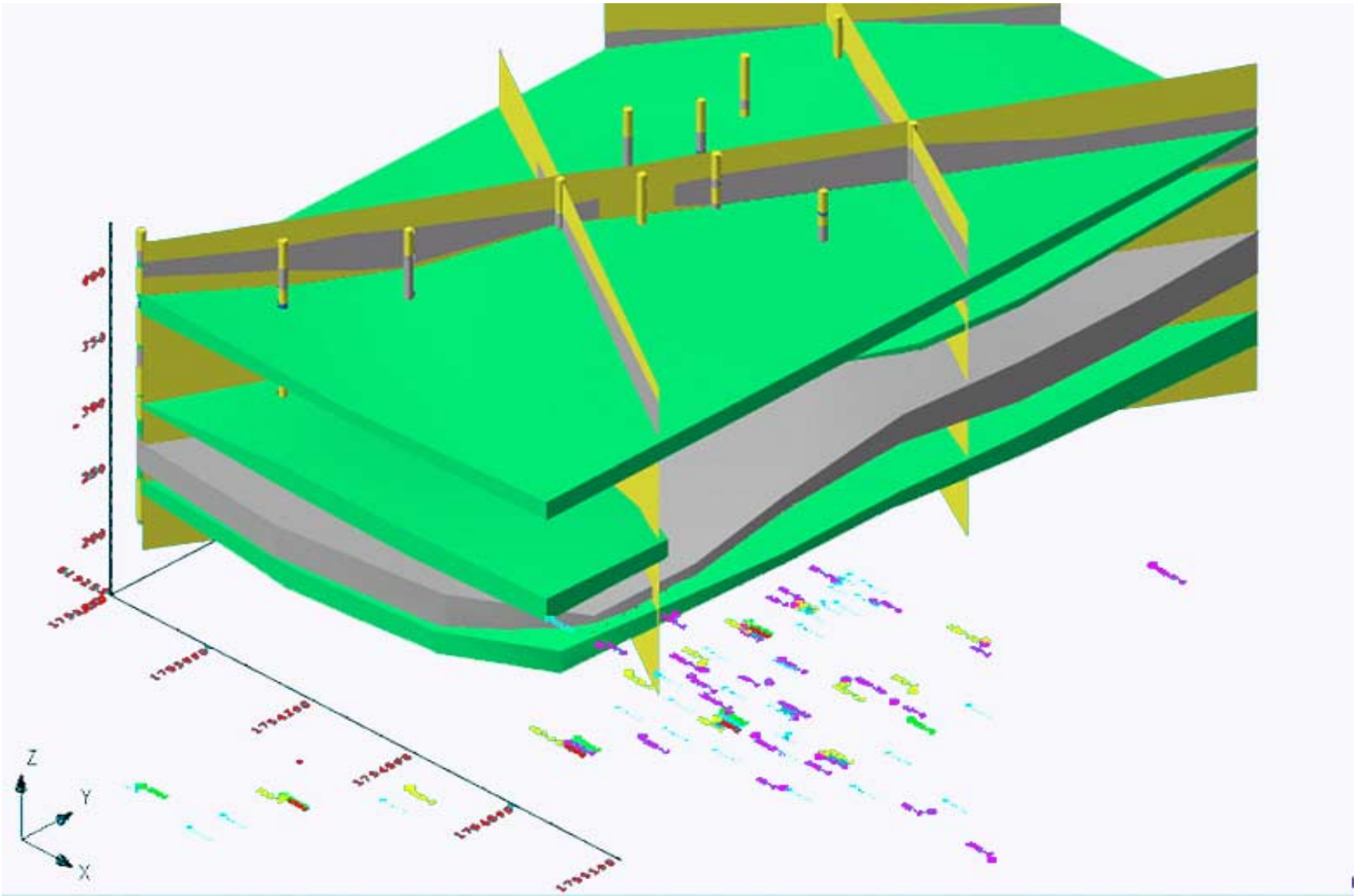

Three-Dimensional Rendering of the Alternative-II Conceptual Hydrogeologic Model of the Area

PANACEA, INC.
Environmental Services

Project No. C00-266	Figure 2- 5

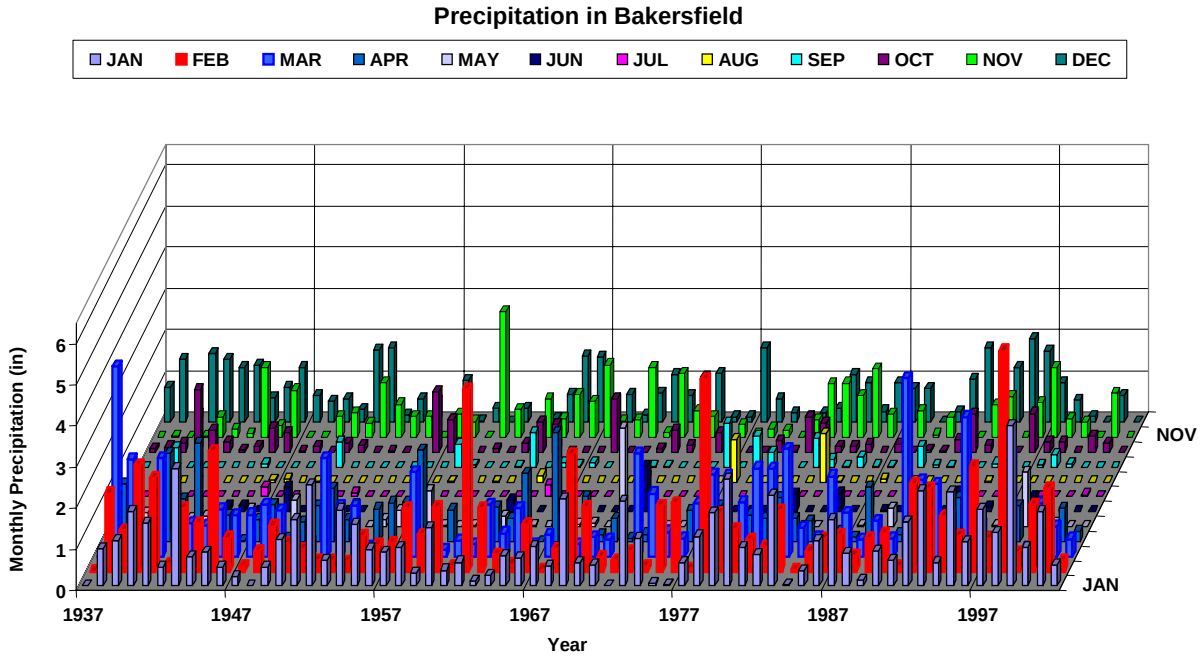

a)

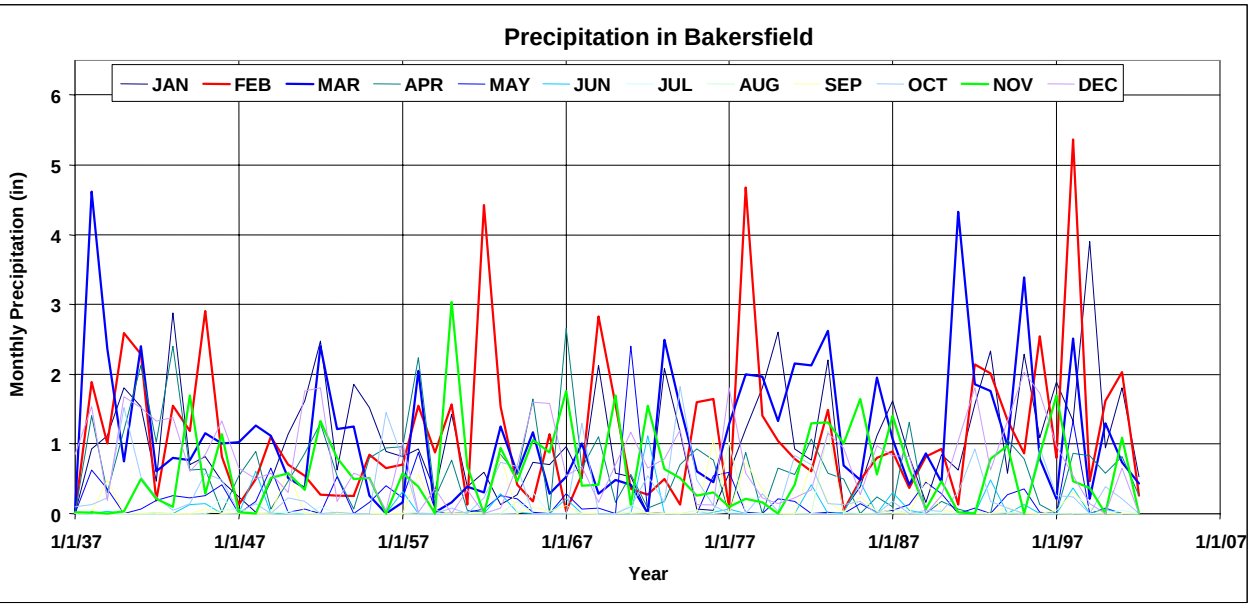

b)

Monthly Precipitation Data for Bakersfield Presented in Three-dimensional View (a) and Line Plot (b)

PANACEA, INC.
Environmental Services

Project No.	Figure
C00-266	2-6

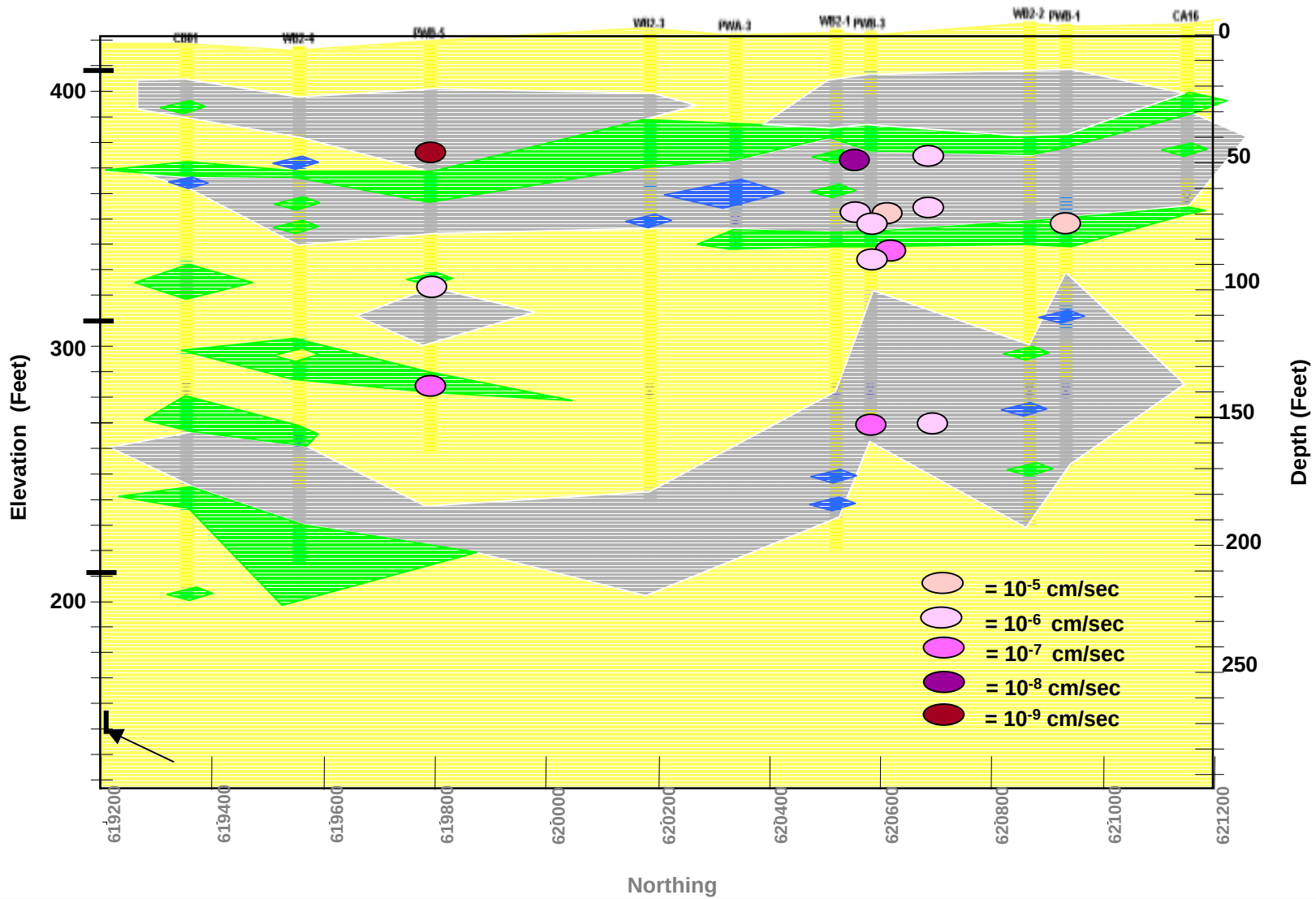

Distribution Available Hydraulic Conductivity Data

PANACEA, INC.
Environmental Services

Project No. C00-266	Figure 2- 7

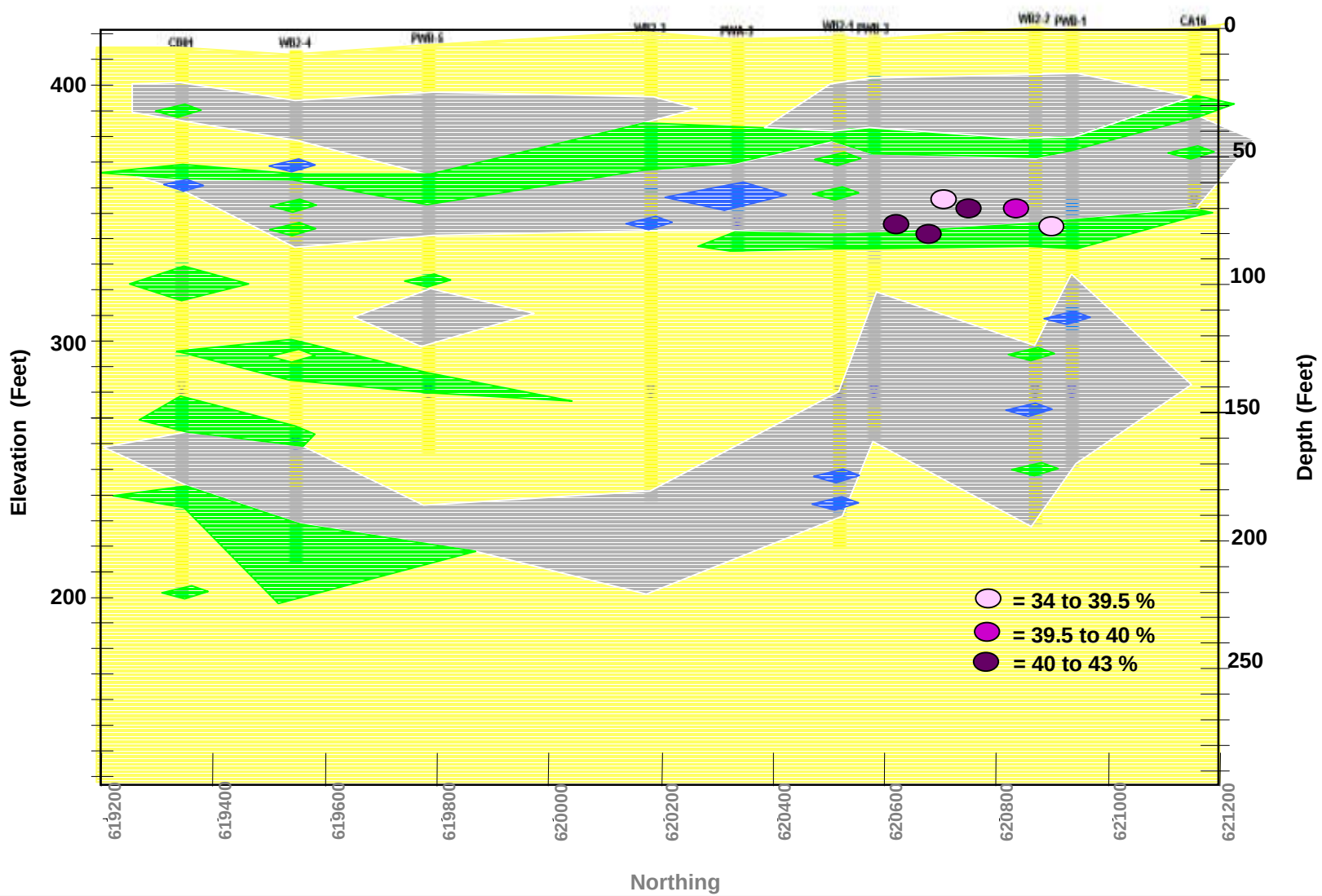

Distribution Available Effective Porosity Data

PANACEA, INC.
Environmental Services

Project No. C00-266	Figure 2- 8

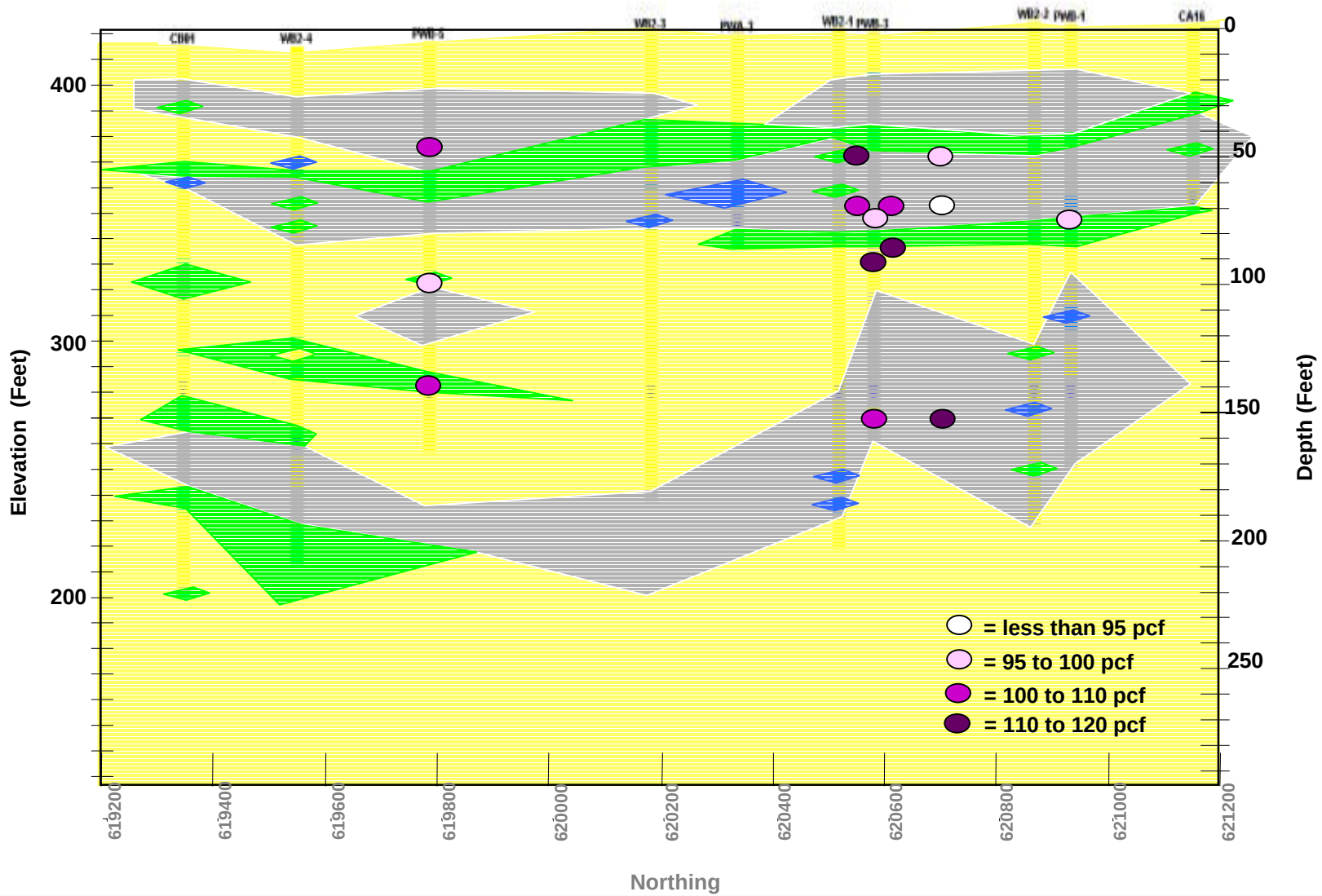

Distribution Available Soil Dry Density Data

PANACEA, INC.
Environmental Services

Project No. C00-266	Figure 2- 9

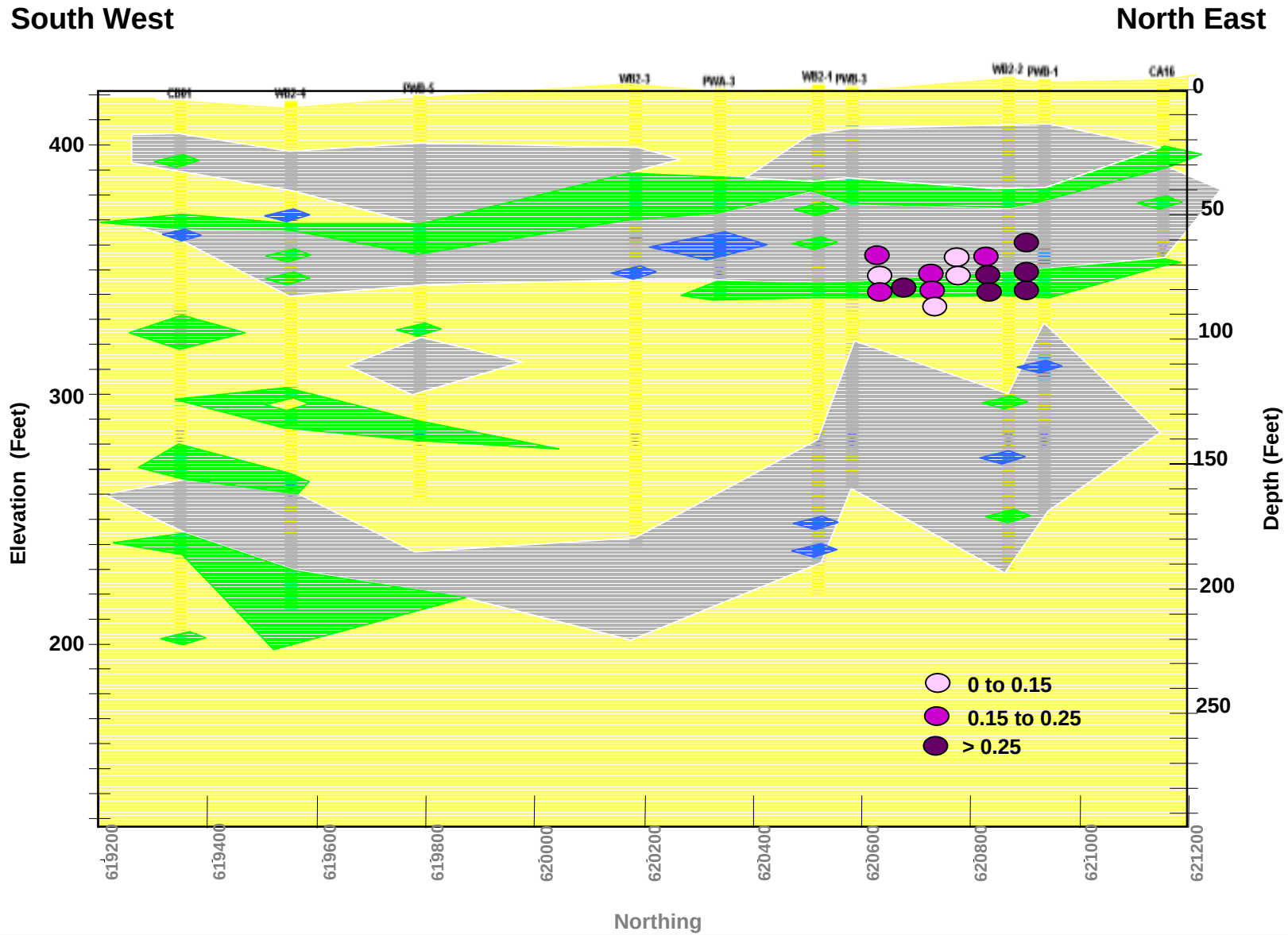

Distribution Available Total Organic Carbon (TOC) Data

PANACEA, INC.
Environmental Services

Project No. C00-266	Figure 2- 10

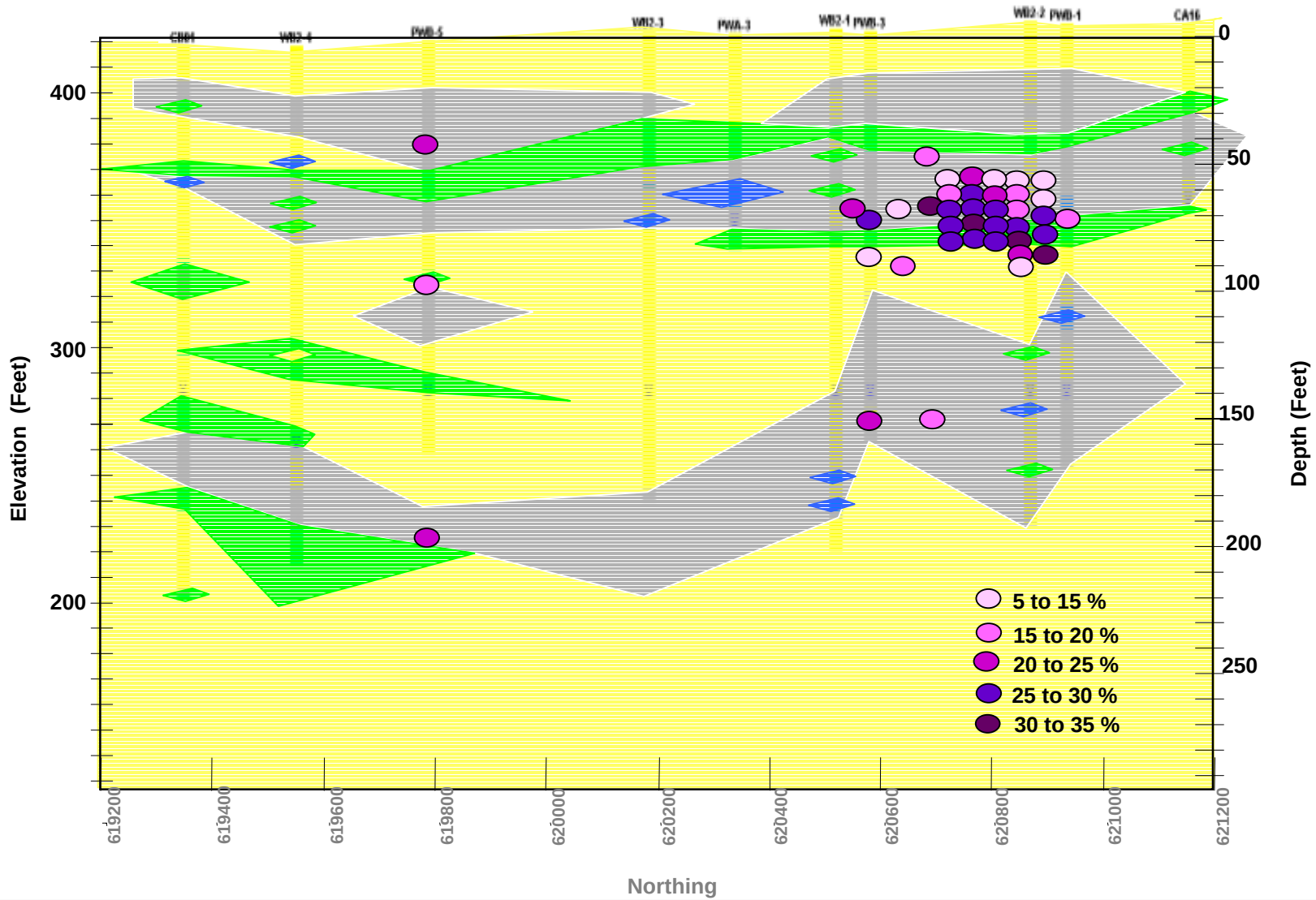

Data Distribution (Moisture Content)

PANACEA, INC.
Environmental Services

Project No. C00-266	Figure 2- 11

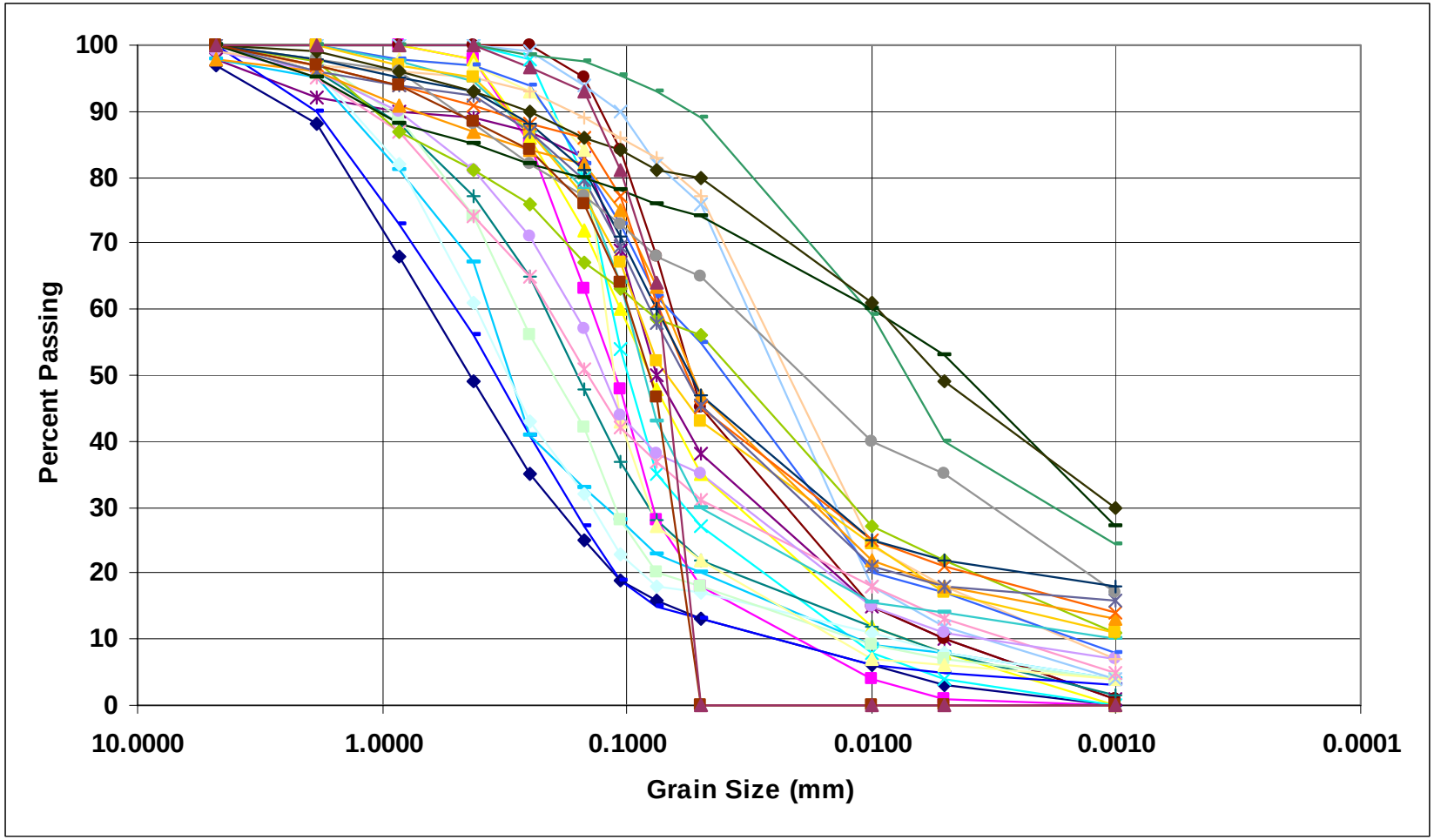

Grain-size Distribution for Various Samples from Boreholes at the Site

PANACEA, INC.
Environmental Services

Project No. C00-266	Figure 2- 12

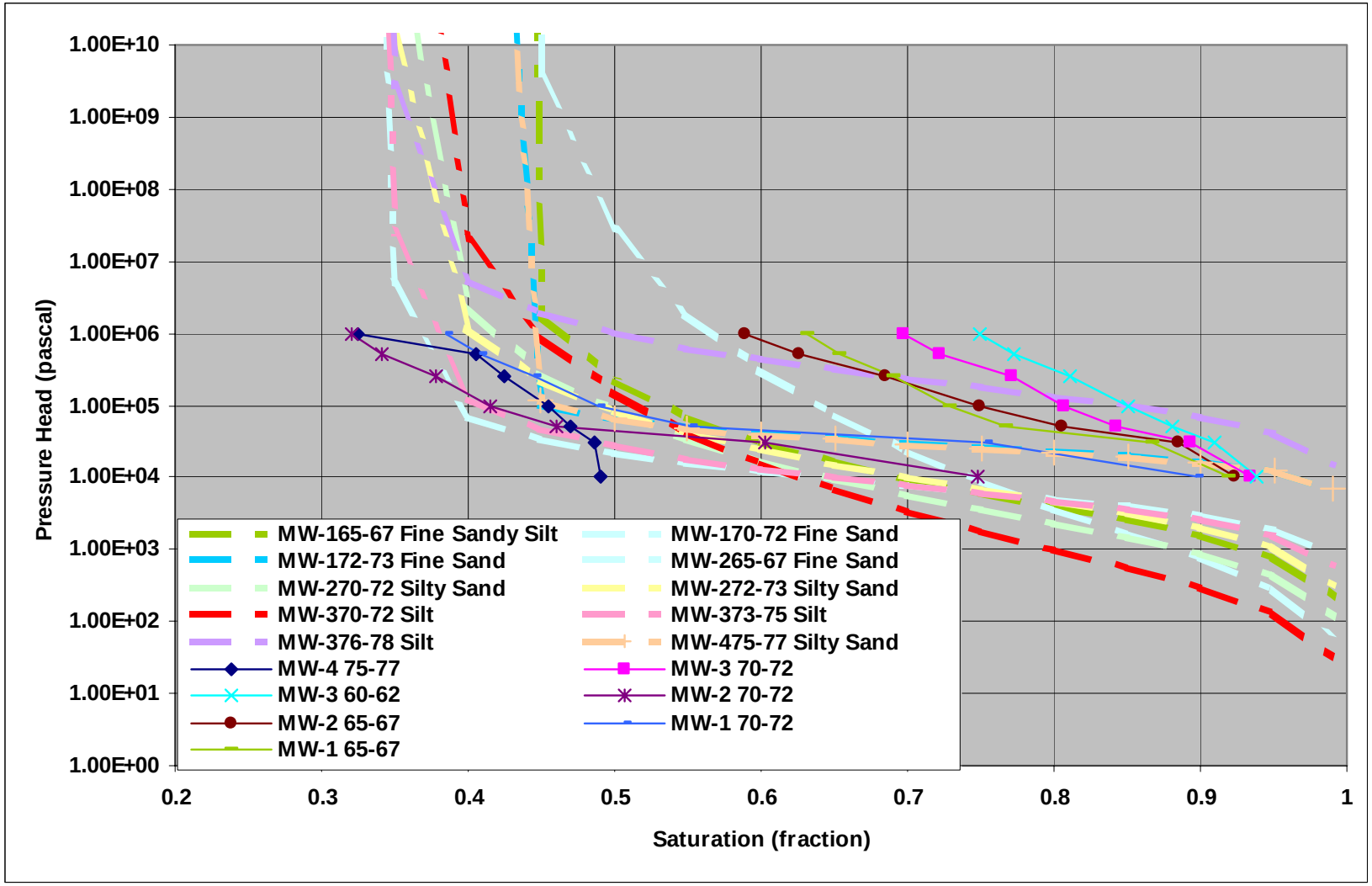

Capillary Pressure Curve for Clays at the Site. Lines With Symbols Represent Measured Data. All Others Are Calculated as Described in Text

PANACEA, INC.
Environmental Services

Project No. C00-266	Figure 2- 13

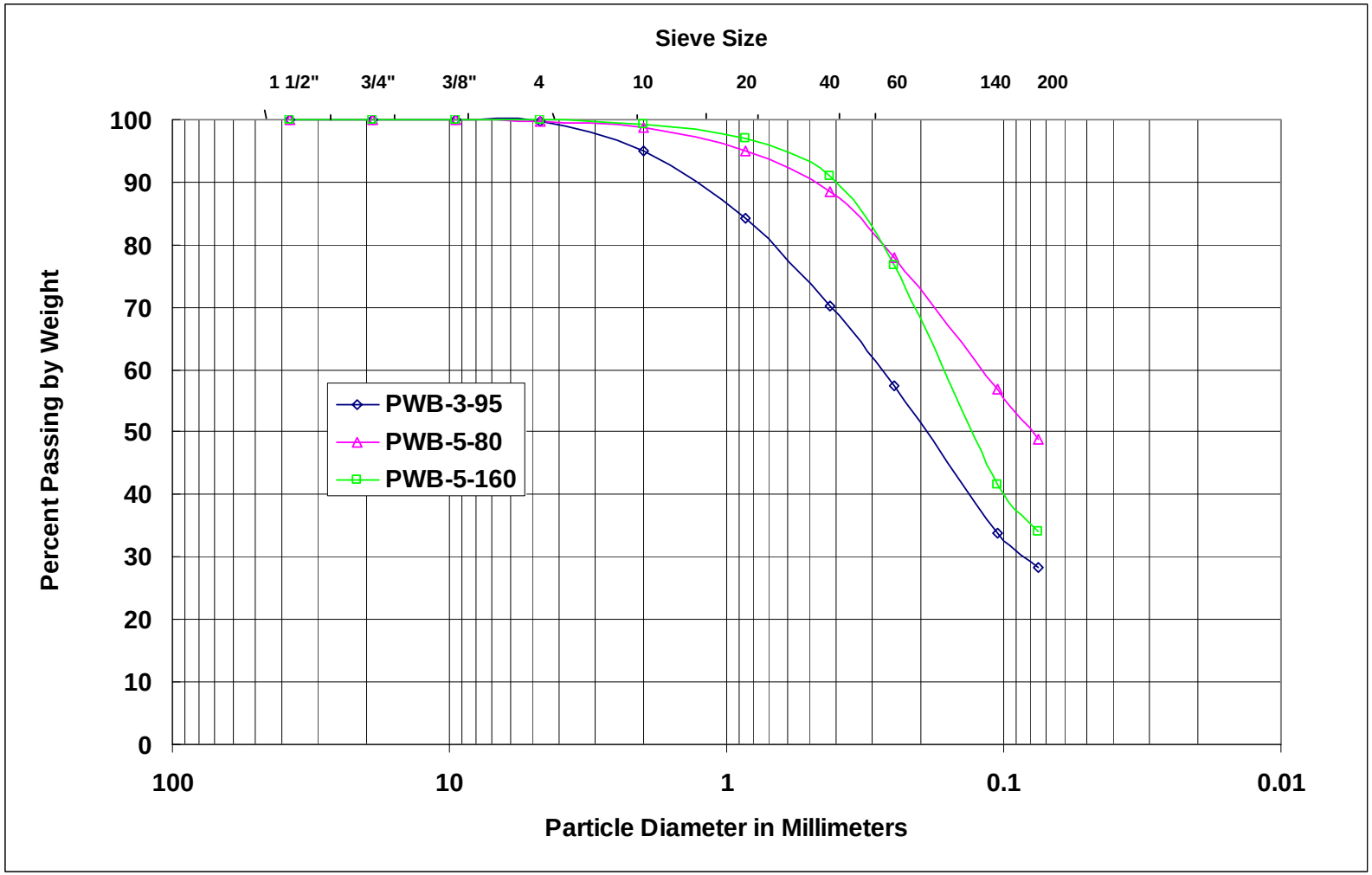

Grain-Size Distribution Curve for Selected Samples at the Site

PANACEA, INC.
Environmental Services

Project No. C00-266	Figure 2- 14

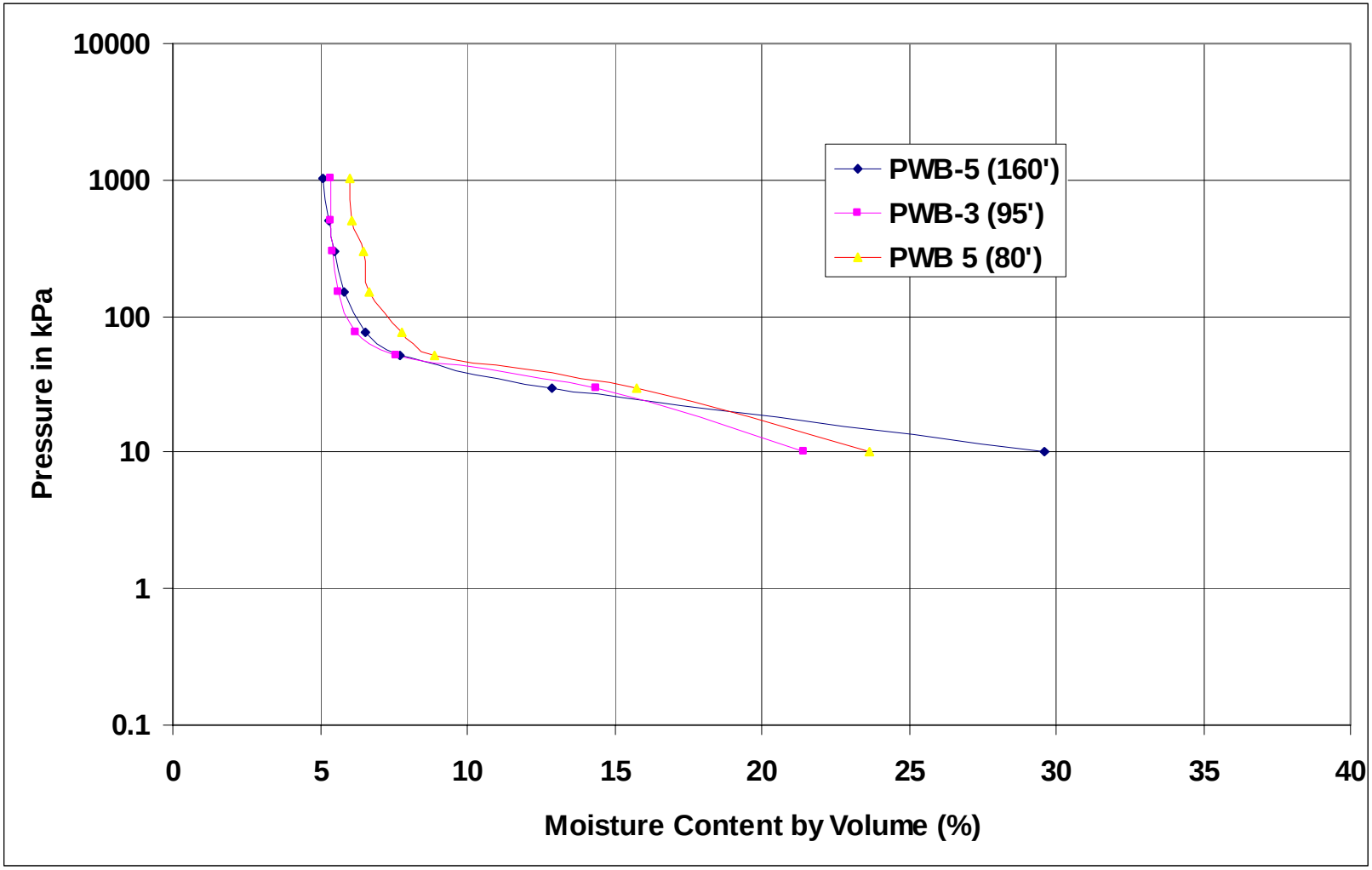

Measured Capillary-Moisture Relations for Selected Soil Samples

PANACEA, INC.
Environmental Services

Project No. C00-266	Figure 2- 15

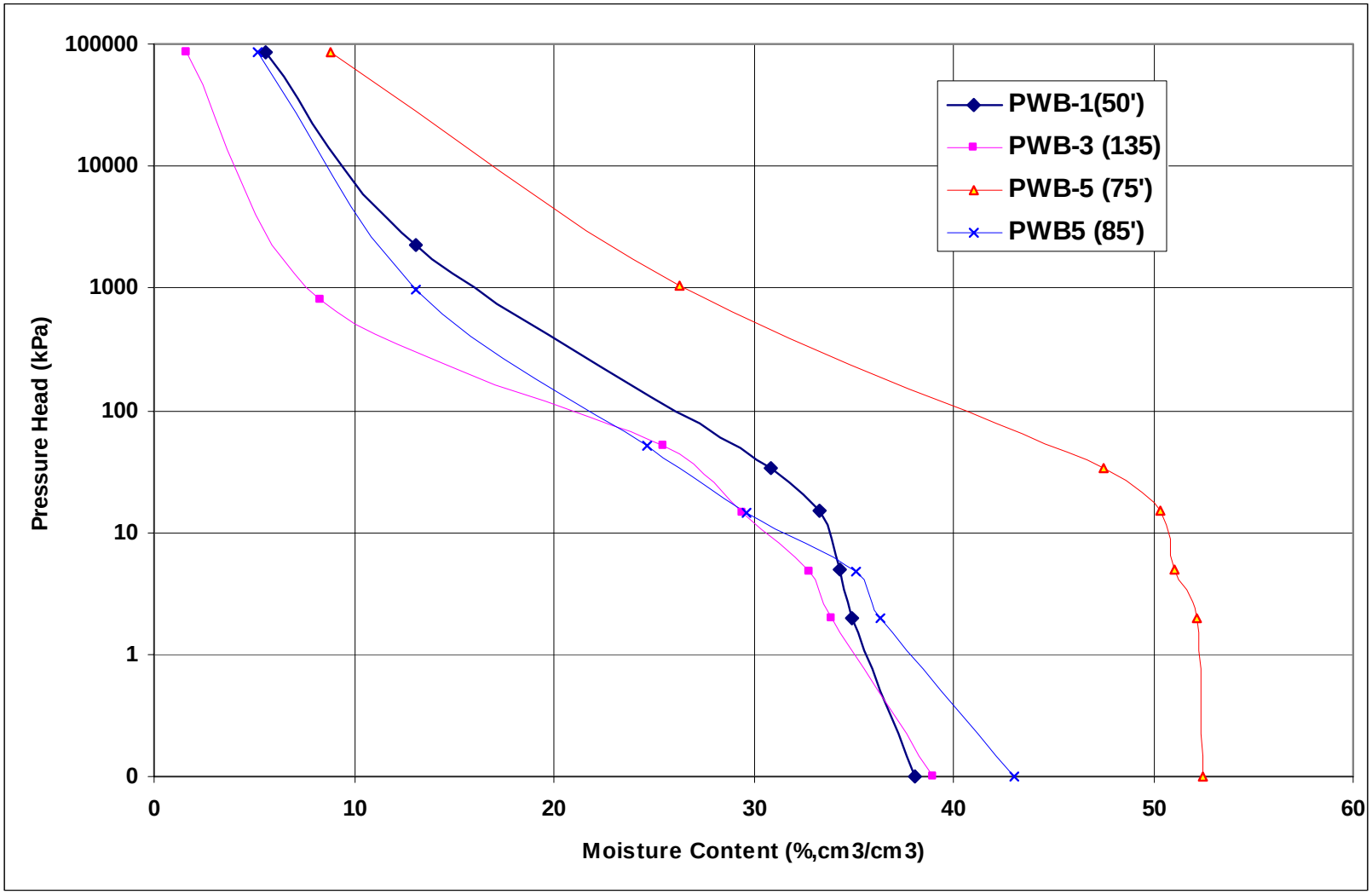

Measured Moisture Retention Curve for Selected Soil Samples

PANACEA, INC.
Environmental Services

Project No. C00-266	Figure 2- 16

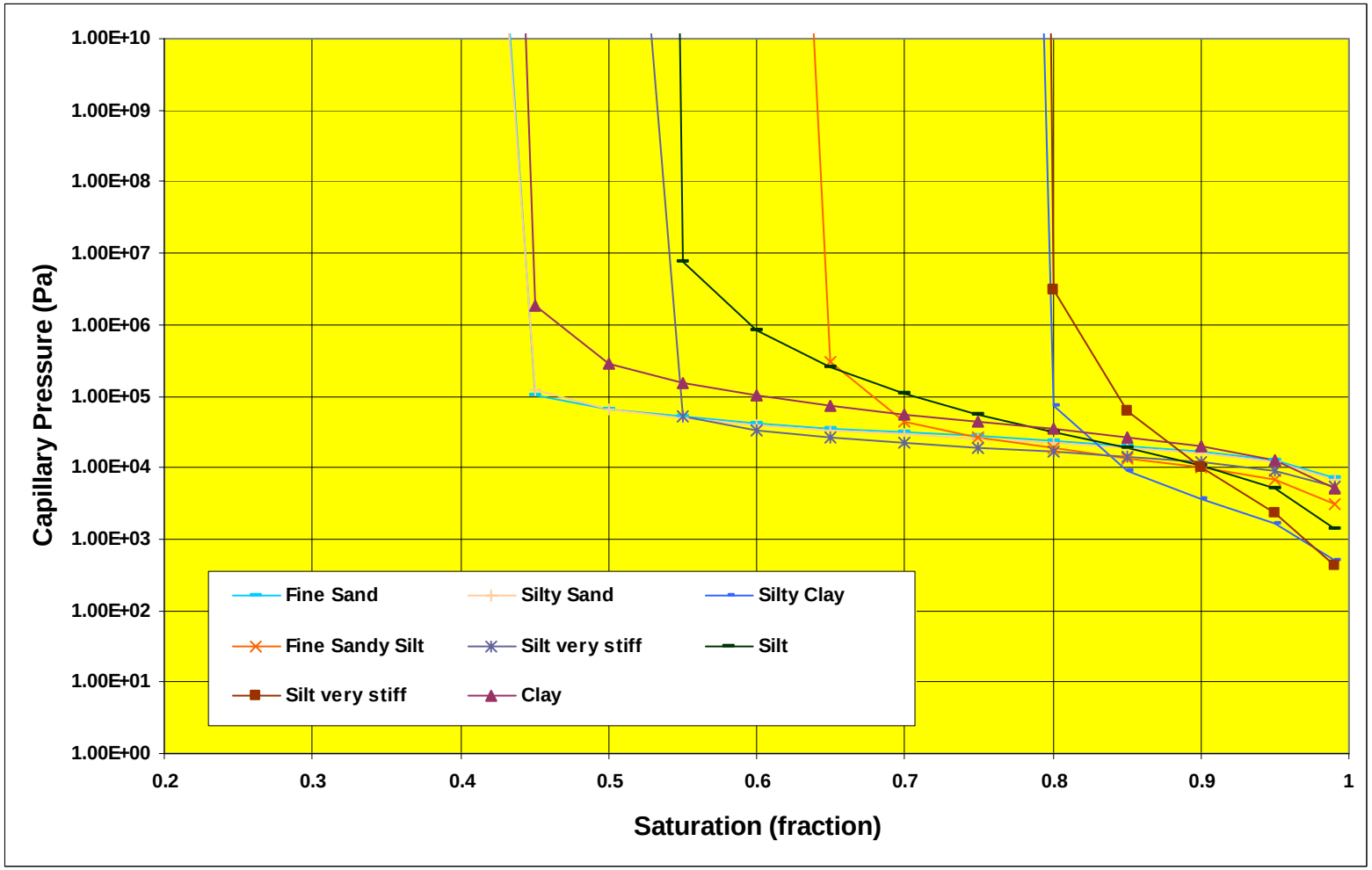

Capillary Pressure Curve for Silt Group at the Site
Calculated as Described in Text

PANACEA, INC.
Environmental Services

Project No. C00-266	Figure 2- 17

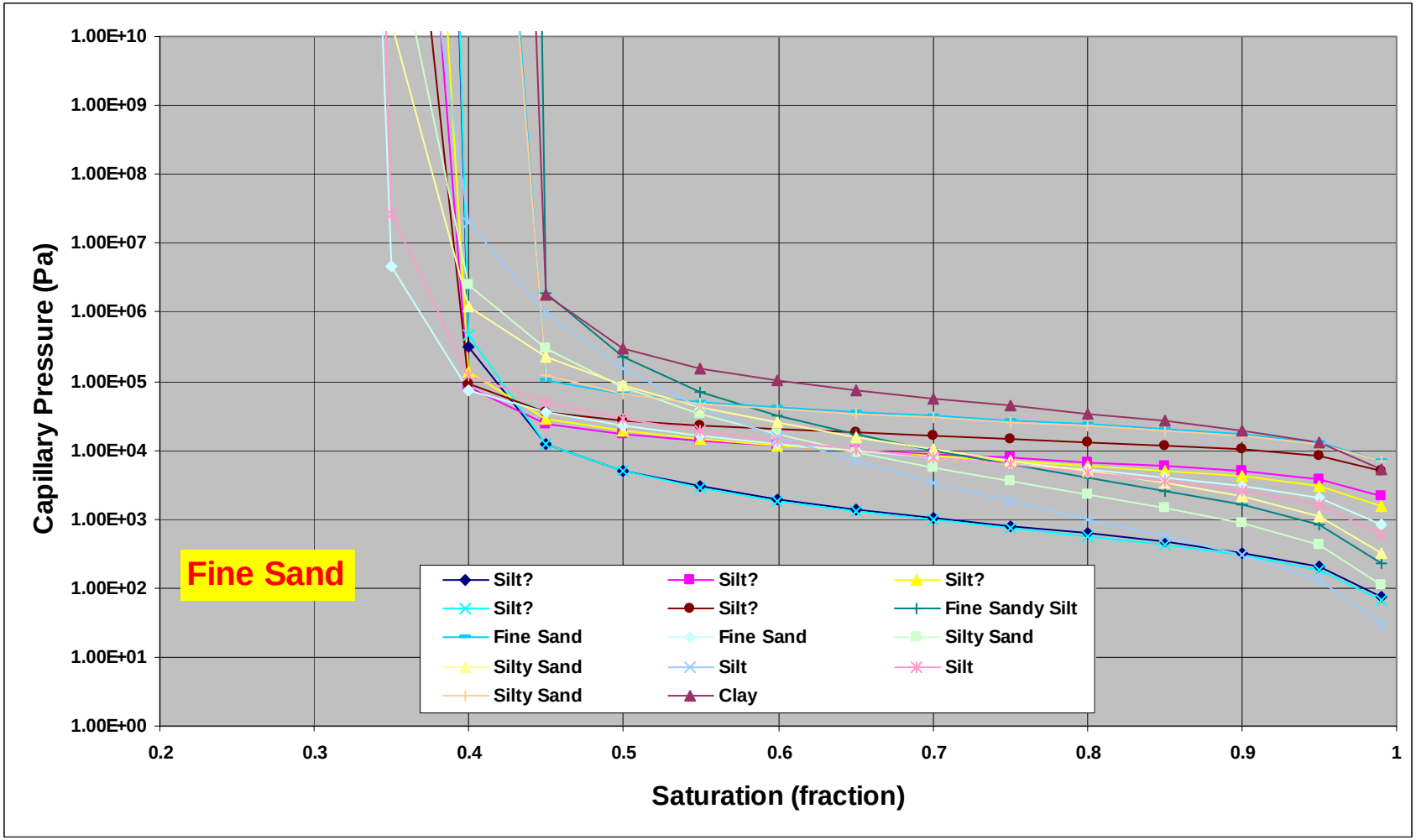

Capillary Pressure Curve for Sand Group at the Site
Calculated as Described in Text

PANACEA, INC.
Environmental Services

Project No. C00-266	Figure 2- 18

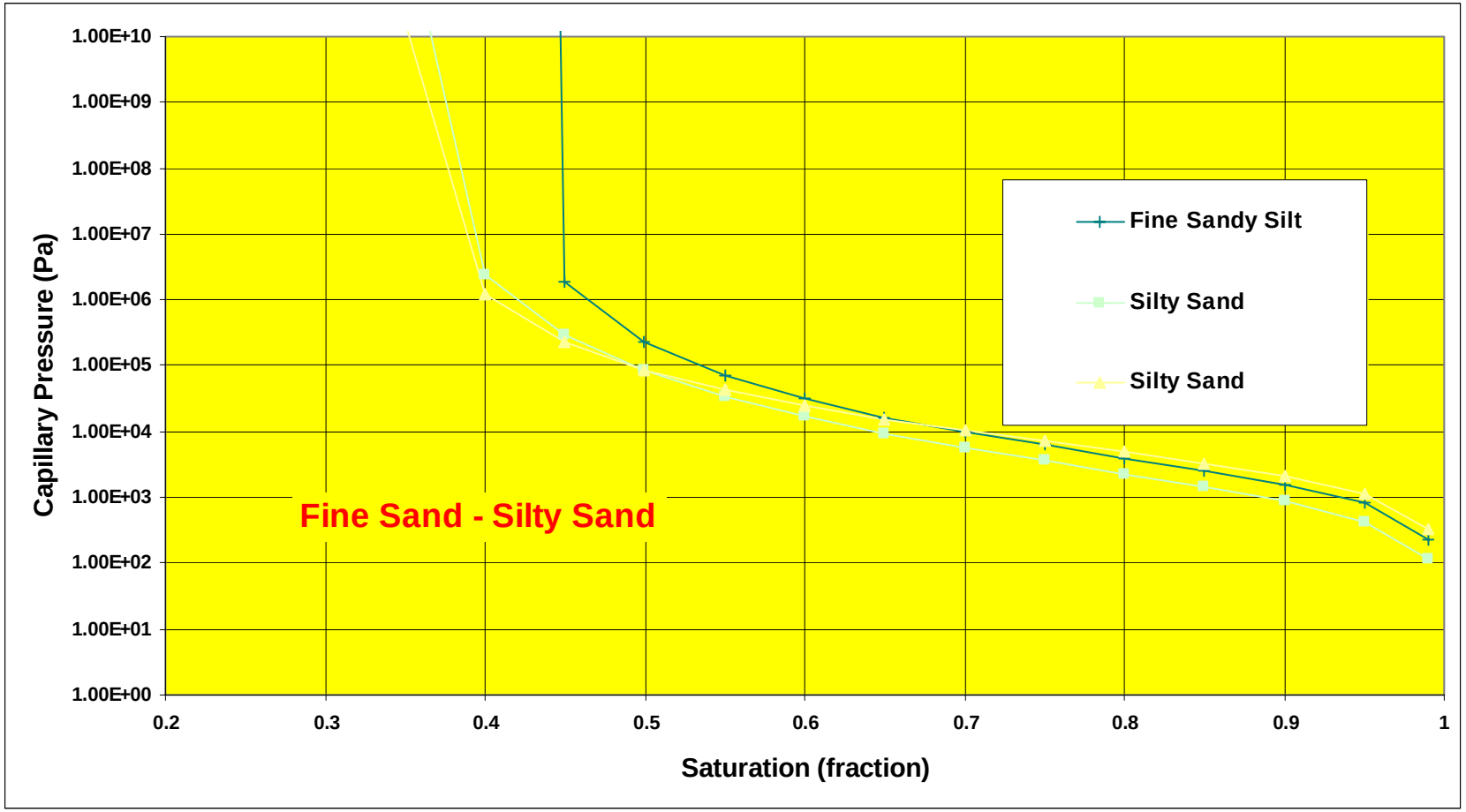

Capillary Pressure Curve for Fine Sand and Silty Sand Group at the Site
Calculated as Described in Text

PANACEA, INC.
Environmental Services

Project No. C00-266	Figure 2- 19

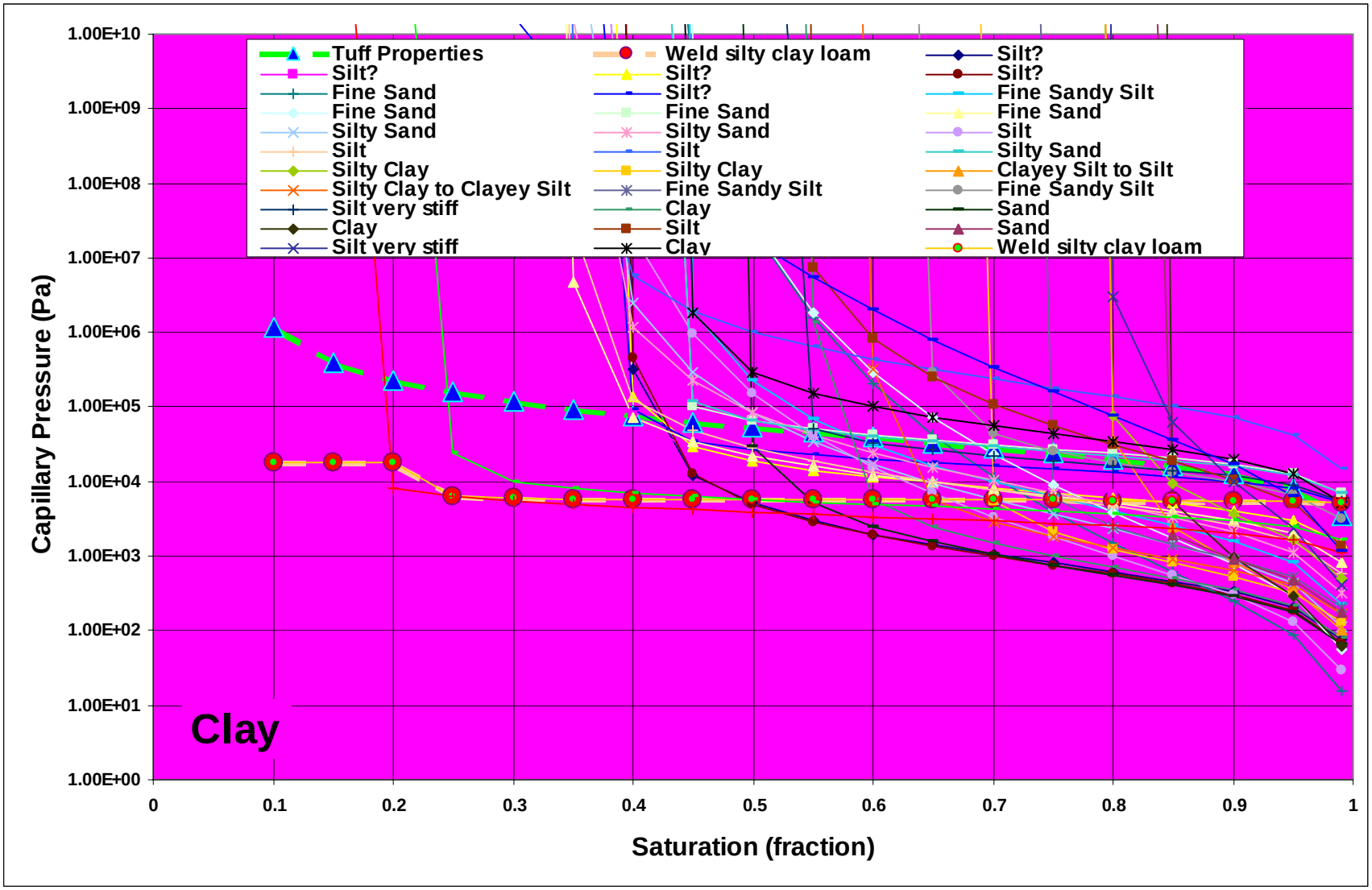

Capillary Pressure Curve for Clay Group at the Site
Calculated as Described in Text Compared with
Typical Distribution in Literature

PANACEA, INC.
Environmental Services

Project No. C00-266	Figure 2- 20

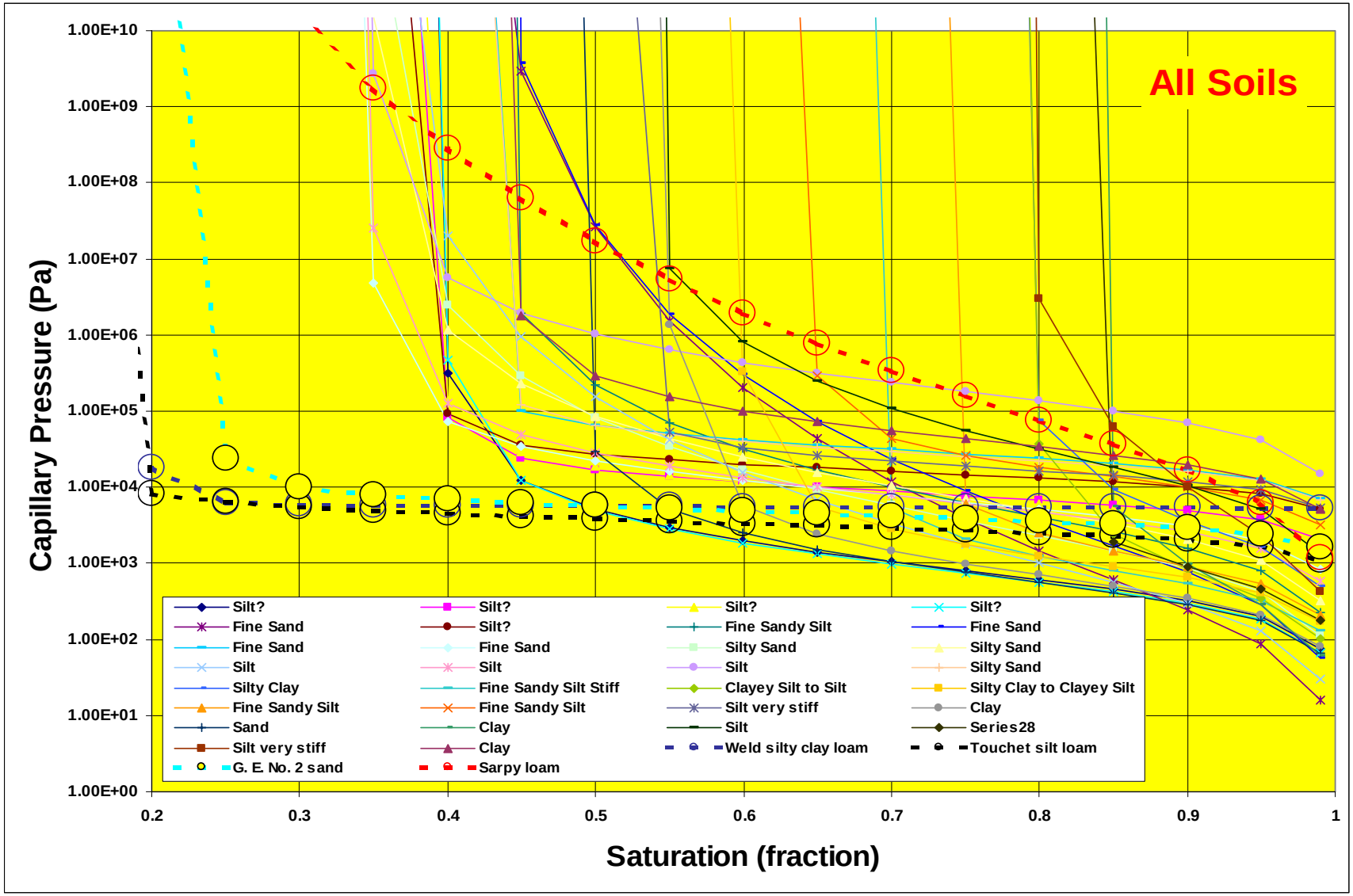

Capillary Pressure Curve for All Soils at the Site Calculated as Described in Text
Compared with Typical Distribution in Literature

PANACEA, INC.
Environmental Services

Project No. C00-266	Figure 2- 21

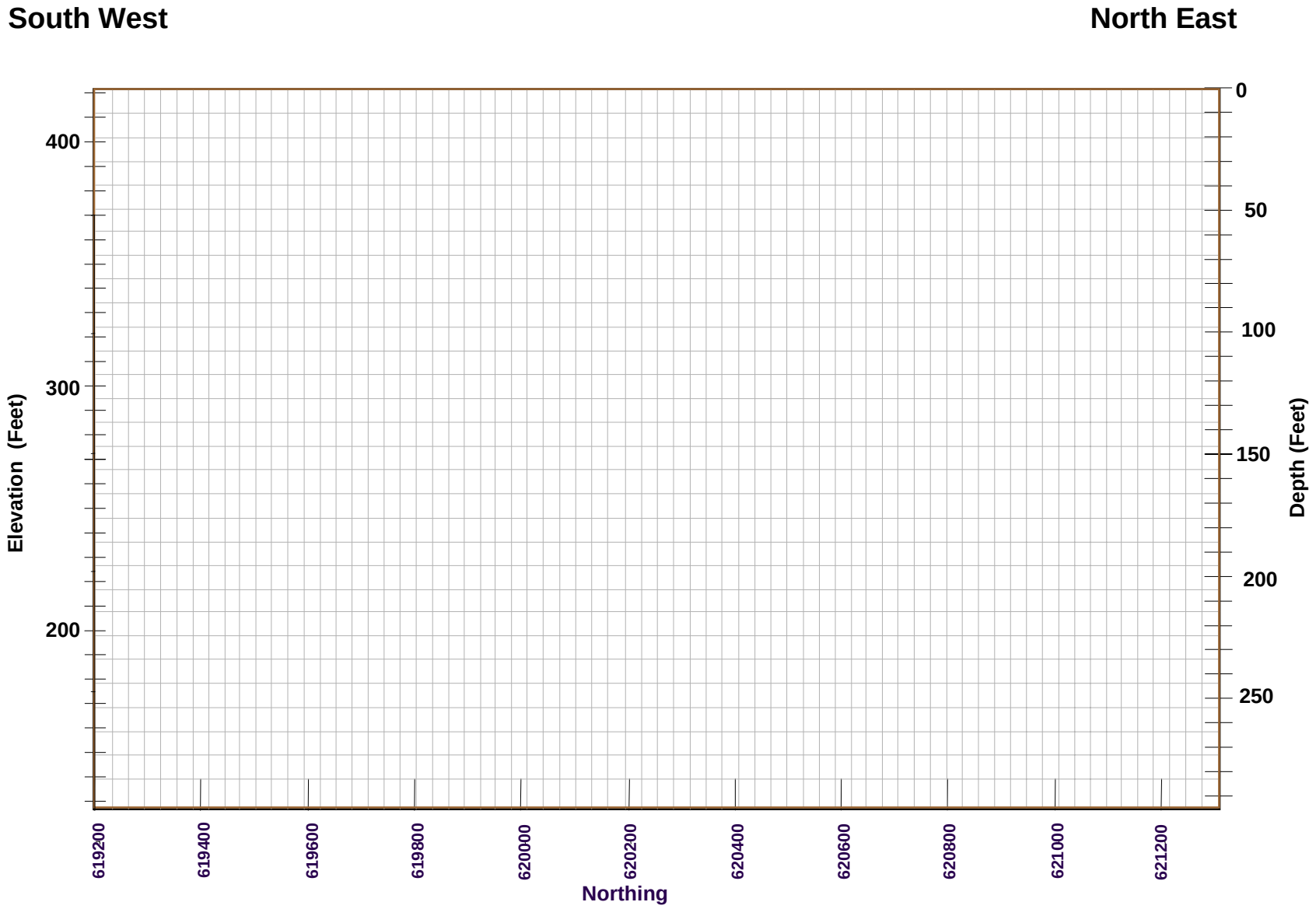

Cross-Sectional Mesh Used for Simulations of Unsaturated Zone

PANACEA, INC.
Environmental Services

Project No. C00-266	Figure 3-1

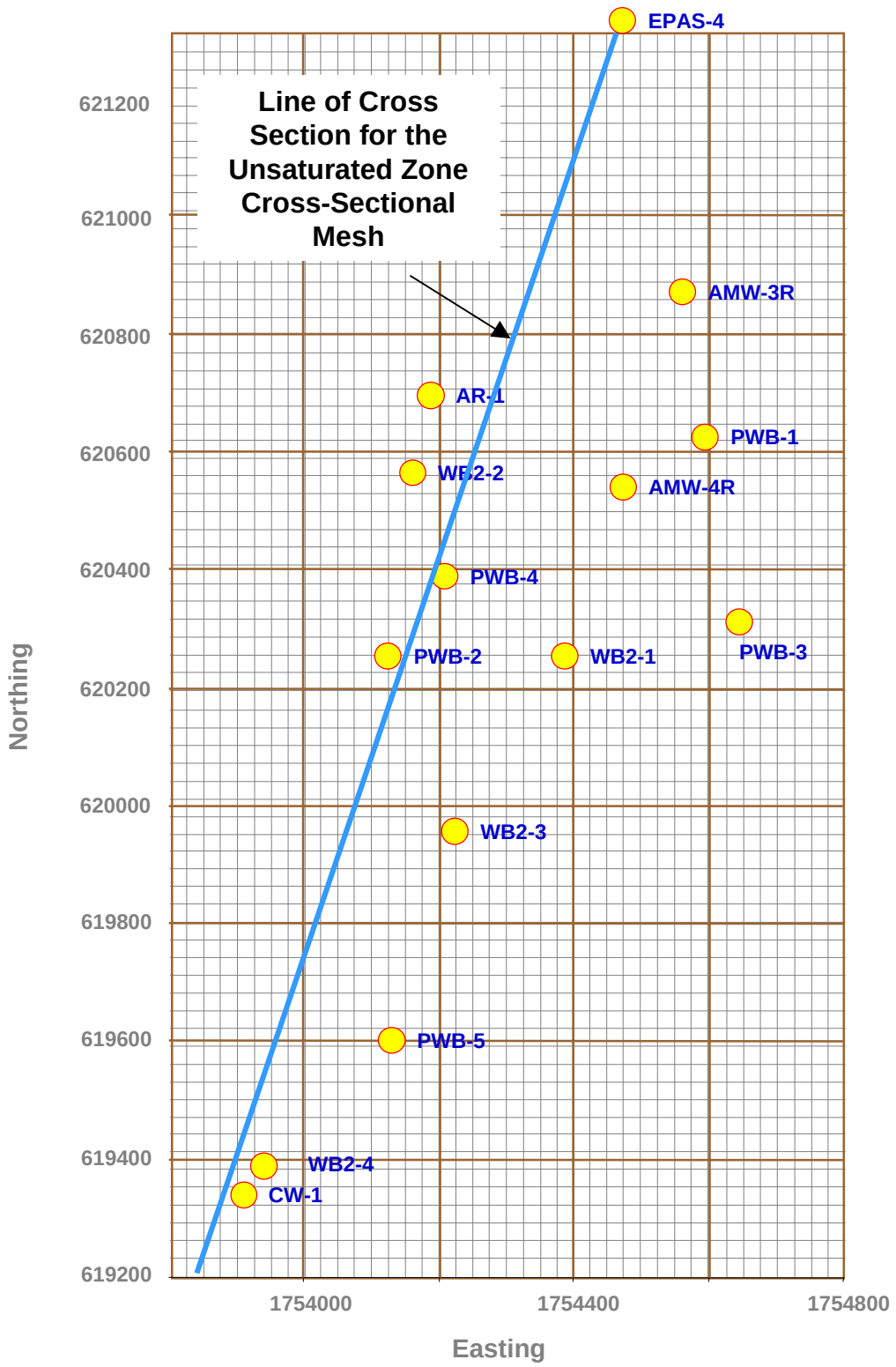

Plan View Mesh Used for Simulations of Saturated B-Zone

PANACEA, INC.
Environmental Services

Project No.
C00-266

Figure 3-2

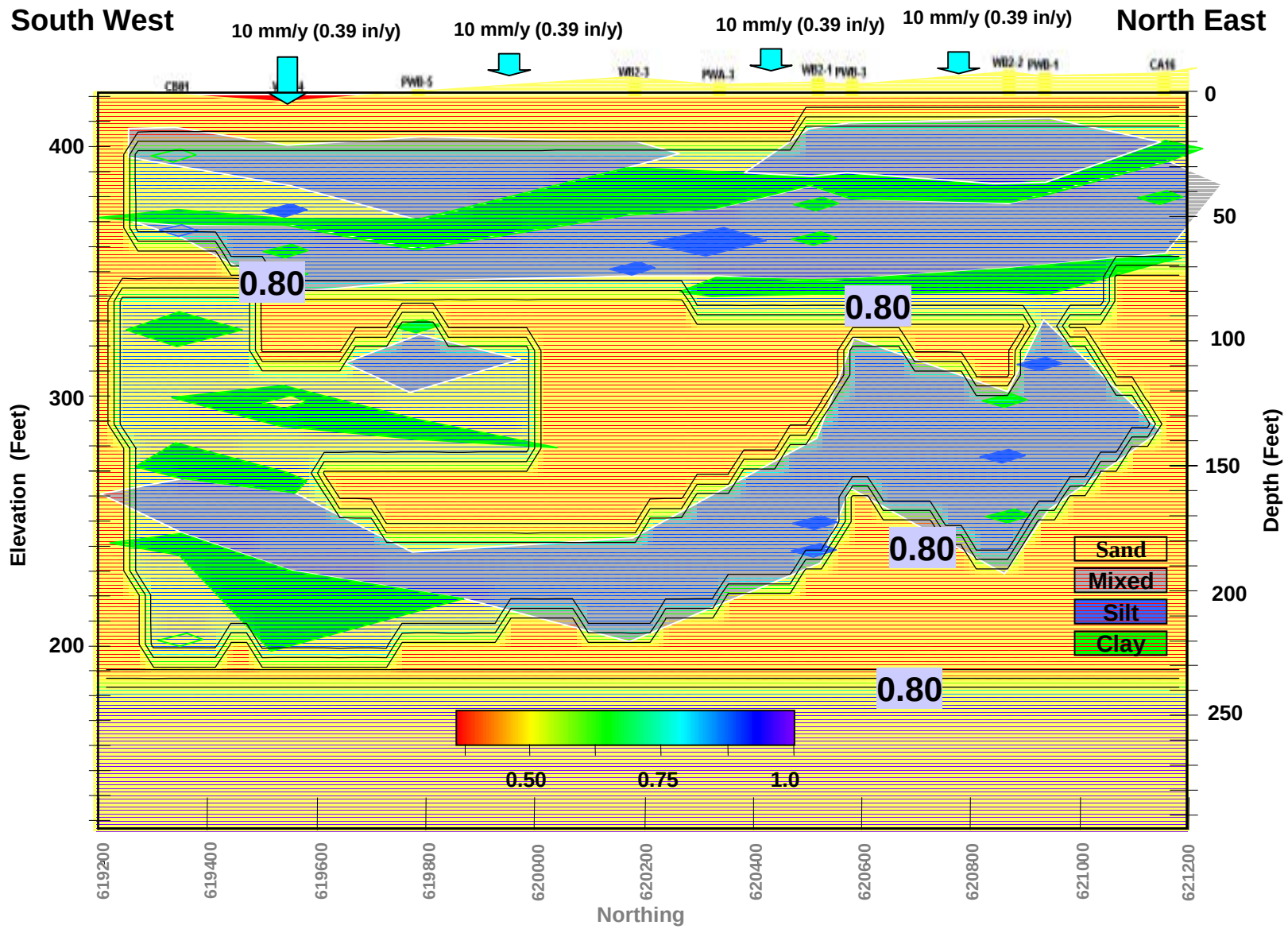

Distribution of Water Saturation Overlain on Conceptual Hydrogeologic Model 1.
A Flat Water Table is Assumed in B-Zone.

PANACEA, INC.
Environmental Services

Project No. C00-266	Figure 4- 1

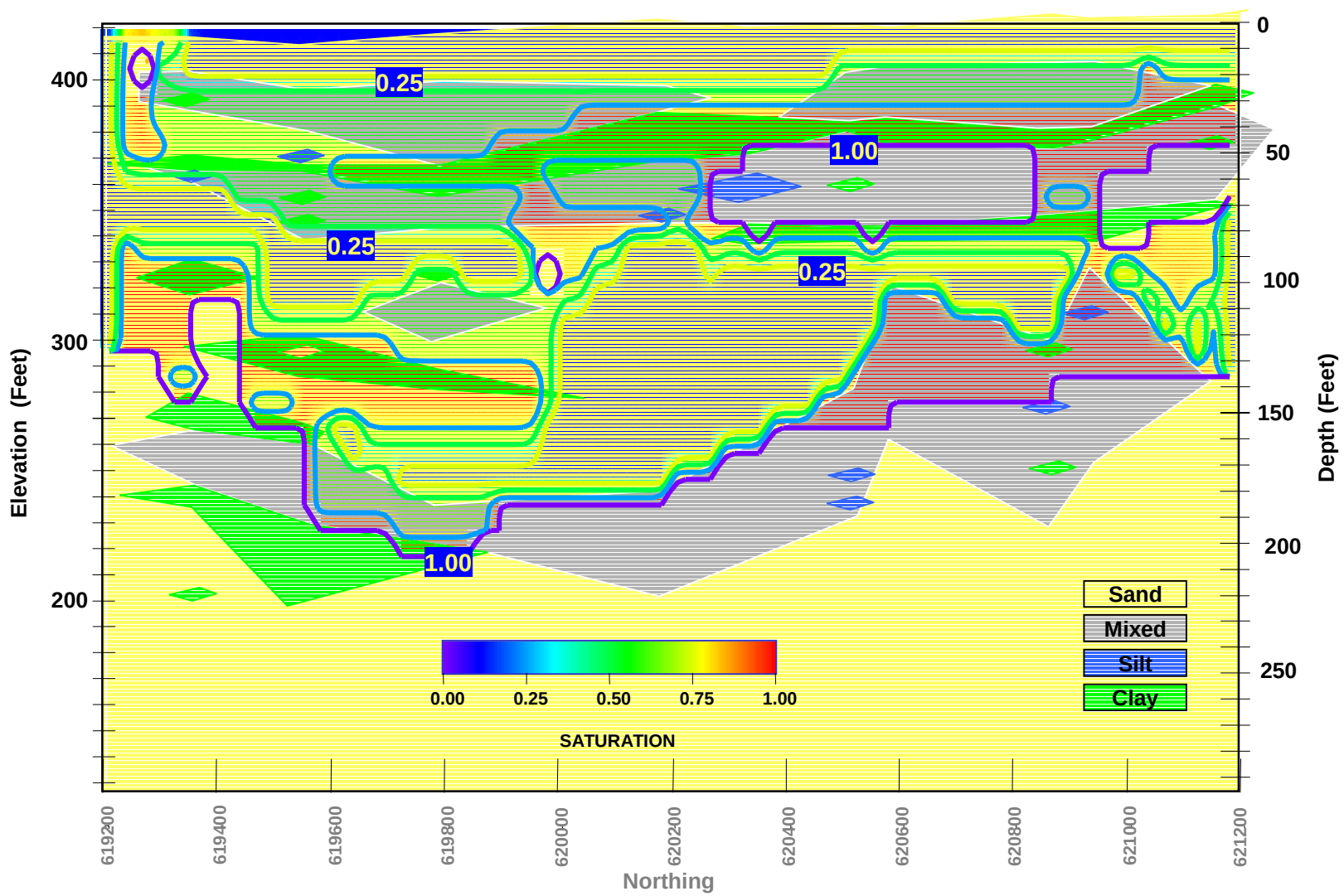

Distribution of Water Saturation Overlain on Conceptual Hydrogeologic Model 1. Alternative Water Table Configuration Assumed for B-Zone Using Data from Existing Wells.

PANACEA, INC.
Environmental Services

Project No. C00-266

Figure 4- 2

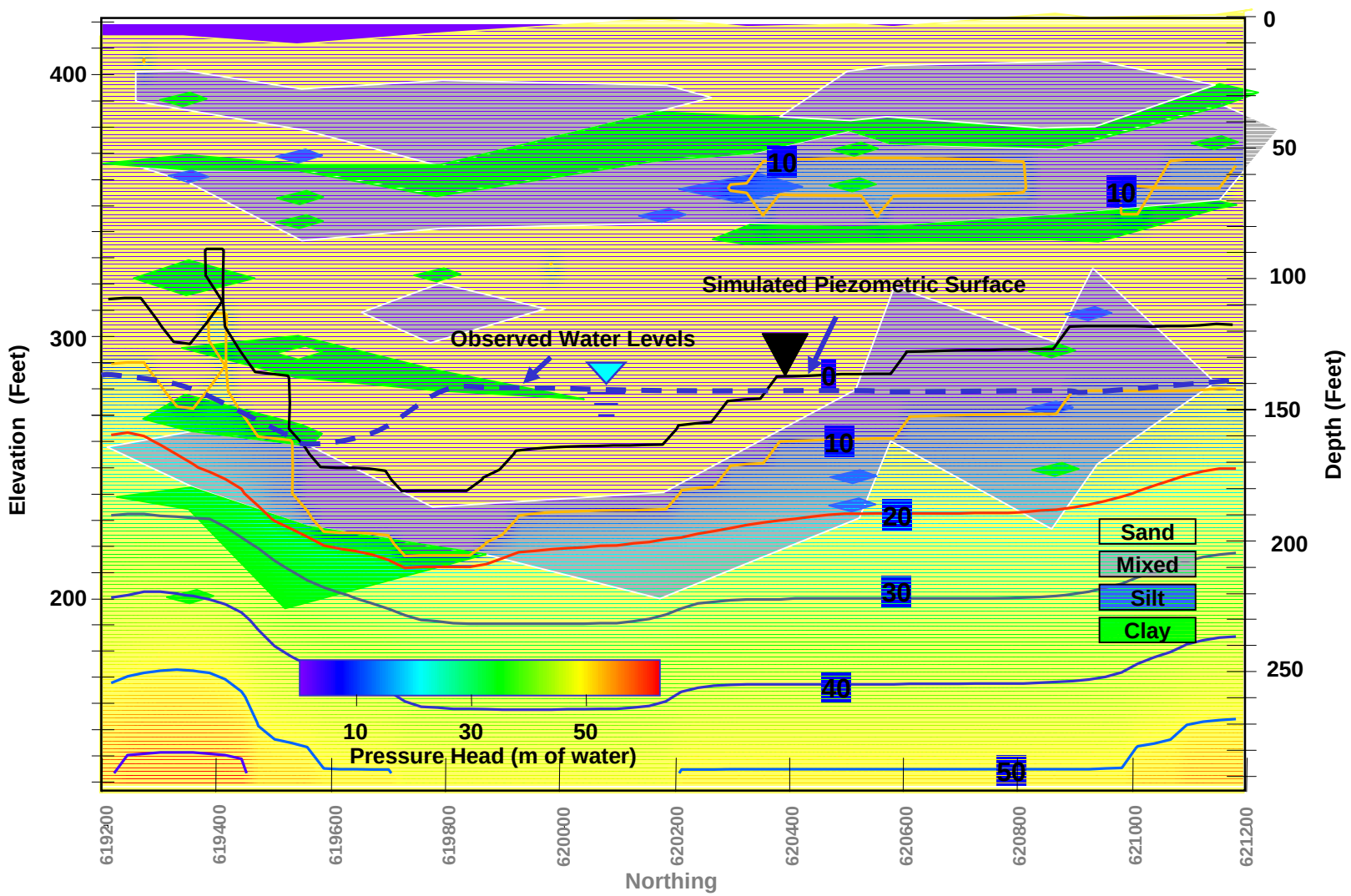

Pressure Head (m) Overlain on Conceptual Hydrogeologic Model 1. Alternative Water Table Configuration Assumed for B-Zone Using Data from Existing Wells.

PANACEA, INC.
Environmental Services

Project No. C00-266

Figure 4- 3

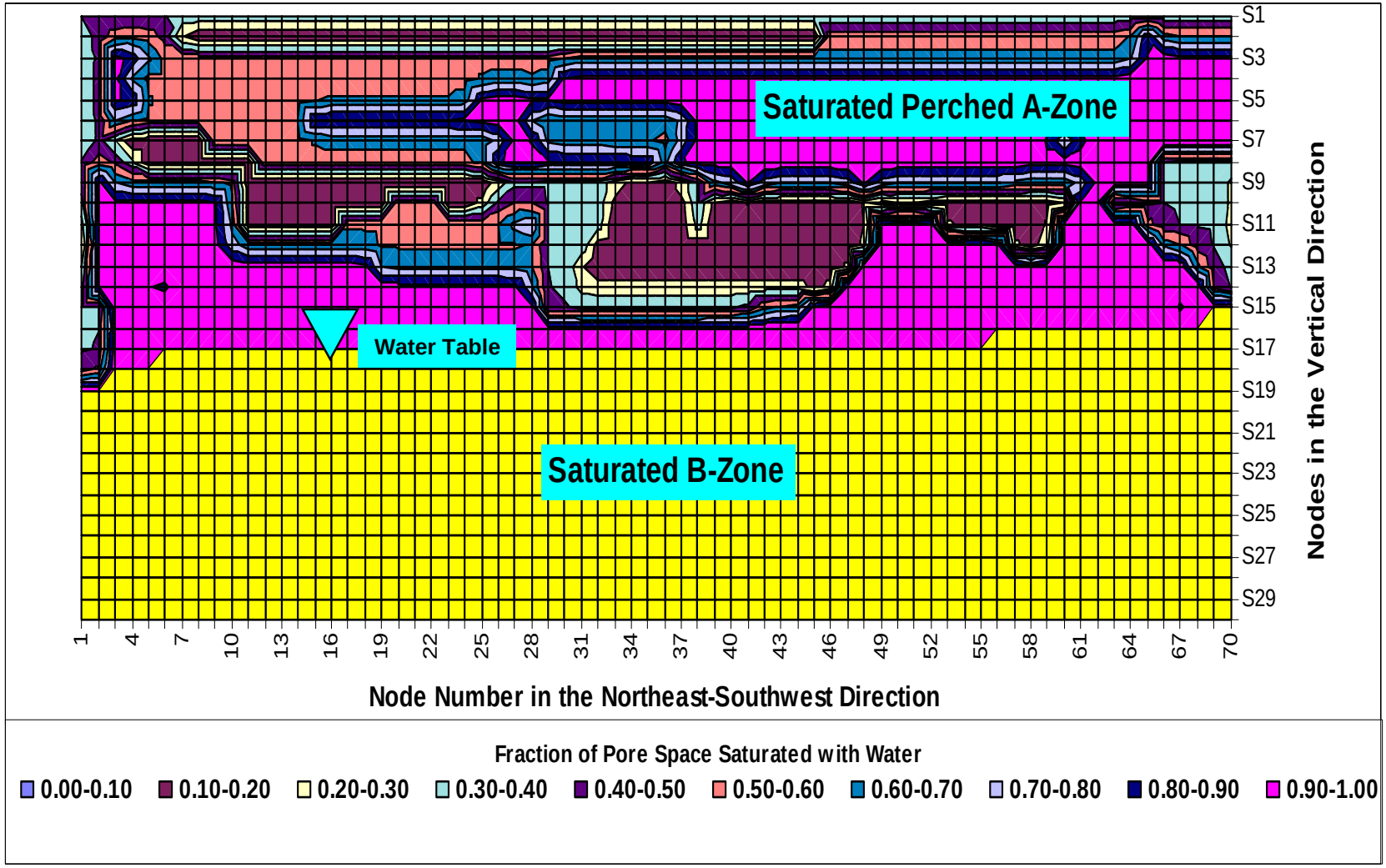

Water Saturation Overlain on Conceptual Hydrogeologic Model 1. Alternative Corrected Water Table for B-Zone is Used Ignoring Data from Existing Wells in the Southwest End of the Cross Section.

PANACEA, INC.
Environmental Services

Project No. C00-266	Figure 4- 4

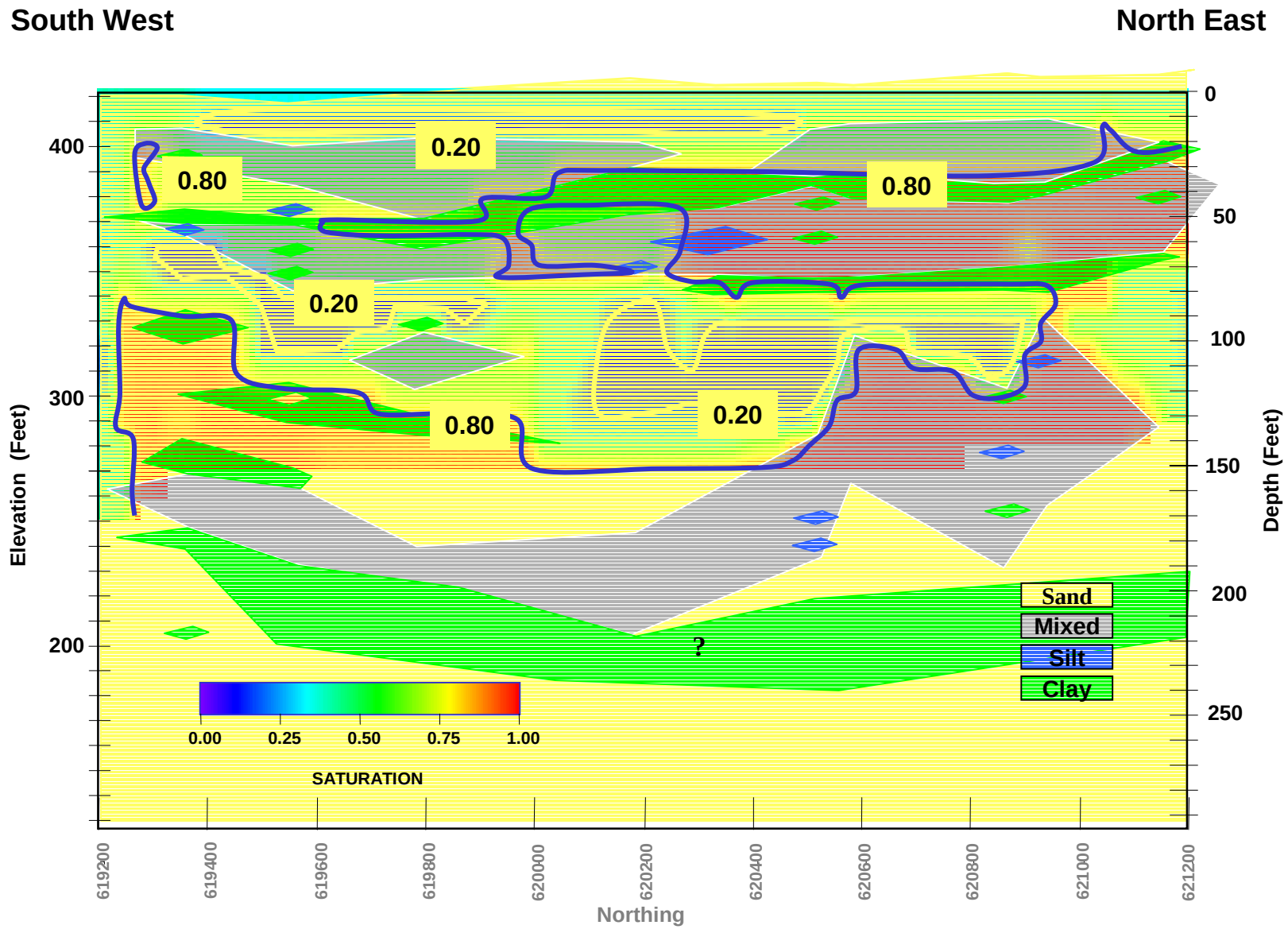

Water Saturation Overlain on Conceptual Hydrogeologic Model 2.
Alternative Corrected Water Table for B-Zone Using Data from
Existing Wells.

PANACEA, INC.
Environmental Services

Project No.
C00-266

Figure 4- 5

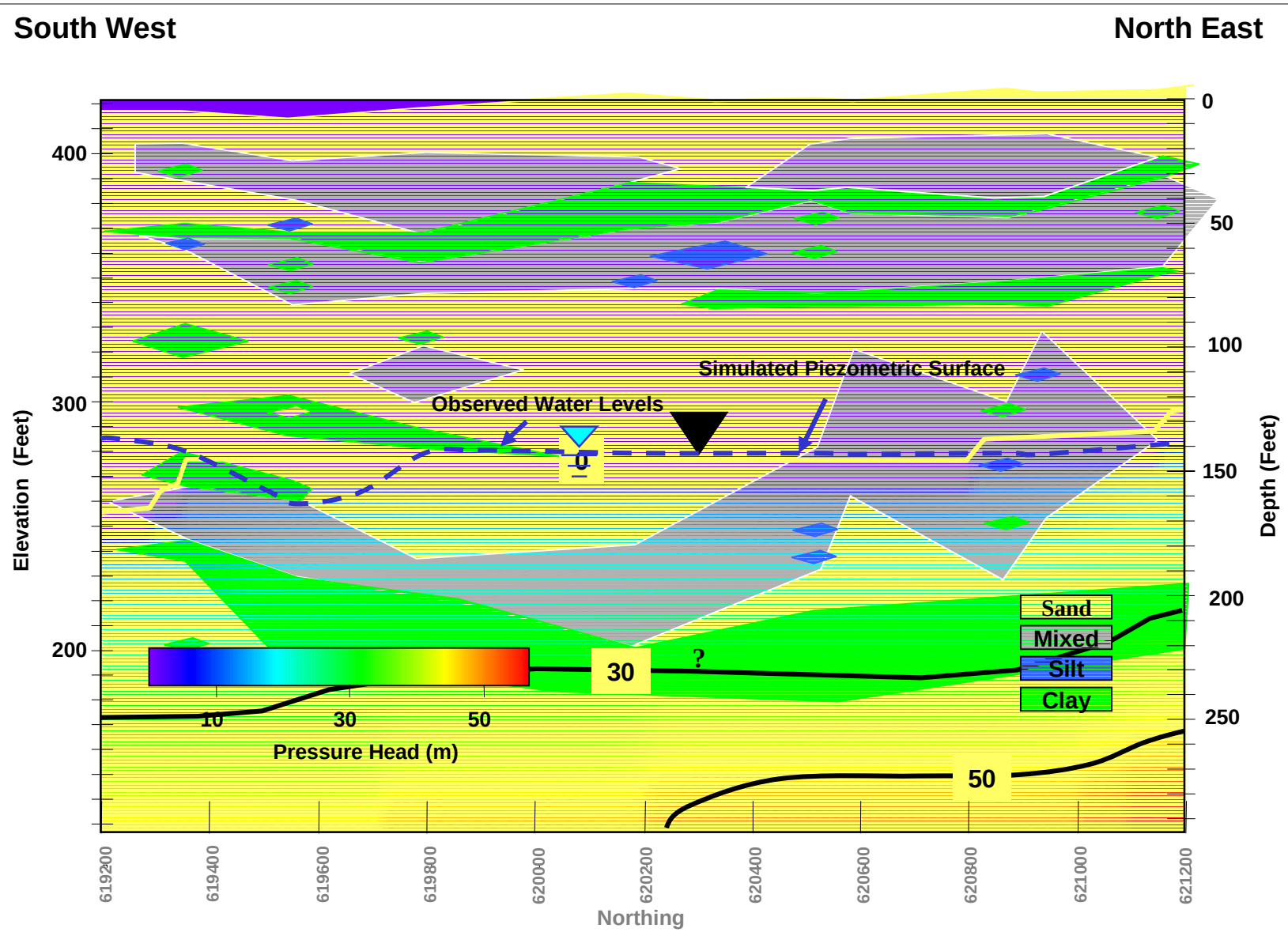

Pressure Head (m) Overlain on Conceptual Hydrogeologic Model 2. Alternative Corrected Water Table for B-Zone is Used Ignoring Data from Existing Wells in the Southwest End of the Cross Section.

PANACEA, INC.
Environmental Services

Project No. C00-266

Figure 4- 6

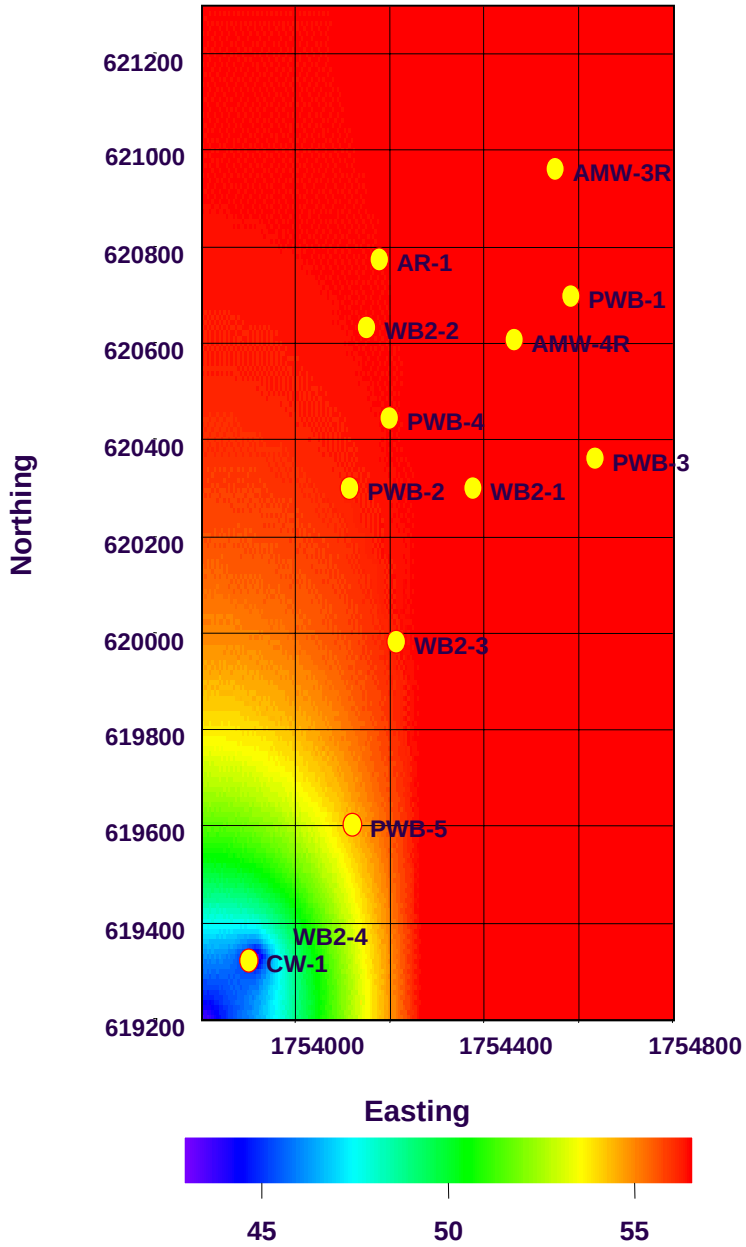

Pressure Head (m) in the B-zone

PANACEA, INC.
Environmental Services

Project No.	Figure
C00-266	4-7

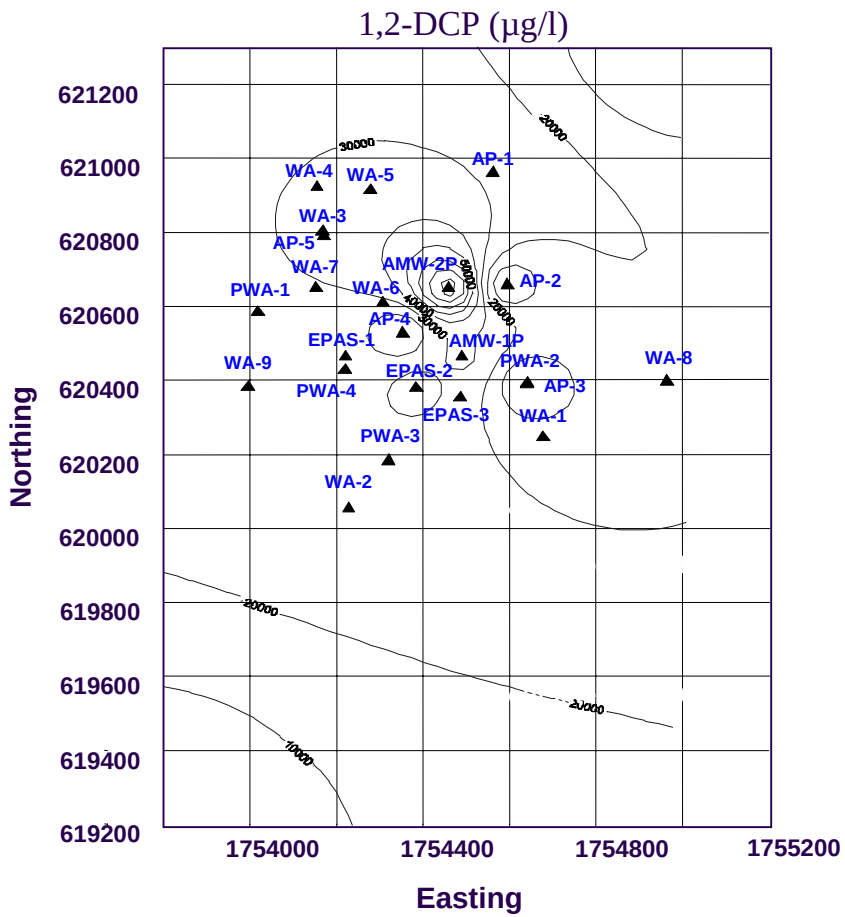

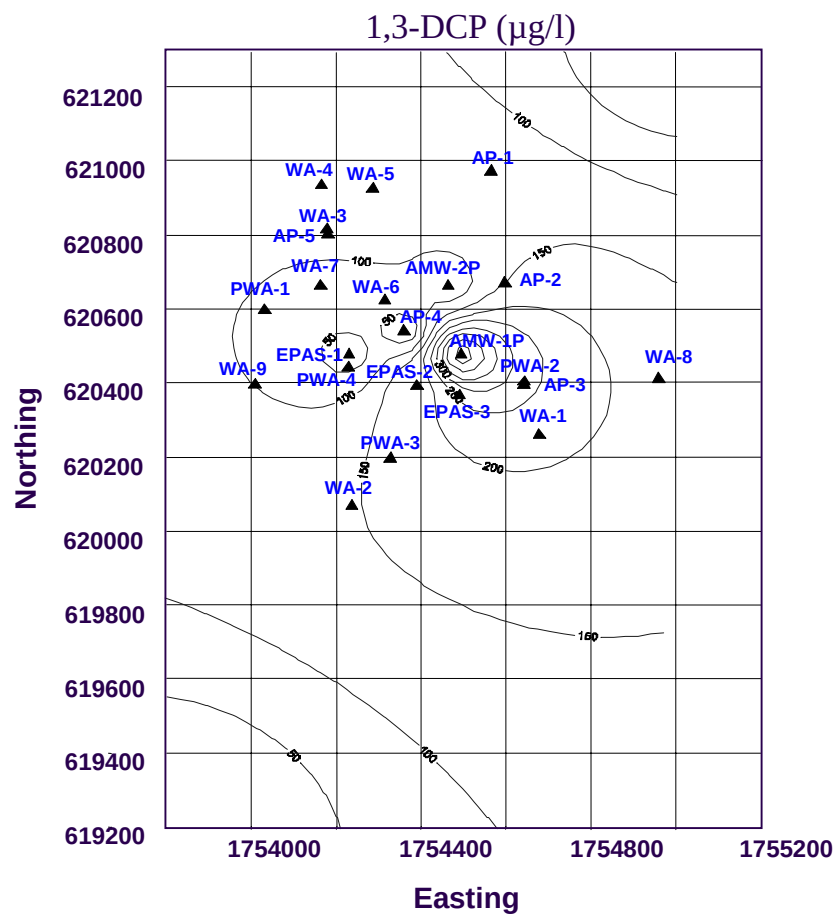

Legend

+ Approximate Location of Borehole

100 Iso-Concentration

Contour Intervals: 500 (µg/l)

Interpolation : Inverse Distance
Software: Surfer

Maximum Chemical Concentration Distribution in A-zone Groundwater in 1991

PANACEA, INC.
Environmental Services

Project No. C00-266	Figure 4-8

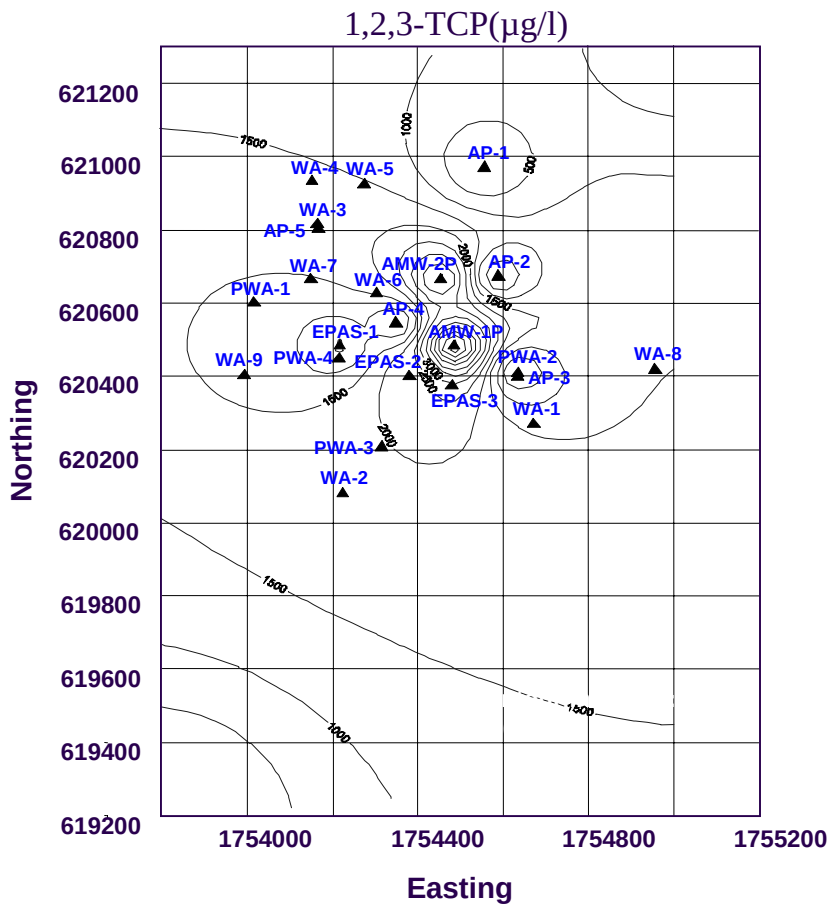

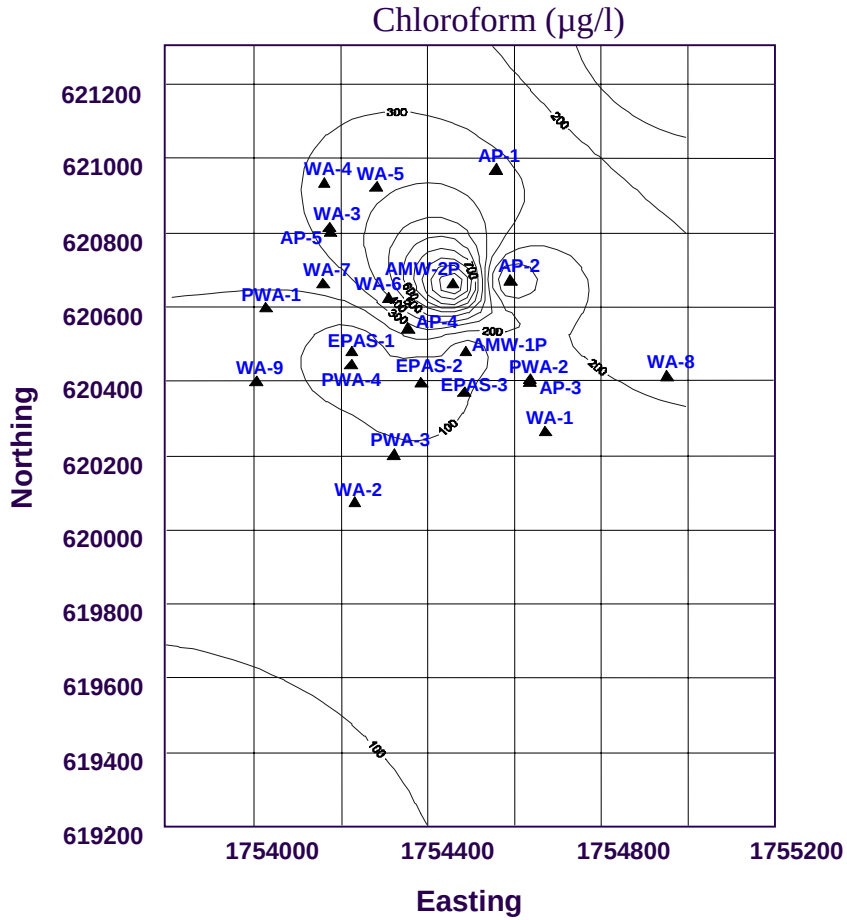

Legend

+ Approximate Location of Borehole

100 Iso-Concentration

Contour Intervals: 500 (µg/l)

Interpolation : Inverse Distance
Software: Surfer

Maximum Chemical Concentration Distribution in A-zone Groundwater in 1991

PANACEA, INC.
Environmental Services

Project No. C00-266	Figure 4-9

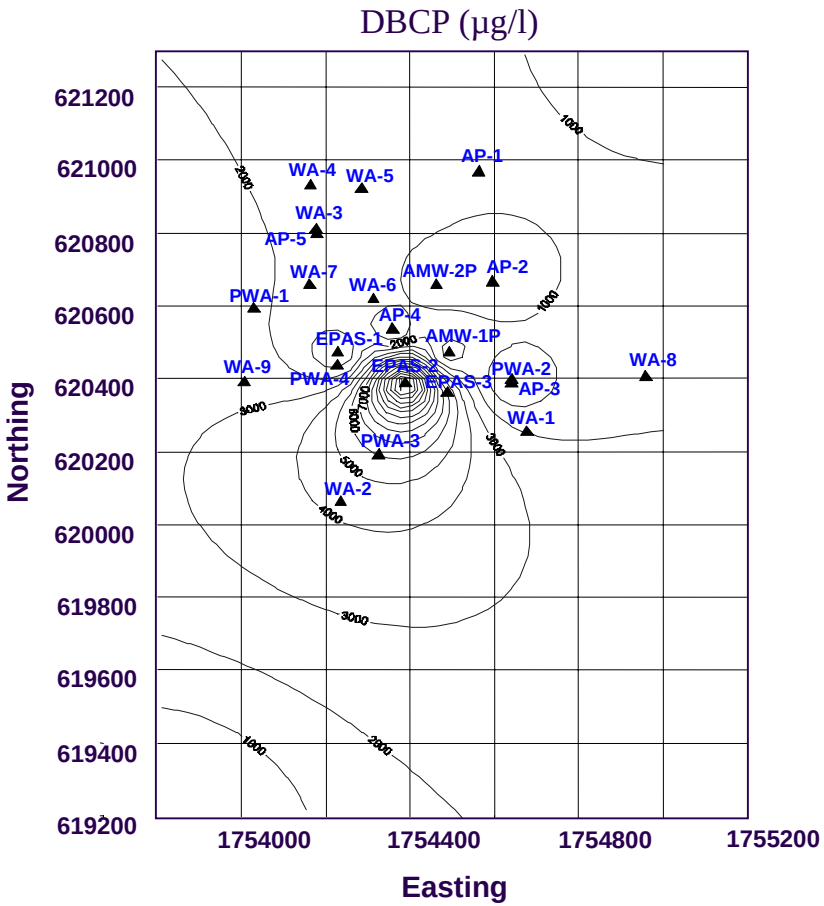

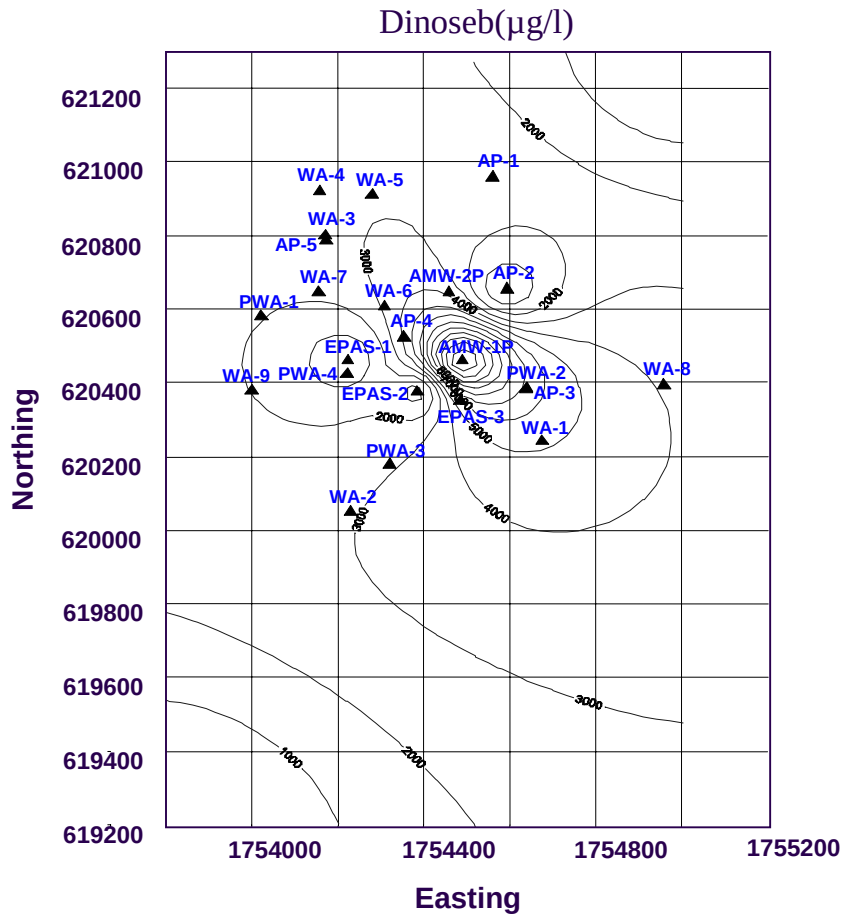

Legend

+ Approximate Location of Borehole

100 Iso-Concentration

Contour Intervals: 500 (µg/l)

Interpolation : Inverse Distance
Software: Surfer

Maximum Chemical Concentration Distribution in A-zone Groundwater in 1991

PANACEA, INC.
Environmental Services

Project No. C00-266	Figure 4-10

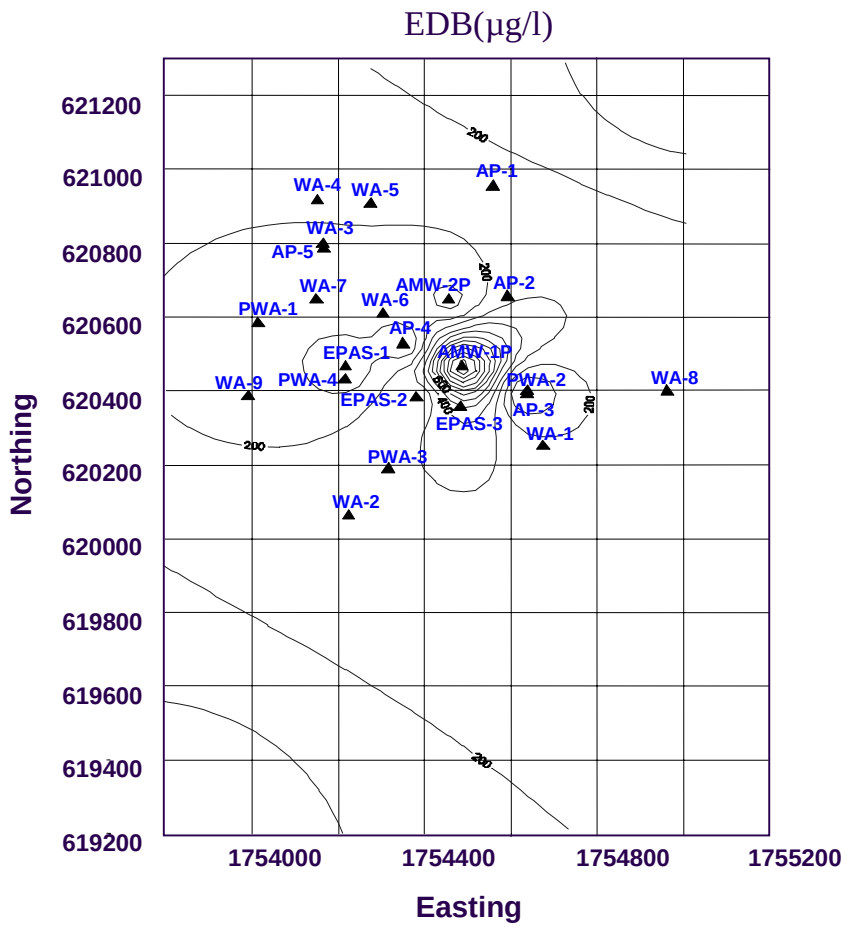

Legend

+ Approximate Location of Borehole

100 Iso-Concentration

Contour Intervals: 500 (µg/l)

Interpolation : Inverse Distance
Software: Surfer

Maximum Chemical Concentration Distribution in A-zone Groundwater in 1991

PANACEA, INC.
Environmental Services

Project No. C00-266	Figure 4-11

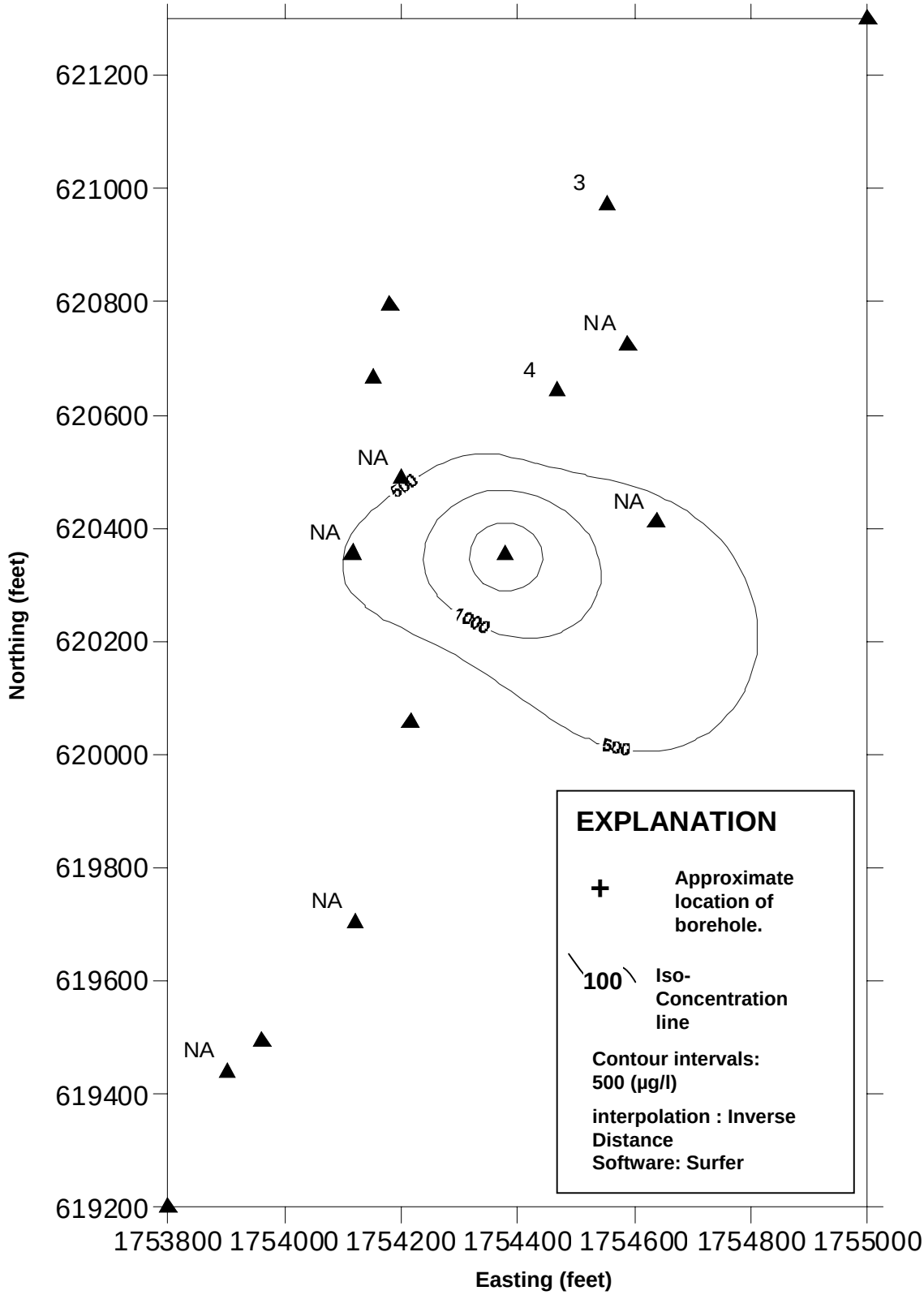

Distribution of Maximum Concentration of 1,2-DCP (µg/l) in B-Zone Groundwater in 1992

PANACEA, INC.
Environmental Services

Project No.	Figure 4-12
C00-266	

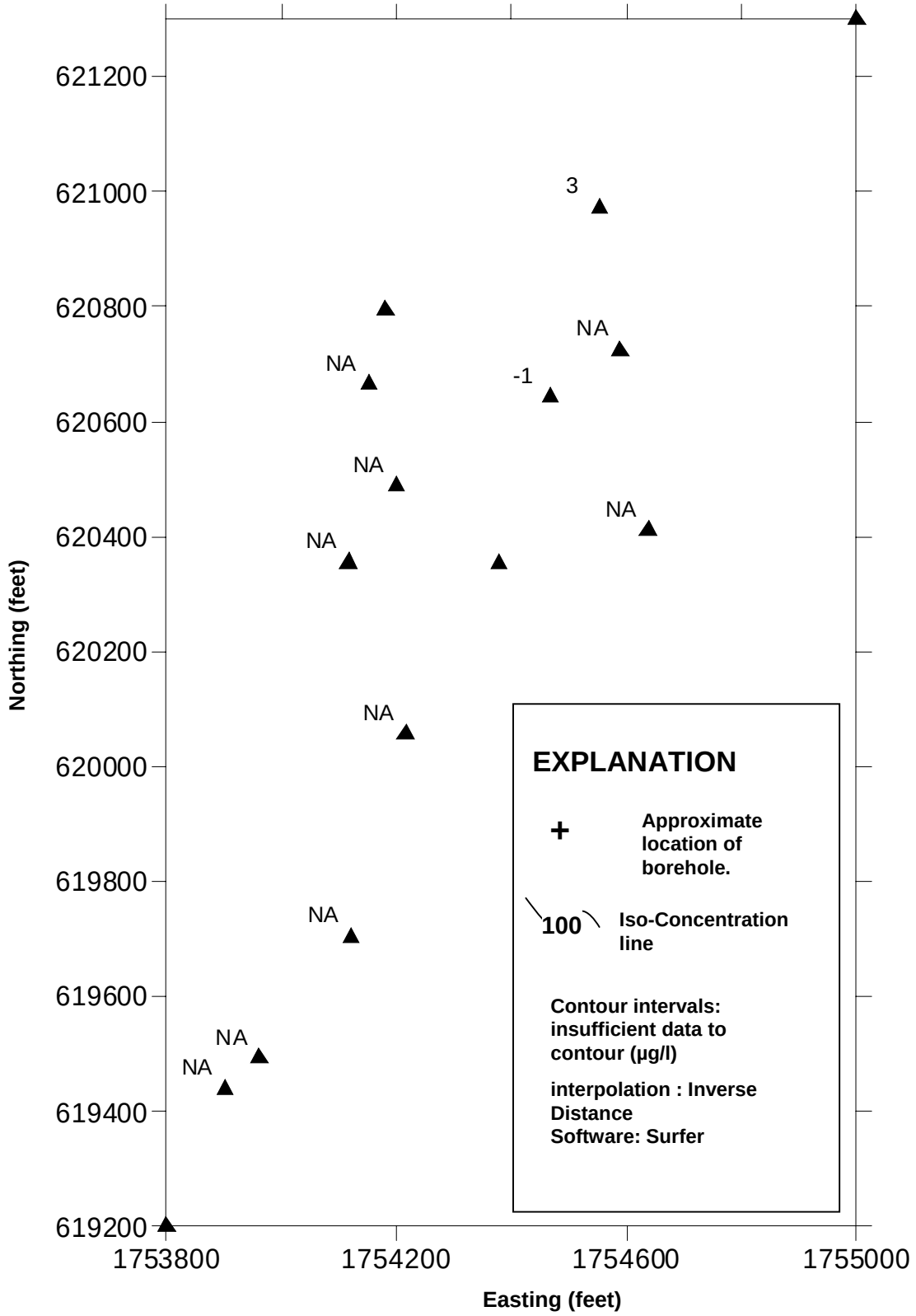

Distribution of Maximum Concentration of 1,3-DCP (µg/l) in B-Zone Groundwater in 1992

PANACEA, INC.
Environmental Services

Project No.	Figure 4-13
C00-266	

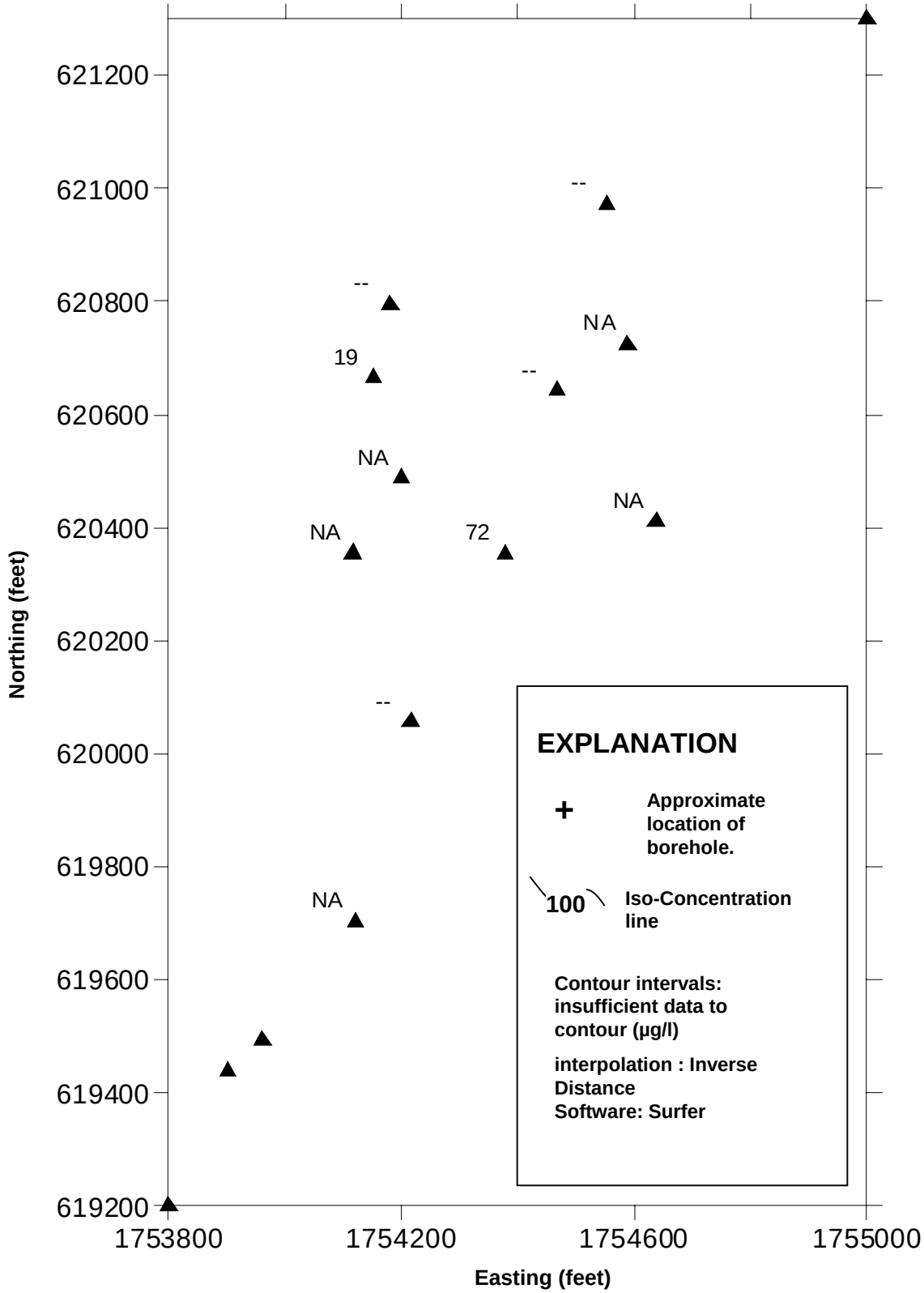

Distribution of Maximum Concentration of 1,2,3-TCP (µg/l) in B-Zone Groundwater in 1992

PANACEA, INC.
Environmental Services

Project No.
C00-266

Figure 4-14

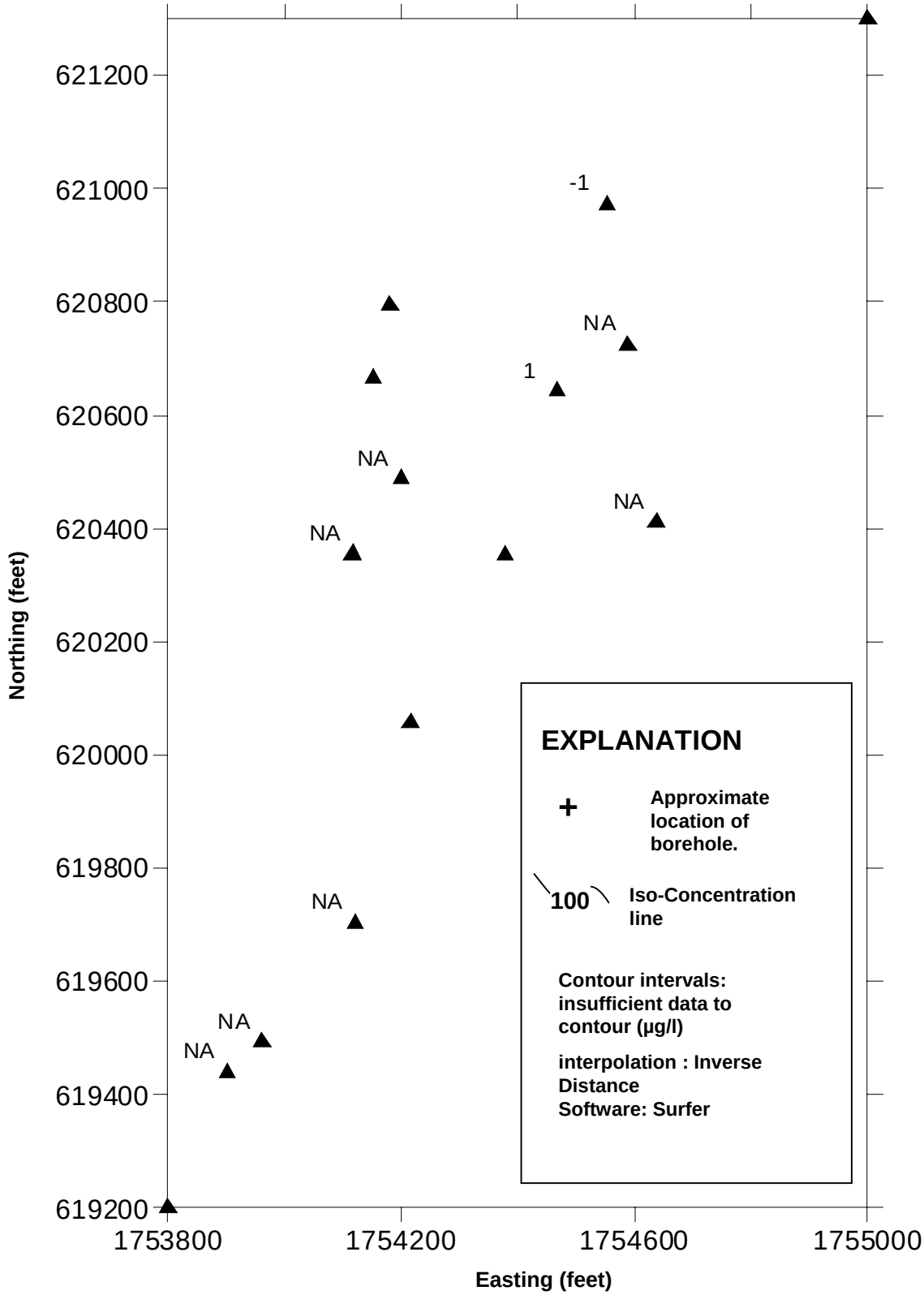

Distribution of Maximum Concentration of Chloroform (µg/l) in B-Zone Groundwater in 1992

PANACEA, INC.
Environmental Services

Project No.
C00-266

Figure 4-15

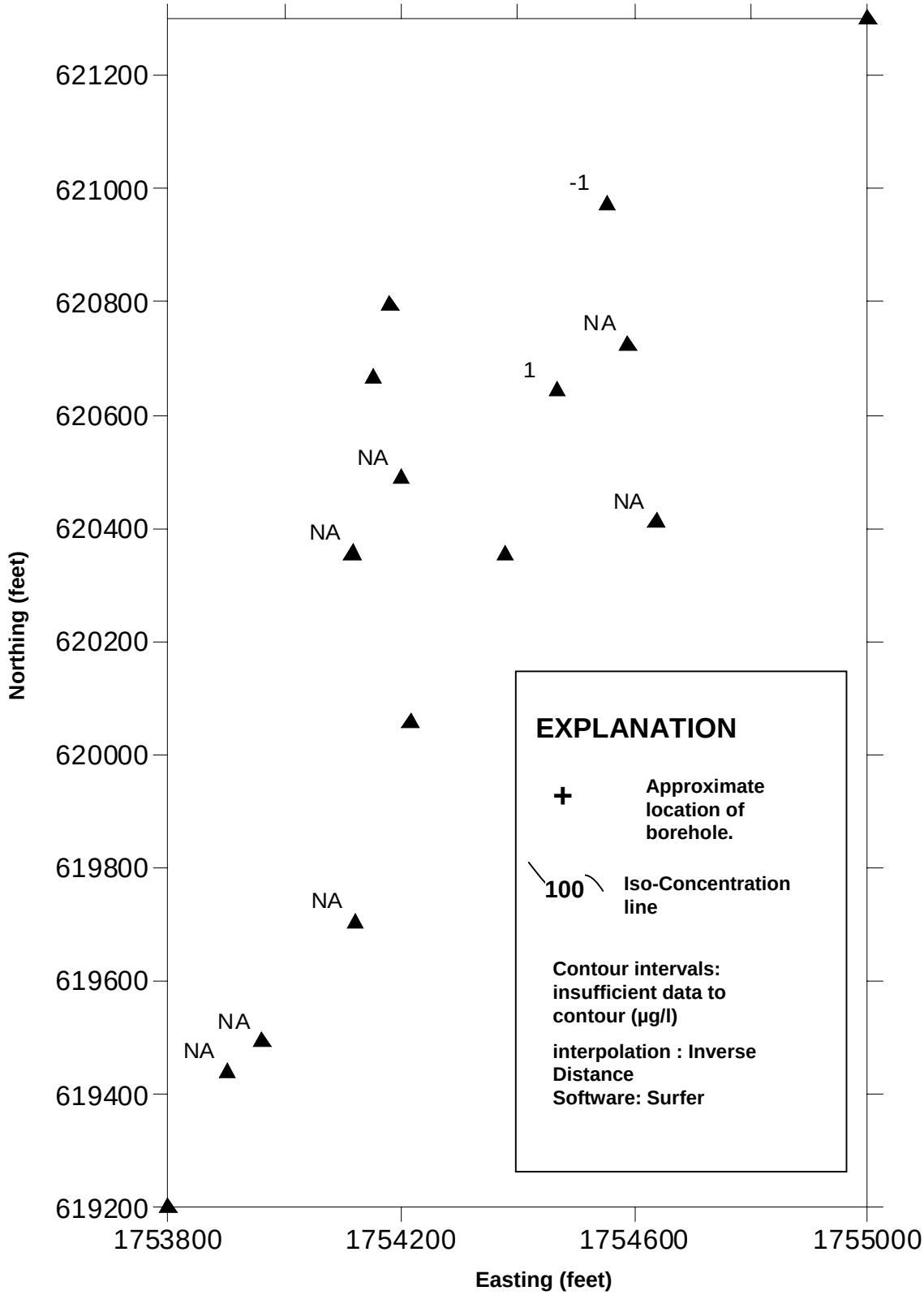

Distribution of Maximum Concentration of DBCP (µg/l) in B-Zone Groundwater in 1992

PANACEA, INC.
Environmental Services

Project No.
C00-266

Figure 4-16

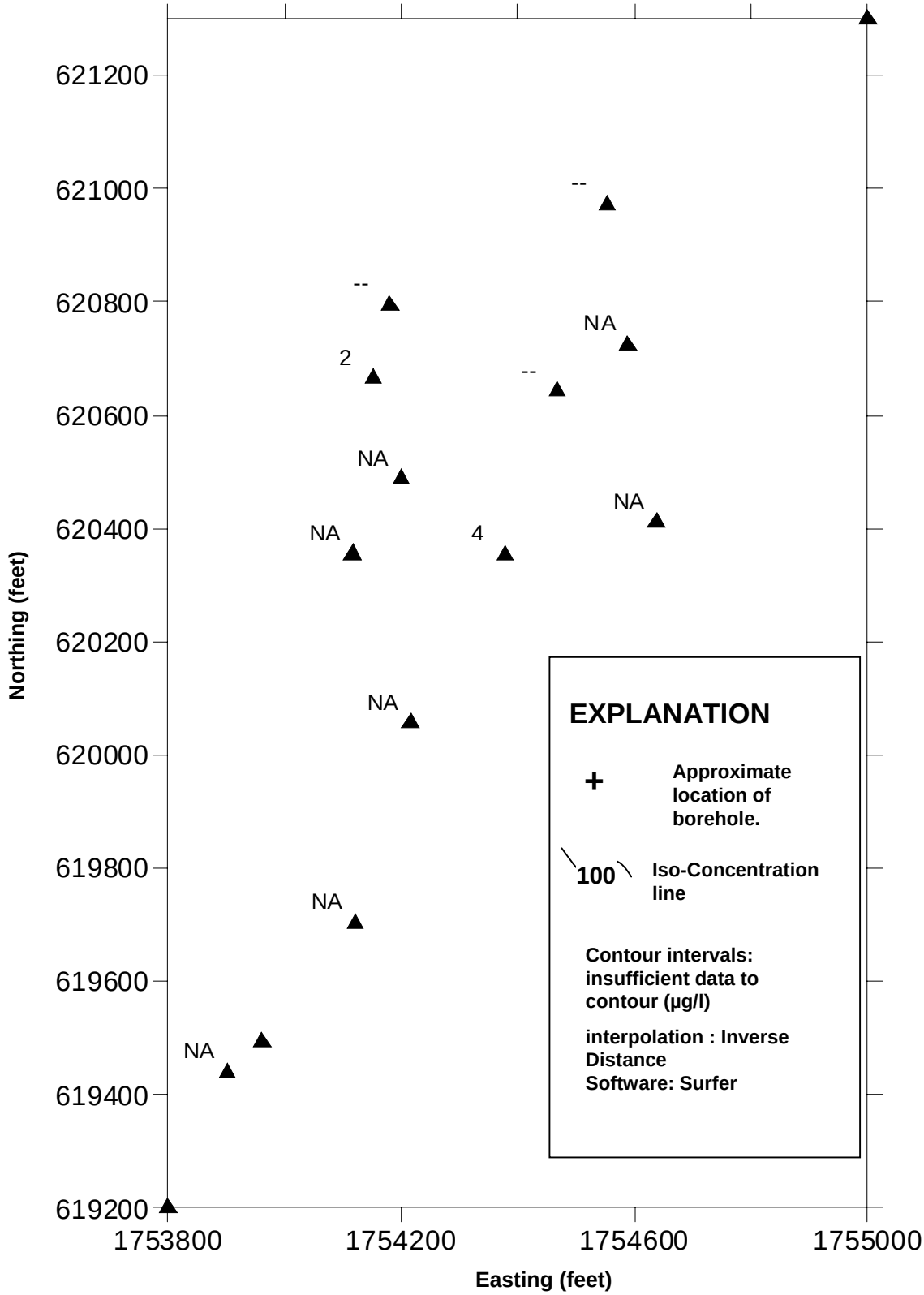

Distribution of Maximum Concentration of Dinoseb (µg/l) in A-Zone Groundwater

PANACEA, INC.
Environmental Services

Project No.
C00-266

Figure 4-17

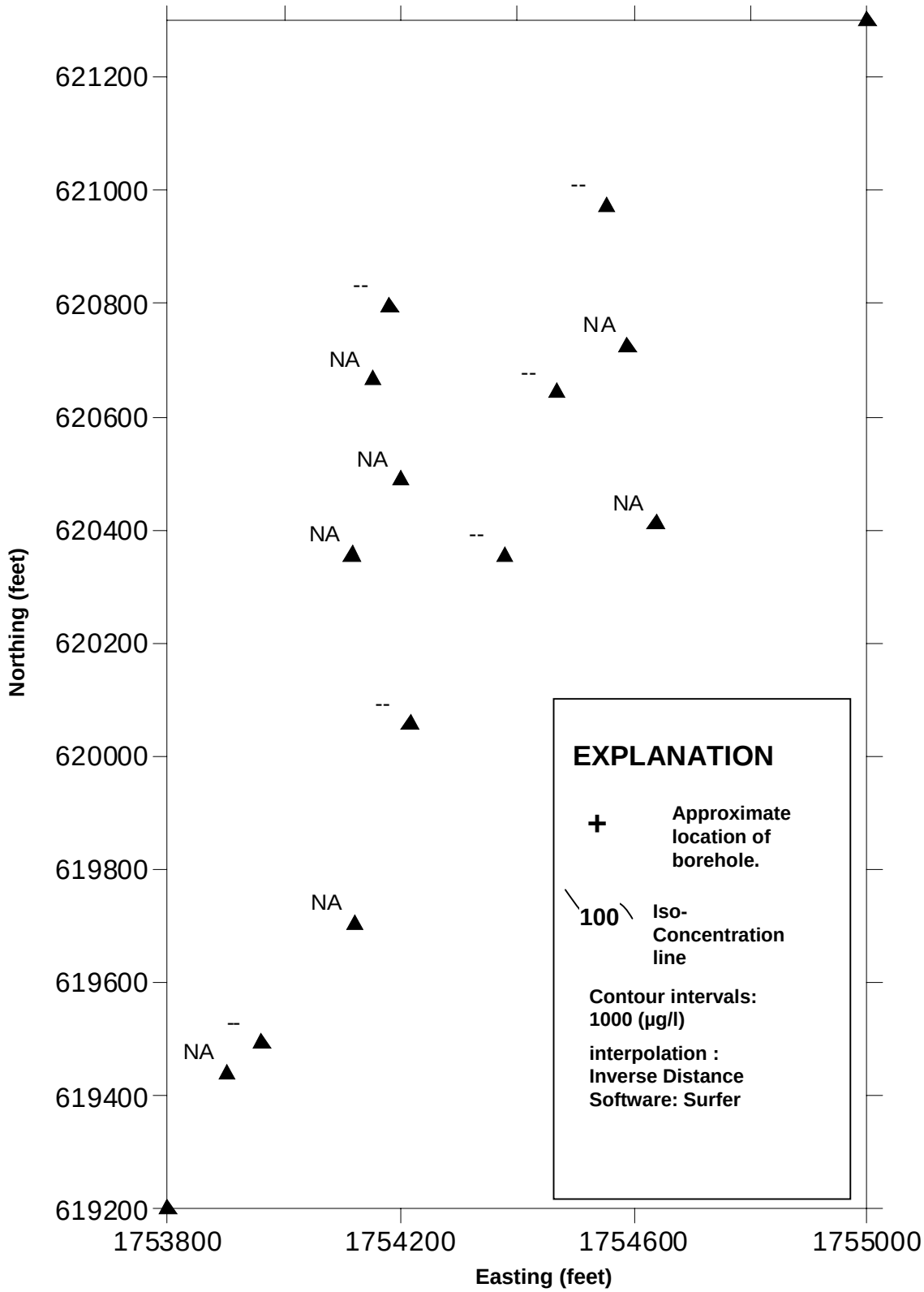

Distribution of Maximum Concentration of EDB (µg/l) in A-Zone Groundwater

PANACEA, INC.
Environmental Services

Project No.	Figure 4-18
C00-266	

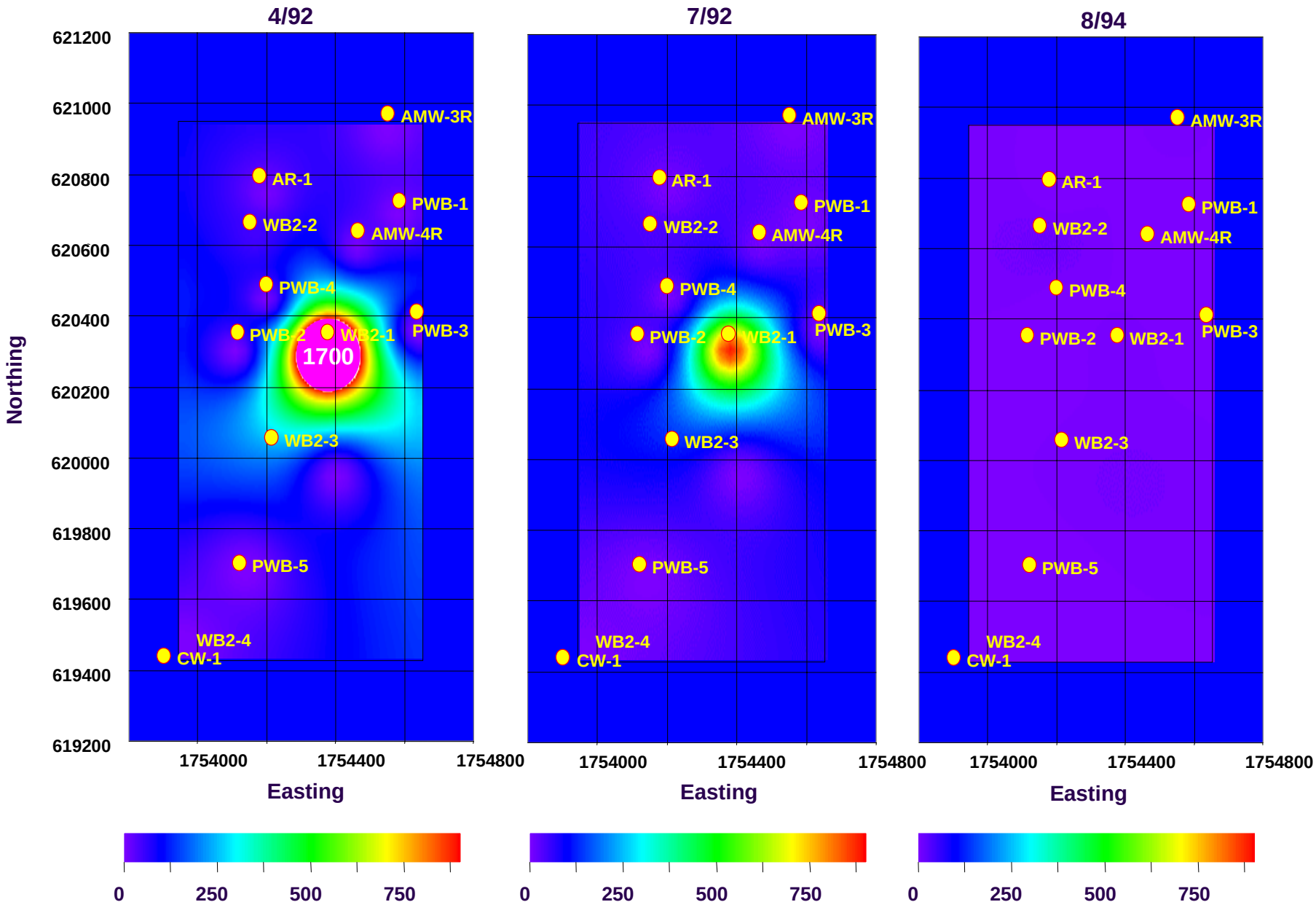

Concentration of 1,2-DCP (µg/l) in the B-zone

PANACEA, INC.
Environmental Services

Project No.	Figure
C00-266	4-19

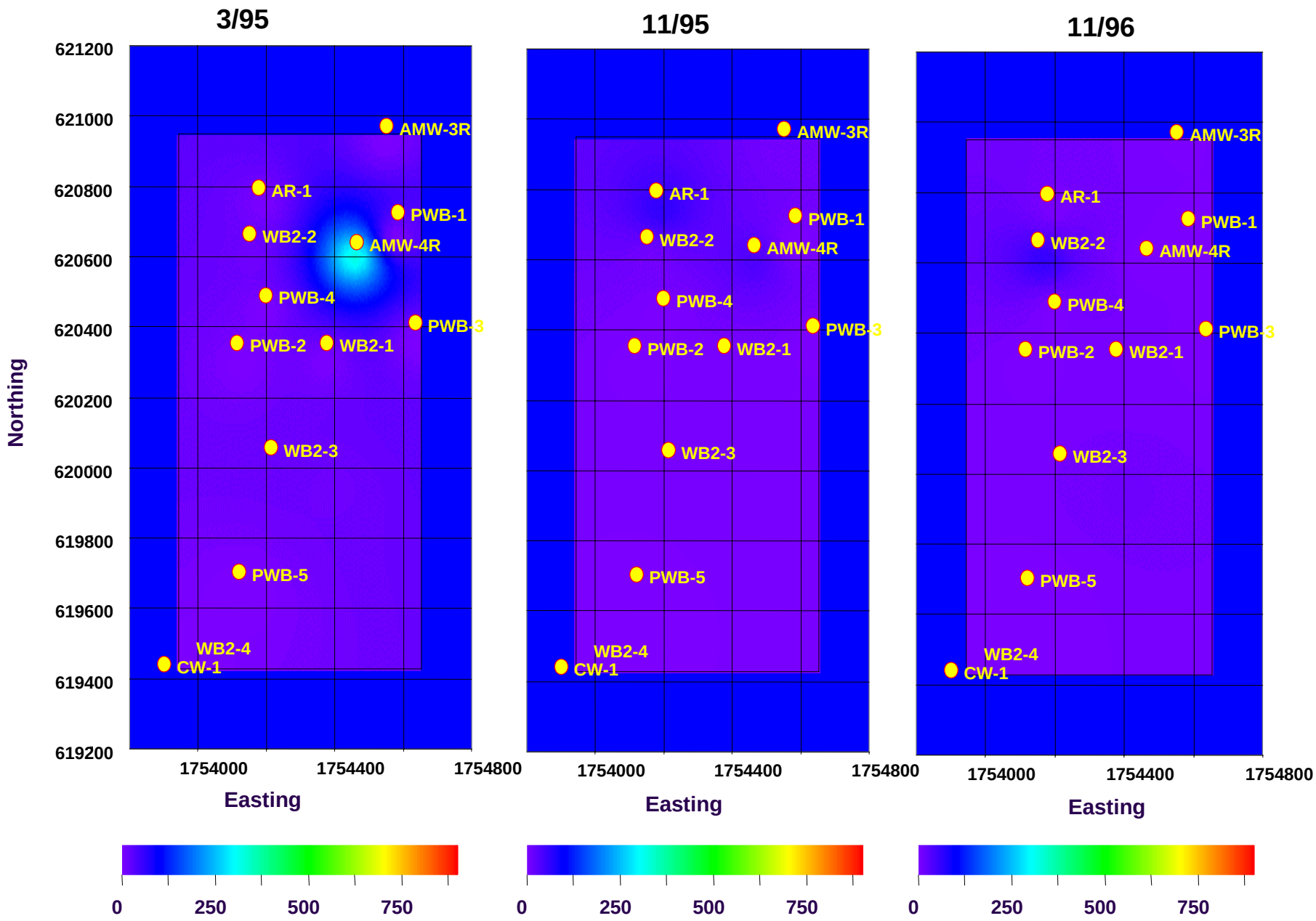

Concentration of 1,2-DCP (µg/l) in the B-zone

PANACEA, INC.
Environmental Services

Project No.	Figure
C00-266	4-20

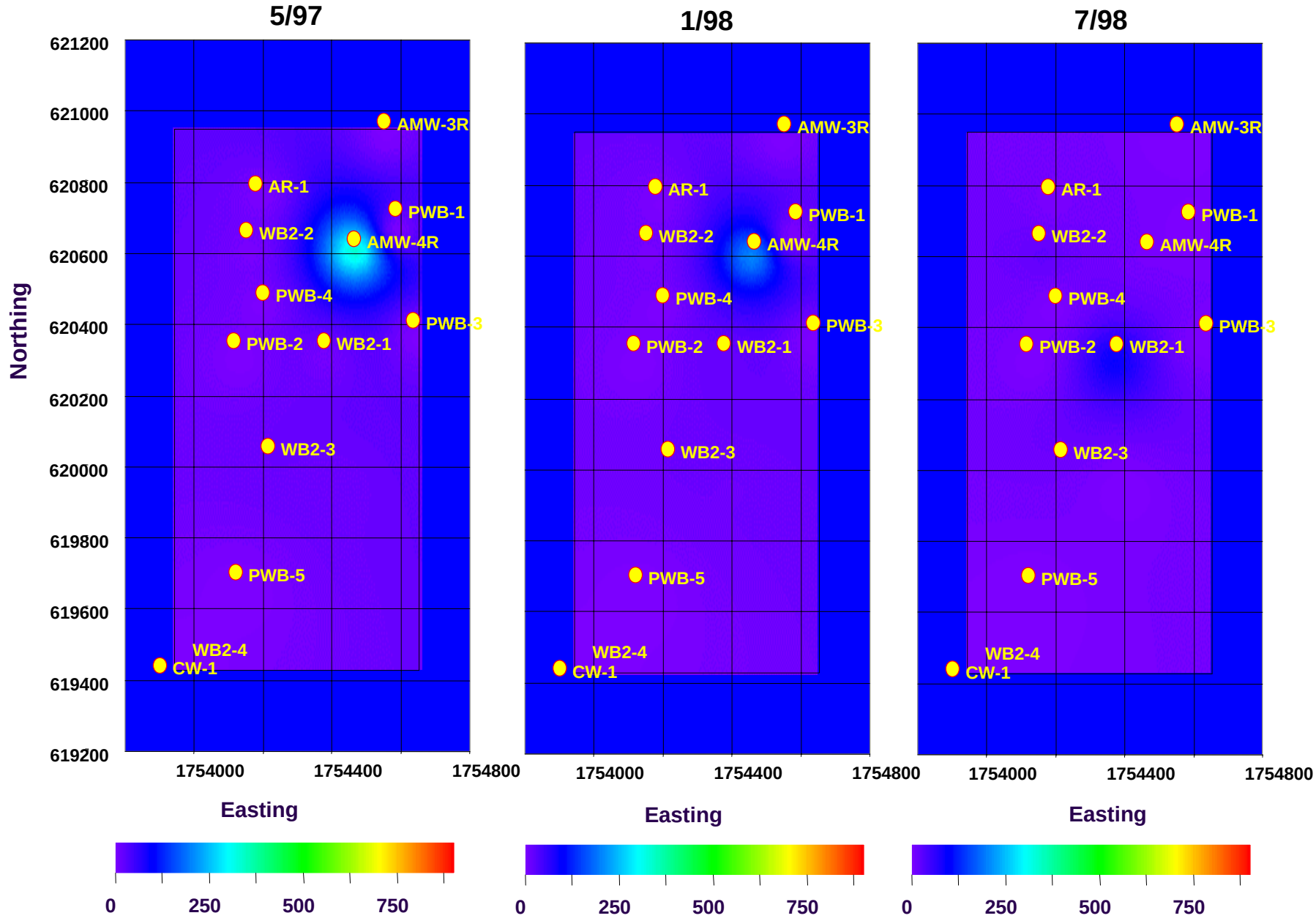

Concentration of 1,2-DCP (µg/l) in the B-zone

PANACEA, INC.
Environmental Services

Project No.	Figure
C00-266	4-21

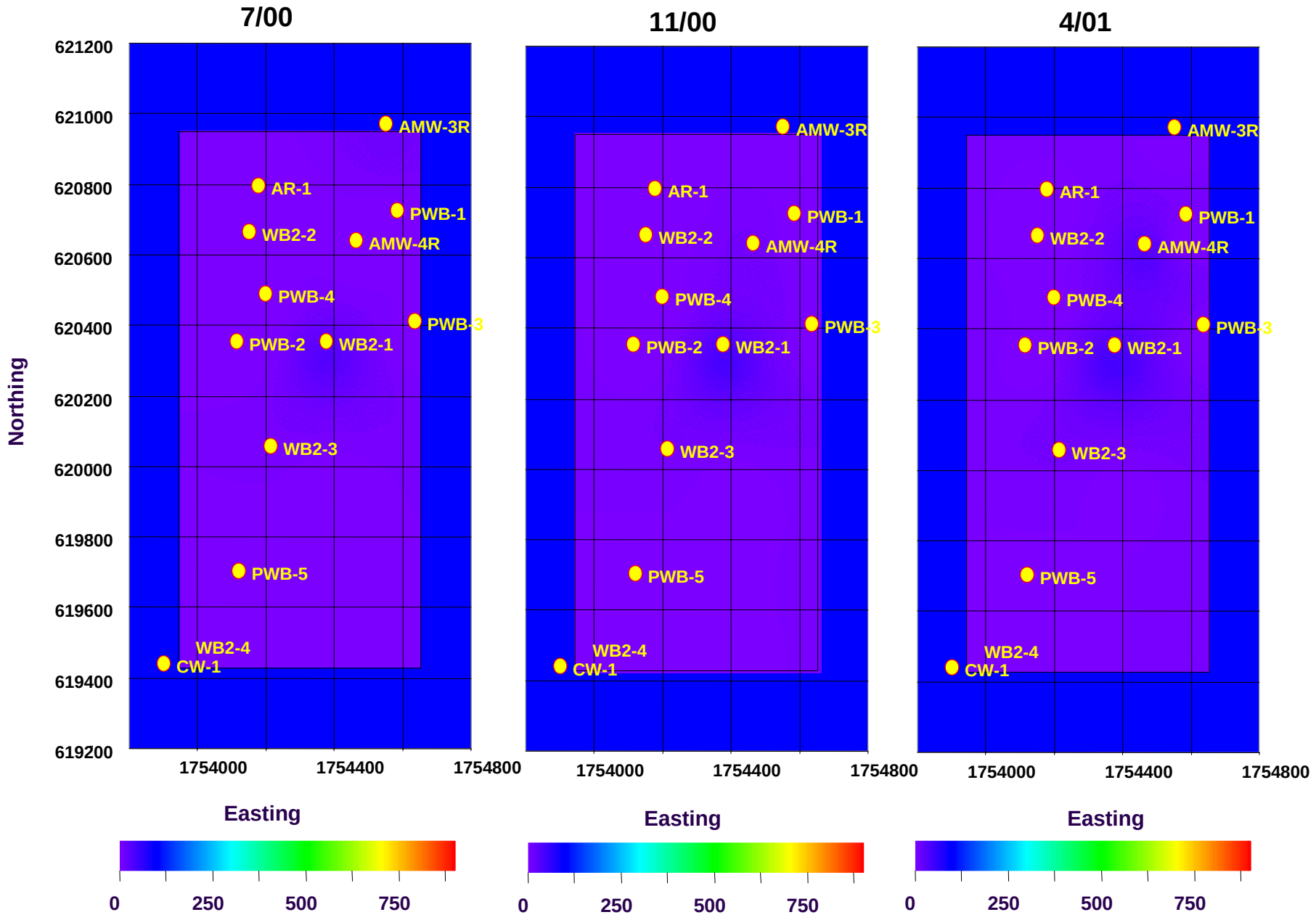

Concentration of 1,2-DCP (µg/l) in the B-zone

PANACEA, INC.
Environmental Services

Project No.	Figure
C00-266	4-22

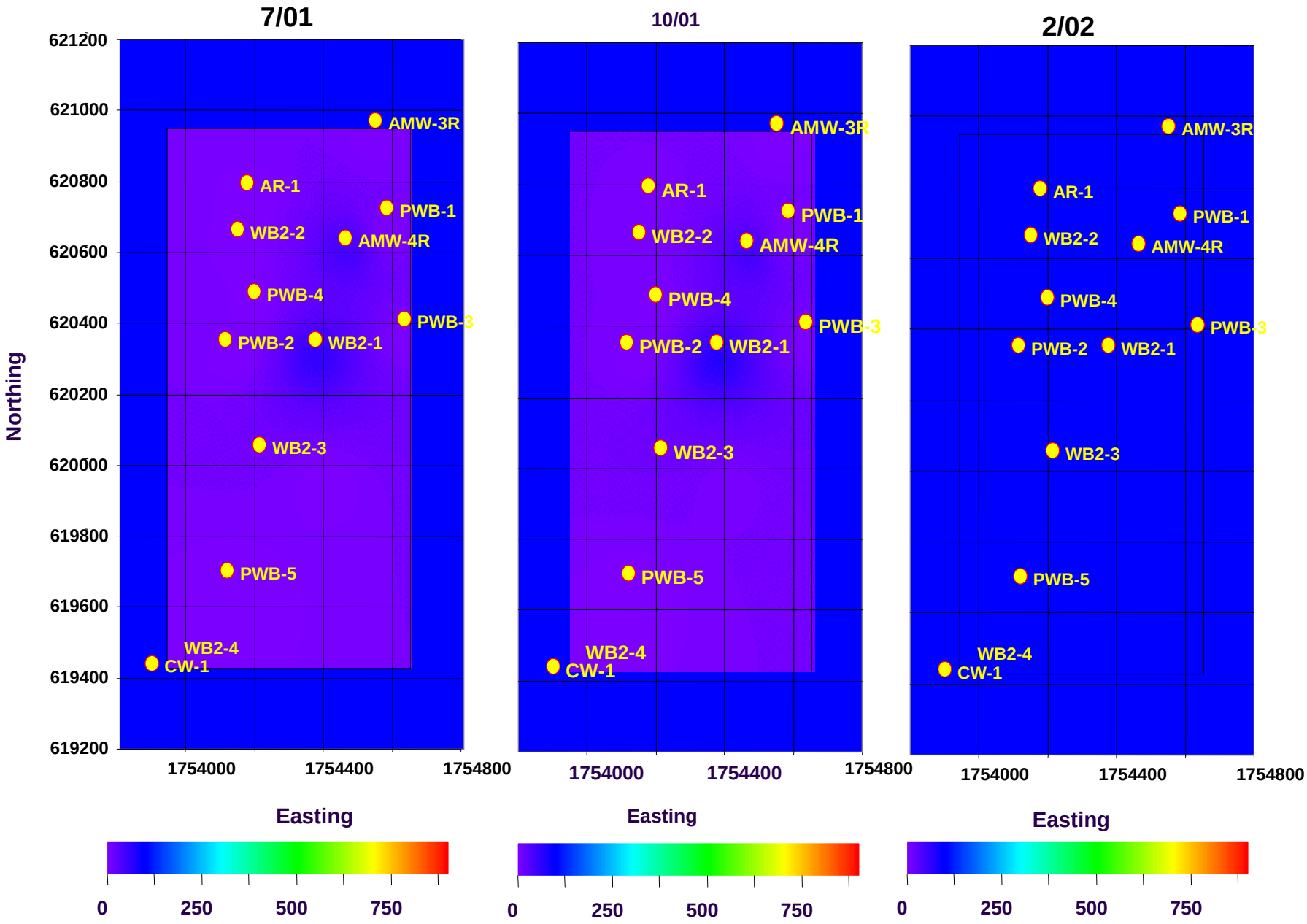

Concentration of 1,2-DCP (µg/l) in the B-zone

PANACEA, INC.
Environmental Services

Project No.	Figure
C00-266	4-23

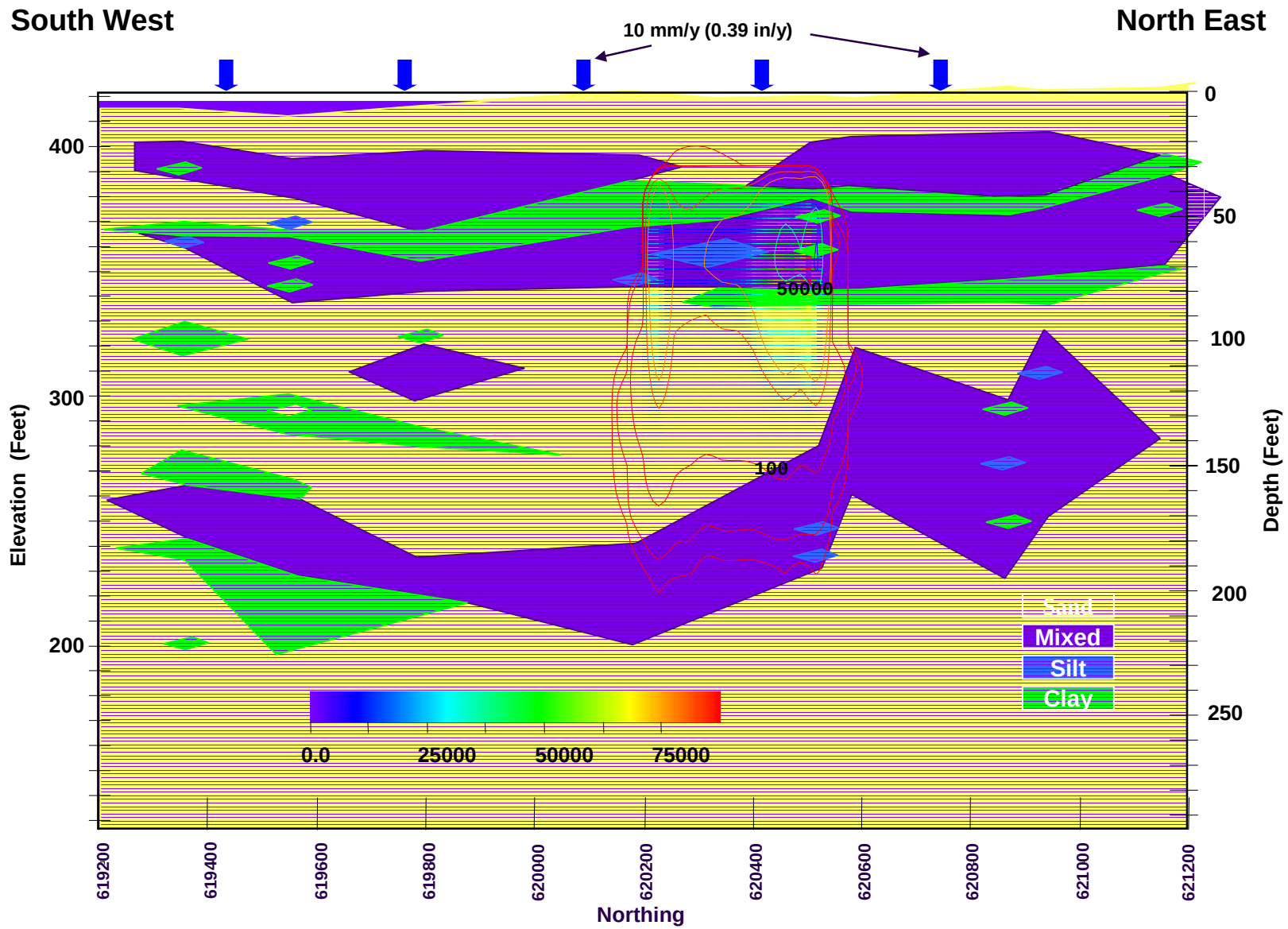

Concentration of 1,2-DCP (µg/l) After 100 Years Overlain on Conceptual Hydrogeologic Model 1 Using 10 mm/yr Infiltration Rate

PANACEA, INC.
Environmental Services

Project No. C00-266	Figure 4-24

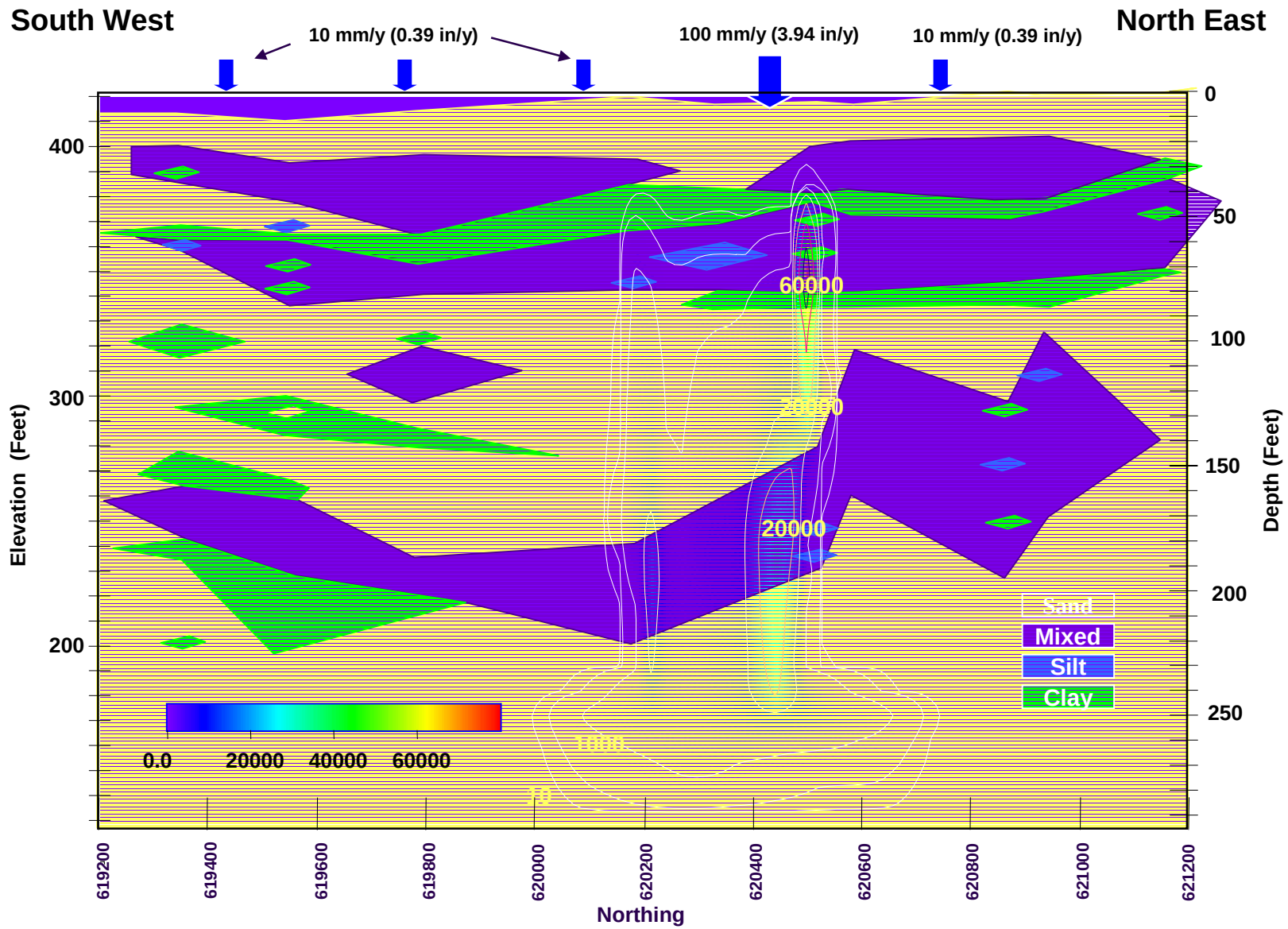

Concentration of 1,2-DCP (µg/l) After 100 Years Overlain on Conceptual Hydrogeologic Model 1 Using 100 mm/yr Infiltration Rate on Site with Flat Water Table

PANACEA, INC.
Environmental Services

Project No. C00-266	Figure 4-25

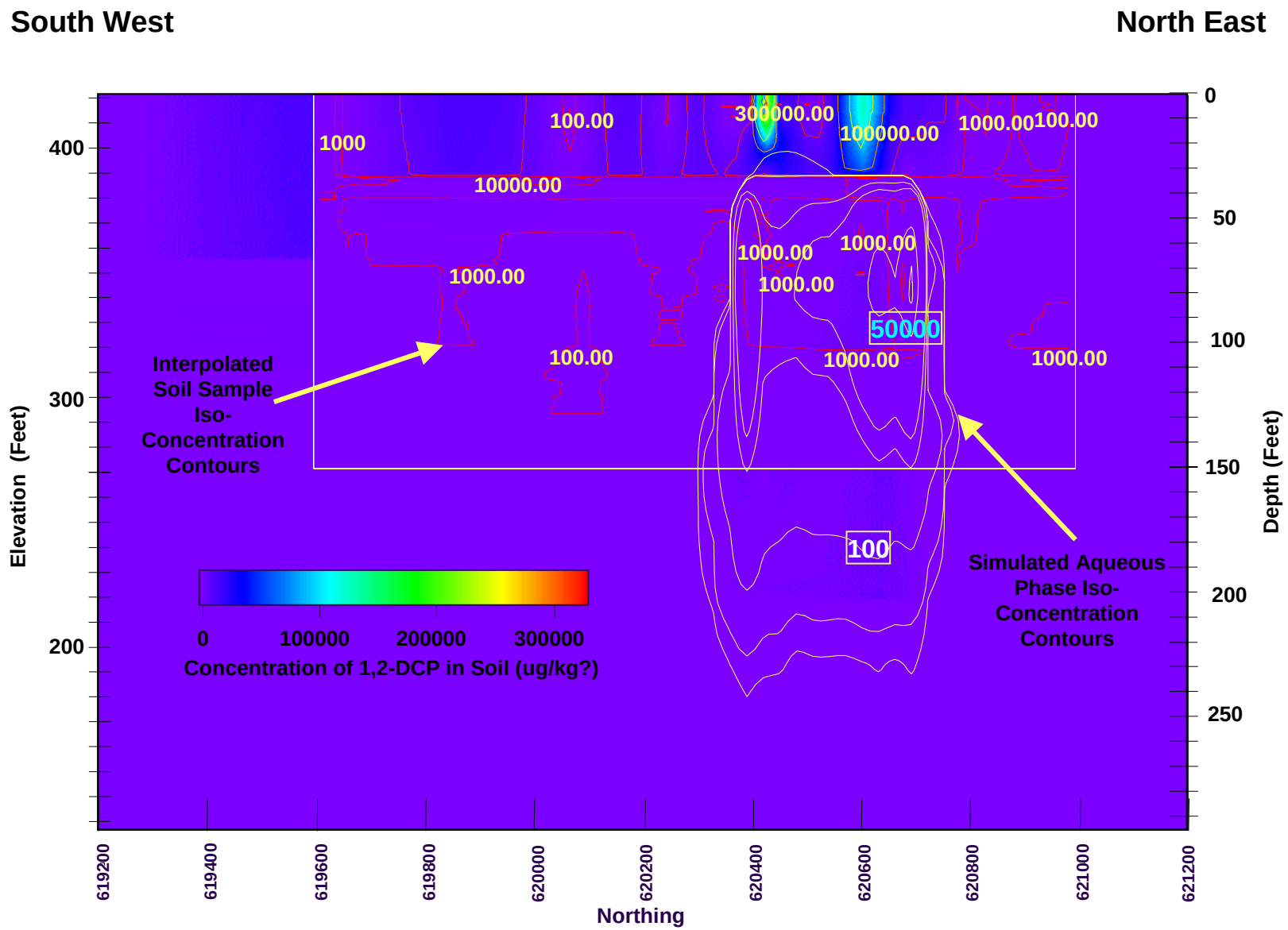

Simulated Concentration of 1,2-DCP (µg/l) After 100 Years with 10 mm/yr Infiltration Rate Compared with Distribution of 1,2-DCP in Unsaturated Zone

PANACEA, INC.
Environmental Services

Project No. C00-266	Figure 4-26

CORRESPONDING DATES FOR SIMULATION TIMES

SIMULATION TIME	CORRESPONDING DATE
0 (days)	1-Apr-1992
0.4 (days)	1-Apr-1992
244 (days)	1-Dec-1992
6.3 (yrs)	20-Jul-1998
9.6 (yrs)	6-Nov-2001
20 (yrs)	1-Apr-2012
40 (yrs)	1-Apr-2032
70 (yrs)	1-Apr-2062
100 (yrs)	1-Apr-2092

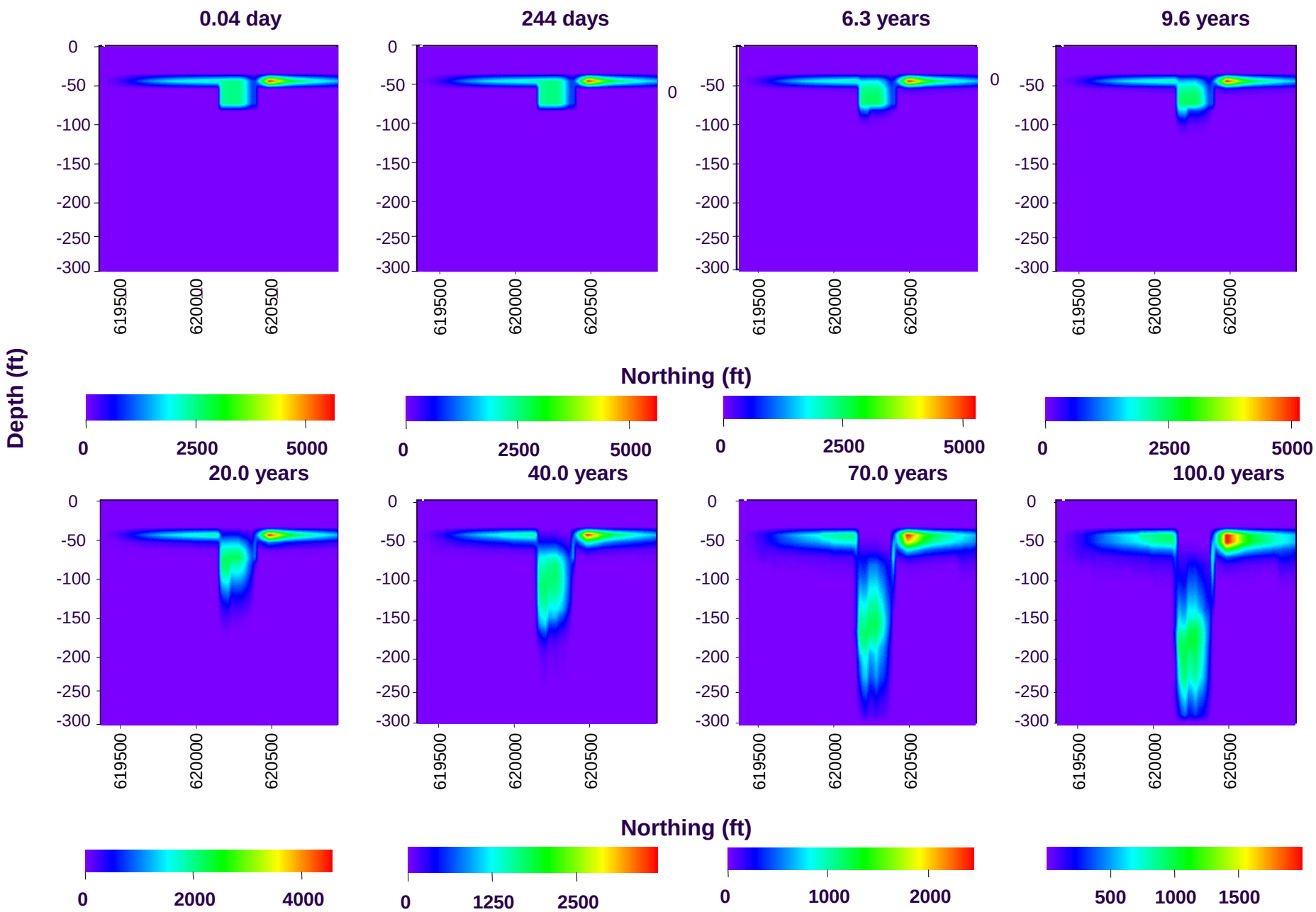

Simulated Concentration of 1,2-DCP (µg/l) in the Unsaturated Zone (Conservative)

PANACEA, INC.
Environmental Services

Project No.	Figure
C00-266	4-27

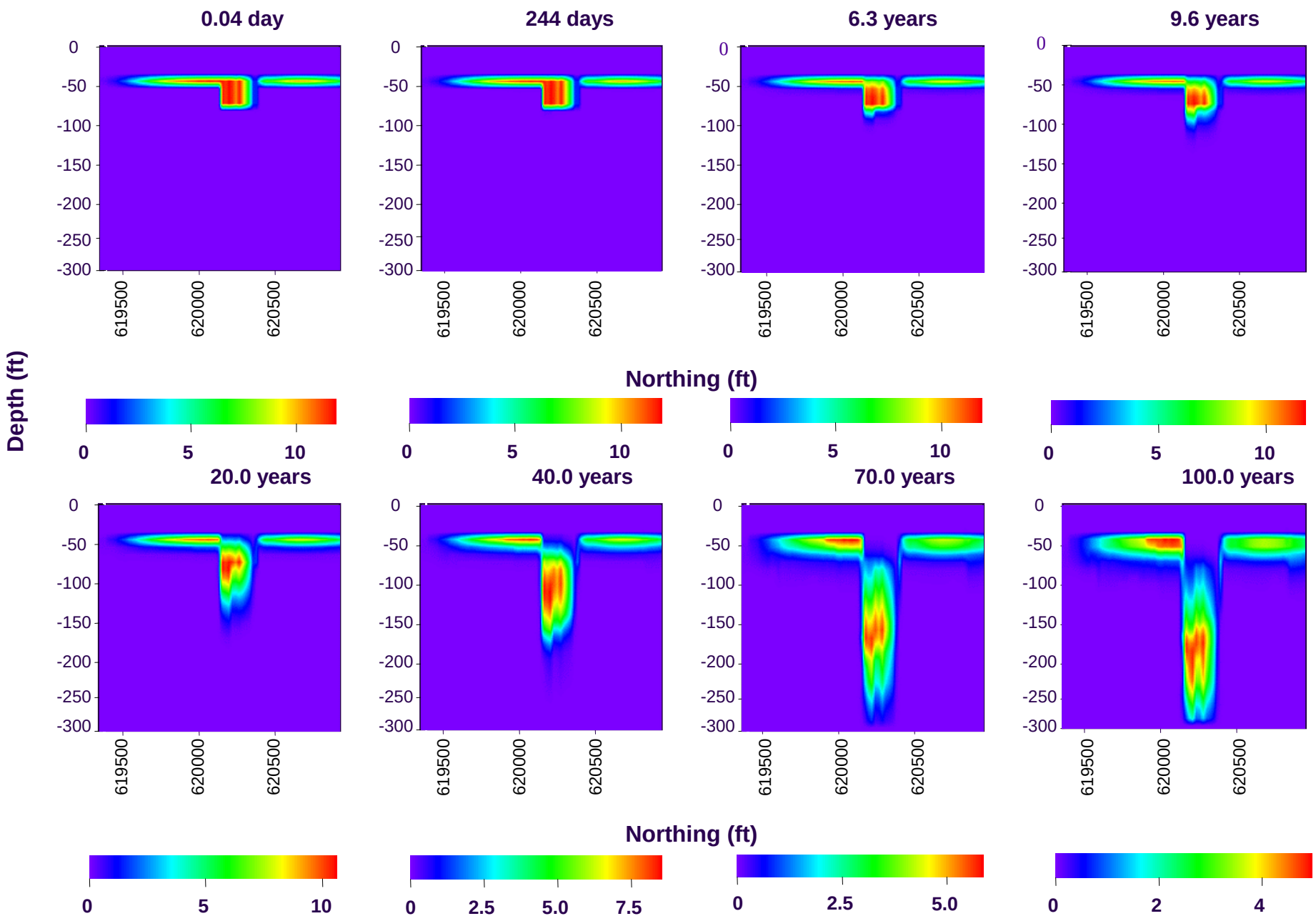

Simulated Concentration of 1,3-DCP (µg/l) in the Unsaturated Zone (Conservative)

PANACEA, INC.
Environmental Services

Project No.	Figure
C00-266	4-28

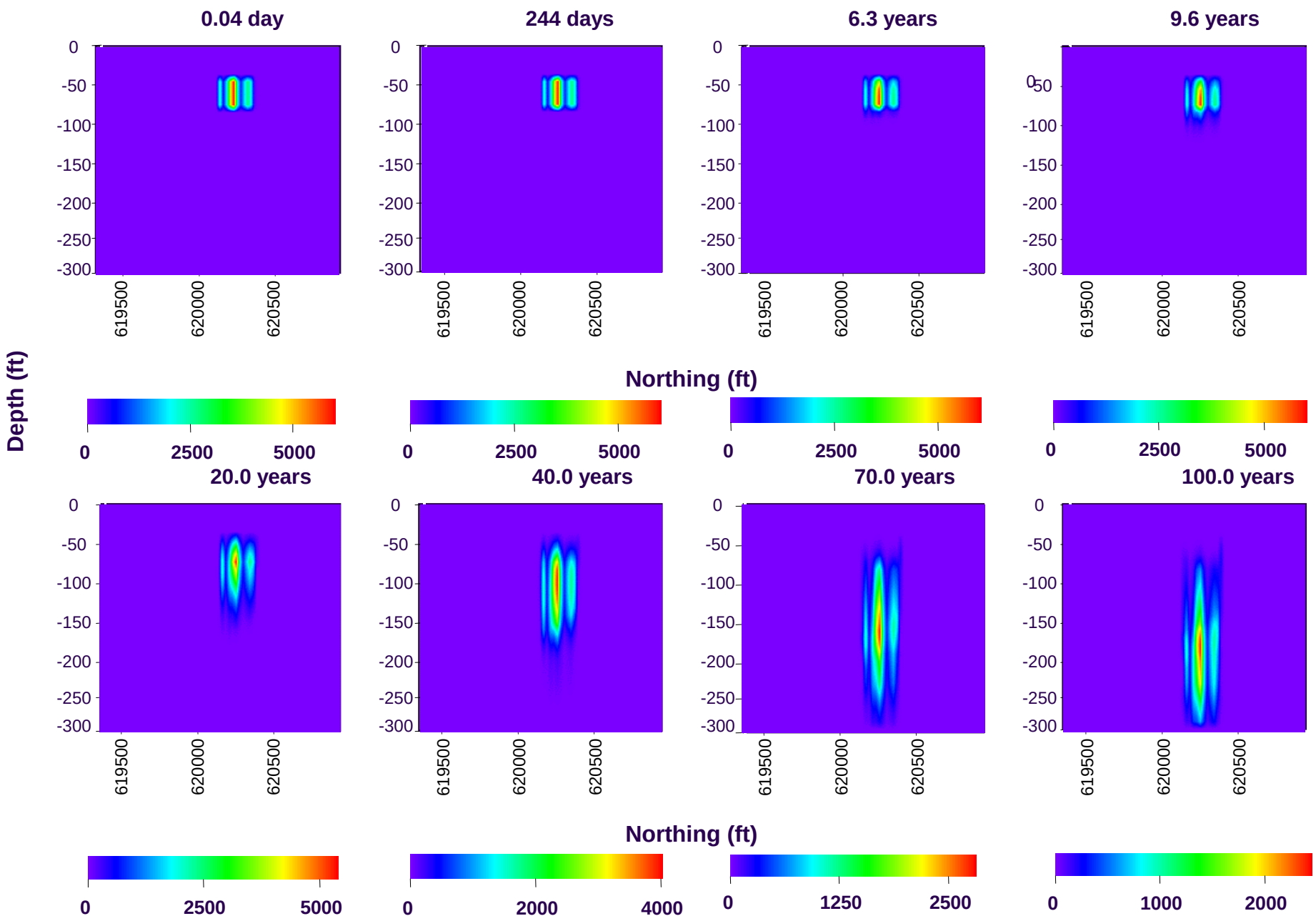

Simulated Concentration of 1,2,3-TCP (µg/l) in the Unsaturated Zone (Conservative)

PANACEA, INC.
Environmental Services

Project No.	Figure
C00-266	4-29

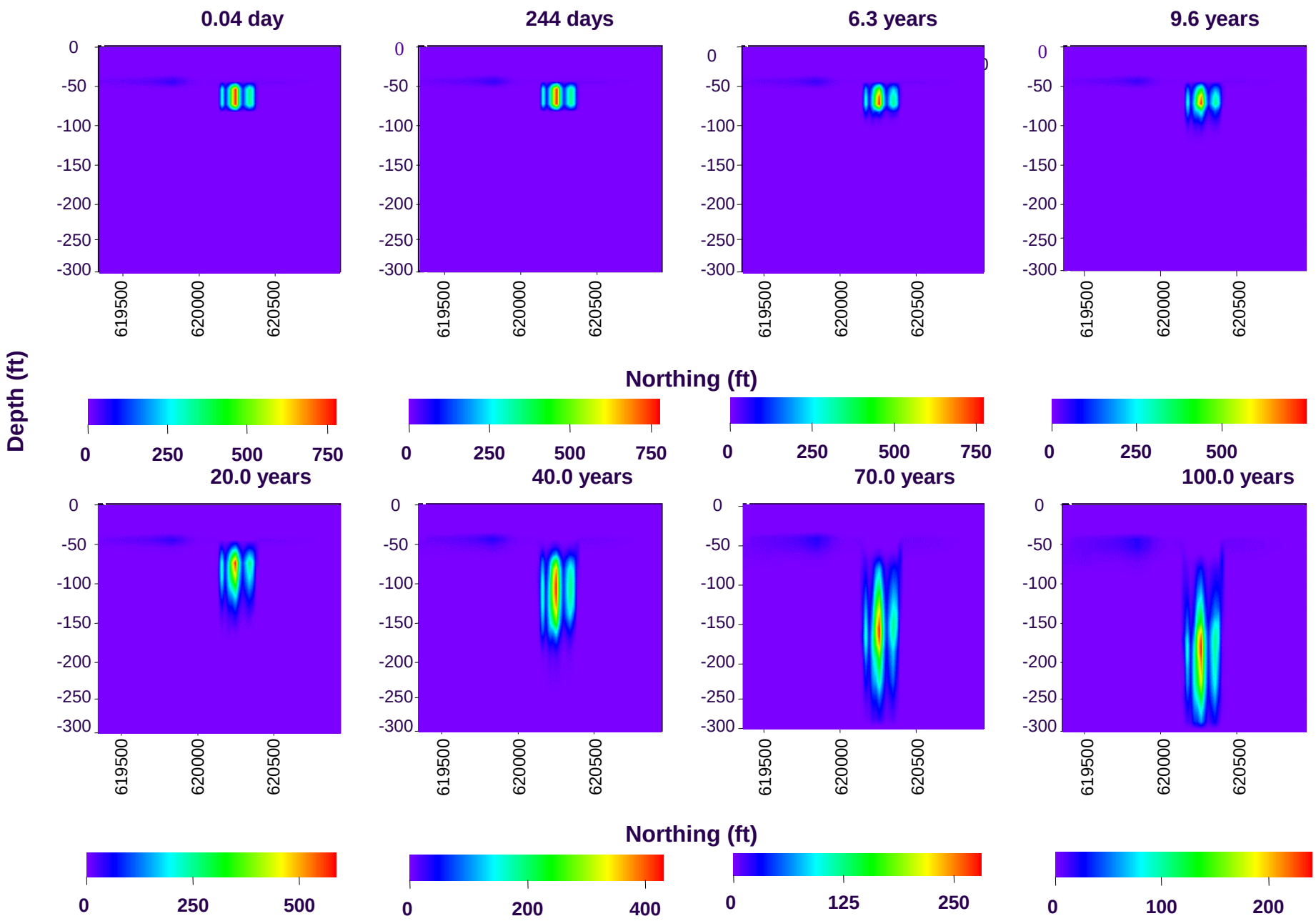

Simulated Concentration of Chloroform (µg/l) in the Unsaturated Zone (Conservative)

PANACEA, INC.
Environmental Services

Project No.	Figure
C00-266	4-30

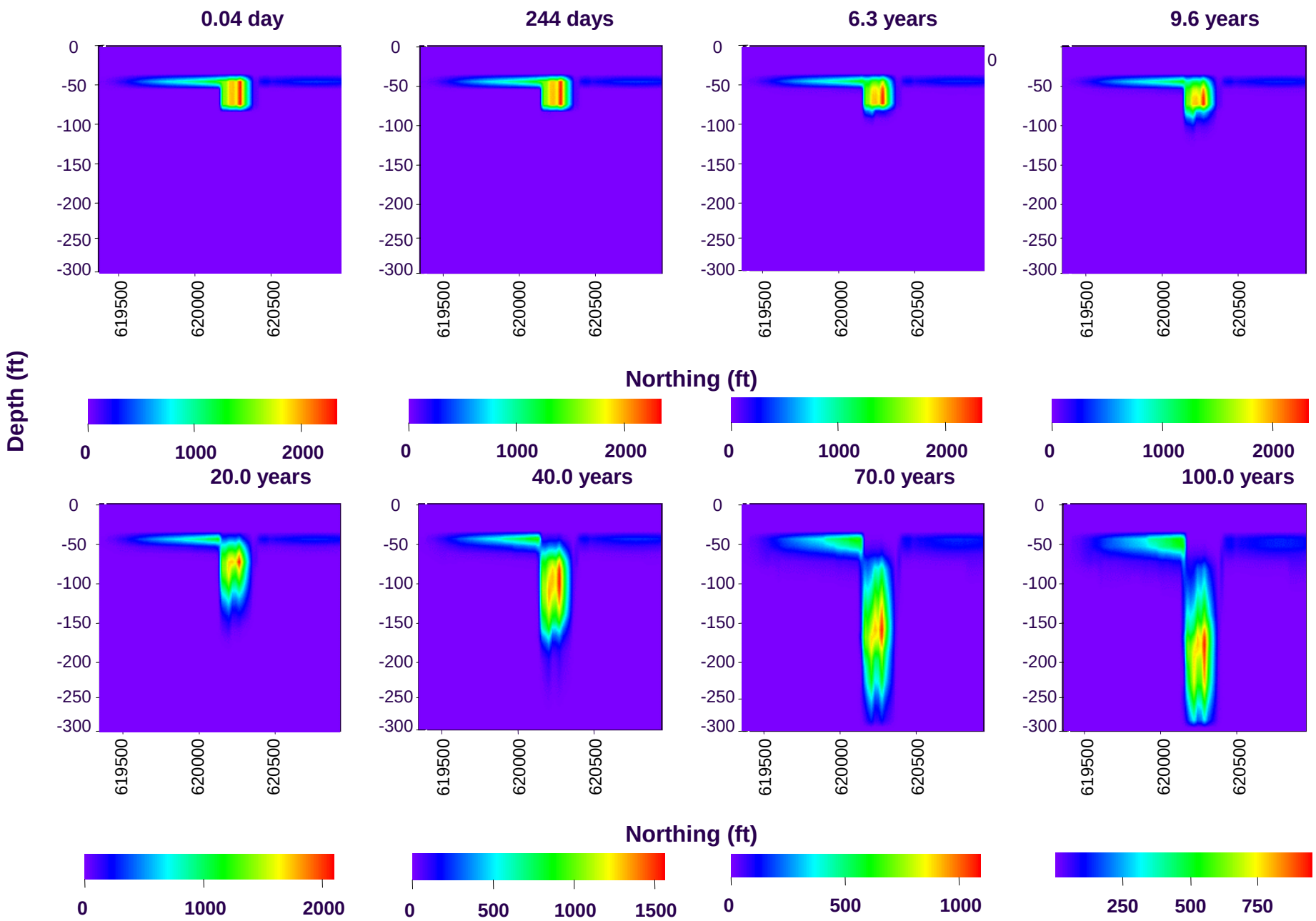

Simulated Concentration of DBCP (µg/l) in the Unsaturated Zone (Conservative)

PANACEA, INC.
Environmental Services

Project No.	Figure
C00-266	4-31

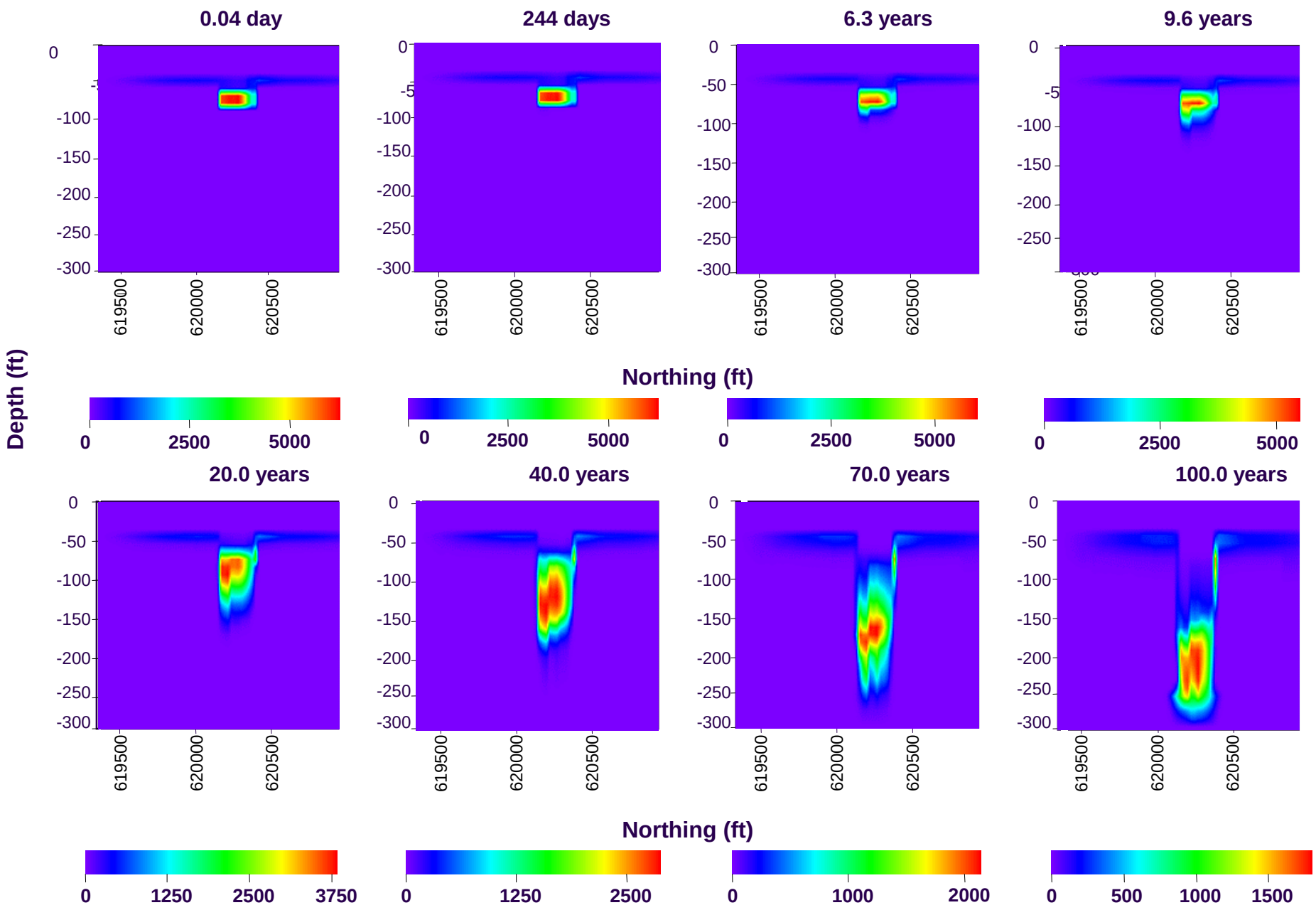

Simulated Concentration of Dinoseb (µg/l) in the Unsaturated Zone (Conservative)

PANACEA, INC.
Environmental Services

Project No.	Figure
C00-266	4-32

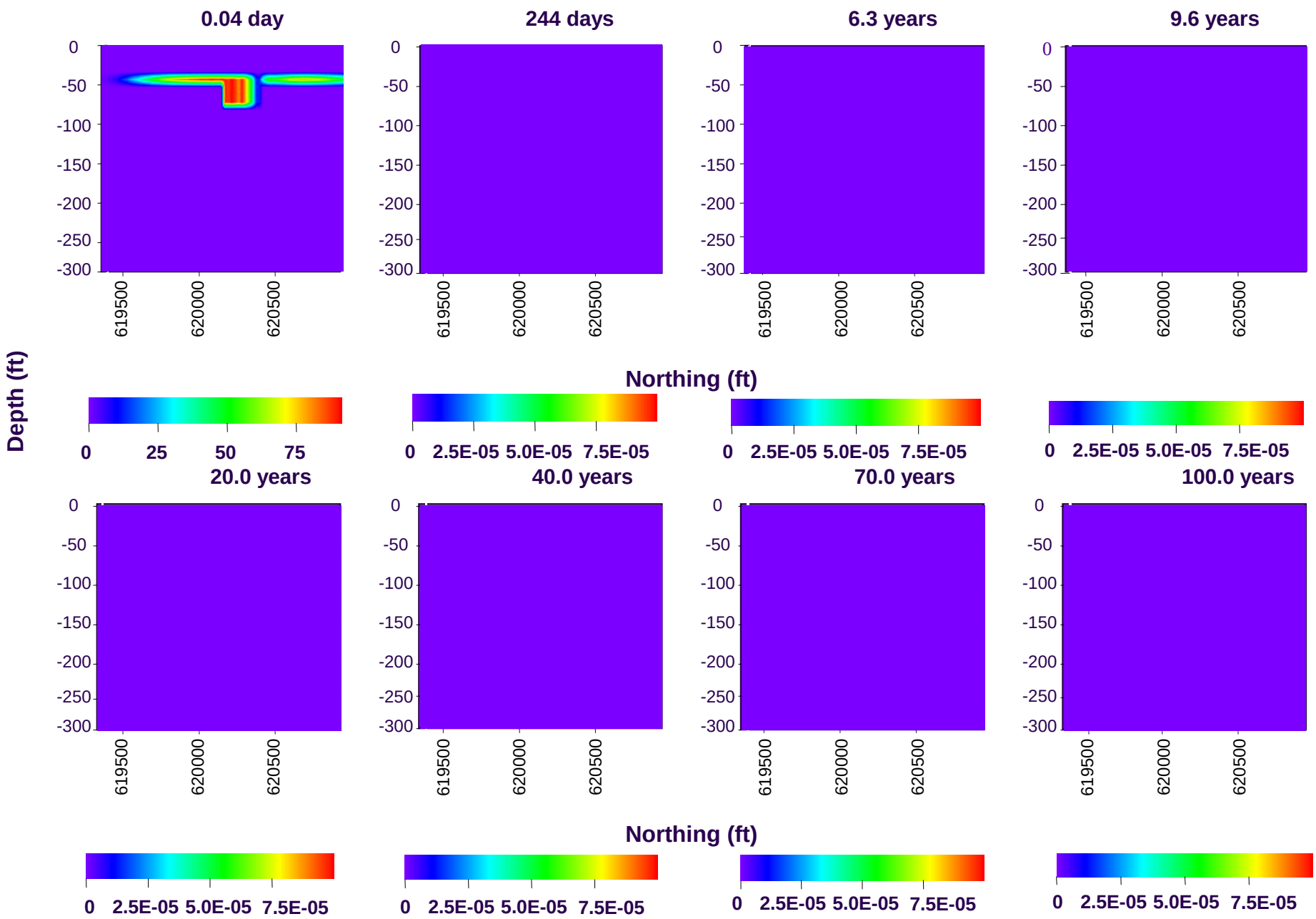

Simulated Concentration of EDB (µg/l) in the Unsaturated Zone (Conservative)

PANACEA, INC.
Environmental Services

Project No.	Figure
C00-266	4-33

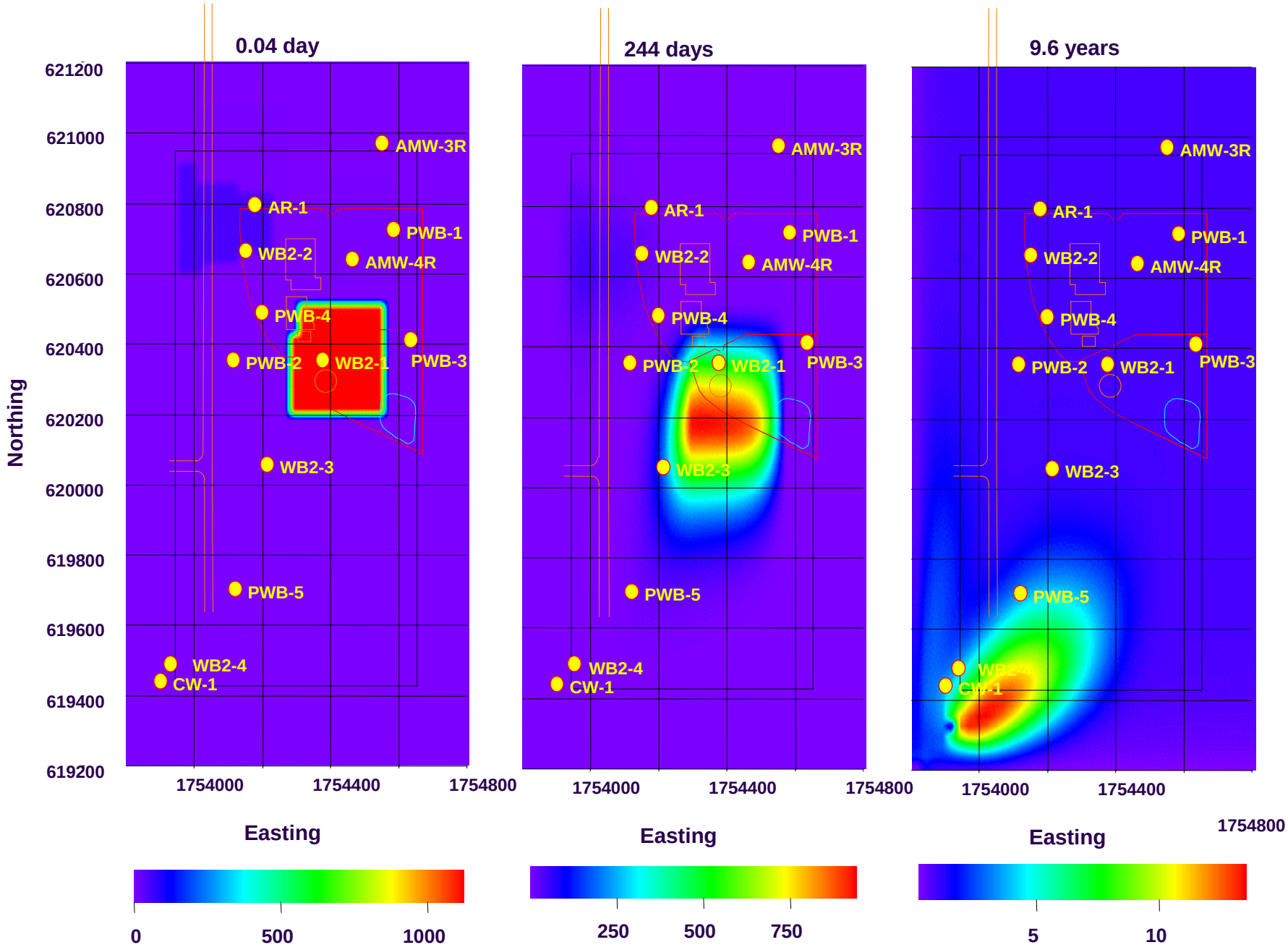

Simulated Concentration of 1,2-DCP (µg/l) in the Saturated Zone (Conservative)

PANACEA, INC.
Environmental Services

Project No.	Figure
C00-266	4-34a

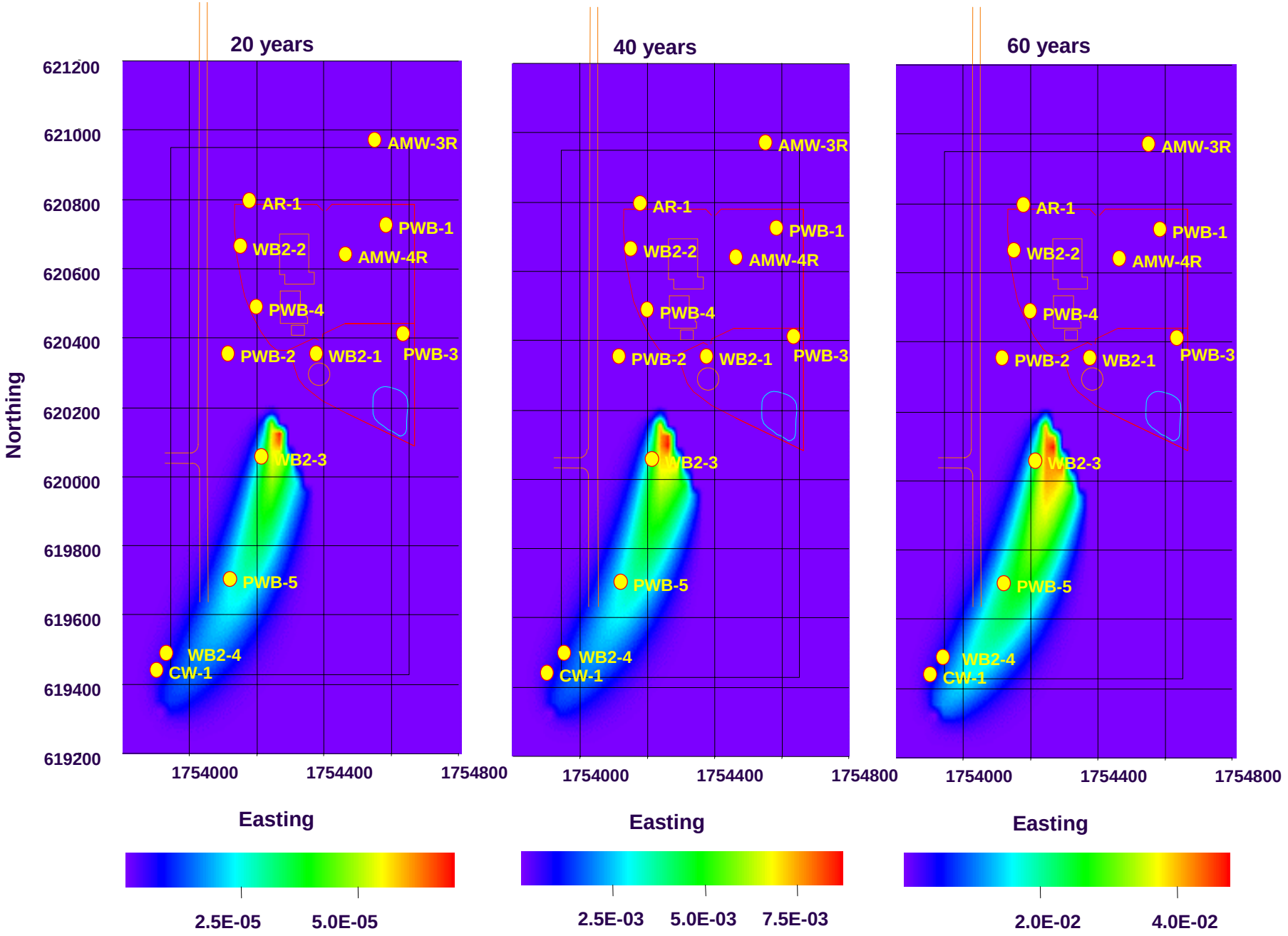

Simulated Concentration of 1,2-DCP (µg/l) in the Saturated Zone (Conservative)

PANACEA, INC.
Environmental Services

Project No.	Figure
C00-266	4-34b

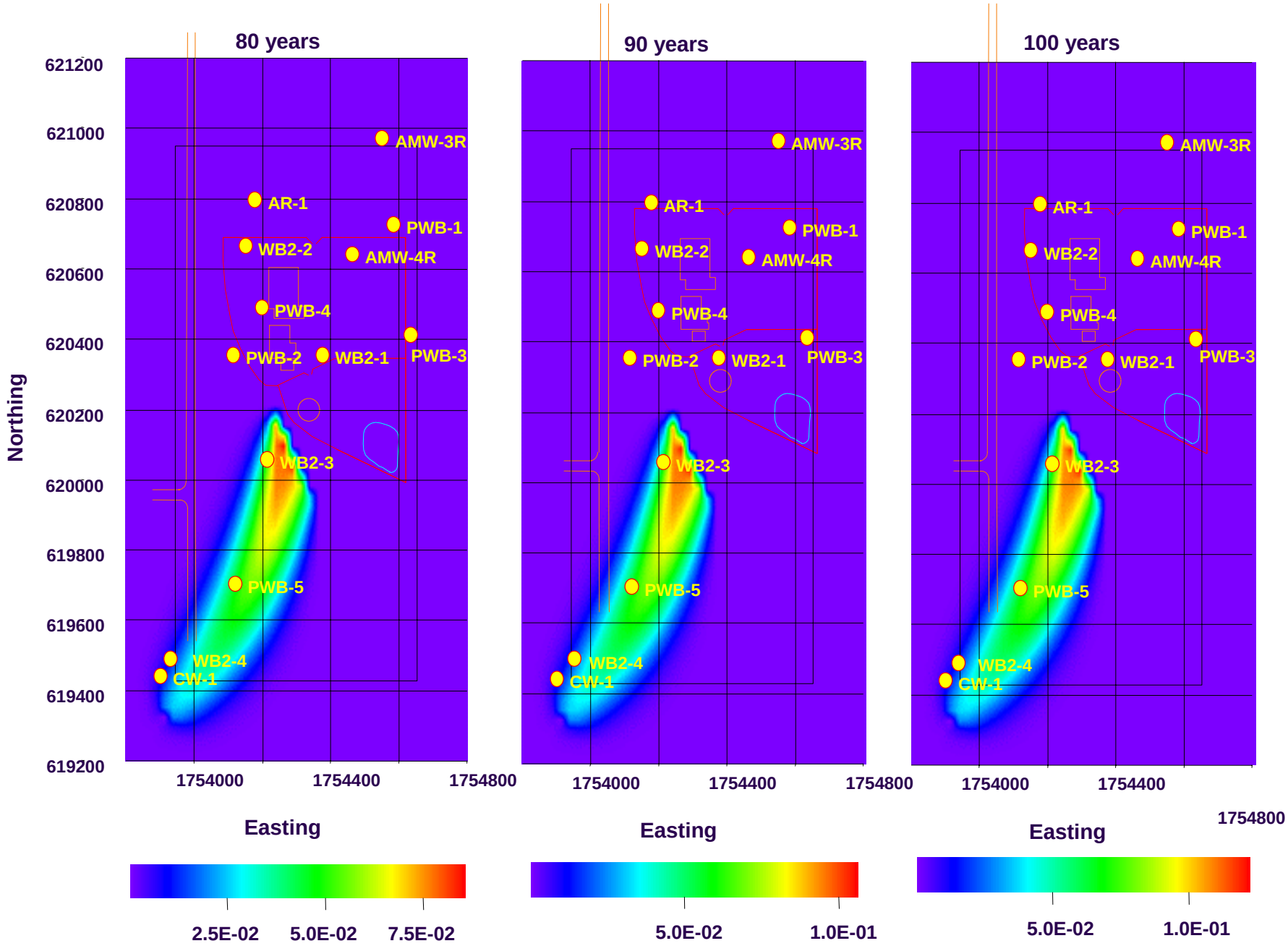

Simulated Concentration of 1,2-DCP (µg/l) in the Saturated Zone (Conservative)

PANACEA, INC.
Environmental Services

Project No.	Figure
C00-266	4-34c

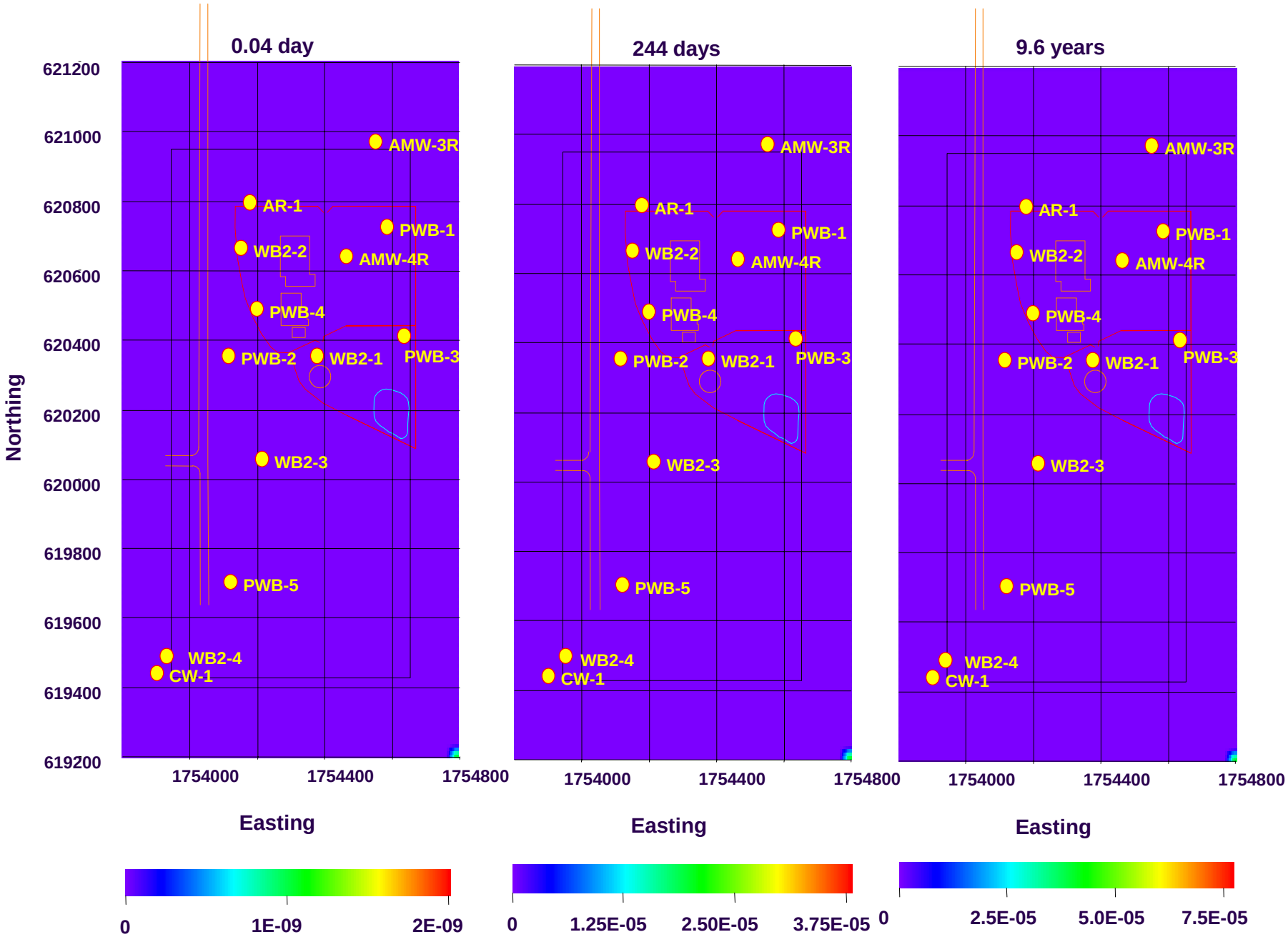

Simulated Concentration of 1,3-DCP (µg/l) in the B-zone Groundwater (Conservative)

PANACEA, INC.
Environmental Services

Project No.	Figure
C00-266	4-35a

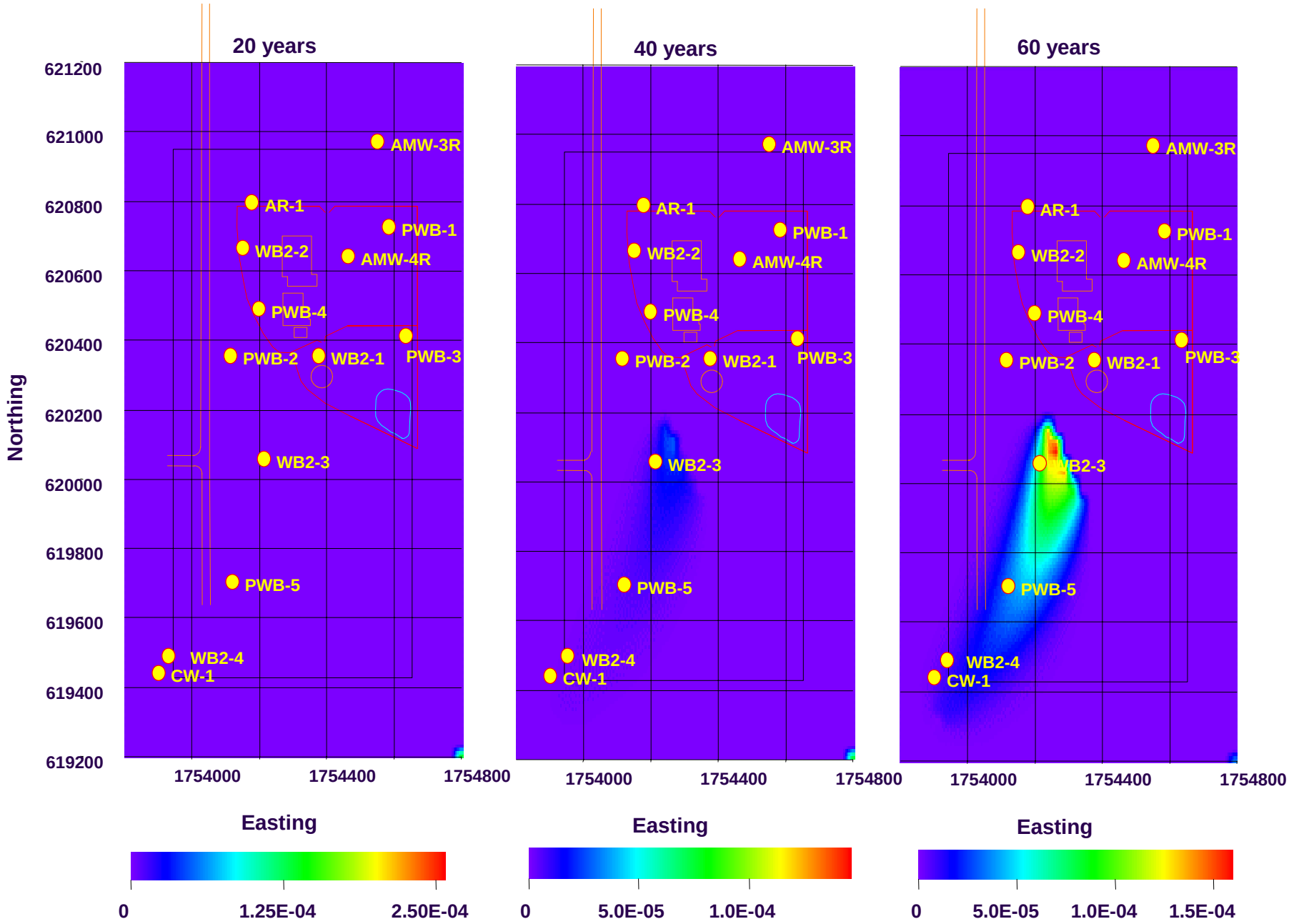

Simulated Concentration of 1,3-DCP (µg/l) in the B-zone Groundwater (Conservative)

PANACEA, INC.
Environmental Services

Project No.	Figure
C00-266	4-35b

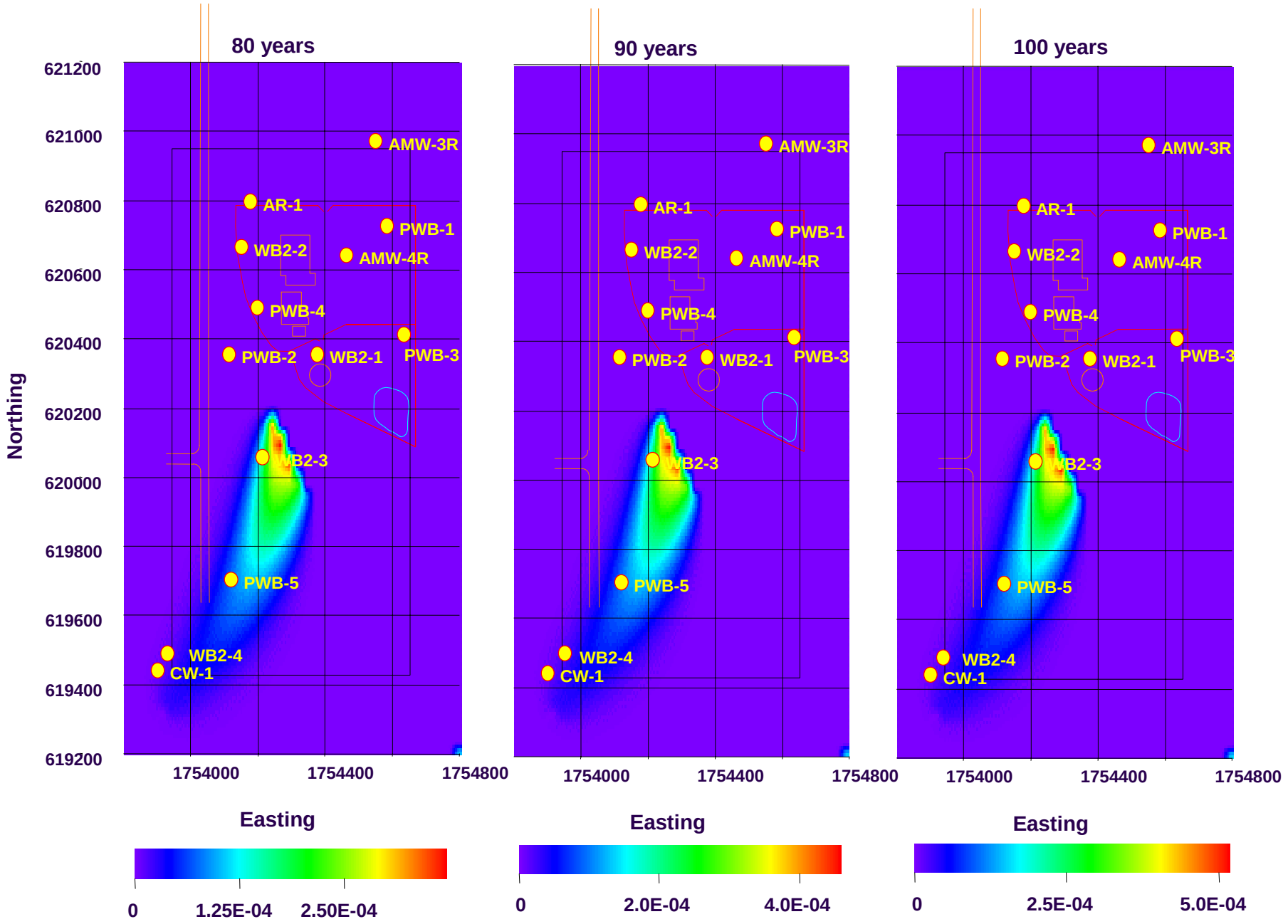

Simulated Concentration of 1,3-DCP (µg/l) in the B-zone Groundwater (Conservative)

PANACEA, INC.
Environmental Services

Project No.	Figure
C00-266	4-35c

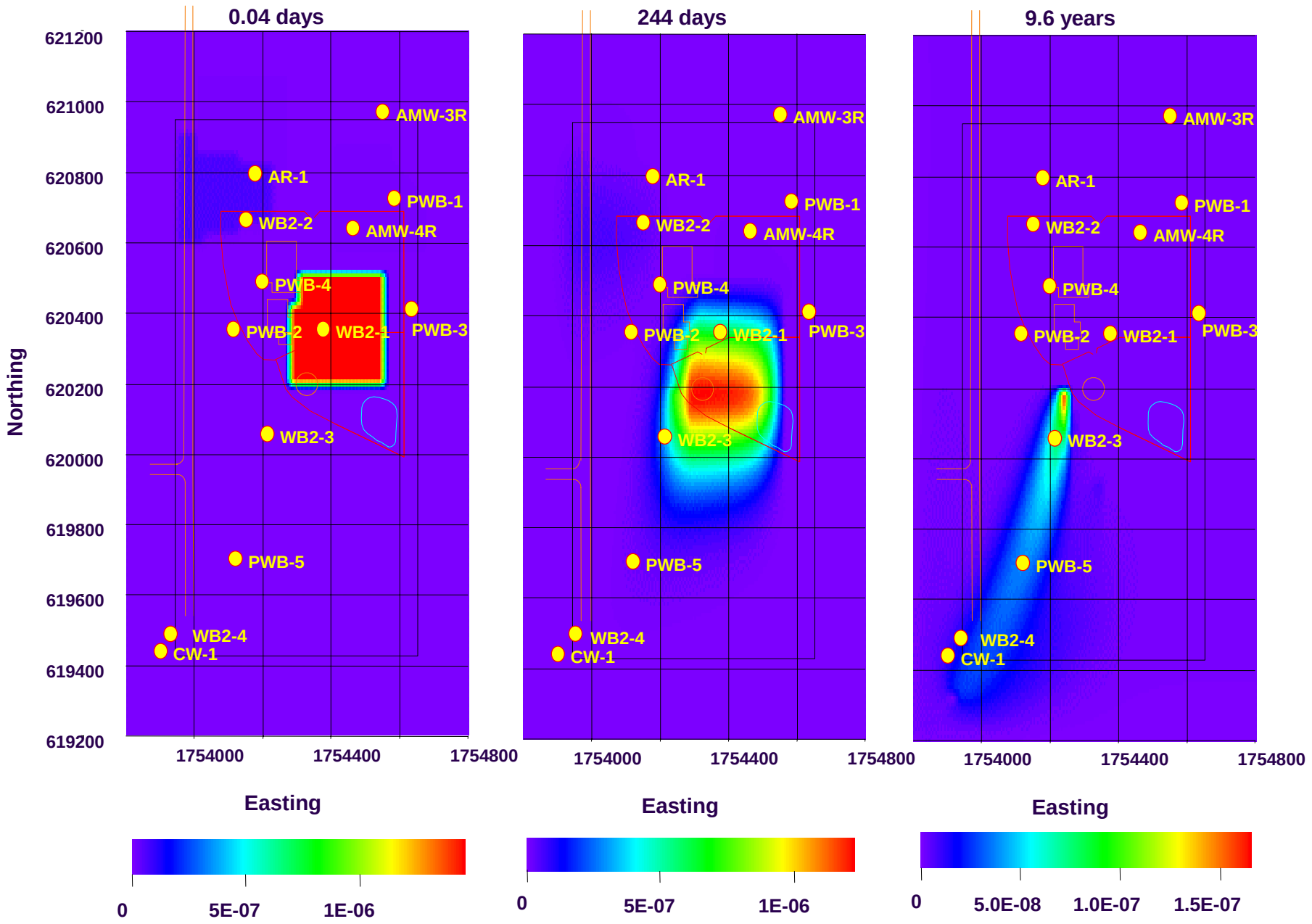

Simulated Concentration of TCP (µg/l) in the Saturated Zone (Conservative)

PANACEA, INC.
Environmental Services

Project No.	Figure
C00-266	4-36a

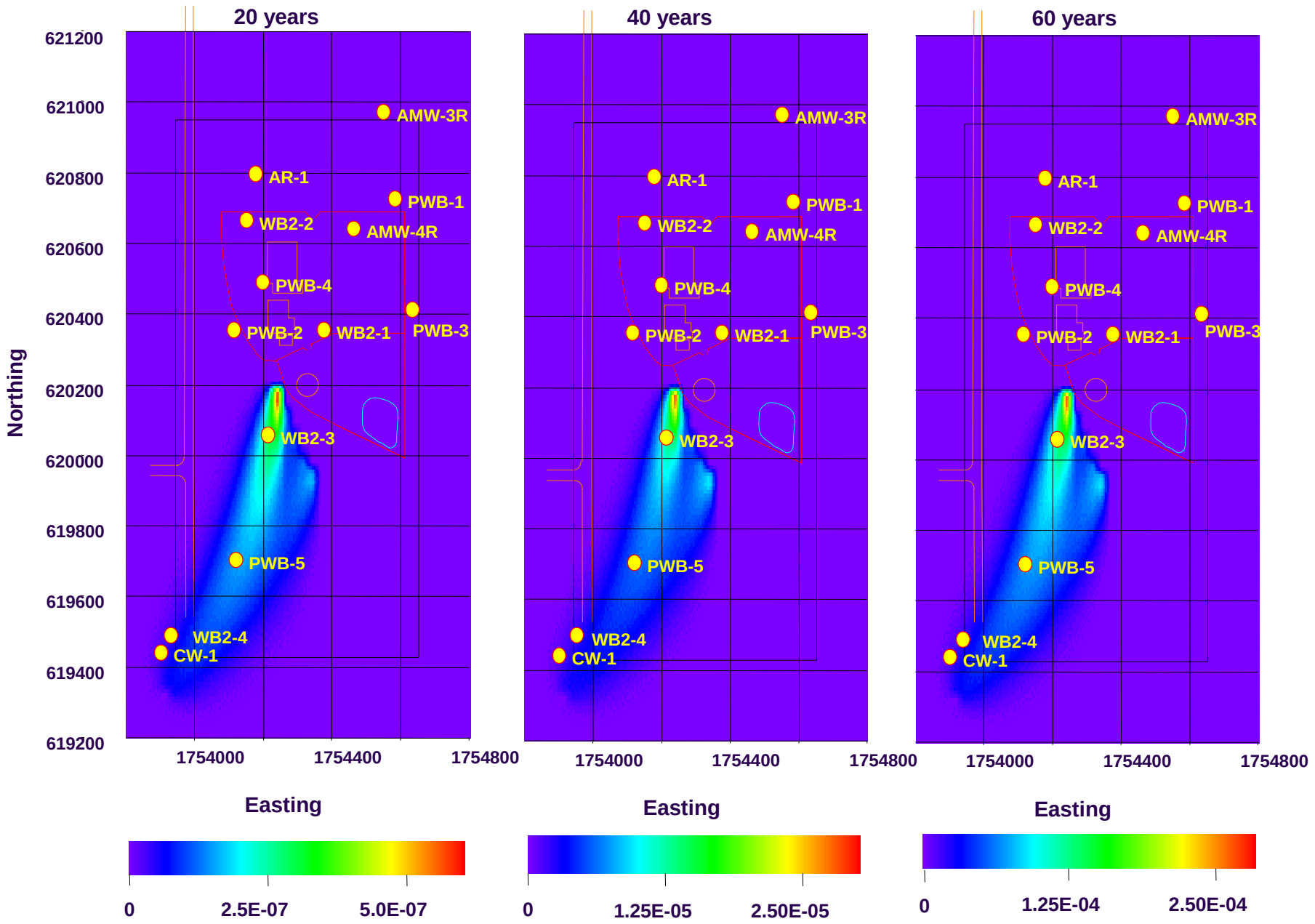

Simulated Concentration of TCP (µg/l) in the Saturated Zone (Conservative)

PANACEA, INC.
Environmental Services

Project No.	Figure
C00-266	4-36b

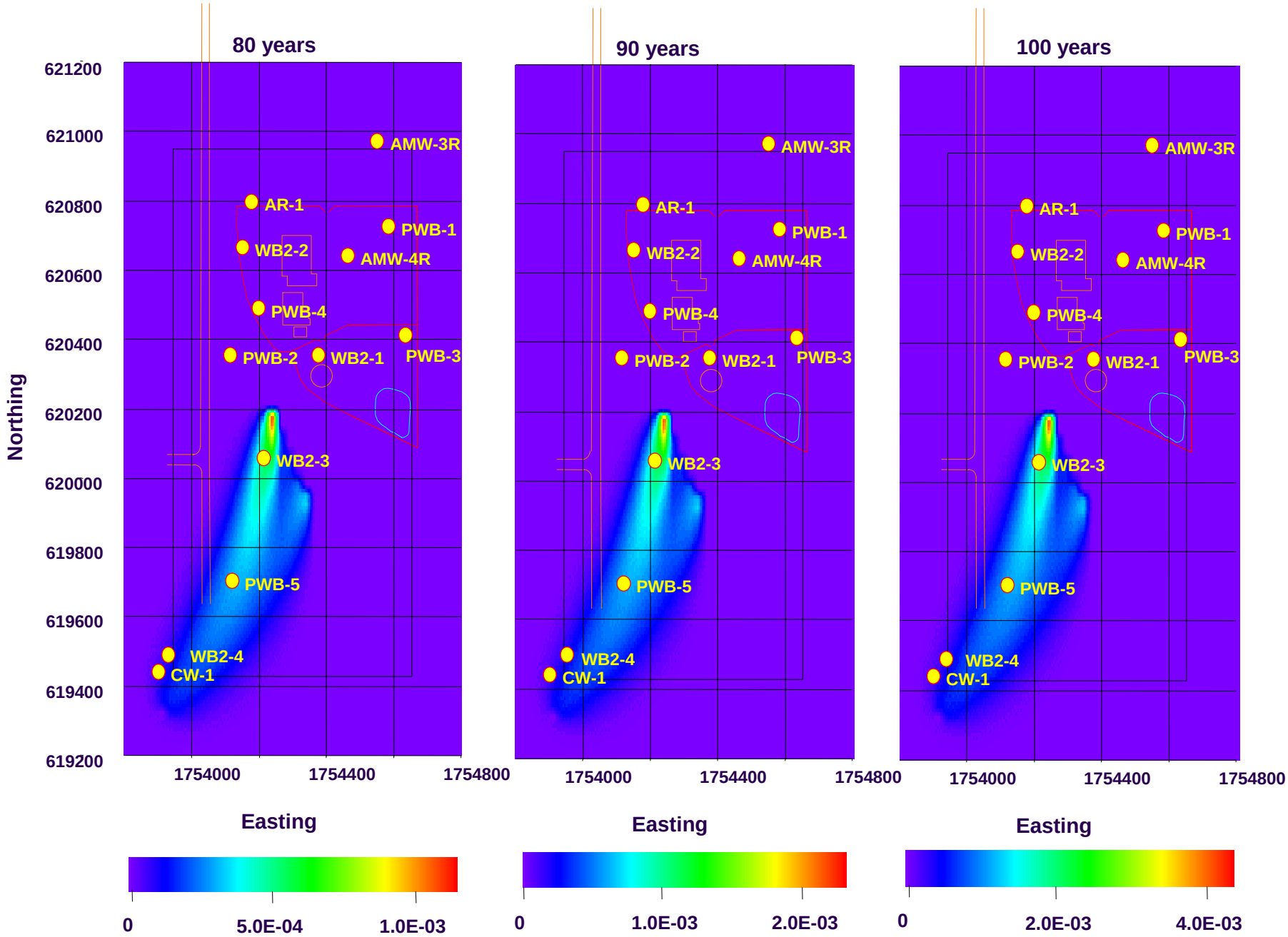

Simulated Concentration of TCP (µg/l) in the Saturated Zone (Conservative)

PANACEA, INC.
Environmental Services

Project No.	Figure
C00-266	4-36c

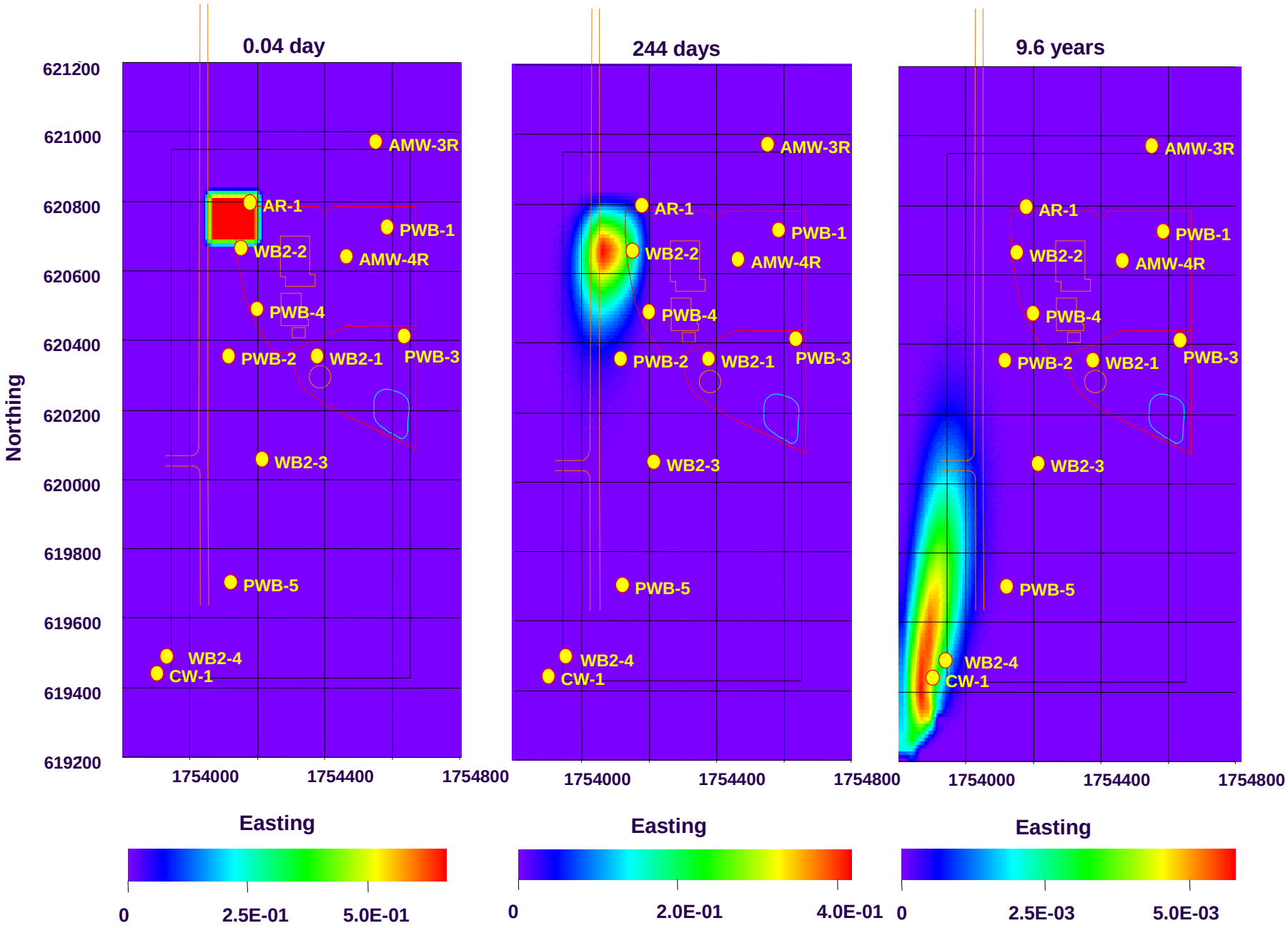

Simulated Concentration of Chloroform (µg/l) in the B-zone Groundwater (Conservative)

PANACEA, INC.
Environmental Services

Project No.	Figure
C00-266	4-37a

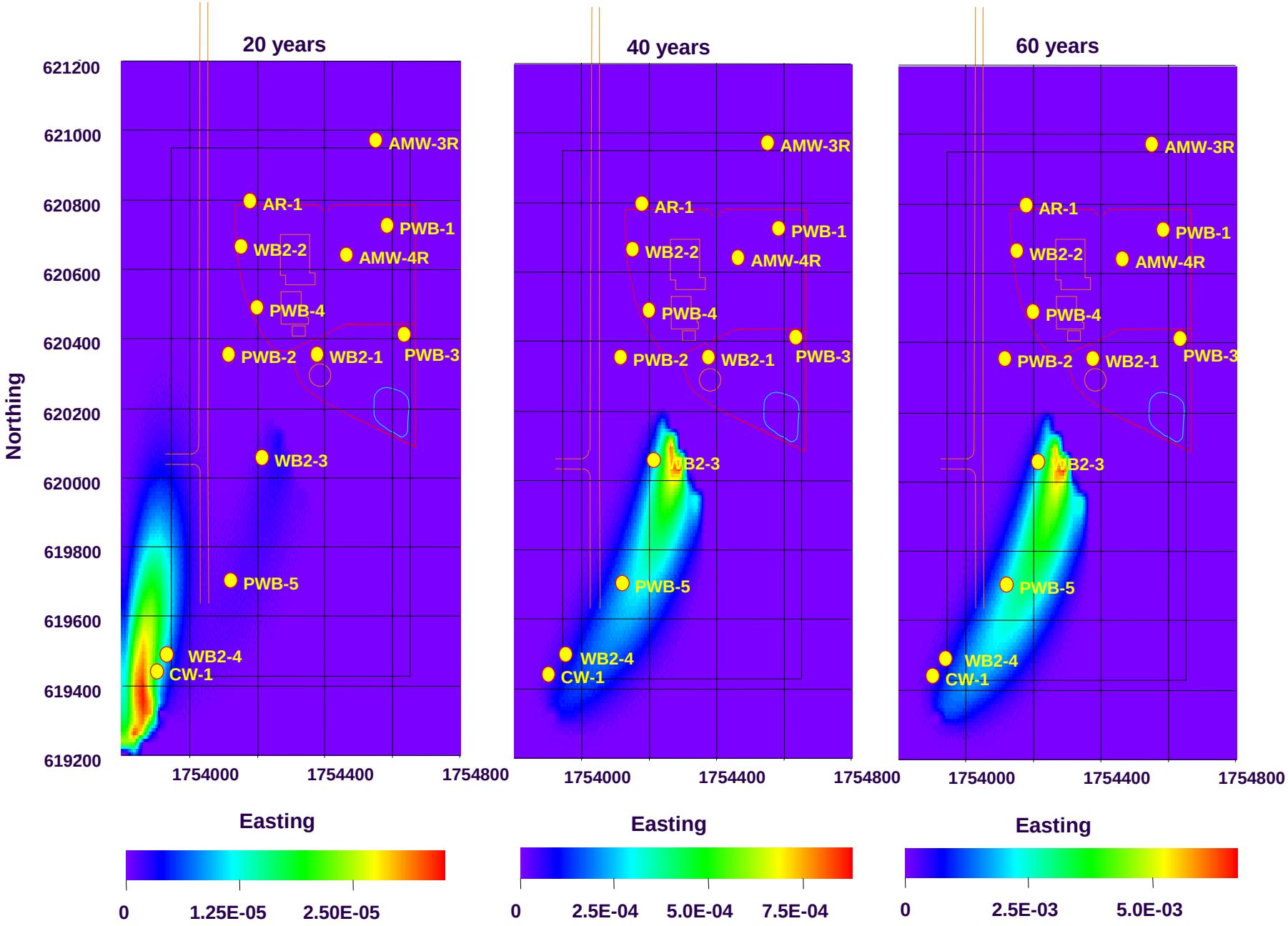

Simulated Concentration of Chloroform (µg/l) in the B-zone Groundwater (Conservative)

PANACEA, INC.
Environmental Services

Project No.	Figure
C00-266	4-37b

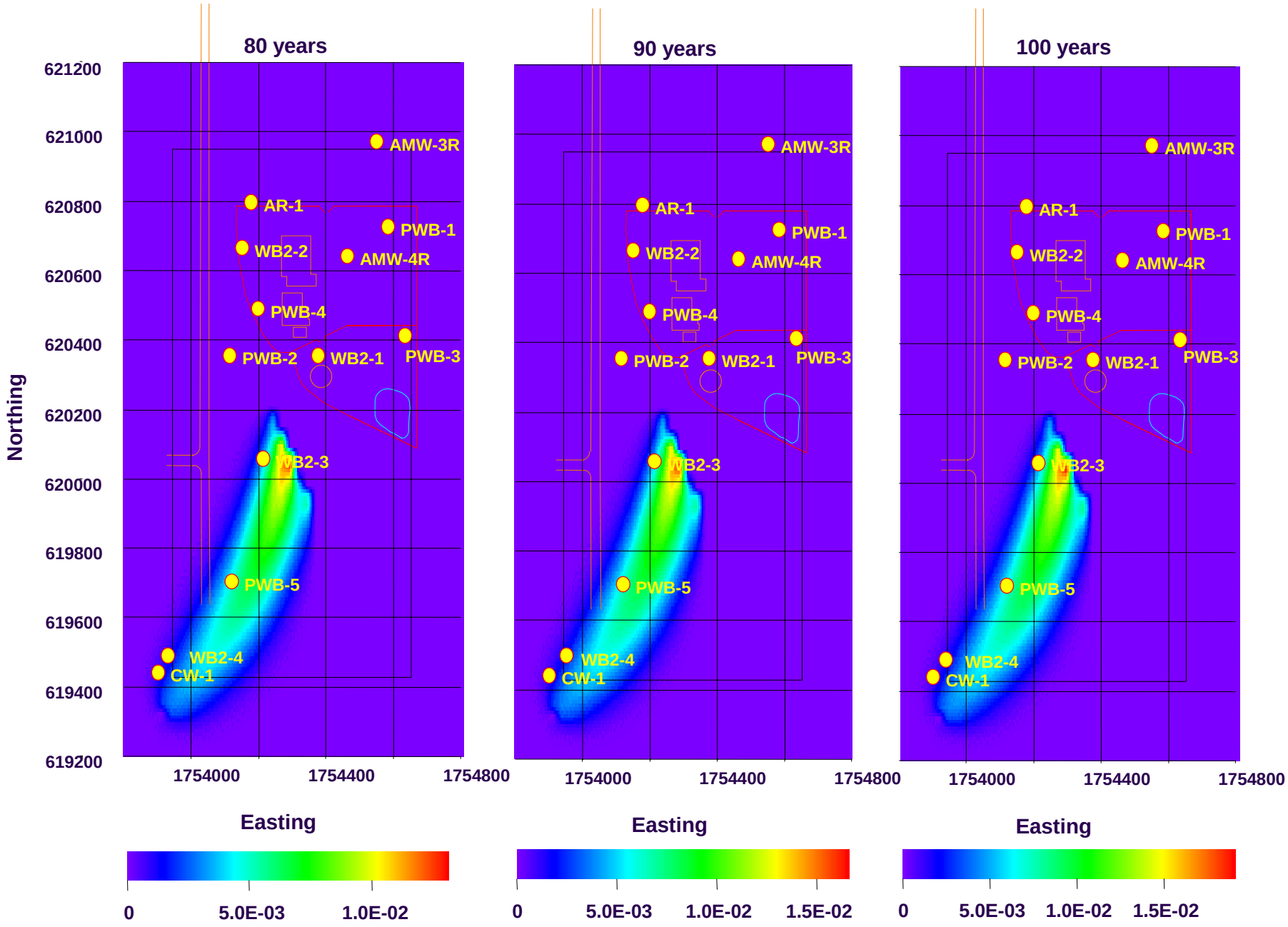

Simulated Concentration of Chloroform (µg/l) in the B-zone Groundwater (Conservative)

PANACEA, INC.
Environmental Services

Project No.	Figure
C00-266	4-37c

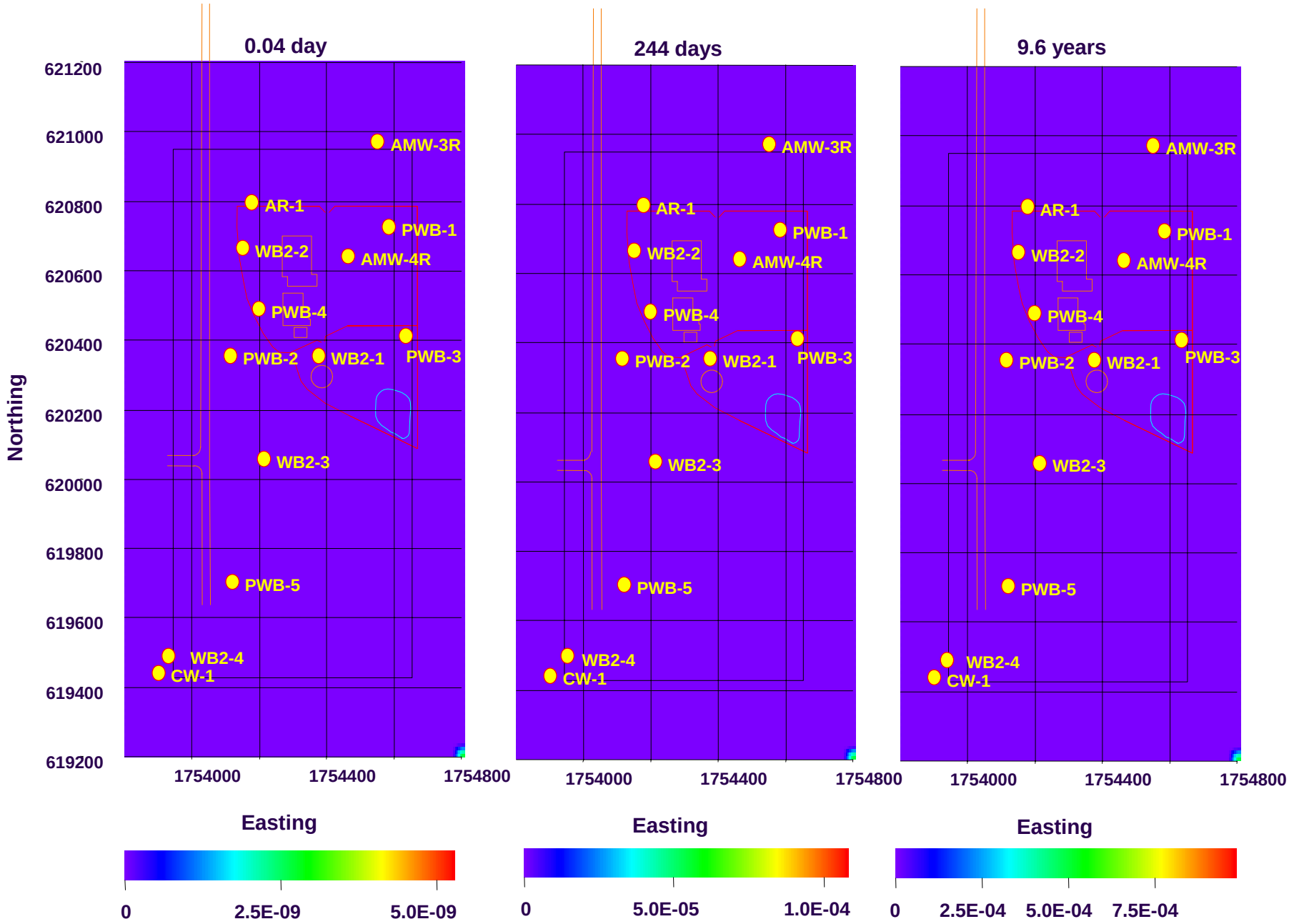

Simulated Concentration of DBCP (µg/l) in the B-zone Groundwater (Conservative)

PANACEA, INC.
Environmental Services

Project No.	Figure
C00-266	4-38a

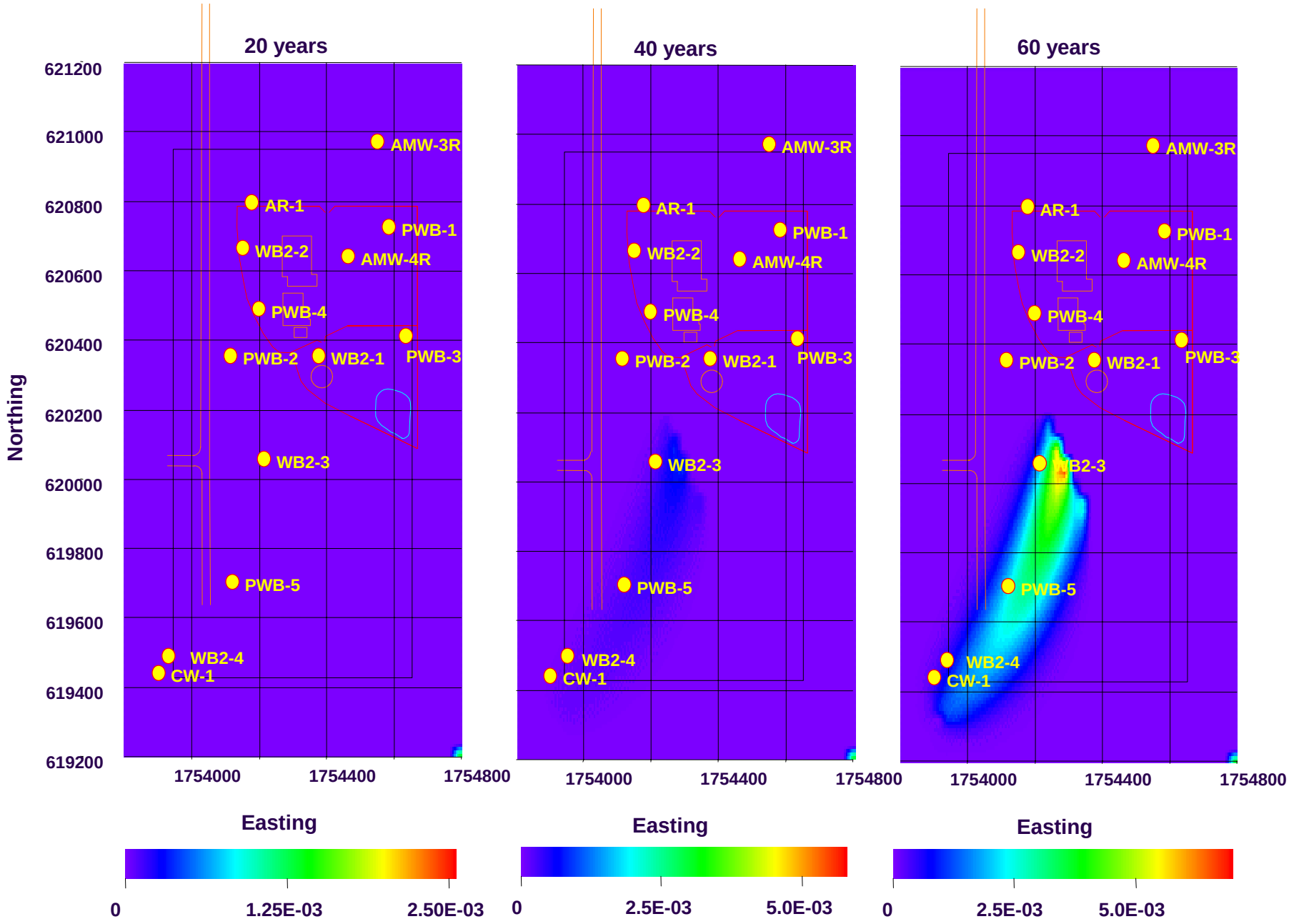

Simulated Concentration of DBCP (µg/l) in the B-zone Groundwater (Conservative)

PANACEA, INC.
Environmental Services

Project No.	Figure
C00-266	4-38b

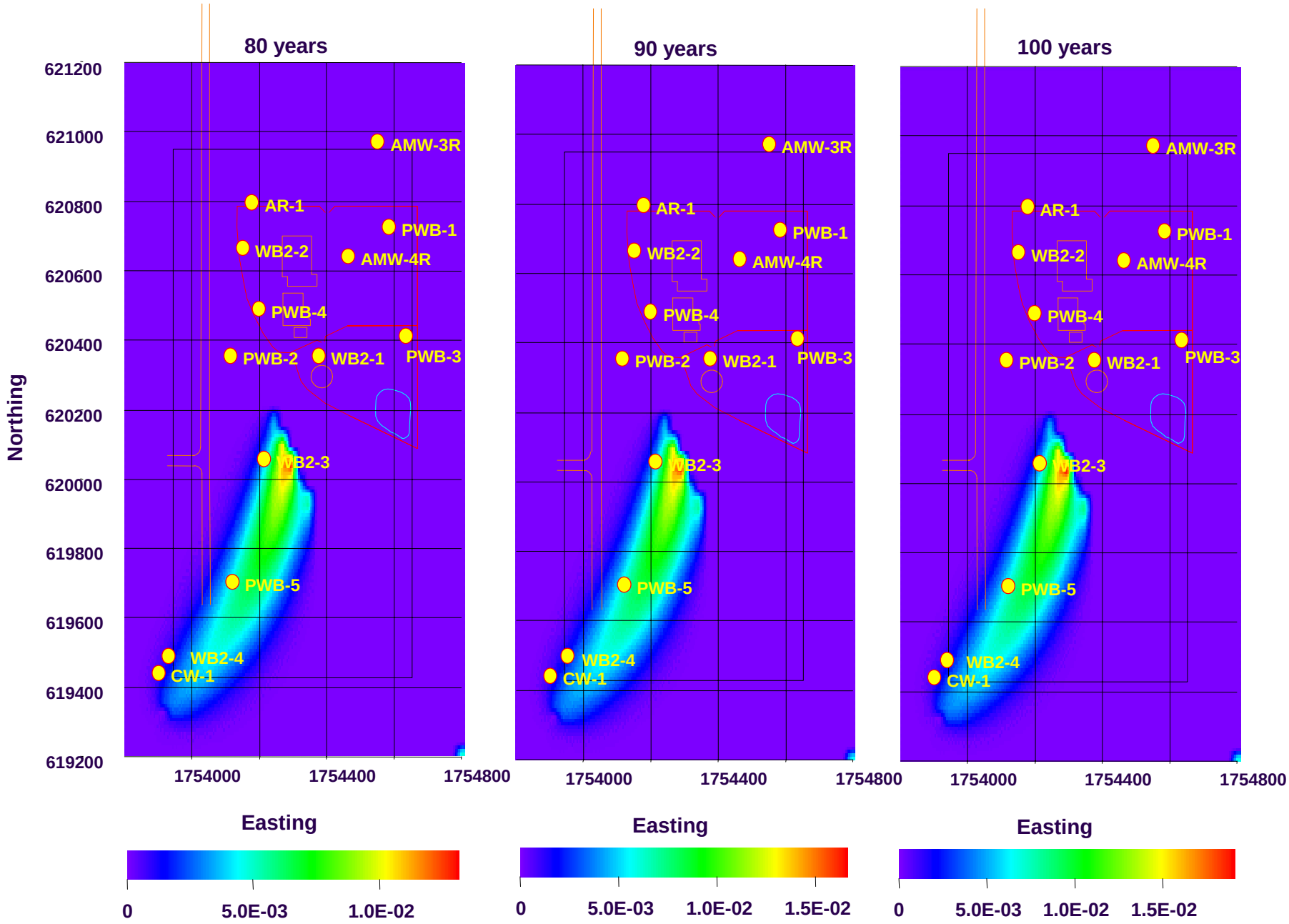

Simulated Concentration of DBCP (µg/l) in the B-zone Groundwater (Conservative)

PANACEA, INC.
Environmental Services

Project No.	Figure
C00-266	4-38c

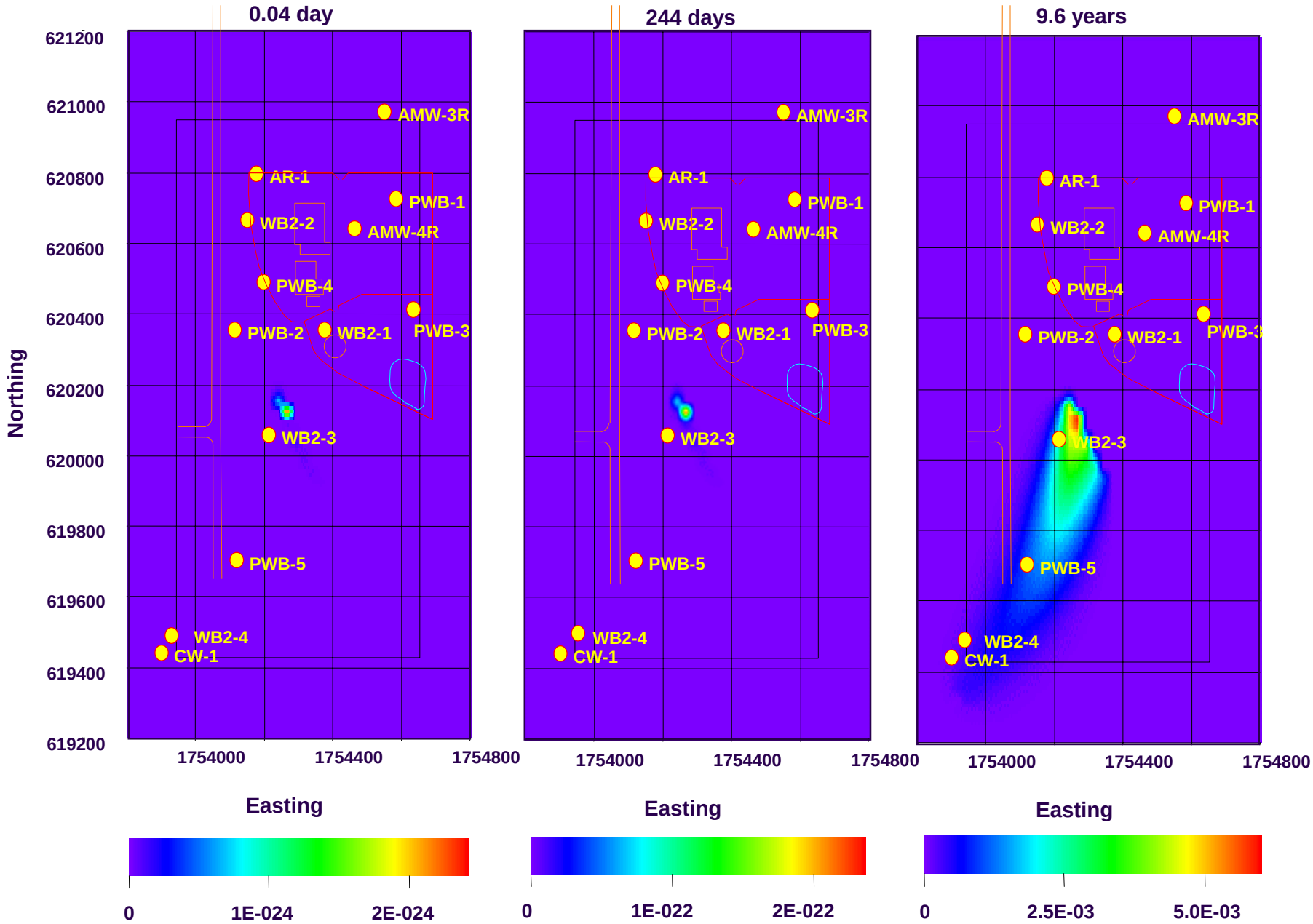

Simulated Concentration of Dinoseb (µg/l) in the Saturated Zone (Conservative)

PANACEA, INC.
Environmental Services

Project No.	Figure
C00-266	4-39a

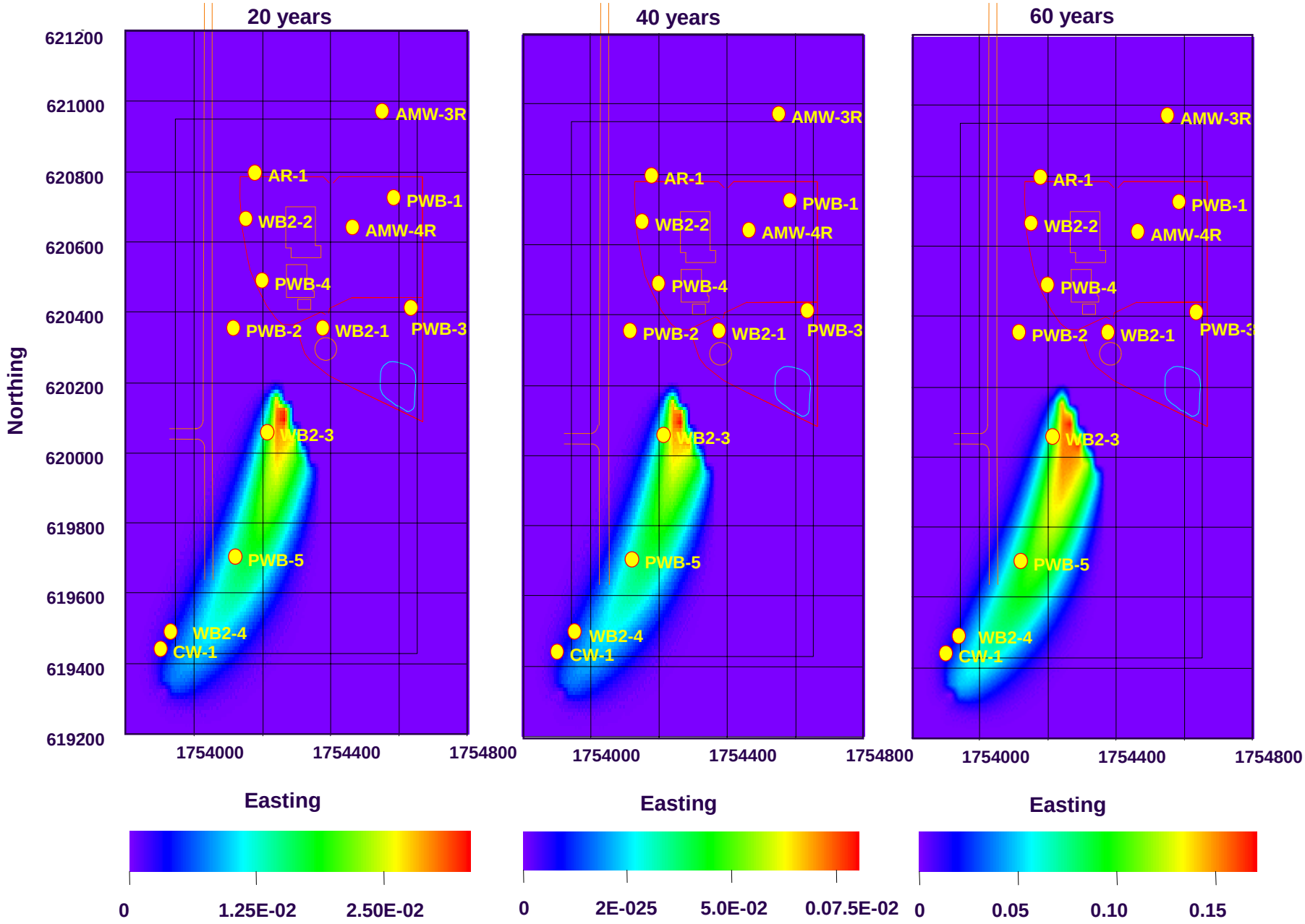

Simulated Concentration of Dinoseb (µg/l) in the Saturated Zone (Conservative)

PANACEA, INC.
Environmental Services

Project No.	Figure
C00-266	4-39b

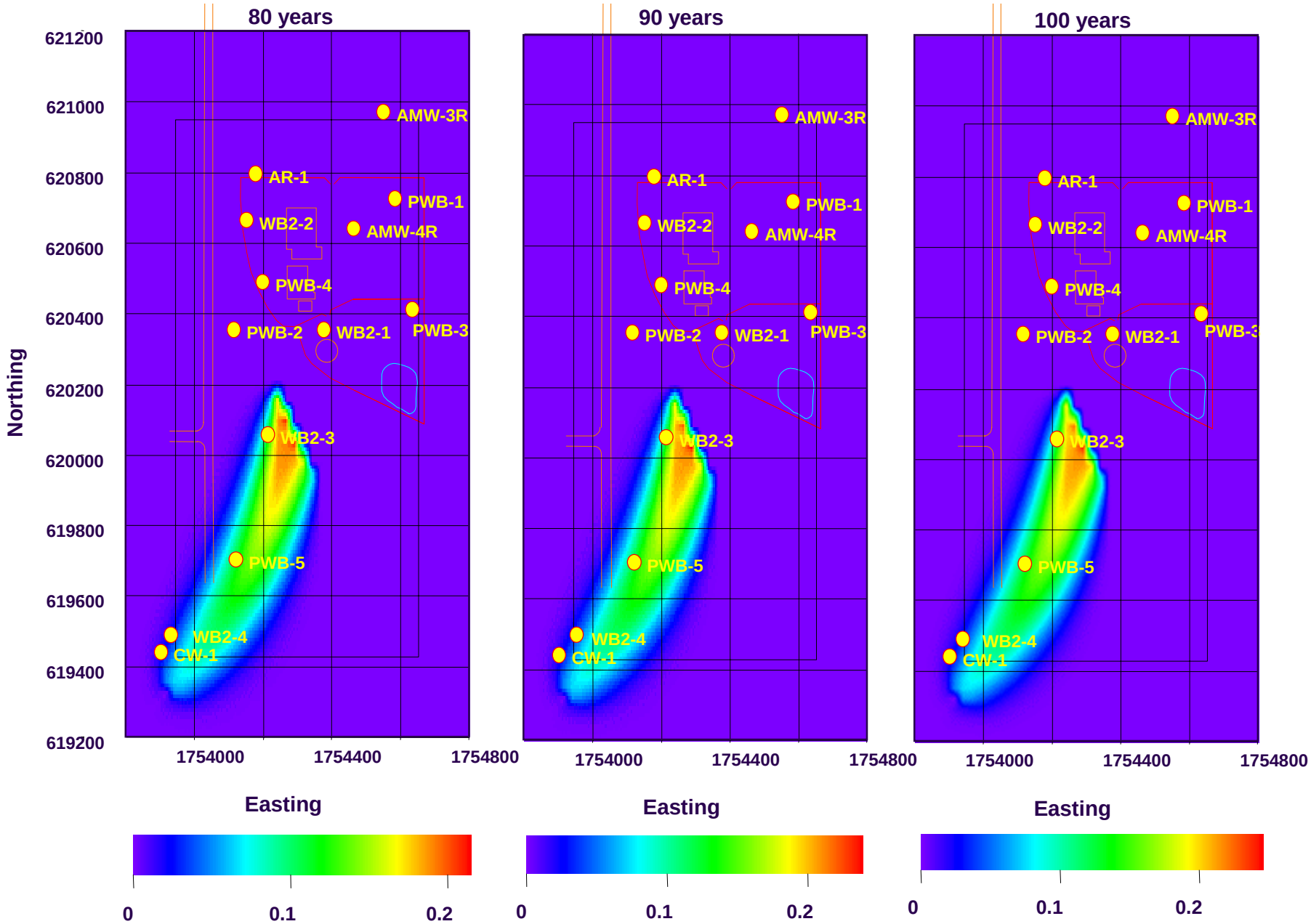

Simulated Concentration of Dinoseb (µg/l) in the Saturated Zone (Conservative)

PANACEA, INC.
Environmental Services

Project No.	Figure
C00-266	4-39c

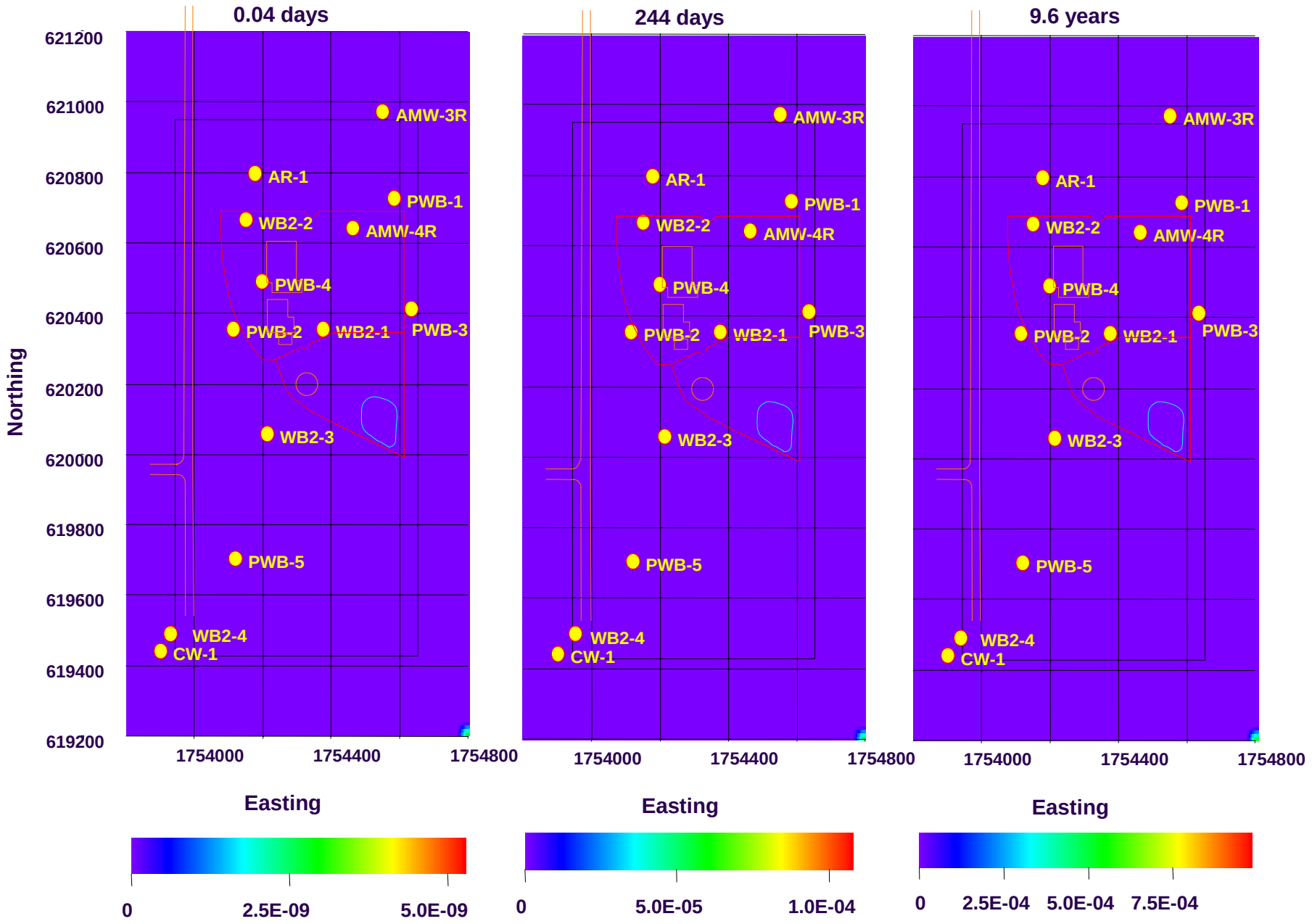

Simulated Concentration of EDB (µg/l) in the Saturated Zone (Conservative)

PANACEA, INC.
Environmental Services

Project No.	Figure
C00-266	4-40a

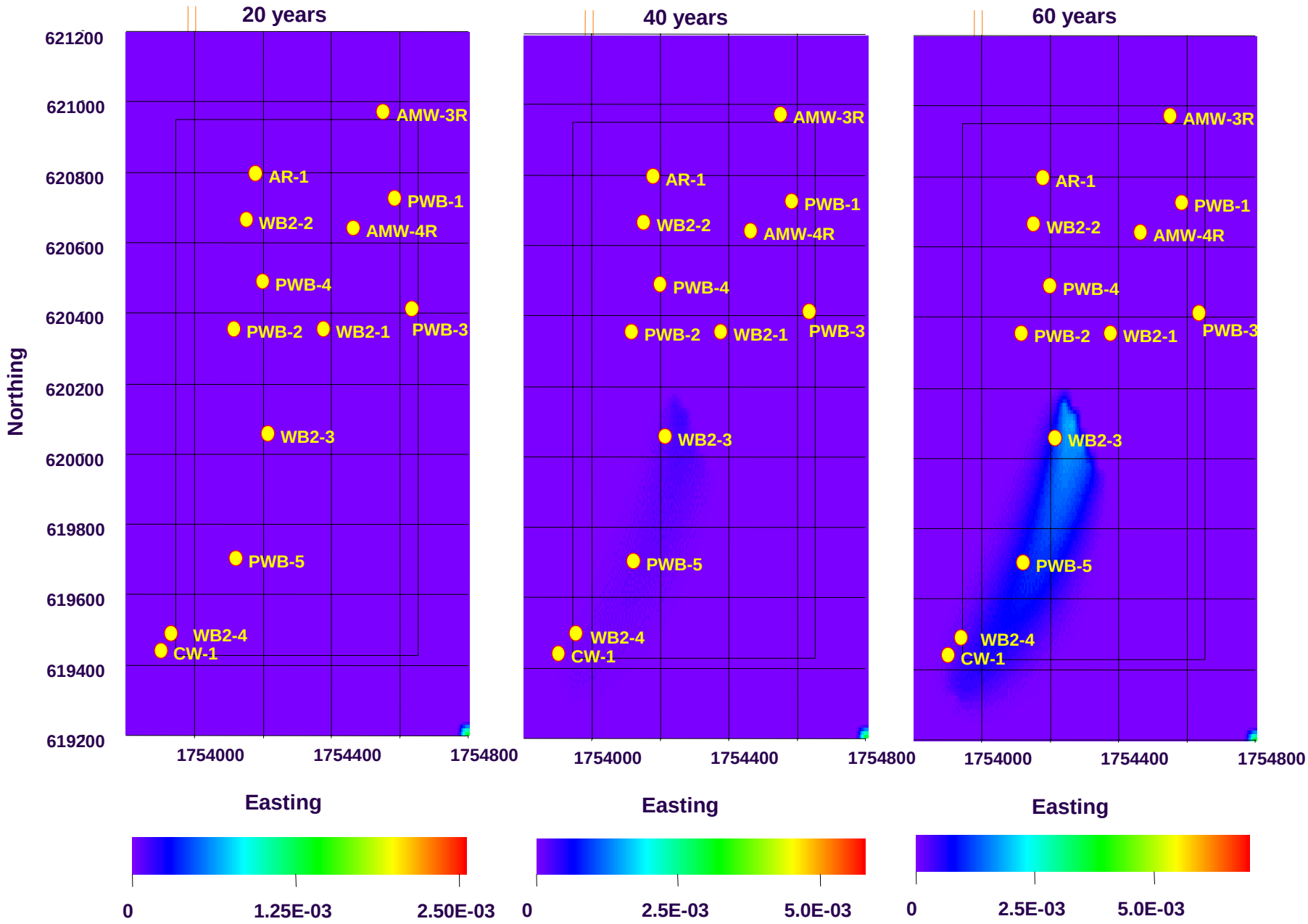

Simulated Concentration of EDB (µg/l) in the Saturated Zone (Conservative)

PANACEA, INC.
Environmental Services

Project No.	Figure
C00-266	4-40b

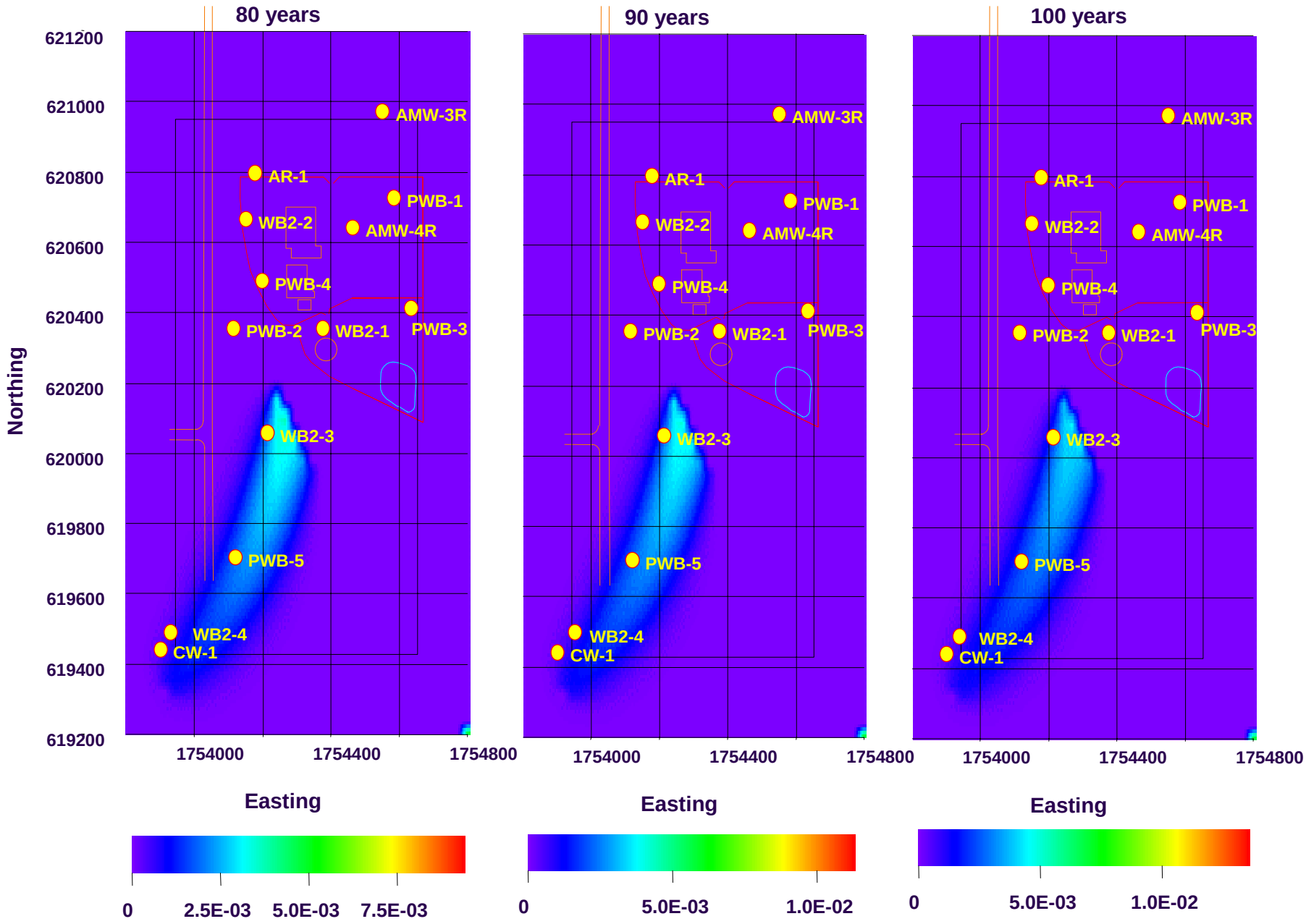

Simulated Concentration of EDB (µg/l) in the Saturated Zone (Conservative)

PANACEA, INC.
Environmental Services

Project No.	Figure
C00-266	4-40c

Appendix A

Photographs of the Site

Photograph A-1 – View looking west at the City of Arvin. Approximate location of the site is marked with the circle.

Photograph A-2 – View looking west at the Brown and Bryant Site. The tank is the upper-left corner and the warehouse is in the upper-right corner of the photograph.

Photograph A-3 – View looking east at the farm adjacent to the Brown and Bryant Site. The tilled soil facilitates infiltration of the runoff from the irrigation water.

Photograph A-4 – View looking northeast at the EPAS-4 well, which is situated on the northeast corner of the modeled area.

Photograph A-5 – View looking west at the City of Arvin water supply well, which is situated near the southeast corner of the modeled area.

Appendix B

Sample of the Database Used for Simulations

Project No. C02-266 June 2004

LabData

Location ID	Borehole ID	Date	Depth	Sample Type	Sample I	Category	Category ID	Unit	Amount	Measure Type	CAS Index
1	1	01-Sep-87	80	-555	MW-001-	BLANK	1	ug/l	1000	1	40
1	1	01-Sep-87	80	1	MW-001-	BLANK	1	ug/l	950	1	1008
1	1	01-Sep-87	80	1	MW-001-	BLANK	1	ug/l	10000	1	1005
1	1	01-Sep-87	80	1	MW-001-	BLANK	1	ug/l	30	1	1486
1	1	01-Sep-87	80	1	MW-001-	BLANK	1	ug/l	10	1	1485
1	1	01-Sep-87	80	1	MW-001-	BLANK	1	ug/l	21000	1	1484
1	1	01-Sep-87	80	1	MW-001-	BLANK	1	ug/l	64000	1	9
1	1	01-Oct-87	80	-555	MW-001-	BLANK	1	ug/l	1000	1	40
1	1	01-Oct-87	80	1	MW-001-	BLANK	1	ug/l	1000	1	1008
1	1	01-Oct-87	80	1	MW-001-	BLANK	1	ug/l	660	1	1486
1	1	01-Oct-87	80	1	MW-001-	BLANK	1	ug/l	10000	1	1005
1	1	01-Oct-87	80	1	MW-001-	BLANK	1	ug/l	3800	1	1484
1	1	01-Oct-87	80	1	MW-001-	BLANK	1	ug/l	63000	1	9
1	1	01-Oct-87	80	1	MW-001-	BLANK	1	ug/l	720	1	1485
1	1	01-Dec-87	80	-999	MW-001-	BLANK	1	ug/l	-999	1	1486
1	1	01-Dec-87	80	-999	MW-001-	BLANK	1	ug/l	-999	1	40
1	1	01-Dec-87	80	-999	MW-001-	BLANK	1	ug/l	-999	1	9
1	1	01-Dec-87	80	-999	MW-001-	BLANK	1	ug/l	-999	1	1484

Location ID	Borehole ID	Date	Depth	Sample Type	Sample I	Category	Category ID	Unit	Amount	Measure Type	CAS Index
1	1	01-Dec-87	80	-999	MW-001-	BLANK		1	ug/l	-999	1 1005
1	1	01-Dec-87	80	-999	MW-001-	BLANK		1	ug/l	-999	1 1008
1	1	01-Dec-87	80	-999	MW-001-	BLANK		1	ug/l	-999	1 1485
1	1	01-Feb-88	80	-999	MW-001-	BLANK		1	ug/l	-999	1 1484
1	1	01-Feb-88	80	-999	MW-001-	BLANK		1	ug/l	-999	1 1005
1	1	01-Feb-88	80	-999	MW-001-	BLANK		1	ug/l	-999	1 1008
1	1	01-Feb-88	80	-999	MW-001-	BLANK		1	ug/l	-999	1 1485
1	1	01-Feb-88	80	-999	MW-001-	BLANK		1	ug/l	-999	1 1486
1	1	01-Feb-88	80	-999	MW-001-	BLANK		1	ug/l	-999	1 9
1	1	01-Feb-88	80	-999	MW-001-	BLANK		1	ug/l	-999	1 40
1	1	01-Mar-88	80	-999	MW-001-	BLANK		1	ug/l	-999	1 1008
1	1	01-Mar-88	80	-999	MW-001-	BLANK		1	ug/l	-999	1 1005
1	1	01-Mar-88	80	-999	MW-001-	BLANK		1	ug/l	-999	1 1486
1	1	01-Mar-88	80	-999	MW-001-	BLANK		1	ug/l	-999	1 9
1	1	01-Mar-88	80	-999	MW-001-	BLANK		1	ug/l	-999	1 1485
1	1	01-Mar-88	80	-999	MW-001-	BLANK		1	ug/l	-999	1 40
1	1	01-Mar-88	80	-999	MW-001-	BLANK		1	ug/l	-999	1 1484
1	1	01-May-90	80	-999	MW-001-	BLANK		1	ug/l	-999	1 1484
1	1	01-May-90	80	-999	MW-001-	BLANK		1	ug/l	-999	1 40
1	1	01-May-90	80	1	MW-001-	BLANK		1	ug/l	380	1 1486

Location ID	Borehole ID	Date	Depth	Sample Type	Sample I	Category	Category ID	Unit	Amount	Measure Type	CAS Index
1	1	01-May-90	80	1	MW-001-	BLANK		1	ug/l	620	1	1008
1	1	01-May-90	80	1	MW-001-	BLANK		1	ug/l	7300	1	1005
1	1	01-May-90	80	1	MW-001-	BLANK		1	ug/l	1200	1	1485
1	1	01-May-90	80	1	MW-001-	BLANK		1	ug/l	30000	1	9
1	1	01-Jan-91	80	-999	MW-001-	BLANK		1	ug/l	-999	1	40
1	1	01-Jan-91	80	1	MW-001-	BLANK		1	ug/l	550	1	1008
1	1	01-Jan-91	80	1	MW-001-	BLANK		1	ug/l	694	1	1486
1	1	01-Jan-91	80	1	MW-001-	BLANK		1	ug/l	6800	1	1005
1	1	01-Jan-91	80	1	MW-001-	BLANK		1	ug/l	1564	1	1485
1	1	01-Jan-91	80	1	MW-001-	BLANK		1	ug/l	16350	1	1484
1	1	01-Jan-91	80	1	MW-001-	BLANK		1	ug/l	29000	1	9
1	1	01-Apr-91	80	1	MW-001-	BLANK		1	ug/l	1300	1	1485
1	1	01-Apr-91	80	1	MW-001-	BLANK		1	ug/l	485	1	1008
1	1	01-Apr-91	80	1	MW-001-	BLANK		1	ug/l	6350	1	1005
1	1	01-Apr-91	80	1	MW-001-	BLANK		1	ug/l	52	1	40
1	1	01-Apr-91	80	1	MW-001-	BLANK		1	ug/l	31500	1	9
1	1	01-Apr-91	80	1	MW-001-	BLANK		1	ug/l	13100	1	1484
1	1	01-Apr-91	80	1	MW-001-	BLANK		1	ug/l	400	1	1486
1	1	01-Aug-91	80	1	MW-001-	BLANK		1	ug/l	670	1	1008
1	1	01-Aug-91	80	1	MW-001-	BLANK		1	ug/l	25000	1	9

Location ID	Borehole ID	Date	Depth	Sample Type	Sample I	Category	Category ID	Unit	Amount	Measure Type	CAS Index
1	1	01-Aug-91	80	1	MW-001-	BLANK	1	ug/l	170	1	1486
1	1	01-Aug-91	80	1	MW-001-	BLANK	1	ug/l	605	1	1485
1	1	01-Aug-91	80	1	MW-001-	BLANK	1	ug/l	11000	1	1005
1	1	01-Aug-91	80	1	MW-001-	BLANK	1	ug/l	6700	1	1484
1	1	01-Aug-91	80	1	MW-001-	BLANK	1	ug/l	38	1	40
1	1	01-Dec-91	80	1	MW-001-	BLANK	1	ug/l	600	1	1008
1	1	01-Dec-91	80	1	MW-001-	BLANK	1	ug/l	35	1	40
1	1	01-Dec-91	80	1	MW-001-	BLANK	1	ug/l	180	1	1486
1	1	01-Dec-91	80	1	MW-001-	BLANK	1	ug/l	19000	1	9
1	1	01-Dec-91	80	1	MW-001-	BLANK	1	ug/l	35000	1	1484
1	1	01-Dec-91	80	1	MW-001-	BLANK	1	ug/l	930	1	1485
1	1	01-Dec-91	80	1	MW-001-	BLANK	1	ug/l	9000	1	1005
1	1	01-Apr-92	80	1	MW-001-	BLANK	1	ug/l	34000	1	1484
1	1	01-Apr-92	80	1	MW-001-	BLANK	1	ug/l	390	1	1008
1	1	01-Apr-92	80	1	MW-001-	BLANK	1	ug/l	18	1	40
1	1	01-Apr-92	80	1	MW-001-	BLANK	1	ug/l	380	1	1485
1	1	01-Apr-92	80	1	MW-001-	BLANK	1	ug/l	64	1	1486
1	1	01-Apr-92	80	1	MW-001-	BLANK	1	ug/l	6900	1	1005
1	1	01-Apr-92	80	1	MW-001-	BLANK	1	ug/l	9800	1	9
1	1	01-Jul-92	80	-999	MW-001-	BLANK	1	ug/l	-999	1	1485

Location ID	Borehole ID	Date	Depth	Sample Type	Sample I	Category	Category ID	Unit	Amount	Measure Type	CAS Index
1	1	01-Jul-92	80	-999	MW-001-	BLANK	1	ug/l	-999	1	9
1	1	01-Jul-92	80	-999	MW-001-	BLANK	1	ug/l	-999	1	1008
1	1	01-Jul-92	80	-999	MW-001-	BLANK	1	ug/l	-999	1	1005
1	1	01-Jul-92	80	-999	MW-001-	BLANK	1	ug/l	-999	1	40
1	1	01-Jul-92	80	-999	MW-001-	BLANK	1	ug/l	-999	1	1486
1	1	01-Jul-92	80	1	MW-001-	BLANK	1	ug/l	40000	1	1484
1	1	01-Dec-92	80	1	MW-001-	BLANK	1	ug/l	22	1	40
1	1	01-Dec-92	80	1	MW-001-	BLANK	1	ug/l	30	1	1485
1	1	01-Dec-92	80	1	MW-001-	BLANK	1	ug/l	5900	1	1005
1	1	01-Dec-92	80	1	MW-001-	BLANK	1	ug/l	15000	1	9
1	1	01-Dec-92	80	1	MW-001-	BLANK	1	ug/l	360	1	1008
1	1	01-Dec-92	80	1	MW-001-	BLANK	1	ug/l	51000	1	1484
1	1	01-Dec-92	80	1	MW-001-	BLANK	1	ug/l	140	1	1486
1	1	01-Aug-94	80	1	MW-001-	BLANK	1	ug/l	4700	1	9
1	1	01-Aug-94	80	1	MW-001-	BLANK	1	ug/l	28000	1	1484
1	1	01-Aug-94	80	1	MW-001-	BLANK	1	ug/l	130	1	1008
1	1	01-Aug-94	80	1	MW-001-	BLANK	1	ug/l	5700	1	1005
1	1	01-Aug-94	80	1	MW-001-	BLANK	1	ug/l	150	1	1485
1	1	01-Aug-94	80	1	MW-001-	BLANK	1	ug/l	48	1	1486
1	1	01-Aug-94	80	1	MW-001-	BLANK	1	ug/l	12	1	40

Location ID	Borehole ID	Date	Depth	Sample Type	Sample I	Category	Category ID	Unit	Amount	Measure Type	CAS Index
1	1	01-Mar-95	80	1	MW-001-	BLANK		1	ug/l	54	1	1486
1	1	01-Mar-95	80	1	MW-001-	BLANK		1	ug/l	135	1	1008
1	1	01-Mar-95	80	1	MW-001-	BLANK		1	ug/l	8250	1	1005
1	1	01-Mar-95	80	1	MW-001-	BLANK		1	ug/l	10	1	40
1	1	01-Mar-95	80	1	MW-001-	BLANK		1	ug/l	5050	1	9
1	1	01-Mar-95	80	1	MW-001-	BLANK		1	ug/l	83000	1	1484
1	1	01-Mar-95	80	1	MW-001-	BLANK		1	ug/l	86	1	1485
1	1	01-Nov-95	80	1	MW-001-	BLANK		1	ug/l	2	1	40
1	1	01-Nov-95	80	1	MW-001-	BLANK		1	ug/l	42000	1	1484
1	1	01-Nov-95	80	1	MW-001-	BLANK		1	ug/l	1900	1	1005
1	1	01-Nov-95	80	1	MW-001-	BLANK		1	ug/l	13	1	1486
1	1	01-Nov-95	80	1	MW-001-	BLANK		1	ug/l	18	1	1008
1	1	01-Nov-95	80	1	MW-001-	BLANK		1	ug/l	19	1	1485
1	1	01-Nov-95	80	1	MW-001-	BLANK		1	ug/l	1000	1	9
1	1	01-Nov-96	80	-999	MW-001-	BLANK		1	ug/l	-999	1	40
1	1	01-Nov-96	80	1	MW-001-	BLANK		1	ug/l	10	1	1486
1	1	01-Nov-96	80	1	MW-001-	BLANK		1	ug/l	11	1	1485
1	1	01-Nov-96	80	1	MW-001-	BLANK		1	ug/l	830	1	1484
1	1	01-Nov-96	80	1	MW-001-	BLANK		1	ug/l	980	1	1005
1	1	01-Nov-96	80	1	MW-001-	BLANK		1	ug/l	9	1	1008

Location ID	Borehole ID	Date	Depth	Sample Type	Sample I	Category	Category ID	Unit	Amount	Measure Type	CAS Index
1	1	01-Nov-96	80	1	MW-001-	BLANK	1	ug/l	700	1	9
1	1	01-May-97	80	-999	MW-001-	BLANK	1	ug/l	-999	1	40
1	1	01-May-97	80	1	MW-001-	BLANK	1	ug/l	5	1	1008
1	1	01-May-97	80	1	MW-001-	BLANK	1	ug/l	10	1	1486
1	1	01-May-97	80	1	MW-001-	BLANK	1	ug/l	840	1	1005
1	1	01-May-97	80	1	MW-001-	BLANK	1	ug/l	1600	1	1484
1	1	01-May-97	80	1	MW-001-	BLANK	1	ug/l	500	1	9
1	1	01-May-97	80	1	MW-001-	BLANK	1	ug/l	2.9	1	1485
1	1	01-Jan-98	80	1	MW-001-	BLANK	1	ug/l	450	1	1005
1	1	01-Jan-98	80	1	MW-001-	BLANK	1	ug/l	1	1	40
1	1	01-Jan-98	80	1	MW-001-	BLANK	1	ug/l	15	1	1484
1	1	01-Jan-98	80	1	MW-001-	BLANK	1	ug/l	670	1	9
1	1	01-Jan-98	80	1	MW-001-	BLANK	1	ug/l	13.8	1	1485
1	1	01-Jan-98	80	1	MW-001-	BLANK	1	ug/l	6	1	1008
1	1	01-Jan-98	80	1	MW-001-	BLANK	1	ug/l	4.8	1	1486
1	1	01-Jul-98	80	-999	MW-001-	BLANK	1	ug/l	-999	1	40
1	1	01-Jul-98	80	-777	MW-001-	BLANK	1	ug/l	-777	1	1485
1	1	01-Jul-98	80	-777	MW-001-	BLANK	1	ug/l	-777	1	1486
1	1	01-Jul-98	80	-777	MW-001-	BLANK	1	ug/l	-777	1	1484
1	1	01-Jul-98	80	1	MW-001-	BLANK	1	ug/l	40	1	1005

Location ID	Borehole ID	Date	Depth	Sample Type	Sample I	Category	Category ID	Unit	Amount	Measure Type	CAS Index
1	1	01-Jul-98	80	1	MW-001-	BLANK	1	ug/l	110	1	9
1	1	01-Jul-98	80	1	MW-001-	BLANK	1	ug/l	1.3	1	1008
1	1	01-Jul-00	80	-999	MW-001-	BLANK	1	ug/l	-999	1	1486
1	1	01-Jul-00	80	-999	MW-001-	BLANK	1	ug/l	-999	1	1485
1	1	01-Jul-00	80	-999	MW-001-	BLANK	1	ug/l	-999	1	1008
1	1	01-Jul-00	80	-999	MW-001-	BLANK	1	ug/l	-999	1	40
1	1	01-Jul-00	80	1	MW-001-	BLANK	1	ug/l	112	1	9
1	1	01-Jul-00	80	1	MW-001-	BLANK	1	ug/l	36	1	1005
1	1	01-Jul-00	80	1	MW-001-	BLANK	1	ug/l	432	1	1484
1	1	02-Nov-00	80	-999	MW-001-	BLANK	1	ug/l	-999	1	40
1	1	02-Nov-00	80	-999	MW-001-	BLANK	1	ug/l	-999	1	1485
1	1	02-Nov-00	80	-999	MW-001-	BLANK	1	ug/l	-999	1	1008
1	1	02-Nov-00	80	1	MW-001-	BLANK	1	ug/l	50	1	1005
1	1	02-Nov-00	80	1	MW-001-	BLANK	1	ug/l	474	1	1484
1	1	02-Nov-00	80	1	MW-001-	BLANK	1	ug/l	17	1	1486
1	1	02-Nov-00	80	1	MW-001-	BLANK	1	ug/l	188	1	9
1	1	01-Apr-01	80	-999	MW-001-	BLANK	1	ug/l	-999	1	1486
1	1	01-Apr-01	80	-999	MW-001-	BLANK	1	ug/l	-999	1	40
1	1	01-Apr-01	80	-999	MW-001-	BLANK	1	ug/l	-999	1	1008
1	1	01-Apr-01	80	1	MW-001-	BLANK	1	ug/l	497	1	1484

Location ID	Borehole ID	Date	Depth	Sample Type	Sample I	Category	Category ID	Unit	Amount	Measure Type	CAS Index
1	1	01-Apr-01	80	1	MW-001-	BLANK		1	ug/l	1.32	1	1485
1	1	01-Apr-01	80	1	MW-001-	BLANK		1	ug/l	34	1	1005
1	1	01-Apr-01	80	1	MW-001-	BLANK		1	ug/l	168	1	9
1	1	20-Jul-01	80	-999	MW-001-	BLANK		1	ug/l	-999	1	40
1	1	20-Jul-01	80	-999	MW-001-	BLANK		1	ug/l	-999	1	1486
1	1	20-Jul-01	80	-999	MW-001-	BLANK		1	ug/l	-999	1	1008
1	1	20-Jul-01	80	1	MW-001-	BLANK		1	ug/l	547	1	1484
1	1	20-Jul-01	80	1	MW-001-	BLANK		1	ug/l	2.3	1	1485
1	1	20-Jul-01	80	1	MW-001-	BLANK		1	ug/l	75	1	1005
1	1	20-Jul-01	80	1	MW-001-	BLANK		1	ug/l	254	1	9
1	1	17-Oct-01	80	-999	MW-001-	BLANK		1	ug/l	-999	1	1486
1	1	17-Oct-01	80	-999	MW-001-	BLANK		1	ug/l	-999	1	40
1	1	17-Oct-01	80	-999	MW-001-	BLANK		1	ug/l	-999	1	1485
1	1	17-Oct-01	80	-999	MW-001-	BLANK		1	ug/l	-999	1	1008
1	1	17-Oct-01	80	1	MW-001-	BLANK		1	ug/l	1710	1	1484
1	1	17-Oct-01	80	1	MW-001-	BLANK		1	ug/l	87	1	1005
1	1	17-Oct-01	80	1	MW-001-	BLANK		1	ug/l	322	1	9
1	1	02-Feb-02	80	-999	MW-001-	BLANK		1	ug/l	-999	1	1008
1	1	02-Feb-02	80	-999	MW-001-	BLANK		1	ug/l	-999	1	40
1	1	02-Feb-02	80	1	MW-001-	BLANK		1	ug/l	4300	1	1484

Location ID	Borehole ID	Date	Depth	Sample Type	Sample I	Category	Category ID	Unit	Amount	Measure Type	CAS Index
1	1	02-Feb-02	80	1	MW-001-	BLANK	1	ug/l	2300	1	9
1	1	02-Feb-02	80	1	MW-001-	BLANK	1	ug/l	320	1	1005
1	1	02-Feb-02	80	1	MW-001-	BLANK	1	ug/l	4.2	1	1485
1	1	02-Feb-02	80	1	MW-001-	BLANK	1	ug/l	12	1	1486
1	2	01-Sep-87	80	1	MW-001-	BLANK	1	ug/l	110000	1	9
1	2	01-Sep-87	80	1	MW-001-	BLANK	1	ug/l	22	1	1485
1	2	01-Sep-87	80	1	MW-001-	BLANK	1	ug/l	4800	1	1005
1	2	01-Sep-87	80	1	MW-001-	BLANK	1	ug/l	1900	1	40
1	2	01-Sep-87	80	1	MW-001-	BLANK	1	ug/l	20000	1	1484
1	2	01-Sep-87	80	-666	MW-001-	BLANK	1	ug/l	-0.1	1	1486
1	2	01-Sep-87	80	-500	MW-001-	BLANK	1	ug/l	-500	1	1008
1	2	01-Oct-87	80	1	MW-001-	BLANK	1	ug/l	930	1	1484
1	2	01-Oct-87	80	1	MW-001-	BLANK	1	ug/l	440	1	1486
1	2	01-Oct-87	80	1	MW-001-	BLANK	1	ug/l	200	1	1008
1	2	01-Oct-87	80	1	MW-001-	BLANK	1	ug/l	130	1	1485
1	2	01-Oct-87	80	1	MW-001-	BLANK	1	ug/l	82000	1	9
1	2	01-Oct-87	80	1	MW-001-	BLANK	1	ug/l	5000	1	1005
1	2	01-Oct-87	80	1	MW-001-	BLANK	1	ug/l	1500	1	40
1	2	01-Dec-87	80	-999	MW-001-	BLANK	1	ug/l	-999	1	1008
1	2	01-Dec-87	80	-999	MW-001-	BLANK	1	ug/l	-999	1	1486

Location ID	Borehole ID	Date	Depth	Sample Type	Sample I	Category	Category ID	Unit	Amount	Measure Type	CAS Index
1	2	01-Dec-87	80	-999	MW-001-	BLANK	1	ug/l	-999	1	9
1	2	01-Dec-87	80	-999	MW-001-	BLANK	1	ug/l	-999	1	1005
1	2	01-Dec-87	80	-999	MW-001-	BLANK	1	ug/l	-999	1	1485
1	2	01-Dec-87	80	-999	MW-001-	BLANK	1	ug/l	-999	1	1484
1	2	01-Dec-87	80	-999	MW-001-	BLANK	1	ug/l	-999	1	40
1	2	01-Feb-88	80	-999	MW-001-	BLANK	1	ug/l	-999	1	1486
1	2	01-Feb-88	80	-999	MW-001-	BLANK	1	ug/l	-999	1	40
1	2	01-Feb-88	80	-999	MW-001-	BLANK	1	ug/l	-999	1	1484
1	2	01-Feb-88	80	-999	MW-001-	BLANK	1	ug/l	-999	1	9
1	2	01-Feb-88	80	-999	MW-001-	BLANK	1	ug/l	-999	1	1008
1	2	01-Feb-88	80	-999	MW-001-	BLANK	1	ug/l	-999	1	1005
1	2	01-Feb-88	80	-999	MW-001-	BLANK	1	ug/l	-999	1	1485
1	2	01-Mar-88	80	-999	MW-001-	BLANK	1	ug/l	-999	1	1005
1	2	01-Mar-88	80	-999	MW-001-	BLANK	1	ug/l	-999	1	1485
1	2	01-Mar-88	80	-999	MW-001-	BLANK	1	ug/l	-999	1	1008
1	2	01-Mar-88	80	-999	MW-001-	BLANK	1	ug/l	-999	1	9
1	2	01-Mar-88	80	-999	MW-001-	BLANK	1	ug/l	-999	1	1484
1	2	01-Mar-88	80	-999	MW-001-	BLANK	1	ug/l	-999	1	40
1	2	01-Mar-88	80	-999	MW-001-	BLANK	1	ug/l	-999	1	1486
1	2	01-May-90	80	-999	MW-001-	BLANK	1	ug/l	-999	1	1485

Location ID	Borehole ID	Date	Depth	Sample Type	Sample I	Category	Category ID	Unit	Amount	Measure Type	CAS Index
1	2	01-May-90	80	-999	MW-001-	BLANK	1	ug/l	-999	1	9
1	2	01-May-90	80	-999	MW-001-	BLANK	1	ug/l	-999	1	1008
1	2	01-May-90	80	-999	MW-001-	BLANK	1	ug/l	-999	1	40
1	2	01-May-90	80	-999	MW-001-	BLANK	1	ug/l	-999	1	1486
1	2	01-May-90	80	-999	MW-001-	BLANK	1	ug/l	-999	1	1484
1	2	01-May-90	80	-999	MW-001-	BLANK	1	ug/l	-999	1	1005
1	2	01-Jan-91	80	1	MW-001-	BLANK	1	ug/l	3400	1	1005
1	2	01-Jan-91	80	1	MW-001-	BLANK	1	ug/l	49	1	1484
1	2	01-Jan-91	80	1	MW-001-	BLANK	1	ug/l	955	1	40
1	2	01-Jan-91	80	1	MW-001-	BLANK	1	ug/l	1.4	1	1485
1	2	01-Jan-91	80	1	MW-001-	BLANK	1	ug/l	76000	1	9
1	2	01-Jan-91	80	1	MW-001-	BLANK	1	ug/l	70	1	1008
1	2	01-Jan-91	80	1	MW-001-	BLANK	1	ug/l	453	1	1486
1	2	01-Apr-91	80	-999	MW-001-	BLANK	1	ug/l	-999	1	1484
1	2	01-Apr-91	80	1	MW-001-	BLANK	1	ug/l	320	1	1486
1	2	01-Apr-91	80	1	MW-001-	BLANK	1	ug/l	1100	1	40
1	2	01-Apr-91	80	1	MW-001-	BLANK	1	ug/l	86000	1	9
1	2	01-Apr-91	80	1	MW-001-	BLANK	1	ug/l	73	1	1008
1	2	01-Apr-91	80	1	MW-001-	BLANK	1	ug/l	4100	1	1005
1	2	01-Apr-91	80	1	MW-001-	BLANK	1	ug/l	67	1	1485

Location ID	Borehole ID	Date	Depth	Sample Type	Sample I	Category	Category ID	Unit	Amount	Measure Type	CAS Index
1	2	01-Aug-91	80	1	MW-001-	BLANK	1	ug/l	2	1	1485
1	2	01-Aug-91	80	1	MW-001-	BLANK	1	ug/l	21	1	1484
1	2	01-Aug-91	80	1	MW-001-	BLANK	1	ug/l	1100	1	40
1	2	01-Aug-91	80	1	MW-001-	BLANK	1	ug/l	3000	1	1005
1	2	01-Aug-91	80	1	MW-001-	BLANK	1	ug/l	89000	1	9
1	2	01-Aug-91	80	1	MW-001-	BLANK	1	ug/l	78	1	1008
1	2	01-Aug-91	80	1	MW-001-	BLANK	1	ug/l	388	1	1486
1	2	01-Dec-91	80	1	MW-001-	BLANK	1	ug/l	855	1	40
1	2	01-Dec-91	80	1	MW-001-	BLANK	1	ug/l	3900	1	1005
1	2	01-Dec-91	80	1	MW-001-	BLANK	1	ug/l	81000	1	9
1	2	01-Dec-91	80	1	MW-001-	BLANK	1	ug/l	2	1	1485
1	2	01-Dec-91	80	1	MW-001-	BLANK	1	ug/l	84	1	1008
1	2	01-Dec-91	80	1	MW-001-	BLANK	1	ug/l	440	1	1484
1	2	01-Dec-91	80	1	MW-001-	BLANK	1	ug/l	485	1	1486
1	2	01-Apr-92	80	1	MW-001-	BLANK	1	ug/l	240	1	1484
1	2	01-Apr-92	80	1	MW-001-	BLANK	1	ug/l	1	1	1485
1	2	01-Apr-92	80	1	MW-001-	BLANK	1	ug/l	45	1	1008
1	2	01-Apr-92	80	1	MW-001-	BLANK	1	ug/l	48000	1	9
1	2	01-Apr-92	80	1	MW-001-	BLANK	1	ug/l	268	1	1486
1	2	01-Apr-92	80	1	MW-001-	BLANK	1	ug/l	435	1	40

Location ID	Borehole ID	Date	Depth	Sample Type	Sample I	Category	Category ID	Unit	Amount	Measure Type	CAS Index
1	2	01-Apr-92	80	1	MW-001-	BLANK		1	ug/l	1700	1	1005
1	2	01-Jul-92	80	-999	MW-001-	BLANK		1	ug/l	-999	1	9
1	2	01-Jul-92	80	-999	MW-001-	BLANK		1	ug/l	-999	1	1486
1	2	01-Jul-92	80	-999	MW-001-	BLANK		1	ug/l	-999	1	1005
1	2	01-Jul-92	80	-999	MW-001-	BLANK		1	ug/l	-999	1	40
1	2	01-Jul-92	80	-999	MW-001-	BLANK		1	ug/l	-999	1	1485
1	2	01-Jul-92	80	-999	MW-001-	BLANK		1	ug/l	-999	1	1008
1	2	01-Jul-92	80	1	MW-001-	BLANK		1	ug/l	190	1	1484
1	2	01-Dec-92	80	1	MW-001-	BLANK		1	ug/l	3000	1	1484
1	2	01-Dec-92	80	1	MW-001-	BLANK		1	ug/l	1300	1	1005
1	2	01-Dec-92	80	1	MW-001-	BLANK		1	ug/l	51	1	1485
1	2	01-Dec-92	80	1	MW-001-	BLANK		1	ug/l	52	1	1008
1	2	01-Dec-92	80	1	MW-001-	BLANK		1	ug/l	390	1	40
1	2	01-Dec-92	80	1	MW-001-	BLANK		1	ug/l	50000	1	9
1	2	01-Dec-92	80	1	MW-001-	BLANK		1	ug/l	150	1	1486
1	2	01-Aug-94	80	1	MW-001-	BLANK		1	ug/l	350	1	40
1	2	01-Aug-94	80	1	MW-001-	BLANK		1	ug/l	325	1	1486
1	2	01-Aug-94	80	1	MW-001-	BLANK		1	ug/l	2450	1	1005
1	2	01-Aug-94	80	1	MW-001-	BLANK		1	ug/l	485	1	1484
1	2	01-Aug-94	80	1	MW-001-	BLANK		1	ug/l	1	1	1485

Location ID	Borehole ID	Date	Depth	Sample Type	Sample I	Category	Category ID	Unit	Amount	Measure Type	CAS Index
1	2	01-Aug-94	80	1	MW-001-	BLANK		1	ug/l	67000	1	9
1	2	01-Aug-94	80	1	MW-001-	BLANK		1	ug/l	94	1	1008
1	2	01-Mar-95	80	-999	MW-001-	BLANK		1	ug/l	-999	1	1485
1	2	01-Mar-95	80	1	MW-001-	BLANK		1	ug/l	1100	1	1484
1	2	01-Mar-95	80	1	MW-001-	BLANK		1	ug/l	350	1	1486
1	2	01-Mar-95	80	1	MW-001-	BLANK		1	ug/l	3500	1	1005
1	2	01-Mar-95	80	1	MW-001-	BLANK		1	ug/l	88000	1	9
1	2	01-Mar-95	80	1	MW-001-	BLANK		1	ug/l	100	1	1008
1	2	01-Mar-95	80	1	MW-001-	BLANK		1	ug/l	520	1	40
1	2	01-Nov-95	80	-999	MW-001-	BLANK		1	ug/l	-999	1	1485
1	2	01-Nov-95	80	1	MW-001-	BLANK		1	ug/l	3250	1	1005
1	2	01-Nov-95	80	1	MW-001-	BLANK		1	ug/l	560	1	40
1	2	01-Nov-95	80	1	MW-001-	BLANK		1	ug/l	96	1	1008
1	2	01-Nov-95	80	1	MW-001-	BLANK		1	ug/l	1085	1	1484
1	2	01-Nov-95	80	1	MW-001-	BLANK		1	ug/l	84000	1	9
1	2	01-Nov-95	80	1	MW-001-	BLANK		1	ug/l	335	1	1486
1	2	01-Nov-96	80	-999	MW-001-	BLANK		1	ug/l	-999	1	1485
1	2	01-Nov-96	80	1	MW-001-	BLANK		1	ug/l	340	1	40
1	2	01-Nov-96	80	1	MW-001-	BLANK		1	ug/l	3800	1	1005
1	2	01-Nov-96	80	1	MW-001-	BLANK		1	ug/l	420	1	1486

Location ID	Borehole ID	Date	Depth	Sample Type	Sample I	Category	Category ID	Unit	Amount	Measure Type	CAS Index
1	2	01-Nov-96	80	1	MW-001-	BLANK	1	ug/l	200	1	1484
1	2	01-Nov-96	80	1	MW-001-	BLANK	1	ug/l	88	1	1008
1	2	01-Nov-96	80	1	MW-001-	BLANK	1	ug/l	110000	1	9
1	2	01-May-97	80	1	MW-001-	BLANK	1	ug/l	0.053	1	1485
1	2	01-May-97	80	1	MW-001-	BLANK	1	ug/l	110	1	1008
1	2	01-May-97	80	1	MW-001-	BLANK	1	ug/l	240	1	40
1	2	01-May-97	80	1	MW-001-	BLANK	1	ug/l	3800	1	1005
1	2	01-May-97	80	1	MW-001-	BLANK	1	ug/l	73000	1	9
1	2	01-May-97	80	1	MW-001-	BLANK	1	ug/l	320	1	1486
1	2	01-May-97	80	1	MW-001-	BLANK	1	ug/l	330	1	1484
1	2	01-Jan-98	80	1	MW-001-	BLANK	1	ug/l	85	1	1484
1	2	01-Jan-98	80	1	MW-001-	BLANK	1	ug/l	96	1	1486
1	2	01-Jan-98	80	1	MW-001-	BLANK	1	ug/l	21	1	1485
1	2	01-Jan-98	80	1	MW-001-	BLANK	1	ug/l	50	1	1008
1	2	01-Jan-98	80	1	MW-001-	BLANK	1	ug/l	1400	1	1005
1	2	01-Jan-98	80	1	MW-001-	BLANK	1	ug/l	51000	1	9
1	2	01-Jan-98	80	1	MW-001-	BLANK	1	ug/l	110	1	40
1	2	01-Jul-98	80	-777	MW-001-	BLANK	1	ug/l	-777	1	1486
1	2	01-Jul-98	80	-777	MW-001-	BLANK	1	ug/l	-777	1	1484
1	2	01-Jul-98	80	1	MW-001-	BLANK	1	ug/l	320	1	40

Location ID	Borehole ID	Date	Depth	Sample Type	Sample I	Category	Category ID	Unit	Amount	Measure Type	CAS Index	
1	2	01-Jul-98	80	-777	MW-001-	BLANK		1	ug/l	-777	1	1485
1	2	01-Jul-98	80	1	MW-001-	BLANK		1	ug/l	77000	1	9
1	2	01-Jul-98	80	1	MW-001-	BLANK		1	ug/l	96	1	1008
1	2	01-Jul-98	80	1	MW-001-	BLANK		1	ug/l	3800	1	1005
1	2	01-Jul-00	80	-999	MW-001-	BLANK		1	ug/l	-999	1	1008
1	2	01-Jul-00	80	-999	MW-001-	BLANK		1	ug/l	-999	1	1485
1	2	01-Jul-00	80	1	MW-001-	BLANK		1	ug/l	274	1	1484
1	2	01-Jul-00	80	1	MW-001-	BLANK		1	ug/l	164	1	40
1	2	01-Jul-00	80	1	MW-001-	BLANK		1	ug/l	1610	1	1005
1	2	01-Jul-00	80	1	MW-001-	BLANK		1	ug/l	46500	1	9
1	2	01-Jul-00	80	1	MW-001-	BLANK		1	ug/l	118	1	1486
1	2	02-Nov-00	80	-999	MW-001-	BLANK		1	ug/l	-999	1	1485
1	2	02-Nov-00	80	1	MW-001-	BLANK		1	ug/l	207	1	40
1	2	02-Nov-00	80	1	MW-001-	BLANK		1	ug/l	220	1	1484
1	2	02-Nov-00	80	1	MW-001-	BLANK		1	ug/l	1970	1	1005
1	2	02-Nov-00	80	1	MW-001-	BLANK		1	ug/l	186	1	1486
1	2	02-Nov-00	80	1	MW-001-	BLANK		1	ug/l	68	1	1008
1	2	02-Nov-00	80	1	MW-001-	BLANK		1	ug/l	68900	1	9
1	2	01-Apr-01	80	1	MW-001-	BLANK		1	ug/l	188	1	1486
1	2	01-Apr-01	80	1	MW-001-	BLANK		1	ug/l	180	1	1484

Location ID	Borehole ID	Date	Depth	Sample Type	Sample I	Category	Category ID	Unit	Amount	Measure Type	CAS Index
1	2	01-Apr-01	80	1	MW-001-	BLANK		1	ug/l	102	1	1008
1	2	01-Apr-01	80	1	MW-001-	BLANK		1	ug/l	0.13	1	1485
1	2	01-Apr-01	80	1	MW-001-	BLANK		1	ug/l	161	1	40
1	2	01-Apr-01	80	1	MW-001-	BLANK		1	ug/l	2420	1	1005
1	2	01-Apr-01	80	1	MW-001-	BLANK		1	ug/l	62800	1	9
1	2	20-Jul-01	80	-999	MW-001-	BLANK		1	ug/l	-999	1	1485
1	2	20-Jul-01	80	1	MW-001-	BLANK		1	ug/l	105000	1	9
1	2	20-Jul-01	80	1	MW-001-	BLANK		1	ug/l	163	1	1008
1	2	20-Jul-01	80	1	MW-001-	BLANK		1	ug/l	3920	1	1005
1	2	20-Jul-01	80	1	MW-001-	BLANK		1	ug/l	197	1	40
1	2	20-Jul-01	80	1	MW-001-	BLANK		1	ug/l	200	1	1484
1	2	20-Jul-01	80	1	MW-001-	BLANK		1	ug/l	307	1	1486
1	2	17-Oct-01	80	-999	MW-001-	BLANK		1	ug/l	-999	1	1485
1	2	17-Oct-01	80	-999	MW-001-	BLANK		1	ug/l	-999	1	1008
1	2	17-Oct-01	80	1	MW-001-	BLANK		1	ug/l	56200	1	9
1	2	17-Oct-01	80	1	MW-001-	BLANK		1	ug/l	5940	1	1005
1	2	17-Oct-01	80	1	MW-001-	BLANK		1	ug/l	191	1	40
1	2	17-Oct-01	80	1	MW-001-	BLANK		1	ug/l	250	1	1484
1	2	17-Oct-01	80	1	MW-001-	BLANK		1	ug/l	300	1	1486
1	2	02-Feb-02	80	-999	MW-001-	BLANK		1	ug/l	-999	1	1485

Location ID	Borehole ID	Date	Depth	Sample Type	Sample I	Category	Category ID	Unit	Amount	Measure Type	CAS Index
1	2	02-Feb-02	80	-999	MW-001-	BLANK	1	ug/l	-999	1	1008
1	2	02-Feb-02	80	1	MW-001-	BLANK	1	ug/l	370	1	1486
1	2	02-Feb-02	80	1	MW-001-	BLANK	1	ug/l	130000	1	9
1	2	02-Feb-02	80	1	MW-001-	BLANK	1	ug/l	300	1	40
1	2	02-Feb-02	80	1	MW-001-	BLANK	1	ug/l	7000	1	1005
1	2	02-Feb-02	80	1	MW-001-	BLANK	1	ug/l	520	1	1484
1	5	01-Sep-87	80	-999	MW-001-	BLANK	1	ug/l	-999	1	1484
1	5	01-Sep-87	80	-999	MW-001-	BLANK	1	ug/l	-999	1	1005
1	5	01-Sep-87	80	-999	MW-001-	BLANK	1	ug/l	-999	1	1486
1	5	01-Sep-87	80	-999	MW-001-	BLANK	1	ug/l	-999	1	40
1	5	01-Sep-87	80	-999	MW-001-	BLANK	1	ug/l	-999	1	1008
1	5	01-Sep-87	80	-999	MW-001-	BLANK	1	ug/l	-999	1	1485
1	5	01-Sep-87	80	-999	MW-001-	BLANK	1	ug/l	-999	1	9
1	5	01-Oct-87	80	-999	MW-001-	BLANK	1	ug/l	-999	1	1485
1	5	01-Oct-87	80	-999	MW-001-	BLANK	1	ug/l	-999	1	1484
1	5	01-Oct-87	80	-999	MW-001-	BLANK	1	ug/l	-999	1	40
1	5	01-Oct-87	80	-999	MW-001-	BLANK	1	ug/l	-999	1	1486
1	5	01-Oct-87	80	-999	MW-001-	BLANK	1	ug/l	-999	1	1005
1	5	01-Oct-87	80	-999	MW-001-	BLANK	1	ug/l	-999	1	9
1	5	01-Oct-87	80	-999	MW-001-	BLANK	1	ug/l	-999	1	1008

Location ID	Borehole ID	Date	Depth	Sample Type	Sample I	Category	Category ID	Unit	Amount	Measure Type	CAS Index
1	5	01-Dec-87	80	-666	MW-001-	BLANK	1	ug/l	-0.02	1	1486
1	5	01-Dec-87	80	1	MW-001-	BLANK	1	ug/l	8	1	1005
1	5	01-Dec-87	80	1	MW-001-	BLANK	1	ug/l	2	1	9
1	5	01-Dec-87	80	-666	MW-001-	BLANK	1	ug/l	-1	1	1008
1	5	01-Dec-87	80	-666	MW-001-	BLANK	1	ug/l	-1	1	40
1	5	01-Dec-87	80	-666	MW-001-	BLANK	1	ug/l	-0.02	1	1485
1	5	01-Dec-87	80	-666	MW-001-	BLANK	1	ug/l	-0.5	1	1484
1	5	01-Feb-88	80	-999	MW-001-	BLANK	1	ug/l	-999	1	1005
1	5	01-Feb-88	80	-999	MW-001-	BLANK	1	ug/l	-999	1	1485
1	5	01-Feb-88	80	-999	MW-001-	BLANK	1	ug/l	-999	1	1484
1	5	01-Feb-88	80	-999	MW-001-	BLANK	1	ug/l	-999	1	1486
1	5	01-Feb-88	80	-999	MW-001-	BLANK	1	ug/l	-999	1	1008
1	5	01-Feb-88	80	-999	MW-001-	BLANK	1	ug/l	-999	1	40
1	5	01-Feb-88	80	-999	MW-001-	BLANK	1	ug/l	-999	1	9
1	5	01-Mar-88	80	-666	MW-001-	BLANK	1	ug/l	-1	1	1008
1	5	01-Mar-88	80	-666	MW-001-	BLANK	1	ug/l	-1	1	40
1	5	01-Mar-88	80	1	MW-001-	BLANK	1	ug/l	5	1	1005
1	5	01-Mar-88	80	-666	MW-001-	BLANK	1	ug/l	-0.5	1	1484
1	5	01-Mar-88	80	-666	MW-001-	BLANK	1	ug/l	-0.02	1	1486
1	5	01-Mar-88	80	-666	MW-001-	BLANK	1	ug/l	-0.02	1	1485

Chemical Properties

Chemical Name	Chemical Property Name	Unit	Property Value	Source ID	Remarks
1,2-Dichloropropane	21) Liquid NAPL viscosity constant-0	Dimensionless	-3.0210E+00	4	Reid
1,2-Dichloropropane	14) Ideal Gas Heat Capacity Constant-3	Dimensionless	7.7410E-08	4	Reid
1,2-Dichloropropane	15) Molecular weight	g/mole	1.1299E+02	4	Reid
1,2-Dichloropropane	16) Reference Temperature	Kelvin	2.9315E+02	4	Reid
1,2-Dichloropropane	17) Reference Binary Diffusivity in Air	m2/s	1.4400E-04	4	Reid
1,2-Dichloropropane	18) Reference Temperature for Gas Diffusivity	Kelvin	2.9315E+02	4	Reid
1,2-Dichloropropane	13) Ideal Gas Heat Capacity Constant-2	Dimensionless	-2.6040E-04	4	Reid
1,2-Dichloropropane	28) Solubility in Water Constant-2	Dimensionless	0.0000E+00		
1,2-Dichloropropane	20) Reference NAPL liquid Density	kg/m3	1.1500E+03	4	Reid
1,2-Dichloropropane	23) Liquid NAPL viscosity constant-2	Dimensionless	0.0000E+00	4	Reid
1,2-Dichloropropane	24) Liquid NAPL viscosity constant-3	Dimensionless	0.0000E+00	4	Reid
1,2-Dichloropropane	25) Chemical Critical Volume	cm3/mole	2.2600E+02	4	Reid
1,2-Dichloropropane	26) Solubility in Water Constant-0	Mole Fraction	4.3014E-04	7	CALCULATED
1,2-Dichloropropane	27) Solubility in Water Constant-1	Dimensionless	0.0000E+00		
1,2-Dichloropropane	32) Koc	m3/kg	5.1286E-02	2	5.1286E+01-2.6977E+01, page 243
1,2-Dichloropropane	19) Exponent for Calculating Chemical Diffusivity	Dimensionless	0.0000E+00	4	Reid
1,2-Dichloropropane	2) Critical Compressibility	Dimensionless	2.1000E-01	4	Reid
1,2-Dichloropropane	22) Liquid NAPL viscosity constant-1	Dimensionless	1.8270E+03	4	Reid

Chemical Name	Chemical Property Name	Unit	Property Value	Source ID	Remarks
1,2-Dichloropropane	12) Ideal Gas Heat Capacity Constant-1	Dimensionless	3.6550E-01	4	Reid
1,2-Dichloropropane	30) Foc	Dimensionless	0.0000E+00		
1,2-Dichloropropane	33) Boiling Point	C	3.6950E+02	4	Reid
1,2-Dichloropropane	1) Critical Pressure	bar	4.4500E+01	4	Reid
1,2-Dichloropropane	31) Decay Constant	1/s	2.4020E-08		Hlf lives GW=8016-61872 hrs, p182, = 2.4020E-08-3.112E-0
1,2-Dichloropropane	3) Pitzner's Acentric Factor	Dimensionless	2.4000E-01	4	Reid
1,2-Dichloropropane	9) Vapor Pressure Constant-3	Dimensionless	-5.0543E+00	4	Reid
1,2-Dichloropropane	11) Ideal Gas Heat Capacity Constant-0	Dimensionless	1.0450E+01	4	Reid
1,2-Dichloropropane	29) Solubility in Water Constant-3	Dimensionless	0.0000E+00		
1,2-Dichloropropane	10) Normal Boiling Point	Kelvin	3.6950E+02	4	Reid
1,2-Dichloropropane	4) Chemical Dipole Moment	debyes	1.9000E+00	4	Reid
1,2-Dichloropropane	8) Vapor Pressure Constant-2	Dimensionless	-1.6000E+00	4	Reid
1,2-Dichloropropane	7) Vapor Pressure Constant-1	Dimensionless	5.4655E-01	4	Reid
1,2-Dichloropropane	6) Vapor Pressure Constant-0	Dimensionless	-6.8223E+00	4	Reid
1,2-Dichloropropane	5) Critical Temperature	Kelvin	5.7700E+02	4	Reid
Chloroform	25) Chemical Critical Volume	cm3/mole	2.3890E+02	4	
Chloroform	18) Reference Temperature for Gas Diffusivity	Kelvin	2.9315E+02	99	Not Available
Chloroform	20) Reference NAPL liquid Density	kg/m3	1.3890E+03	9	TOXNET
Chloroform	21) Liquid NAPL viscosity constant-0	Dimensionless	-4.1720E+00	4	Reid
Chloroform	22) Liquid NAPL viscosity constant-1	Dimensionless	9.1530E+02		
Chloroform	23) Liquid NAPL viscosity constant-2	Dimensionless	2.7000E-03		

Chemical Name	Chemical Property Name	Unit	Property Value	Source ID	Remarks
Chloroform	24) Liquid NAPL viscosity constant-3	Dimensionless	-4.1080E-06		
Chloroform	19) Exponent for Calculating Chemical Diffusivity	Dimensionless	0.0000E+00	99	Not Available
Chloroform	26) Solubility in Water Constant-0	Mole Fraction	1.1662E-03	9	Water solubility = 7,710 mg/l at 25 deg C
Chloroform	27) Solubility in Water Constant-1	Dimensionless	0.0000E+00		
Chloroform	28) Solubility in Water Constant-2	Dimensionless	0.0000E+00		
Chloroform	29) Solubility in Water Constant-3	Dimensionless	0.0000E+00		
Chloroform	30) Foc	Dimensionless	0.0000E+00		
Chloroform	31) Decay Constant	1/s	2.2285E-08	3	Hlf lives GW=1344-43200 hrs, p99, = 1.4326E-07-4.4570E-0
Chloroform	33) Boiling Point	C	3.6950E+02	4	Reid
Chloroform	17) Reference Binary Diffusivity in Air	m2/s	1.4400E-04	99	Not Available
Chloroform	32) Koc	m3/kg	1.5300E-01	10	TOXNET, 153-196
Chloroform	8) Vapor Pressure Constant-2	Dimensionless	-2.1397E+00	4	Reid
Chloroform	1) Critical Pressure	bar	5.3700E+01	4	Reid
Chloroform	34) Henry's Law Constant	atm-cu m/mole	3.6700E-03	0	
Chloroform	3) Pitzner's Acentric Factor	Dimensionless	2.1800E-01	4	Reid
Chloroform	4) Chemical Dipole Moment	debyes	1.1000E+00	4	Reid
Chloroform	5) Critical Temperature	Kelvin	5.3640E+02	4	Reid
Chloroform	2) Critical Compressibility	Dimensionless	2.9300E-01	4	Reid
Chloroform	7) Vapor Pressure Constant-1	Dimensionless	1.1663E+00	4	Reid
Chloroform	16) Reference Temperature	Kelvin	2.9315E+02	4	Reid
Chloroform	9) Vapor Pressure Constant-3	Dimensionless	-3.4442E+00	4	Reid

Chemical Name	Chemical Property Name	Unit	Property Value	Source ID	Remarks
Chloroform	10) Normal Boiling Point	Kelvin	3.3430E+02	4 Reid	
Chloroform	11) Ideal Gas Heat Capacity Constant-0	Dimensionless	2.4000E+01	4 Reid	
Chloroform	12) Ideal Gas Heat Capacity Constant-1	Dimensionless	1.8930E-01	4 Reid	
Chloroform	13) Ideal Gas Heat Capacity Constant-2	Dimensionless	-1.8410E-04	4 Reid	
Chloroform	14) Ideal Gas Heat Capacity Constant-3	Dimensionless	6.6570E-08	4 Reid	
Chloroform	15) Molecular weight	g/mole	1.1938E+02	4 Reid	
Chloroform	6) Vapor Pressure Constant-0	Dimensionless	-6.9555E+00	4 Reid	
1,2,3-Trichloropropane	24) Liquid NAPL viscosity constant-3	K	2.9371E+02	9 TOXNET p.3 20 C	
1,2,3-Trichloropropane	7) Vapor Pressure Constant-1	Dimensionless	3.4173E+03	4 Reid	
1,2,3-Trichloropropane	16) Reference Temperature	Kelvin	2.9315E+02	4 Reid	
1,2,3-Trichloropropane	15) Molecular weight	g/mole	1.4743E+02	4 Reid	
1,2,3-Trichloropropane	14) Ideal Gas Heat Capacity Constant-3	Dimensionless	8.7880E-08	4 Reid	
1,2,3-Trichloropropane	13) Ideal Gas Heat Capacity Constant-2	Dimensionless	-2.7870E-04	4 Reid	
1,2,3-Trichloropropane	12) Ideal Gas Heat Capacity Constant-1	Dimensionless	3.6220E+01	4 Reid	
1,2,3-Trichloropropane	10) Normal Boiling Point	Kelvin	4.2900E+02	9 TOXNET	
1,2,3-Trichloropropane	17) Reference Binary Diffusivity in Air	m2/s	1.4400E-04	99 Not Available	
1,2,3-Trichloropropane	8) Vapor Pressure Constant-2	Dimensionless	-6.9150E+01	4 Reid	
1,2,3-Trichloropropane	11) Ideal Gas Heat Capacity Constant-0	Dimensionless	2.6880E+01	4 Reid	
1,2,3-Trichloropropane	6) Vapor Pressure Constant-0	Dimensionless	9.5044E+00	4 Reid	
1,2,3-Trichloropropane	5) Critical Temperature	Kelvin	6.5100E+02	4 Reid	
1,2,3-Trichloropropane	4) Chemical Dipole Moment	debyes	1.6000E+00	4 Reid	

Chemical Name	Chemical Property Name	Unit	Property Value	Source ID	Remarks
1,2,3-Trichloropropane	3) Pitzner's Acentric Factor	Dimensionless	3.1000E-01	4	Reid
1,2,3-Trichloropropane	2) Critical Compressibility	Dimensionless	2.5000E-01	4	Reid
1,2,3-Trichloropropane	1) Critical Pressure	bar	3.9500E+01	4	Reid
1,2,3-Trichloropropane	26) Solubility in Water Constant-0	Mole Fraction	2.1366E-04	9	TOXNET, P. 3 1750 mg/l
1,2,3-Trichloropropane	32) Koc	m3/kg	7.2000E-02	9	TOXNET
1,2,3-Trichloropropane	9) Vapor Pressure Constant-3	Dimensionless	0.0000E+00	4	Reid
1,2,3-Trichloropropane	33) Boiling Point	C	3.6950E+02	4	Reid
1,2,3-Trichloropropane	18) Reference Temperature for Gas Diffusivity	Kelvin	2.9315E+02	99	Not Available
1,2,3-Trichloropropane	31) Decay Constant	1/s	2.2285E-08		Hlf lives GW=8640-17280 hrs, p312, = 2.22850E-08-1.1142
1,2,3-Trichloropropane	30) Foc	Dimensionless	0.0000E+00		
1,2,3-Trichloropropane	29) Solubility in Water Constant-3	Dimensionless	0.0000E+00		
1,2,3-Trichloropropane	28) Solubility in Water Constant-2	Dimensionless	0.0000E+00		
1,2,3-Trichloropropane	27) Solubility in Water Constant-1	Dimensionless	0.0000E+00		
1,2,3-Trichloropropane	25) Chemical Critical Volume	cm3/mole	3.4800E+02	4	Reid
1,2,3-Trichloropropane	23) Liquid NAPL viscosity constant-2	centipoise	2.5000E-04	9	TOXNET
1,2,3-Trichloropropane	22) Liquid NAPL viscosity constant-1	Dimensionless	0.0000E+00	13	"
1,2,3-Trichloropropane	21) Liquid NAPL viscosity constant-0	Dimensionless	0.0000E+00	13	When only one value of viscosity, constants 1 and 2 = 0 & 3
1,2,3-Trichloropropane	20) Reference NAPL liquid Density	kg/m3	1.3890E+03	9	TOXNET
1,2,3-Trichloropropane	19) Exponent for Calculating Chemical Diffusivity	Dimensionless	0.0000E+00	99	Not Available
1,3-Dichloropropane	4) Chemical Dipole Moment	debyes	1.9000E+00	4	Reid assumed equivalent to 1,2-Dichloropropane
1,3-Dichloropropane	15) Molecular weight	g/mole	1.1299E+02	4	Reid assumed equivalent to 1,2-Dichloropropane

Chemical Name	Chemical Property Name	Unit	Property Value	Source ID	Remarks
1,3-Dichloropropane	14) Ideal Gas Heat Capacity Constant-3	Dimensionless	7.7410E-08	4	Reid assumed equivalent to 1,2-Dichloropropane
1,3-Dichloropropane	13) Ideal Gas Heat Capacity Constant-2	Dimensionless	-2.6040E-04	4	Reid assumed equivalent to 1,2-Dichloropropane
1,3-Dichloropropane	12) Ideal Gas Heat Capacity Constant-1	Dimensionless	3.6550E-01	9	TOXNET
1,3-Dichloropropane	11) Ideal Gas Heat Capacity Constant-0	Dimensionless	1.0450E+01	4	Reid assumed equivalent to 1,2-Dichloropropane
1,3-Dichloropropane	10) Normal Boiling Point	Kelvin	3.7000E+02	4	Reid assumed equivalent to 1,2-Dichloropropane
1,3-Dichloropropane	9) Vapor Pressure Constant-3	Dimensionless	-5.0543E+00	4	Reid assumed equivalent to 1,2-Dichloropropane
1,3-Dichloropropane	8) Vapor Pressure Constant-2	Dimensionless	-1.6000E+00	4	Reid assumed equivalent to 1,2-Dichloropropane
1,3-Dichloropropane	7) Vapor Pressure Constant-1	Dimensionless	5.4655E-01	4	Reid assumed equivalent to 1,2-Dichloropropane
1,3-Dichloropropane	2) Critical Compressibility	Dimensionless	2.1000E-01	4	Reid assumed equivalent to 1,2-Dichloropropane
1,3-Dichloropropane	5) Critical Temperature	Kelvin	5.7700E+02	4	Reid assumed equivalent to 1,2-Dichloropropane
1,3-Dichloropropane	16) Reference Temperature	Kelvin	2.9315E+02	4	Reid assumed equivalent to 1,2-Dichloropropane
1,3-Dichloropropane	3) Pitzner's Acentric Factor	Dimensionless	2.4000E-01	4	Reid assumed equivalent to 1,2-Dichloropropane
1,3-Dichloropropane	1) Critical Pressure	bar	4.1750E+01	9	TOXNET
1,3-Dichloropropane	19) Exponent for Calculating Chemical Diffusivity	Dimensionless	0.0000E+00	4	Reid assumed equivalent to 1,2-Dichloropropane
1,3-Dichloropropane	6) Vapor Pressure Constant-0	Dimensionless	-6.8223E+00	4	Reid assumed equivalent to 1,2-Dichloropropane
1,3-Dichloropropane	32) Koc	m3/kg	2.9000E-01	9	
1,3-Dichloropropane	17) Reference Binary Diffusivity in Air	m2/s	1.4400E-04	4	Reid assumed equivalent to 1,2-Dichloropropane
1,3-Dichloropropane	18) Reference Temperature for Gas Diffusivity	Kelvin	2.9315E+02	4	Reid assumed equivalent to 1,2-Dichloropropane
1,3-Dichloropropane	33) Boiling Point	C	3.6950E+02	4	Reid
1,3-Dichloropropane	31) Decay Constant	1/s	2.4020E-08	3	Hlf lives GW=8016-61872 hrs, p182, = 2.4020E-08-3.112E-0
1,3-Dichloropropane	30) Foc	Dimensionless	0.0000E+00		

Chemical Name	Chemical Property Name	Unit	Property Value	Source ID	Remarks
1,3-Dichloropropane	29) Solubility in Water Constant-3	Dimensionless	0.0000E+00		
1,3-Dichloropropane	28) Solubility in Water Constant-2	Dimensionless	0.0000E+00		
1,3-Dichloropropane	27) Solubility in Water Constant-1	Dimensionless	0.0000E+00		
1,3-Dichloropropane	25) Chemical Critical Volume	cm3/mole	2.2600E+02	4	Reid assumed equivalent to 1,2-Dichloropropane
1,3-Dichloropropane	24) Liquid NAPL viscosity constant-3	Dimensionless	0.0000E+00	4	Reid assumed equivalent to 1,2-Dichloropropane
1,3-Dichloropropane	23) Liquid NAPL viscosity constant-2	Dimensionless	0.0000E+00	4	Reid assumed equivalent to 1,2-Dichloropropane
1,3-Dichloropropane	22) Liquid NAPL viscosity constant-1	Dimensionless	1.8270E+03	4	Reid assumed equivalent to 1,2-Dichloropropane
1,3-Dichloropropane	21) Liquid NAPL viscosity constant-0	Dimensionless	-3.0210E+00	4	Reid assumed equivalent to 1,2-Dichloropropane
1,3-Dichloropropane	20) Reference NAPL liquid Density	kg/m3	1.1876E+03	9	TOXNET
1,3-Dichloropropane	26) Solubility in Water Constant-0	Mole Fraction	3.8106E-04	9	TOXNET; In water, 2.75X10+3 mg/l @ 25 deg C
2,4-dinitro-6-sec-butylphe	29) Solubility in Water Constant-3	Dimensionless	0.0000E+00	99	Assume
2,4-dinitro-6-sec-butylphe	13) Ideal Gas Heat Capacity Constant-2	Dimensionless	0.0000E+00	99	Assumed
2,4-dinitro-6-sec-butylphe	12) Ideal Gas Heat Capacity Constant-1	Dimensionless	0.0000E+00	99	Assumed
2,4-dinitro-6-sec-butylphe	11) Ideal Gas Heat Capacity Constant-0	Dimensionless	2.1260E+02	6	p. 6-124, ChloroNaphtalene,TC,Pc, Critical Density of Napht
2,4-dinitro-6-sec-butylphe	10) Normal Boiling Point	Kelvin	3.5130E+02	99	Not Availble, Assumed
2,4-dinitro-6-sec-butylphe	9) Vapor Pressure Constant-3	Dimensionless	4.0000E+00	99	Assumed
2,4-dinitro-6-sec-butylphe	8) Vapor Pressure Constant-2	Dimensionless	0.0000E+00	99	Assumed
2,4-dinitro-6-sec-butylphe	7) Vapor Pressure Constant-1	Dimensionless	1.5570E+01	99	Calculated
2,4-dinitro-6-sec-butylphe	6) Vapor Pressure Constant-0	Dimensionless	-9.4141E+03	99	Calculated
2,4-dinitro-6-sec-butylphe	4) Chemical Dipole Moment	debyes	0.0000E+00	99	Not Available
2,4-dinitro-6-sec-butylphe	31) Decay Constant	1/s	2.0056E-06	3	Hlf lives GW=96-5904 hrs, p248, = 2.0056E-06-3.2612E-08/

Chemical Name	Chemical Property Name	Unit	Property Value	Source ID	Remarks
2,4-dinitro-6-sec-butylphe	32) Koc	m3/kg	2.4000E-05	7	Units unknown, Ref gives Kd ??2.4000E-05m3/kg??
2,4-dinitro-6-sec-butylphe	30) Foc	Dimensionless	0.0000E+00	99	Not Available
2,4-dinitro-6-sec-butylphe	14) Ideal Gas Heat Capacity Constant-3	Dimensionless	0.0000E+00	99	Assumed
2,4-dinitro-6-sec-butylphe	22) Liquid NAPL viscosity constant-1	Dimensionless	2.5170E+03	4	Reid, et. al., p452, naphtalene used
2,4-dinitro-6-sec-butylphe	5) Critical Temperature	Kelvin	7.4840E+02	6	TC,Pc, Critical Density of Naphtalene were used from CRC
2,4-dinitro-6-sec-butylphe	23) Liquid NAPL viscosity constant-2	Dimensionless	1.0980E-02	4	Reid, et. al., p452, naphtalene used
2,4-dinitro-6-sec-butylphe	1) Critical Pressure	bar	4.0510E+01	6	TC,Pc, Critical Density of Naphtalene were used from CRC
2,4-dinitro-6-sec-butylphe	2) Critical Compressibility	Dimensionless	2.6900E-01	6	TC,Pc, Critical Density of Naphtalene were used from CRC
2,4-dinitro-6-sec-butylphe	33) Boiling Point	C	3.2000E+01	7	32-42 degrees C, The Pesticide Management Education Pro
2,4-dinitro-6-sec-butylphe	28) Solubility in Water Constant-2	Dimensionless	0.0000E+00	99	Assumed
2,4-dinitro-6-sec-butylphe	27) Solubility in Water Constant-1	Dimensionless	0.0000E+00	99	Assumed
2,4-dinitro-6-sec-butylphe	26) Solubility in Water Constant-0	Mole Fraction	3.7500E-06	999	Calculated based on 50ppm (ref. 7) cpnverted to mole/mole
2,4-dinitro-6-sec-butylphe	20) Reference NAPL liquid Density	kg/m3	1.2900E+00	1	Karel Vaerschueren, 1983
2,4-dinitro-6-sec-butylphe	24) Liquid NAPL viscosity constant-3	Dimensionless	-5.8670E-06	4	Reid, et. al., p452, naphtalene used
2,4-dinitro-6-sec-butylphe	15) Molecular weight	g/mole	2.4000E+02	7	The Pesticide Management Education Program at Cornell U
2,4-dinitro-6-sec-butylphe	21) Liquid NAPL viscosity constant-0	Dimensionless	-1.0270E+01	4	Reid, et. al., p452, naphtalene used
2,4-dinitro-6-sec-butylphe	3) Pitzner's Acentric Factor	Dimensionless	0.0000E+00	99	Not Available
2,4-dinitro-6-sec-butylphe	19) Exponent for Calculating Chemical Diffusivity	Dimensionless	1.0000E-05		TC,Pc, Critical Density of Naphtalene were used from CRC
2,4-dinitro-6-sec-butylphe	18) Reference Temperature for Gas Diffusivity	Kelvin	3.0000E+02	99	Assumed
2,4-dinitro-6-sec-butylphe	17) Reference Binary Diffusivity in Air	m2/s	1.0000E-05	99	Assumed
2,4-dinitro-6-sec-butylphe	16) Reference Temperature	Kelvin	3.0000E+02	99	Assumed

Chemical Name	Chemical Property Name	Unit	Property Value	Source ID	Remarks
2,4-dinitro-6-sec-butylphe	25) Chemical Critical Volume	cm3/mole	1.5159E+00	999	Calculated from Oc and Tc
1,2-Dibromoethane	26) Solubility in Water Constant-0	Mole Fraction	4.1297E-04		In water, 4,310 mg/l @ 30 deg C
1,2-Dibromoethane	7) Vapor Pressure Constant-1	Dimensionless	2.2285E+00	4	Reid
1,2-Dibromoethane	28) Solubility in Water Constant-2	Dimensionless	0.0000E+00		
1,2-Dibromoethane	14) Ideal Gas Heat Capacity Constant-3	Dimensionless	5.6460E-08	4	Reid
1,2-Dibromoethane	13) Ideal Gas Heat Capacity Constant-2	Dimensionless	-1.8330E-04	4	Reid
1,2-Dibromoethane	12) Ideal Gas Heat Capacity Constant-1	Dimensionless	2.5100E-01	4	Reid
1,2-Dibromoethane	11) Ideal Gas Heat Capacity Constant-0	Dimensionless	2.5000E+01	4	Reid
1,2-Dibromoethane	10) Normal Boiling Point	Kelvin	4.0470E+02	4	Reid
1,2-Dibromoethane	16) Reference Temperature	Kelvin	2.9315E+02	4	Reid
1,2-Dibromoethane	8) Vapor Pressure Constant-2	Dimensionless	-3.9779E+00	4	Reid
1,2-Dibromoethane	17) Reference Binary Diffusivity in Air	m2/s	1.4400E-04	99	Not Available
1,2-Dibromoethane	6) Vapor Pressure Constant-0	Dimensionless	-7.4500E+00	4	Reid
1,2-Dibromoethane	5) Critical Temperature	Kelvin	6.4600E+02	4	Reid
1,2-Dibromoethane	4) Chemical Dipole Moment	debyes	1.0000E+00	4	Reid
1,2-Dibromoethane	3) Pitzner's Acentric Factor	Dimensionless	7.9500E-01	4	Reid
1,2-Dibromoethane	2) Critical Compressibility	Dimensionless	2.9300E-01	99	Critical temperature: 309.8 deg C; critical pressure: 7154 kP
1,2-Dibromoethane	1) Critical Pressure	bar	5.3500E+01	4	Reid
1,2-Dibromoethane	9) Vapor Pressure Constant-3	Dimensionless	-2.4734E-01	4	Reid
1,2-Dibromoethane	25) Chemical Critical Volume	cm3/mole	2.3890E+02	4	Assumed
1,2-Dibromoethane	33) Boiling Point	C	3.6950E+02	4	Reid

Chemical Name	Chemical Property Name	Unit	Property Value	Source ID	Remarks
1,2-Dibromoethane	32) Koc	m3/kg	1.4000E-02	9	TOXNET, 14-160
1,2-Dibromoethane	31) Decay Constant	1/s	7.1311E-07	3	Hlf lives GW=470-2880 hrs, p378 (6.6854E-08)
1,2-Dibromoethane	30) Foc	Dimensionless	0.0000E+00		
1,2-Dibromoethane	29) Solubility in Water Constant-3	Dimensionless	0.0000E+00		
1,2-Dibromoethane	15) Molecular weight	g/mole	1.8786E+02	4	Reid
1,2-Dibromoethane	27) Solubility in Water Constant-1	Dimensionless	0.0000E+00		
1,2-Dibromoethane	34) Henry's Law Constant	atm-cu m/mole	6.5000E-04	0	
1,2-Dibromoethane	24) Liquid NAPL viscosity constant-3	Dimensionless	0.0000E+00		
1,2-Dibromoethane	23) Liquid NAPL viscosity constant-2	Dimensionless	0.0000E+00		
1,2-Dibromoethane	22) Liquid NAPL viscosity constant-1	Dimensionless	1.2990E+03		
1,2-Dibromoethane	21) Liquid NAPL viscosity constant-0	Dimensionless	-3.8990E+00	4	Reid
1,2-Dibromoethane	20) Reference NAPL liquid Density	kg/m3	2.1720E+03	9	TOXNET
1,2-Dibromoethane	19) Exponent for Calculating Chemical Diffusivity	Dimensionless	0.0000E+00	99	Not Available
1,2-Dibromoethane	18) Reference Temperature for Gas Diffusivity	Kelvin	2.9315E+02	99	Not Available
1,2-Dibromo-3-Chloropro	32) Koc	m3/kg	3.0500E-01	9	TOXNET
1,2-Dibromo-3-Chloropro	33) Boiling Point	C	3.6950E+02	4	Reid, Assumed same as 1,2,3-TCP
1,2-Dibromo-3-Chloropro	3) Pitzner's Acentric Factor	Dimensionless	3.1000E-01	4	Reid, Assumed same as 1,2,3-TCP
1,2-Dibromo-3-Chloropro	17) Reference Binary Diffusivity in Air	m2/s	1.4400E-04	99	Not Available
1,2-Dibromo-3-Chloropro	34) Henry's Law Constant	atm-cu m/mole	1.5000E-04	0	
1,2-Dibromo-3-Chloropro	1) Critical Pressure	bar	3.9500E+01	4	Reid, Assumed same as 1,2,3-TCP
1,2-Dibromo-3-Chloropro	2) Critical Compressibility	Dimensionless	2.5000E-01	4	Reid, Assumed same as 1,2,3-TCP

Chemical Name	Chemical Property Name	Unit	Property Value	Source ID	Remarks
1,2-Dibromo-3-Chloropro	4) Chemical Dipole Moment	debyes	1.6000E+00	4	Reid, Assumed same as 1,2,3-TCP
1,2-Dibromo-3-Chloropro	6) Vapor Pressure Constant-0	Dimensionless	9.5044E+00	4	Reid, Assumed same as 1,2,3-TCP
1,2-Dibromo-3-Chloropro	7) Vapor Pressure Constant-1	Dimensionless	3.4173E+03	4	Reid, Assumed same as 1,2,3-TCP
1,2-Dibromo-3-Chloropro	8) Vapor Pressure Constant-2	Dimensionless	-6.9150E+01	4	Reid, Assumed same as 1,2,3-TCP
1,2-Dibromo-3-Chloropro	9) Vapor Pressure Constant-3	Dimensionless	0.0000E+00	4	Reid, Assumed same as 1,2,3-TCP
1,2-Dibromo-3-Chloropro	10) Normal Boiling Point	Kelvin	4.3765E+02	9	TOXNET
1,2-Dibromo-3-Chloropro	11) Ideal Gas Heat Capacity Constant-0	Dimensionless	2.6880E+01	4	Reid, Assumed same as 1,2,3-TCP
1,2-Dibromo-3-Chloropro	12) Ideal Gas Heat Capacity Constant-1	Dimensionless	3.6220E+01	4	Reid, Assumed same as 1,2,3-TCP
1,2-Dibromo-3-Chloropro	13) Ideal Gas Heat Capacity Constant-2	Dimensionless	-2.7870E-04	4	Reid, Assumed same as 1,2,3-TCP
1,2-Dibromo-3-Chloropro	14) Ideal Gas Heat Capacity Constant-3	Dimensionless	8.7880E-08	4	Reid, Assumed same as 1,2,3-TCP
1,2-Dibromo-3-Chloropro	5) Critical Temperature	Kelvin	6.5100E+02	4	Reid, Assumed same as 1,2,3-TCP
1,2-Dibromo-3-Chloropro	23) Liquid NAPL viscosity constant-2	Dimensionless	2.5000E-04	9	TOXNET
1,2-Dibromo-3-Chloropro	30) Foc	Dimensionless	0.0000E+00		
1,2-Dibromo-3-Chloropro	29) Solubility in Water Constant-3	Dimensionless	0.0000E+00		
1,2-Dibromo-3-Chloropro	28) Solubility in Water Constant-2	Dimensionless	0.0000E+00		
1,2-Dibromo-3-Chloropro	27) Solubility in Water Constant-1	Dimensionless	0.0000E+00		
1,2-Dibromo-3-Chloropro	26) Solubility in Water Constant-0	Mole Fraction	7.6155E-05	9	TOXNET
1,2-Dibromo-3-Chloropro	15) Molecular weight	g/mole	2.3636E+02	4	Reid, Assumed same as 1,2,3-TCP
1,2-Dibromo-3-Chloropro	24) Liquid NAPL viscosity constant-3	Dimensionless	2.9315E+02	99	Assumed
1,2-Dibromo-3-Chloropro	16) Reference Temperature	Kelvin	2.9315E+02	9	TOXNET
1,2-Dibromo-3-Chloropro	22) Liquid NAPL viscosity constant-1	Dimensionless	0.0000E+00		

Chemical Name	Chemical Property Name	Unit	Property Value	Source ID	Remarks
1,2-Dibromo-3-Chloropro	21) Liquid NAPL viscosity constant-0	Dimensionless	0.0000E+00		
1,2-Dibromo-3-Chloropro	20) Reference NAPL liquid Density	kg/m3	2.0800E+03	9 TOXNET	
1,2-Dibromo-3-Chloropro	19) Exponent for Calculating Chemical Diffusivity	Dimensionless	0.0000E+00	99 Not Available	
1,2-Dibromo-3-Chloropro	18) Reference Temperature for Gas Diffusivity	Kelvin	2.9315E+02	99 Not Available	
1,2-Dibromo-3-Chloropro	31) Decay Constant	1/s	2.2285E-08	Unknown	
1,2-Dibromo-3-Chloropro	25) Chemical Critical Volume	cm3/mole	3.4800E+02	4 Reid for 1,2,3-TCP	

Appendix C

Excerpts from Van Genuchten

Project No. C02-266 June 2004

Appendix C

Excerpts from van Genuchten

van Genuchten [1980]

Several continuously differentiable (smooth) equations have been proposed to improve the description of soil water retention near saturation. Most of these functions are mathematically too complicated to be easily incorporated into predictive pore-size distribution models for the hydraulic conductivity, or lack a simple inverse relationship, which makes them less attractive for many soil-water studies. A related smooth function with attractive properties is the equation of van Genuchten [1980], hereinafter referred to as the VG-equation:

$$Se = [\lambda+(\alpha h)^n]^{-m} \qquad (3)$$

where α, n and m are empirical constants affecting the shape of the retention curve.

The limiting curve follows from 3 by removing the factor 1 from the denominator. This shows that the VG- and BC-functions become equivalent at low Se when $\lambda=mn$. The same limiting curve also appears when n in 3 is allowed to go to infinity, while simultaneously decreasing m such that the product, mn, remains at 0.4. The limiting BC equation exhibits a sharp break in the curve at the air entry value $h\alpha=1/\alpha$. For finite values of n, the curves remain smooth and more or less sigmoidally shaped on a semi-logarithmic plot. Note, however, that the curves become markedly nonsigmoidal on the regular $\theta(h)$ plot, especially when n is relatively small.

The results of fitting 3 to retention data of four different soils are shown in Table C-1. The examples were previously discussed by van Genuchten and Nielsen [1985]. The table contains fitted parameter values and the calculated sum of squares, SSQ, of the fitted versus observed water contents. The SSQ values reflect the relative accuracy of the retention models in describing the observed data. For Weld silty clay loam, the BC equation ($n\rightarrow\infty$) matches the data equally well as the variable m,n case, whereas the VG curves associated with the restrictions m=1-1/n and m=1-2/n produced relatively poor results. This situation is different for Touchet silt loam and G.E. No. 2 sand where the BC equation produces an unacceptable fit, while the VG equation with restricted m,n values produces results which are essentially identical to those for the general case when m and n are independent. Finally, there is a progressively better fit to the Sarpy loam data going from the BC limiting curve via the restricted cases m=12/n and m=1-1/n, to the more general case of variable m,n.

From these results, and many other examples not further discussed here, we conclude that 3 with variable m,n gives an excellent fit to observed retention data for most soils. The only exceptions are certain structured or aggregated soils characterized by very distinct bimodal pore-size distributions. Of the three cases with restricted m values, m=1-1/n seems to perform best for many but not all soils, while the BC equation generally performs best for selected coarse-textured and/or repacked, sieved soils with relatively narrow pore-size distributions. Although the variable m,n case produced always superior results, its use is not necessarily recommended when only a limited range of retention data (usually in the wet range) is available. Unless augmented with laboratory measurements at relatively low Se values, such data sets may not lead to accurate description of the retention curve in the dry range. Keeping both m and n variables may then lead to uniqueness problems in the parameter estimation process.

TABLE C-1

FITTED SOIL HYDRAULIC PARAMETERS FOR THE RETENTION CURVES [AFTER VAN GENUCHTEN AND NIELSEN, 1985]

Type of curve	θr	θs	α	n	λ, m†	SSQ
	(cm3/cm3)	(cm3/cm3)	(1/cm)	(-)	(-)	(10-5)

Weld silty clay loam

variable m, n	0.116	0.469	0.0173	61.54	m=0.0308	18
m=1-1/n	0.159	0.496	0.0136	5.45	(m=0.816)	487
m=1-2/n	0.155	0.495	0.0143	5.87	(m=0.659)	425

n goes to ∞	0.116	0.465	0.0172	-	λ=1.896	21

Touchet silt loam

variable m, n	0.081	0.524	0.0313	3.98	m=0.493	14
m=1-1/n	0.102	0.526	0.0278	3.59	(m=0.721)	17
m=1-2/n	0.082	0.524	0.0312	3.98	(m=0.497)	14

n goes to ∞	0.018	0.499	0.0377	-	λ=1.146	367

G. E. No. 2 sand

variable m, n	0.091	0.369	0.0227	4.11	m=4.80	24
m=1-1/n	0.057	0.367	0.0364	5.05	(m=0.802)	34
m=1-2/n	0.0	0.370	0.0382	4.51	(m=0.557)	56
n goes to ∞	0.0	0.352	0.0462	-	l=1.757	354

Sarpy loam

variable m, n	0.051	0.410	0.0127	1.11	m=0.886	60
m=1-1/n	0.032	0.400	0.0279	1.60	(m=0.374)	99
m=1-2/n	0.012	0.393	0.0393	2.45	(m=0.185)	199
n goes to ∞	0.0	0.380	0.0444	-	l=0.387	539

†Values for m in parentheses were calculated from the fitted n values.

Appendix D

Summary of the Runs for Unsaturated Zone Flow Sensitivity Analyses

Project No. C02-266 **June 2004**

Appendix D

Summary of the Runs for Unsaturated Zone Flow Sensitivity Analyses

Run and File Name	Soil Unit	Porosity	Kx m^2	Ky m^2	Kz m^2	Length of Run	Upper Boundary
Pan001.inp(9)	ClyA1	2.53E-01	3.86E-15	3.86E-15	**3.86E-15**		
	ClyA2	2.03E-01	9.23E-17	9.23E-17	**9.23E-17**		
	ClyC1	5.30E-02	6.32E-17	6.32E-17	**6.32E-17**		
	ClyA1	2.53E-01	3.86E-15	3.86E-15	**3.86E-15**		
	ClyA2	2.03E-01	9.23E-17	9.23E-17	**9.23E-17**		
	ClyB1	2.03E-01	9.23E-17	9.23E-17	**9.23E-17**		
	ClyC1	5.30E-02	6.32E-17	6.32E-17	**6.32E-17**		
Pan002.inp(9)	ClyA1	2.53E-01	2.42E-15	2.42E-15	**2.42E-15**		
	ClyA2	2.53E-01	2.42E-15	2.42E-15	**2.42E-15**		
	ClyB1	2.53E-01	2.42E-15	2.42E-15	**2.42E-15**		
	ClyC1	2.53E-01	2.42E-15	2.42E-15	**2.42E-15**		
Pan003.inp(9)	ClyA1	2.53E-01	2.42E-15	2.42E-15	**2.42E-15**		
	ClyA2	2.53E-01	2.42E-15	2.42E-15	**2.42E-15**		
	ClyB1	2.53E-01	2.42E-15	2.42E-15	**2.42E-15**		
	ClyC1	2.53E-01	2.42E-15	2.42E-15	**2.42E-15**		
Pan004.inp(9)	ClyA1	4.00E-01	2.42E-15	2.42E-15	**2.42E-15**		
	ClyA2	4.00E-01	2.42E-15	2.42E-15	**2.42E-15**		
	ClyB1	4.00E-01	2.42E-15	2.42E-15	**2.42E-15**		
	ClyC1	4.00E-01	2.42E-15	2.42E-15	**2.42E-15**		
Pan004a.inp(9)	ClyA1	4.00E-01	2.42E-15	2.42E-15	**2.42E-15**		
	ClyA2	4.00E-01	2.42E-15	2.42E-15	**2.42E-15**		
	ClyB1	4.00E-01	2.42E-15	2.42E-15	**2.42E-15**		
	ClyC1	4.00E-01	2.42E-15	2.42E-15	**2.42E-15**		
Pan005.inp(9)	ClyA1	4.00E-01	2.42E-15	2.42E-15	**2.42E-15**		
	ClyA2	4.00E-01	2.42E-15	2.42E-15	**2.42E-15**		
	ClyB1	4.00E-01	2.42E-15	2.42E-15	**2.42E-15**		
	ClyC1	4.00E-01	2.42E-15	2.42E-15	**2.42E-15**		
Pan10t2.inp(5)	ClyA1	4.00E-01	2.42E-15	2.42E-15	**2.42E-17**	30 Yrs	100mm/yr on every other site nodes
	ClyA2	4.00E-01	2.42E-15	2.42E-15	**2.42E-15**		
	ClyB1	4.00E-01	2.42E-15	2.42E-15	**2.42E-15**		
	ClyC1	4.00E-01	2.42E-15	2.42E-15	**2.42E-15**		
Pan11t2.inp(5)	ClyA1	4.00E-01	2.42E-15	2.42E-15	**2.42E-17**	30 Yrs	100mm/yr on every other site nodes
	ClyA2	4.00E-01	2.42E-15	2.42E-15	**2.42E-17**		
	ClyB1	4.00E-01	2.42E-15	2.42E-15	**2.42E-17**		
	ClyC1	4.00E-01	2.42E-15	2.42E-15	**2.42E-15**		

Pan12t2.inp(5)	ClyA1	4.00E-01	2.42E-15	2.42E-15	**2.42E-16**	15 yrs	10 mm/yr on all nodes
	ClyA2	4.00E-01	2.42E-15	2.42E-15	**2.42E-16**		
	ClyB1	4.00E-01	2.42E-15	2.42E-15	**2.42E-16**		
	ClyC1	4.00E-01	2.42E-15	2.42E-15	**2.42E-15**		
Pan6tst2.inp(15)	ClyA1	4.00E-01	2.42E-15	2.42E-15	**2.42E-15**		
	ClyA2	4.00E-01	2.42E-15	2.42E-15	**2.42E-15**		
	ClyB1	4.00E-01	2.42E-15	2.42E-15	**2.42E-15**		
	ClyC1	4.00E-01	2.42E-15	2.42E-15	**2.42E-15**		
Pan7tst2.inp(5)	ClyA1	4.00E-01	2.42E-15	2.42E-15	**2.42E-15**		
	ClyA2	4.00E-01	2.42E-15	2.42E-15	**2.42E-15**		
	ClyB1	4.00E-01	2.42E-15	2.42E-15	**2.42E-15**		
	ClyC1	4.00E-01	2.42E-15	2.42E-15	**2.42E-15**		
Pan8tst2.inp(5)	ClyA1	4.00E-01	2.42E-15	2.42E-15	**2.42E-15**		
	ClyA2	4.00E-01	2.42E-15	2.42E-15	**2.42E-15**		
	ClyB1	4.00E-01	2.42E-15	2.42E-15	**2.42E-15**		
	ClyC1	4.00E-01	2.42E-15	2.42E-15	**2.42E-15**		
Pan9tst2.inp(5)	ClyA1	4.00E-01	2.42E-15	2.42E-15	**2.42E-15**		
	ClyA2	4.00E-01	2.42E-15	2.42E-15	**2.42E-15**		
	ClyB1	4.00E-01	2.42E-15	2.42E-15	**2.42E-15**		
	ClyC1	4.00E-01	2.42E-15	2.42E-15	**2.42E-15**		
Pan4VOC.inp(9)	ClyA1	4.00E-01	2.42E-15	2.42E-15	**2.42E-15**	100 yrs	10 mm/yr on all nodes
	ClyA2	4.00E-01	2.42E-15	2.42E-15	**2.42E-15**		Only Node 36 had 100 mm/yr
	ClyB1	4.00E-01	2.42E-15	2.42E-15	**2.42E-15**		
	ClyC1	4.00E-01	2.42E-15	2.42E-15	**2.42E-15**		
Pan5VOC.inp(9)	ClyA1	4.00E-01	2.42E-15	2.42E-15	**2.42E-15**	38.5 yrs	10 mm/yr on all nodes
	ClyA2	4.00E-01	2.42E-15	2.42E-15	**2.42E-15**	38.5 yrs	
	ClyB1	4.00E-01	2.42E-15	2.42E-15	**2.42E-15**	38.5 yrs	
	ClyC1	4.00E-01	2.42E-15	2.42E-15	**2.42E-15**	38.5 yrs	
Pan6VOC.inp(9)	ClyA1	4.00E-01	2.42E-15	2.42E-15	**2.42E-15**	100 yrs	10 mm/yr on all nodes
	ClyA2	4.00E-01	2.42E-15	2.42E-15	**2.42E-15**	100 yrs	
	ClyB1	4.00E-01	2.42E-15	2.42E-15	**2.42E-15**	100 yrs	
	ClyC1	4.00E-01	2.42E-15	2.42E-15	**2.42E-15**	100 yrs	
Pan7VOC.inp(9)	ClyA1	4.00E-01	2.42E-15	2.42E-15	**2.42E-15**	100 yrs	100mm/yr on site nodes
	ClyA2	4.00E-01	2.42E-15	2.42E-15	**2.42E-15**	100 yrs	
	ClyB1	4.00E-01	2.42E-15	2.42E-15	**2.42E-15**	100 yrs	
	ClyC1	4.00E-01	2.42E-15	2.42E-15	**2.42E-15**	100 yrs	
Pan8VOC.inp(9)	ClyA1	4.00E-01	2.42E-15	2.42E-15	**2.42E-17**	3.0 Yrs	100mm/yr on site nodes
	ClyA2	4.00E-01	2.42E-15	2.42E-15	**2.42E-15**	3.0 Yrs	
	ClyB1	4.00E-01	2.42E-15	2.42E-15	**2.42E-15**	3.0 Yrs	
	ClyC1	4.00E-01	2.42E-15	2.42E-15	**2.42E-15**	3.0 Yrs	
Pan11TCP.inp(5)	ClyA1	4.00E-01	2.42E-15	2.42E-15	**2.42E-17**	Non-Convergent	
	ClyA2	4.00E-01	2.42E-15	2.42E-15	**2.42E-17**	Non-Convergent	
	ClyB1	4.00E-01	2.42E-15	2.42E-15	**2.42E-17**	Non-Convergent	
	ClyC1	4.00E-01	2.42E-15	2.42E-15	**2.42E-15**	Non-Convergent	
Pan8TCP.inp(9)	ClyA1	4.00E-01	2.42E-15	2.42E-15	**2.42E-17**	3.05E+00	Yrs
	ClyA2	4.00E-01	2.42E-15	2.42E-15	**2.42E-15**	3.05E+00	
	ClyB1	4.00E-01	2.42E-15	2.42E-15	**2.42E-15**	3.05E+00	
	ClyC1	4.00E-01	2.42E-15	2.42E-15	**2.42E-15**	3.05E+00	

Appendix E

Calculation of Concentration of COCs in Soil Water (Aqueous Phase)

Project No. C02-266 **June 2004**

Appendix E

Calculation of Concentration of COCs in Soil Water (Aqueous Phase)

ASSUMPTIONS AND PROCEDURES

This appendix summarizes the procedures used to calculate concentrations of chemicals of concern (COCs) in the aqueous phase from the reported values of soil concentration. These values have been used to arrive at initial concentrations for simulations presented in the main body of this report. Several assumptions were used to arrive at these results as outlined in the following paragraphs.

The soil concentrations reported by laboratories represent the total mass of the COC per unit mass of soil. This assumption implies that there was no loss of volatiles during sampling and laboratory analyses.

Constant average values of water content, porosity, and bulk density were used.

Total concentration in soil is approximated by the following equations:

Total mass of COC (M_t) = Adsorbed mass (M_s) + Dissolved mass (M_w) + Volatilized mass (M_v)

M_s = Adsorbed concentration (C_s) x Mass of soil (W_s)

$W_s = \rho_b \times V_s$

C_s = Aqueous-phase concentration (C_w) / Distribution coefficient (K_d)

$M_s = (C_w / K_d) \times \rho_b \times V_s$

$M_w = C_w$ x Volumetric water content (θ_w) x V_s

$M_v = C_v$ x Volumetric air content (θ_v) x V_s

θ_v = Porosity (n) - θ_w

$C_v = C_w$ x Henry's law constant (H) /[Gas law constant (R) x Absolute Temperature (T)]

$M_v = C_w \times H / (R \times T) \times V_s$

Therefore,

$M_t = (C_w / K_d) \times \rho_b \times V_s + C_w \times \theta_w \times V_s + C_w \times H / (R \times T) \times (n - \theta_w) \times V_s$

Reported soil concentration (C'_s) = M_t / V_s

$C'_s = C_w [(\rho_b / K_d) + \theta_w + H / (R \times T) \times (n - \theta_w)]$

Apparent distribution coefficient (K'_d) = $1/[(\rho_b / K_d) + \theta_w + H / (R \times T)) \times (n - \theta_w)]$

Therefore, aqueous-phase concentrations (Cw) may be estimated by the following equation:

$C_w = C'_s \times K_d$

If both soil and water samples are analyzed in the saturated zone, Kd may be estimated by the following equations:

$K'_d = C_w / C'_s = 1/[(\rho_b / K_d) + \theta_w + H / (R \times T)) \times (n - \theta_w)]$

$C'_s / C_w = [(\rho_b / K_d) + \theta_w + H / (R \times T) \times (n - \theta_w)]$

$\rho_b / K_d = C'_s / C_w - \theta_w - H / (R \times T) \times (n - \theta_w)$

$K_d = \rho_b / [C'_s / C_w - \theta_w - H/(R \times T) \times (n - \theta_w)]$

Appendix F

Calculation of Kd from Laboratory Batch Adsorption Test

Project No. C02-266 **June 2004**

Appendix F

Calculation of Kd from Laboratory Batch Adsorption Test

Two soil samples and a groundwater sample were tested to obtain an estimate of distribution coefficient. The procedure was as follows:

Twenty-five grams (25 g) of soil samples (PWA-3-80 and PWB-5-45) were used, which were collected during drilling of boreholes PWA-3 at 80 feet below ground surface (bgs) and PWB-5 at 45 feet bgs, respectively. These samples were analyzed for COCs and water content prior to mixing with the groundwater sample. The groundwater sample was obtained from the A-zone in well AMW-1P and analyzed for COCs prior to mixing with the soil samples. The analytical results are shown in Table F-1. Each soil sample was then agitated with 250 milliliters (ml) of the groundwater sample separately and the final concentration of the COCs was measured in the aqueous phase.

The distribution coefficient (Kd) is calculated by:

$$K_d = C^2_s / C^2_w$$

Where, C2s is the mass of COC adsorbed per unit bulk dry mass of soil and C2w is the final mass of COC in the aqueous phase after completion of agitation of the batch of soil and groundwater mix. The mass C2s is not measured and needs to be calculated as follows:

$$C^2_s = M^2_{COCs}/W_{soil} = (M^1_{COCs} + M^1_{COCw} - M^2_{COCw})/ W_{soil\text{-}dry}$$

Where, M2COCs and M2COCw are the mass of the COC adsorbed on solids and dissolved in water after agitation, respectively. M1COCs is the total mass of COC in soil before mixing with water, and M1COCw is the mass of COC in the groundwater sample. Wsoil-dry is the bulk dry mass of soil. The mass C2w is measured and, therefore, Kd may be estimated. It should be noted that the Kd estimated with such a method is exaggerated because the nature of the soil in-situ is disturbed and sorption sites that may not have been available in a natural state have been made available as a result of disturbance of the soil.

TABLE F-1

Bulk Density	Water Content	Concentration (ug/kg)	Sample Number	Sample Type	Bulk Density	Water Content	Concentration (ug/kg)	Post Agitation Concentration with PWA-3-80 (ug/l)	Post Agitation Concentration with PWB-5-45 (ug/l)
113.47	34.539	ND	PWB-5-45	Soil	97.75	32.886	ND	ND	ND
113.47	34.539	ND	PWB-5-45	Soil	97.75	32.886	ND	ND	ND
113.47	34.539	ND	PWB-5-45	Soil	97.75	32.886	ND	ND	ND
113.47	34.539	2.85	PWB-5-45	Soil	97.75	32.886	ND	570	560
113.47	34.539	ND	PWB-5-45	Soil	97.75	32.886	ND	4440	3340
113.47	34.539	ND	PWB-5-45	Soil	97.75	32.886	ND	ND	ND
113.47	34.539	ND	PWB-5-45	Soil	97.75	32.886	ND	3300	3300

Appendix I-B

Baseline Human Health Risk Assessment Report

Project No. C00-266.2 September 2005